Mechanisms of transcriptional regulation in Waldenström's macroglobulinemia and multiple myeloma

Kimberley Jade Anderson

Thesis for the degree of Philosophiae Doctor

Supervisor:
Erna Magnúsdóttir

April 2019

UNIVERSITY OF ICELAND
SCHOOL OF HEALTH SCIENCES
FACULTY OF MEDICINE

Sameindaferlar umritunarstjórnunar í Waldenströms risaglóbúlínblæði og mergæxlum

Kimberley Jade Anderson

Ritgerð til doktorsgráðu

Leiðbeinandi:
Erna Magnúsdóttir

Doktorsnefnd:
Þórarinn Gúðjónsson
Eiríkur Steingrímsson
Arnar Pálsson
Þórunn Rafnar

Apríl 2019

UNIVERSITY OF ICELAND
SCHOOL OF HEALTH SCIENCES
FACULTY OF MEDICINE

ISBN 978-9935-9455-6-3

Printing by Háskólaprent ehf.

Reykjavik, Iceland 2019

Ágrip

Stjórnferlar umritunar stýra þroska B-fruma yfir í plasma-frumur, þar sem stórbrotnar breytingar á umritunarferlum eiga sér stað. Þessar breytingar eru háðar fjölmörgum þáttum, en þar á meðal er umritunarþátturinn “B lymphocyte- induced maturation protein-1” (BLIMP1), auk ferla sem stjórna umframerfðamörkunum. Í þessari ritgerð lýsi ég tveimur verkefnum sem skoða sameindaferla umritunarstjórnar í krabbameinum mótefnaseytandi fruma.

Waldenströms risaglóbúlínblæði er krabbamein mótefnaseytandi fruma í beinmerg sem hafa svipgerð eitil- og plasmafruma. Umritunarþátturinn BLIMP1 er mikilvægur fyrir seytingu mótefna en hlutverk hans í Waldenströms risaglóbúlínblæði hefur þó ekki verið rannsakað. Í þessari rannsókn sýni ég fram á að frumur Waldenström’s risaglóbúlínblæðis eru háðar BLIMP1 til að lifa Rannsóknir á plasmablöstum músa og mótefnaseytandi frumum hafa bent til að bæði bein- sem og erfðafræðileg víxlverkun sé á milli BLIMP1 og histónumetýltransferasans „enhancer of zeste homologue 2“ (EZH2). Í þessari rannsókn sýni ég fram á áður óskilgreint hlutverk BLIMP1 í að viðhalda prótínstyrk EZH2 í frumum Waldenströms risaglóbúlínblæðis. Niðursláttur á BLIMP1 og hindrun á EZH2 sýndu fram á að mikil skörun er í markgenum þessara tveggja þátta. Þrátt fyrir þessa skörun bindast BLIMP1 og EZH2 á mismunandi bindiset í erfðamenginu, en oft á sömu genin. Þetta bendir til þess að skörun í virkni þáttanna sé að mestu vegna samhliða stjórnun á umritun auk viðhalds BLIMP1 á EZH2 fremur en að þeir bindist saman við litni. Loks sýni ég fram á hlutverk BLIMP1 og EZH2 í að forða frumum sjúkdómsins frá frumudauða af völdum náttúrulegra drápsfruma, auk stjórnunar á frumuhringnum. Þessar uppgötvanir veita nýja innsýn inní meingerð Waldenströms risaglóbúlínblæðis.

Einstofna mótefnahækkun, eða „monoclonal gammopathy of undetermined significance“ (MGUS) er góðkynja forstig mergæxla. Um 0.5-1% MGUS tilfella þróast yfir í mergæxli árlega og núverandi viðmið sem notast er við til að spá fyrir um áhættuna á þessari framþróun eru ófullnægjandi. Þeir ferlar sem hafa áhrif á það að frumur breytist úr MGUS í mergæxli eru ekki vel þekktir. Rannsóknir á tjáningarmynstrum hafa ekki bent til stórfellds munar í umritun á milli þessara tveggja stiga. Ein leið til þess að afhjúpa ný merki er með því að lýta á mismunandi virkjun eflirða sem geta

gefið til kynna breytingu á eðli fruma jafnvel í fjarveru samsvarandi breytinga í genatjáningu. Hægt er að bera kennsl á mismunandi virkjaðar efliraðir með tilvist mismunandi markana á histónum og umrituðum efliraða RNA (eRNA). Í þessari rannsókn set ég upp vinnuferil til þess að rannsaka histónumörk á efliröðum og stýrlum auk vinnurferils fyrir RNA raðgreiningu á heildar RNA úr frumum með því að nota lágan fjölda fruma úr sjúklingum með einstofna mótefnahækkun og mergæxlum sem upphafsefnivið. Þessar aðferðir má nota í framtíðinni til þess að bera kennsl á þætti sem hafa forspárgildi um sjúkdómsframvindu MGUS og mergæxla.

Lykilorð:

Umritunarþáttur, efliröð umritunar, Waldenströms risaglóbúlínblæði, mergæxli, histónumörk

Abstract

Transcriptional regulatory mechanisms drive the maturation of B cells to plasma cells, with a dramatic transcriptional rewiring taking place during the transition. This rewiring is dependent on a number of factors, including the transcription factor B lymphocyte induced maturation protein 1 (BLIMP1), and epigenetic mechanisms, amongst others. In this thesis, I present two projects investigating mechanisms of transcriptional regulation in antibody-secreting cell malignancies.

Waldenström's macroglobulinemia is a cancer of antibody-secreting lymphoplasmacytic cells in the bone marrow. The transcription factor BLIMP1 is important for antibody secretion and yet its role has not been studied in Waldenström's macroglobulinemia. Here I demonstrate that Waldenström's macroglobulinemia cell lines rely on BLIMP1 for survival. Studies in mouse plasmablasts and antibody secreting cells have suggested both a physical and genetic interaction between BLIMP1 and the histone methyltransferase enhancer of zeste homologue 2 (EZH2). In this study I reveal a novel role of BLIMP1 maintaining the protein levels of EZH2 in Waldenström's macroglobulinemia. BLIMP1 knock-down and EZH2 inhibition reveal a large overlap in transcriptional targets of the two factors. Despite this, BLIMP1 and EZH2 bind to the genome at mostly distinct sites, although often on the same genes, indicating that the functional overlap of the two factors is mostly due to parallel transcriptional regulation and through maintenance of EZH2 by BLIMP1, rather than through co-binding to chromatin. Finally, I uncover novel roles for BLIMP1 and EZH2 in evasion from natural killer (NK) cell mediated cytotoxicity and regulation of the cell cycle. These findings provide novel insights into the pathology of Waldenström's macroglobulinemia.

Multiple myeloma is preceded by the pre-malignant monoclonal gammopathy of undetermined significance (MGUS). Around 0.5-1% of MGUS cases progress to myeloma each year and current standards for predicting the risk of progression are inadequate. The drivers of the transition from MGUS to multiple myeloma are still not well understood, and gene expression profiling studies have failed to identify major transcriptional differences between the two stages. One opportunity for uncovering novel markers is in the study of differential activation of transcriptional enhancers, which can indicate changes in cellular states even without corresponding

gene expression changes. Differentially activated enhancers can be identified by the presence of different histone modifications and transcribed enhancer RNA (eRNA). Here, I establish a protocol for profiling histone modifications at enhancer and promoter regions and for total RNAseq using small numbers of cells from MGUS and myeloma patient material. These techniques may be used in the future to identify novel prognostic markers for MGUS and multiple myeloma.

Keywords:

Transcription factor, transcriptional enhancer, Waldenström's macroglobulinemia, multiple myeloma, histone modifications.

Acknowledgements

The work involved in this project was mostly carried out at the Biomedical Centre at the University of Iceland, and in the departments of Anatomy, Biomedical Science and Biochemistry and Molecular Biology, Faculty of Medicine, School of Health Sciences at the University of Iceland.

I would like to specially thank my supervisor Erna Magnúsdóttir for teaching and guiding me so carefully through the years of my PhD. It has been an invaluable learning experience due to her guidance and the many hours spent going over ideas, hypotheses and interpretations together. I would like to thank the members of the EM lab, especially Árný Björg Ósvaldsdóttir for enormous technical and moral support during my PhD. Also many thanks to Birgit Atzinger, Aðalheiður Elín Lárusdóttir and Kristján Hólm Gretarson for their contribution to the project. Thanks to Daisy Awiti, Juan Manuel Sacnun, Árni Ásbjarnarson and Halla Rós Eyólfsdóttir for many good chats and advice.

I would like to thank the members of my PhD committee, Eiríkur Steingrímsson, Þórarinn Guðjónsson, Þórunn Rafnar and Arnar Pálsson for their input, support and advice during the years of the project.

Thanks to SCRU lab members especially Gunnhildur Ásta Traustadóttir for help with reagents and experiments. I would also like to thank members of the RTL lab, especially Diahann Atacho, Fatich Mechmet and Alba Sabate for their help, advice and good company in the office for the past years. Thanks to Eiríkur Steingrímsson and members of his lab for including me as a part of their group for the first two years of my PhD. Special thanks go out to Ramile Dilshat for invaluable advice and help with bioinformatics analyses, and for teaching me in the lab during the first years of my project. Thanks to Valerie Fock for technical advice and help with reagents over the years. Also thanks to Ramile and Valerie for great company in the first years of my PhD.

Thanks to Kirstine Nolling Jensen and Sunnefa Yeatman Ómarsdóttir for their invaluable help with the isolation and analysis of NK cells. Thanks to Jóna Freysdóttir and Ingibjörg Harðardóttir for allowing me to use their lab space and for providing feedback on my manuscript. Special thanks to Jón Þór Bergþórsson for an enormous amount of help with all things related to

flow cytometry and analysis of the MGUS and myeloma patient samples. Also thanks to Katrín Birna Péturdóttir for help with setting up the apoptosis assays. Special thanks to Þórunn Rafnar for giving me the opportunity to investigate my sets of lncRNAs for variants using the databases at deCODE Genetics. Thanks to Arnar Pálsson and Dagný Ásta Rúnarsdóttir for very helpful advice regarding my bioinformatics analyses. Thanks to Sigurður Yngvi Kristinsson for providing the MGUS and muliple myeloma patient bone marrow extracts and for advice in setting up the $CD138^+$ cell isolations. Also, special thanks to Margrét S Steinarsdóttir for her invaluable help in teaching me how to isolate $CD138^+$ cells and for providing me with additional patient samples.

Finally, I would like to thank my husband Arnar Össur Harðarson for his tireless love, help and support in my life outside of work, without which the completion of this PhD project would not have been possible.

This work was supported by project grants from the Icelandic Research fund (grant no. 140950-051) and the Icelandic Cancer Society, a doctoral fellowship from the University of Iceland, and grant from the University of Iceland Eggertssjóður and funds from the COST Project EpiChemBio.

Contents

List of abbreviations

ABC-DLBCL	Activated B cell type diffuse large B cell lymphoma
APC	Antigen presenting cell
BCR	B cell receptor
BSA	Bovine serum albumin
CD40L	CD40 ligand
CDK	Cyclin-dependant kinase
C_H	Heavy chain constant region
ChIP	Chromatin immunoprecipitation
CIITA	MHC class II transactivator
CLP	Common lymphoid progenitor
CRAB	Hypercalcaemia, renal failure, anaemia, and bone lesions
CSR	Class switch recombination
D	Diversity region
DLBCL	Diffuse large B cell lymphoma
dox	Doxycycline
DSB	Double-strand break
EGFP	Enhanced green fluorescent protein
eRNA	Enhancer RNA
FBS	Foetal bovine serum
FSC	Forward scatter
GFP	Green fluorescent protein
GTF	General transcription factor
H3K27Ac	Histone 3, lysine 27 acetylation
H3K27me3	Histone 3, lysine 27 tri-methylation
H3K4me1	Histone 3, lysine 4 mono-methylation
H3K4me3	Histone 3, lysine 4 tri-methylation
H3K9me3	Histone 3, lysine 9 tri-methylation

HDAC	Histone deacetylase
IgH	Immunoglobulin heavy chain
IgL	Immunoglobulin light chain
IgV	Immunoglobulin variable region
IL	Interleukin
IP	Immunoprecipitation
J	Joining region
KD	Knock-down
KIR	Killer immunoglobulin-like receptor
MGUS	Monoclonal gammopathy of undetermined significance
MHC	Major histocompatibility
miRNA	Micro RNA
mRNA	Messenger RNA
NELF	Negative elongation factor
NHEJ	Non-homologous end joining
NK cell	Natural killer cell
NT	Non-targeting control
PBS	Phosphate buffered saline
PcG	Polycomb group
PCNA	Proliferating cell nuclear antigen
PFA	Paraformaldehyde
PIC	Transcriptional pre-initiation complex
PRC2	Polycomb repressive complex 2
Pre-BCR	pre-B cell receptor
RLU	Relative luminescence units
RNA pol	RNA polymerase
rRNA	Ribosomal RNA
RT-qPCR	Quantitative reverse-transcription PCR
SDS-PAGE	SDS-polyacrylamide gel electrophoresis
SHM	Somatic hypermutation
SSB	Single-strand break

SSC	Side scatter
TBST	Tris-buffered saline with 0.1% tween-20
TEB	Triton extraction buffer
TIR	TLR/IL-1R domain
TLR	Toll-like receptor
TLS	Translesion synthesis
tRNA	transfer RNA
TSS	Transcription start site
UNG	Uracil DNA glycosylase
V	Variable region
WGA	Whole-genome amplification

List of figures

List of tables

List of original papers

This thesis is based on the following original publication, which is referred to in the text by the Roman numeral I:

I. **The BLIMP1 - EZH2 nexus in a non-Hodgkin lymphoma**

Kimberley Jade Anderson, Árný Björg Ósvaldsdóttir, Birgit Atzinger, Gunnhildur Ásta Traustadóttir, Kirstine Nolling Jensen, Aðalheiður Elín Lárusdóttir, Jón Þór Bergþórsson, Ingibjörg Harðardóttir, Erna Magnúsdóttir. *Manuscript in preparation*

In addition, a large body of unpublished data is presented.

Declaration of contribution

I performed all of the experimental work presented in this thesis, with a few exceptions. Two of the stable cell lines used in the study were generated by my supervisor, Erna Magnúsdóttir and two by another student, Aðalheiður E Lárusdóttir. Gunnhildur Á Traustadóttir produced a number of batches of lentivirus which were used for the rescue experiments, and I also produced a number of batches. Árný B Ósvaldsdóttir optimised the immunofluorescence stainings for BLIMP1 and performed two of the three stains for BLIMP1 in the OPM-2 cell line. Jón Þór Bergþórsson and Kirstine Nolling Jensen assisted with and performed some of the flow cytometric analyses.

Beyond the experimental work, I also contributed to planning and devising methodologies and experimental designs. I performed all of the bioinformatics analyses. I contributed to hypothesis generation, planning and interpretation of results together with my supervisor Erna Magnúsdóttir. Our paper manuscript, which is currently in preparation for submission, was written by me together with my supervisor.

1 Introduction

Transcriptional regulation is central to maintenance of cellular states, both in normal differentiation and disease. Waldenström's macroglobulinemia and multiple myeloma are malignancies of antibody-secreting cells derived from the B cell to plasma cell differentiation spectrum. In this thesis I describe transcriptional regulatory mechanisms underlying these disease states. In order to understand these mechanisms, it is important to acknowledge the diseases and their regulation in the context of B cell and plasma cell development (Figure 1).

1.1 B cell and plasma cell development

One of the most striking features of B cells is the diversity of their B cell receptor (BCR), with at least 10^{11} possible molecules with different specificities (Janeway Jr et al., 2001). The BCR consists of a membrane-bound immunoglobulin molecule, which acts as a transmembrane receptor, and later is secreted from plasma cells as an antibody. Immunoglobulins are molecules that can recognise and bind to sites on pathogens, known as antigens, which can lead to BCR signalling, direct neutralisation of the pathogen, or recruitment of other immune effectors. The clonal selection theory of acquired immunity proposed the now accepted paradigm of "one B cell, one antibody". This hypothesis suggested that each developing B cell produces its own unique BCR with specificity for a particular antigen. The BCR is then clonally selected for upon contact with this antigen (Burnet, 1957). The enormous diversity of immunoglobulins is achieved through alterations of the DNA encoding the BCR in processes of V(D)J recombination, somatic hypermutation and class switch recombination.

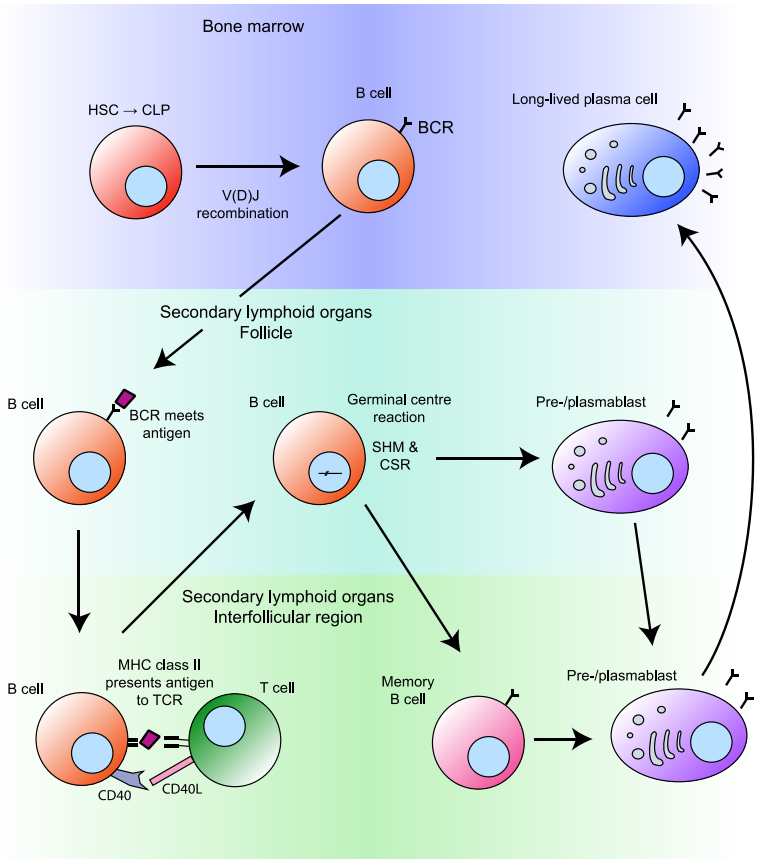

Figure 1: A simplified overview of B cell and plasma cell development

B cells develop from in the bone marrow from CLPs and undergo the process of V(D)J recombination. They then migrate to the periphery and collect in secondary lymphoid organs. Upon antigen recognition, the B cells internalize the antigen-bound BCR and can present it to T cells via MHC class II. With T cell help, B cells can initiate the germinal centre reaction in the lymphoid follicles where they undergo SHM and CSR. Following the germinal centre reaction, the B cells can differentiate into memory B cells or pre-/plasmablasts, which migrate away from lymphoid organs and can form long-lived plasma cells in the bone marrow.

B cells originate from hematopoietic stem cells, which develop in the foetal liver and in the bone marrow (Gathings et al., 1977; Raff et al., 1976). Some of the earliest involved factors are the chromatin remodeller IKAROS (Georgopoulos et al., 1994; Kim et al., 1999), and the transcription factors PU.1(DeKoter & Singh, 2000) and E2A (encoded by *TCF3*) (Mercer et al., 2011; Welinder et al., 2011), whose expression results in lymphoid primed multipotent progenitors that develop into common lymphoid progenitors. Common lymphoid progenitors can develop into B cells, T cells and NK cells. Downstream of this, EBF1, PAX5 and other factors are activated to induce B cell-specific gene expression (Decker et al., 2009; Lin, Y. C. et al., 2010).

1.1.1 V(D)J recombination

The genes that encode immunoglobulins are present as fragments in the germ-line genome, known as the variable region (V), diversity region (D), and joining region (J), and are assembled into their functional state in B lymphocytes (Brack et al., 1978; Tonegawa, 1983). This step, known as V(D)J recombination is essential in generating diversity of antigen-recognition and occurs during the development of B cells in the foetal liver and adult bone marrow. Firstly, the DNA is cleaved by the RAG complex introducing single-strand nicks at recombination signal sequences, then double-strand breaks to remove these sequences. The fragments are then repaired by non-homologous end joining together with the RAG complex and fused together into the assembled gene (McBlane et al., 1995; Oettinger et al., 1990; Taccioli et al., 1993; van Gent et al., 1995). Immunoglobulins comprise four polypeptide chains, made up of two known as the heavy chain and two known as the light chain. The heavy chain locus (*IgH*) is typically recombined prior to the light chain locus (*IgL*). The imprecise nature of this joining leads to antigen receptor diversity, but can also have consequences such as lymphoid cancers, due to improper recombination and genomic instability (Schatz & Ji, 2011).

Somatic cells bear two alleles for each gene under normal circumstances. Most genes are expressed equally from both alleles, however in specific cases, genes are expressed from only one allele in a process termed monoallelic expression. This can result in a proportion of cells expressing one allele, while another proportion expresses the second allele. Alternatively, one allele can be epigenetically silenced in all cells through imprinting (Zakharova et al., 2009). However, in B cells, the immunoglobulin VDJ transcripts are expressed from both alleles simultaneously in the same cell. In order to maintain “one B cell, one antibody”, one of the alleles is

inactivated via allelic exclusion. This occurs during V(D)J recombination by a number of mechanisms. Firstly, the timing of V(D)J recombination is staggered, such that one allele is rearranged before the second. This may occur through inaccessible chromatin blocking the recombination machinery, making it probable for one allele to be rearranged before the other (Vettermann & Schlissel, 2010). Another proposed mechanism is that asynchronous DNA replication timing leads to the recombination of the allele that is replicated first (Mostoslavsky et al., 2001).

During their early development, B cells pass through distinct developmental stages known as pro- or progenitor B cells, which do not express the BCR on their surface, and pre-B cells, which express the pre-B cell receptor (pre-BCR), comprising the heavy chains together with surrogate light chains (Kerr et al., 1989; LeBien & Tedder, 2008). The expression of this pre-BCR serves as a developmental checkpoint. This allows for another mechanism of allelic exclusion to take place, whereby signals from the pre-BCR send negative feedback to prevent V(D)J recombination from the second allele (Alt et al., 1984; Hewitt et al., 2009). In those cells whose rearrangement of the first allele did not produce an in-frame immunoglobulin gene and cannot express the pre-BCR, rearrangement of the second allele then takes place (Vettermann & Schlissel, 2010). Following this, cells whose VDJ recombination process did not generate in-frame *IgH* VDJ joints in either allele undergo apoptosis (Ehlich et al., 1993; Rajewsky, 1996). The cells that survive send further signals via their pre-BCR, which is capable of signalling in the absence of any exogenous ligand (Geier & Schlissel, 2006). Pre-BCR signalling induces a cascade of events mediated by BTK and MAPK signalling to induce a short burst of proliferation (Geier & Schlissel, 2006; Rolink et al., 2000). A negative feedback loop is then initiated, inducing quiescence of the cell cycle (Geier & Schlissel, 2006), silencing transcription of surrogate light chain genes (Parker et al., 2005; Thompson et al., 2007) and promoting VJ recombination of the *IgL* gene (Reth et al., 1987). Signalling via the pre-BCR also induces the transcription factors NFκB, IRF4 and PAX5 to bind to and transcriptionally activate the *IgL* promoter (Shaffer et al., 1997). Again, following *IgL* genetic recombination, many unproductive *IgL* loci are formed without in-frame joints, and are given the opportunity to recombine their second *IgL* allele. Additionally, many autoreactive BCRs are produced and the cells expressing them, or not expressing functional *IgL* are driven towards apoptosis (Melchers et al., 2000). The remaining cells enter a quiescent state that is activated upon antigenic stimulation.

1.1.2 Antigen-dependent maturation of B cells

The B cells with their newly recombined immunoglobulin genes, expressing BCRs on their surfaces, then enter the periphery of the body where the BCRs can come into contact with their specific antigens. To increase the chance of a B cell encountering its specific antigen, antigens are collected and concentrated in secondary lymphoid organs such as lymph nodes and spleen. Here, B cells migrate to the follicles, directed by chemokines and interactions with follicular dendritic cells (Bajénoff et al., 2006; Gunn et al., 1998; Schiemann et al., 2001). Small soluble antigens can pass through pores in the sinuses of lymphoid organs to meet follicular B cells directly, but larger antigens need to be presented to B cells via macrophages and follicular dendritic cells (Batista & Harwood, 2009). This initiates the activation of the B cell via separate pathways, either independent or dependent on T-cell help. In the T-dependent pathway, the antigen is first internalised and processed, and then can be presented to T cells via major histocompatibility (MHC) class II molecules (Lanzavecchia, 1985). Having met their antigen, the B cells move to the interfollicular region, where they come into contact with T cells that have previously had antigen presented to them by dendritic cells (Bajénoff et al., 2003; Kerfoot et al., 2011; Kitano et al., 2011; Stoll et al., 2002). The MHC class II molecule on the B cell forms a complex with the antigen and the T cell receptor, and the CD40 surface molecule on the B cell binds to the CD40 ligand (CD40L) on the T cell. This activates the T cells to form T_{FH} cells and activates the B cells to either differentiate into short-lived plasma cells or to re-enter the follicle along with the T_{FH} cells and initiate the germinal centre reaction (De Silva & Klein, 2015).

The germinal centre is a close grouping of cells within secondary lymphoid organs such as the spleen or lymph nodes. The purpose of the germinal centre reaction is to generate high-affinity BCRs, which are then clonally selected for. This process is termed affinity maturation. In the early germinal centre, activated B cells collect in the centre of a follicle and rapidly proliferate, displacing the naïve B cells which are pushed to the outside of the germinal centre. The proliferating B cells arrange into two distinct groupings, termed the light zone and the dark zone. The dark zone, organised by CXCR4 expression contains proliferating B cells and reticular cells, whereas the light zone, organised by CXCR5 expression contains B cells as well as T_{FH} cells and follicular dendritic cells (De Silva & Klein, 2015). Somatic hypermutation, the process of generating small mutations in the immunoglobulin variable region (IgV), takes place in the dark zone, whereas T-cell dependent selection occurs in the light zone. The B cells cycle between the two zones during affinity maturation (Allen et al., 2007; Victora et al., 2010).

1.1.3 Somatic hypermutation

The key process in affinity maturation is somatic hypermutation (SHM), which involves the generation of point mutations in the variable regions (*IgV*) of the immunoglobulin gene, with the goal of increasing the affinity of the immunoglobulin to its antigen (Jacob et al., 1991). Both SHM and class switch recombination are orchestrated by the cytosine deaminase AID (encoded by *AICDA*) (Muramatsu et al., 2000). AID acts by converting cytosine (C) to uracil (U) only on single stranded-DNA, and so acts with much higher efficiency at sites of active transcription (Chaudhuri et al., 2003). Thus, during SHM, AID physically interacts with members of the stalled RNA pol II complex and localises to *IgV* (Nambu et al., 2003; Pavri et al., 2010). Following *IgV* deamination by AID, SHM occurs through three predominant mechanisms. Firstly, the C to U changes can act as an altered template for replication, where the sites of previous C are changed to T (Methot & Di Noia, 2017). Secondly, uracil DNA glycosylase (UNG) removes U, leaving abasic sites in the DNA strand (Di Noia & Neuberger, 2002; Rada et al., 2002). The pathway of base excision repair, which would normally repair the abasic sites, most often does not occur at these sites of AID deamination. As normal replicative polymerases cannot pass over abasic sites, alternative polymerases including REV1 and Pol η initiate translesion synthesis (TLS), which leads to insertion of C opposite to U or A/T mutations (Delbos et al., 2007; Delbos et al., 2005; Jansen et al., 2006). The choice of alternative polymerase engagement is regulated by ubiquitination of proliferating cell nuclear antigen (PCNA) (Choe & Moldovan, 2017; Guo et al., 2006; Kannouche et al., 2004; Watanabe et al., 2004). Finally, the third mechanism for generation of point mutations in SHM involves the action of MutSα (comprising the MSH2-MSH6 heterodimer) independent of UNG (Rada et al., 2004). In the canonical mismatch repair pathway, MutSα recruits MutLα to create a nick in the DNA, which provides access for EXO1 to chew back the DNA over the mismatched site, and allows Pol δ or ε to repair the gap (Hsieh & Zhang, 2017). Instead, during SHM, MutSα recognises the U:G mismatch, recruiting EXO1 and then activating an inaccurate TLS polymerase such as Pol η, which often generates mutations at these sites (Methot & Di Noia, 2017; Wilson et al., 2005).

1.1.4 Class switch recombination

Immunoglobulins can be separated into 5 different classes or isotypes that are defined by the constant region of their heavy chain (C_H), IgD, IgM, IgG, IgA and IgE. Each of these classes can work against different pathogens,

and can localise to different sites in the body. Naïve B cells express only IgD and IgM, and so class switch recombination (CSR) is the process by which the other classes of antibody are produced. The primary immunoglobulin C_H locus comprises 5 regions of exon clusters termed μ, δ, γ, ε, and α, with specific upstream or downstream switch regions. During CSR, the transcribed exon cluster is replaced by the cluster of another isotype without any changes to the already-mutated antigen-recognising variable region. This occurs through the generation of double-strand breaks (DSBs) followed by joining of two switch regions, which creates an extrachromosomal circle of the intermediate regions that is then removed, leaving behind the recombined genomic locus (Xu, Z. et al., 2012). CSR is initiated by transcriptional activation of the primary *IgH* locus and recruitment of AID to tandem repeats in the centres of switch regions (Maul et al., 2011). Following deamination by AID, UNG removes U as in SHM (Rada et al., 2002), then nucleases known as APEs induce single-strand breaks (SSBs) at these abasic sites, ultimately leading to DSB formation. Endonuclease G and topoisomerase I can also play a role in DSB formation in switch regions (Kobayashi et al., 2009; Zan et al., 2011).

1.1.5 Plasma cell differentiation

B cells can also be activated independently of the germinal center reaction, and differentiate much more quickly into non-somatically mutated or class switched antibody secreting plasma cells. This is particularly useful with respect to blood-borne pathogens, which require a fast immune response. However, the downside of this is that the antibodies produced have a lower affinity towards their antigen, and the plasma cells produced by this method are typically short-lived (Fairfax et al., 2008).

Either following the germinal centre reaction, or independently of it, B cells can then differentiate into memory B cells, which upon antigen re-stimulation can differentiate into plasma cells or rapidly mobilise germinal centre reactions (Dogan et al., 2009). In humans, memory B cells, even those that have not passed through the germinal centre reaction bear somatically mutated *IgV* loci (Cerutti et al., 2013). During foetal development, SHM can occur independently of the germinal centre or T cell help (Scheeren et al., 2008), and SHM can also occur independently of antigen stimulation in the first two years of human life (Weller et al., 2004; Weller et al., 2008). Indeed, in humans lacking a functional CD40L, there exists a population of somatically mutated memory B cells formed independently of T cell help (Weller et al., 2001). In adults, stimulatory signals from neutrophils (Puga et

al., 2011) or pattern recognition receptors such as toll-like receptors (TLRs) can also trigger SHM independently of T cells (Aranburu et al., 2010; Capolunghi et al., 2008).

Post-germinal centre or memory B cells can differentiate into pre-plasmablasts, which lose expression of B cell markers such as CD20, but have not yet gained plasma cell markers such as CD38 (Jourdan et al., 2011), followed by plasmablasts, which express early plasma cell markers such as CD38, and then plasma cells, which express CD138. Plasmablasts migrate and enter the circulation where they will either die or find a survival niche such as lymphoid organs, inflamed tissue, or the bone marrow where they are able to differentiate into long lived plasma cells (Radbruch et al., 2006). While pre-plasmablasts, plasmablasts and plasma cells all have the ability for antibody secretion, only pre-plasmablasts and plasmablasts have proliferative capacity (Jourdan et al., 2011; Nutt et al., 2015).

During the development from a B cell to a plasma cell, the immunoglobulin undergoes a switch from its membrane-bound to secreted form. The form of immunoglobulin protein is dictated by differential mRNA processing on the *IgH* gene (Early et al., 1980; Peterson & Perry, 1989). It is negatively regulated by factors such as hnRNP (Veraldi et al., 2001) and U1A (Ma et al., 2006), and positively regulated by ELL2 (Martincic et al., 2009). As well as changes to the form of the immunoglobulin protein, the B cell to plasma cell transition induces immense changes to hundreds of genes, and is considered a “lineage switch” due to the almost complete cellular rewiring (Nutt et al., 2015). In order to achieve this profound switch, competing transcriptional programs are turned off and on.

Perturbations that occur during B cell and plasma cell differentiation can lead to the development of B/plasma cell malignancies. The different types of these malignancies often retain some properties of their cell of origin, and it is often the same mechanisms that lead to development of normal activated B cells and plasma cells that drives the malignant transformation. For example, diffuse large B cell lymphoma (DLBCL) is derived from a stage between a germinal centre B cell and a plasmablast (Basso & Dalla-Favera, 2015). Here we focus on two antibody-secreting cell malignancies, Waldenström’s macroglobulinemia and multiple myeloma. Because the literature on Waldenström’s macroglobulinemia is still somewhat sparse, we also find it useful to include an analysis of some literature focusing on DLBCL.

1.2 Waldenström's macroglobulinemia

Waldenström's macroglobulinemia is a lymphoplasmacytic lymphoma, characterised by an expansion of B cells in the bone marrow that secrete monoclonal IgM (Treon, 2015). The bone marrow infiltrate in Waldenström's macroglobulinemia can vary from cells with a distinct B cell phenotype to those with a plasmacytic phenotype. Typically the cells express B cell markers including CD19 and CD20, and can also co-express plasma cell markers such as CD38 and CD138 on the same cell (Ghobrial et al., 2003; Konoplev et al., 2005). Patients present with anaemia resulting from the high burden of infiltrating lymphoplasmacytic cells in the bone marrow, and fatigue is the most common symptom (Gertz, 2019). Hyperviscosity of the serum occurs due to high levels of secreted IgM, leading to headaches, blurred vision, nasal/retinal haemorrhage and muscle cramps. Lymphadenopathy and organomegaly especially of the spleen and liver are also common in Waldenström's macroglobulinemia, with cells leaving the bone marrow to infiltrate other organs (Ghobrial et al., 2003). Peripheral neuropathies can occur due to the high levels of IgM, often with the antibody targeting myelin and causing demyelination. The symptoms can include numbness of the feet and weakness (Ropper & Gorson, 1998). However, at the early stages many Waldenström's macroglobulinemia patients are asymptomatic. Waldenström's macroglobulinemia is preceded by IgM monoclonal gammopathy of undetermined significance (MGUS), which is characterised by lymphoplasmacytic expansion and antibody secretion, but is by definition asymptomatic. IgM MGUS is differentiated from Waldenström's macroglobulinemia by having a bone marrow infiltration of < 10% and the absence of adenopathy or organomegaly (Gertz, 2019). In a long-term study of MGUS patients over a median of 34.1 years, 5% of those with IgM MGUS progressed to Waldenström's macroglobulinemia, whereas 8% progressed to other forms of non-hodgkin lymphoma (Kyle et al., 2018). The 10 year survival rate for Waldenström's macroglobulinemia is 66% for patients diagnosed in the years 2001-2010 (Castillo et al., 2014), although the average length of survival decreases with age (Castillo et al., 2015). While survival rates have been improving, there is still no cure for Waldenström's macroglobulinemia.

1.2.1 The MYD88^{L265P} mutation

The most common mutation in Waldenström's macroglobulinemia, present in >90% of patients is the MYD88^{L265P} somatic mutation, where a single nucleotide is changed from a T to a C in the *MYD88* gene, resulting in a

change from leucine to proline (Treon et al., 2012). The MYD88 protein is an adaptor molecule for all TLRs except for TLR3, and for the interleukin (IL)-1 and -18 receptors (Hoshino et al., 2000; Kawai et al., 1999; Medzhitov et al., 1998; O'Neill & Bowie, 2007). MYD88 signalling initiates a cascade involving downstream players IRAKs (Lin, S.-C. et al., 2010; Muzio et al., 1997; Wesche et al., 1997) and TRAF6 (Deng et al., 2000; Takeda & Akira, 2004). This can lead to the activation of NFκB and AP-1 via two branching pathways involving IKKs/BTK and JNK/MAPK respectively (Takeda & Akira, 2004; Yang et al., 2013). Recently, MYD88 was also shown to function as part of a large complex involving TLR9, the BCR, and mTOR to activate both NFκB and PI3K (Phelan et al., 2018). The MYD88 protein has two main domains separated by a short linker, the death-domain at the N-terminal, and the TLR/IL-1R (TIR) domain at the C-terminal (Bonnert et al., 1997; Hardiman et al., 1996). The protein functions by forming oligomers and interacting with IRAKs and BTK to initiate two diverging pathways for activation of NFκB (Lin, S.-C. et al., 2010; Yang et al., 2013). The L265P mutation is present within the TIR domain of the protein and causes constitutive activation of MYD88 signalling through increased ability to form oligomers with both its WT and mutated forms (Avbelj et al., 2014; Ngo et al., 2010). The effect of hyperactive MYD88 signalling in Waldenström's macroglobulinemia has been mostly attributed to high NFκB activity. Although there has been much investigation into the role of $MYD88^{L265P}$ in Waldenström's macroglobulinemia pathogenesis, whether the mutation affects survival is still controversial, with some finding that the mutation is associated with shorter survival (Treon et al., 2018), and others finding no difference between the mutant and wild-type carriers (Abeykoon et al., 2018). At least in cell line models, $MYD88^{L265P}$ is associated with increased Waldenström's macroglobulinemia cell survival (Yang et al., 2013).

1.2.2 Treatments, the cell of origin, and representative cell lines

The main treatments for Waldenström's macroglobulinemia depend on the characteristics of the individual patient's disease, but may involve plasmapheresis for immediate treatment of symptomatic hyperviscosity. One of the most commonly used agents is rituximab, a monoclonal antibody targeting CD20 (Treon, 2015). However, use of rituximab alone tends to cause a "flare" in IgM levels shortly after treatment, which itself can lead to increased morbidity (Branagan et al., 2004). Furthermore, a combination of two or more drugs produces a better response rate than rituximab alone (Santos-Lozano et al., 2016). Proteasome inhibitors such as bortezomib are

also frequently used. Proteasomal inhibition works against Waldenström's macroglobulinemia and multiple myeloma cells by a number of mechanisms, including preventing degradation of anti-apoptosis factors (Gomez-Bougie et al., 2007; Zhu et al., 2005), and inducing endoplasmic reticulum stress (Meister et al., 2007). Another method is to use nucleoside analogues such as fludarabine and cladribine, which prevent DNA replication and induce apoptosis (Huang & Plunkett, 1995). The glucocorticoid dexamethasone is also active against Waldenström's macroglobulinemia and multiple myeloma cells and is frequently used in combination with the above-mentioned agents in the treatment of Waldenström's macroglobulinemia. Dexamethasone is able to induce apoptosis of multiple myeloma cells and has effects on JNK (Chauhan et al., 1997) and NFκB (Sharma & Lichtenstein, 2008). More recently, the mTOR inhibitor everolimus (Ghobrial et al., 2014) and the histone deacetylase inhibitor panobinostat (Ghobrial, I. M. et al., 2013) have been tested and shown promising results in Waldenström's macroglobulinemia. Despite improved outcomes from drug treatments, relapses are still frequent. In the event of relapse, autologous stem cell transplantation can be used, with good response rates (Bachanova & Burns, 2012; Kyriakou et al., 2017). One of the most effective treatments available at present is ibrutinib, commonly used for rituximab refractory patients (Dimopoulos et al., 2017; Treon et al., 2015). Ibrutinib is a kinase inhibitor of BTK and HCK, both downstream targets of $MYD88^{L265P}$ in Waldenström's macroglobulinemia (Yang et al., 2016; Yang et al., 2013). More recently, ibrutinib has demonstrated effectiveness for use as a single agent first line therapy in Waldenström's macroglobulinemia (Treon et al., 2017a), and as a first line therapy in combination with rituximab, with a 30 month progression free survival rate of 82% (Dimopoulos et al., 2018). Taken together, effective treatments for Waldenström's macroglobulinemia depend on disturbing the signalling and survival mechanisms that the cells rely on.

The cell of origin for the Waldenström's macroglobulinemia clone poses an interesting question. Waldenström's macroglobulinemia cells have undergone SHM, but not CSR, and although they secrete antibody, they maintain expression of B cell surface markers. It has been proposed that the origin of the Waldenström's macroglobulinemia clone is an activated B cell that has been blocked in the process of plasma cell differentiation (Paiva et al., 2015; Zhou et al., 2014).

The use of representative cell lines provides an accessible method for studying disease properties. For Waldenström's macroglobulinemia, there are three main cell lines, which were used in this project. Firstly, the BCWM.1

cell line, which was derived from $CD19^+$ selected cells from the bone marrow of an untreated Waldenström's macroglobulinemia patient (Ditzel Santos et al., 2007). Secondly, the MWCL-1 cell line, derived from unsorted bone marrow mononuclear cells of a previously treated Waldenström's macroglobulinemia patient, with a monoallelic loss of *TP53* (Hodge et al., 2011). And finally, the RPCI-WM1 cell line, which was derived from tumour-bearing lymph nodes of a previously treated Waldenström's macroglobulinemia patient. The RPCI-WM1 primary cells were implanted into mice for a xenograft model, and the cell line is derived from the xenograft tumours. The cell line contains deletions at the *CDKN2A*, *RB1* and 6q21 loci, and amplification of the *IgH* gene (Chitta et al., 2013). All three of the cell lines secrete monoclonal IgM and bear the $MYD88^{L265P}$ mutation (Ansell et al., 2014; Chitta et al., 2013).

1.3 Multiple myeloma

Multiple myeloma is characterised by a clonal expansion of malignant terminally differentiated plasma cells primarily in the bone marrow. Unlike Waldenström's macroglobulinemia, myeloma cells have a mature plasma cell phenotype. The most common myelomas secrete IgG immunoglobulin, but they can also secrete all the other immunoglobulin classes, including light chains only, and a small proportion of myelomas do not secrete antibody (Kyle et al., 2003). The symptoms of multiple myeloma are often referred to as CRAB symptoms, standing for hypercalcaemia, renal failure, anaemia, and bone lesions (Rajkumar et al., 2014). Hypercalcaemia arises from bone destruction from within the bone marrow, with osteoclast activity causing lytic bone lesions increased in myeloma patients (Mundy et al., 1974; Yaccoby et al., 2002). Renal failure is often caused by the toxicity of secreted immunoglobulin light chains and hypercalcaemia, and rarely by plasma cell infiltrate and hyperviscosity (Dimopoulos et al., 2010). In addition to these symptoms, 10% or higher levels of bone marrow plasma cell infiltrate, and other non-CRAB organ damage can lead to a diagnosis of multiple myeloma. These include hyperviscosity, amyloid light chain amyloidosis, and peripheral neuropathy. Amyloid light chain amyloidosis is caused by the build-up of fibril aggregates of immunoglobulin light chain proteins, which then accumulate on organs (Bahlis & Lazarus, 2006). Peripheral neuropathy is also common and is thought to be caused by the effects of immunoglobulins on peripheral nerves (Rajkumar et al., 2014).

Mutiple myeloma is preceded by two stages, MGUS (typically non-IgM) and smouldering myeloma. Non IgM MGUS is classified as having a serum Ig

level less than 30g/L, and having less than 10% bone marrow infiltrate. Only 0.5-1% of MGUS cases progress to myeloma each year, and the underlying cause of progression is unknown (Rajkumar et al., 2014). Surprisingly, MGUS is relatively common, being present in 4% of the white population over the age of 50 (Landgren et al., 2009). Smouldering myeloma is an intermediate stage between MGUS and multiple myeloma, which has a 10% annual risk of progression to multiple myeloma within the first five years of diagnosis (Kyle et al., 2007). Smouldering myeloma is defined as having a serum immunoglobulin concentration of > 30g/L and bone marrow infiltrate of 10-60% (Rajkumar et al., 2014). Furthermore, multiple myeloma can develop from solitary plasmacytoma, which is classified as having a localised infiltration of plasma cells, without spreading to multiple sites. For plasmacytomas within the bone marrow, approximately 50% will ultimately develop into multiple myeloma (Hill et al., 2014). In the latest stages, multiple myeloma can develop into plasma cell leukaemia (Fernández de Larrea et al., 2012).

Chromosomal alterations are seen as one of the key initiating steps in multiple myeloma. The multiple rounds of DNA double-strand breaks and repair that B cells undergo in their immunoglobulin loci during their development towards plasma cells can often result in abnormal translocations. These are typically not propagated, as unfavourable rearrangements lead the cells into apoptosis. However occasionally, these rearrangements, especially those occurring during class switch recombination, can persist into plasma cells, and lead to myeloma (Bergsagel et al., 1996). Common genetic abnormalities include translocation of the *IgH* locus to *CCND1* (11q14) (Gabrea et al., 1999), *MMSET/FGFR3* (4p16) (Chesi et al., 1998b), *CCND3* (6p21) (Shaughnessy et al., 2001), *MAF* (16q23) (Chesi et al., 1998a), and *MAFB* (20q11) (Hanamura et al., 2001). Chromosomal trisomies are also common in myeloma, with trisomy 21 conferring a poor outcome for patients (Chretien et al., 2015). More likely to be secondary events, other common genetic abnormalities are the deletion of 17p13, harbouring the *TP53* gene, and the translocation of *IgH* to *MYC* (Avet-Loiseau et al., 2007). In terms of pathways, the most frequently mutated are RAS/MAPK with mutations in *KRAS*, *NRAS* and *BRAF*, and the NFκB pathway, with mutations/deletions of *TRAF3*, *CYLD* and *LTB*. Some of the most commonly mutated genes are *FAM46C, DIS3* and *FGFR3.* Furthermore, mutations in plasma cell genes *PRDM1* and *IRF4*, the MYC interaction partner *MAX*, and DNA repair pathway genes such as *RB1*, *TP53*, *ATM* and *ATR* can be present (Walker et al., 2015). A key question is in

understanding the drivers for progression from MGUS to myeloma. Interestingly, many of the initial genetic abnormalities mentioned above are already present in MGUS plasma cells, although at lower frequencies than in multiple myeloma (López-Corral et al., 2011).

Treatments for multiple myeloma include pharmacologic therapy and autologous stem cell transplantation. Eligibility for stem cell transplantation often determines the choice of pharmacologic therapy. Early on, corticosteroids such as dexamethasone were most frequently used (Alexanian et al., 1992). Today, the most effective treatment involves the use of dexamethasone in combination with bortezomib and lenalidomide (Durie et al., 2017). Lenalidomide is an immunomodulatory drug, which leads to apoptosis (Hideshima et al., 2000), decreased IL-6 and VEGF secretion (Gupta et al., 2001), and increased natural killer (NK) cell mediated cytotoxicity against myeloma cells (Davies et al., 2001). Recent data shows survival for patients under 65 years to be 7.7 years, and 3.4 years for older patients (Blimark et al., 2018), and survival rates are constantly improving (Fonseca et al., 2016). Despite this, there is still no cure for multiple myeloma. Predicting which MGUS cases will progress to myeloma is an interesting avenue for disease prevention. At present, the guidelines suggest that the frequency of clinical follow-up for MGUS should be based on the serum immunoglobulin levels (Kyle et al., 2010). However, a recent investigation found that MGUS patients with lower serum immunoglobulin levels have poorer myeloma survival (Sigurdardottir et al., 2015). Thus, the predictive value of current MGUS criteria is imperfect. Further investigation into the drivers of the MGUS to myeloma transition may yield better outcomes for patients in the future.

1.4 Immune evasion of DLBCL and multiple myeloma

A hallmark of cancer is the ability to evade killing by the immune system (Hanahan & Weinberg, 2011) and perturbations of transcriptional programs have recently been implicated in tumour immune evasion (Hugo et al., 2016). Modulating the immune system to target malignant B and plasma cells offers effective and promising new therapeutic avenues in DLBCL and multiple myeloma. For example, as mentioned above, lenalidomide increases the interactions between myeloma plasma cells and NK cells (Davies et al., 2001). Immune checkpoint blockade has also shown promise in multiple myeloma (Görgün et al., 2015) and is being investigated in DLBCL (Goodman et al., 2016). In light of this, investigating the mechanisms underlying immune evasion may provide further insights into the pathology of

Waldenström's macroglobulinemia and multiple myeloma.

A few main mechanisms exist for escape from immune surveillance. These include "hiding" from the immune system by reducing expression of surface molecules that can be recognised by and activate immune effector cells. Cancer cells can also increase expression of immune checkpoint ligands on the cell surface, and secrete inhibitory cytokines to dampen the response of immune effector cells and create an immunosuppressive microenvironment. Also, the cancer cells can suppress their own responses to cells of the immune system, through apoptosis resistance (de Charette & Houot, 2018).

The two main effector immune cell types are NK cells and $CD8^+$ T cells. NK cells are the innate killer cells of the immune system, with "ready-to-go" cytolytic activity. Their choice of activation or deactivation is dependant upon a balance of signals received by their surface receptors (Morvan & Lanier, 2015). NK cells bear several types of activating receptors and inhibitory receptors. One of the most important is the killer immunoglobulin-like receptor (KIR) class, some of which recognise the MHC class I molecules (HLA-A, HLA-B and HLA-C). MHC class I molecules are expressed on all nucleated cells and transmit a "self" signal, actively inhibiting killing by NK cells (Kärre et al., 1986; Ljunggren & Kärre, 1990). In some cancers, where MHC class I is lost, this loss of inhibition of the NK cell provides a strong signal for activation. Furthermore, expression of activating ligands can overcome inhibitory signals. For example, the stress ligand MICA, when expressed on target cells can stimulate NK cell cytolytic activity (Bauer et al., 1999).

T cells on the other hand, as part of the adaptive immune system, recognise antigen presented to them by MHC molecules. Antigen presented on MHC class I can stimulate $CD8^+$ T cells to carry out their cytotoxic activity against the cells. In this way, T cells and NK cells play a complementary role, whereby if cancer or infected cells lose their MHC class I to evade killing by $CD8^+$ T cells, they can instead induce killing by NK cells. However, T cells are also affected by activating and inhibitory ligands. For example, the activation of the co-stimulatory receptor 4-1BB (encoded by *TNFRSF9*) can enhance the T cell receptor response in cytotoxic T cells (Shuford et al., 1997). The PD-L1 ligand can be expressed on cancer cells, and interacts with the PD-1 receptor of $CD8^+$ T cells to inhibit their responses. Blockade of PD-L1 can restore tumour-antigen specific $CD8^+$ T cell cytotoxicity (Blank et al., 2006).

Two important factors to take into account when looking at B cell malignancies are that B cells are themselves professional antigen presenting cells (APCs), and that they are also related immune cells, so they respond to many of the same signals as NK cells and T cells. MHC class I is frequently lost on the surface of DLBCL cells along with the surface molecule CD58, which is necessary for NK cell stimulation (Challa-Malladi et al., 2011). While MHC class I is lost on early stage myeloma cells, it is highly expressed on late-stage myeloma cells to evade killing by NK cells (Carbone et al., 2005). As professional APCs, B cells naturally express MHC class II, however DLBCL cells can downregulate this in order to evade the immune system. Loss of histone acetylation at the class II transactivator (*CIITA*) locus leads to transcriptional inactivation and loss of MHC class II proteins (Hashwah et al., 2017). Loss of MHC class II correlates with decreased $CD8^+$ T cell infiltration at the sites of DLBCL tumours and poorer patient outcomes (Rimsza et al., 2004). Changes in surface ligand expression are frequent in myeloma, with altered expression of activating surface markers shifting to balance out altered MHC class I expression (Bernal et al., 2009). PD-L1 expression on multiple myeloma cells can induce T cell apoptosis and anergy (Tamura et al., 2012). Interestingly, inhibitory receptors are also expressed on lymphoma and myeloma cells, and their activation can inhibit the cancer cell growth. For example, the immune inhibitory checkpoint molecule CD85j is lost on myeloma cells, and its re-introduction leads to increased targeting by NK cells and cytotoxic T cells (Lozano et al., 2018). Additionally, engagement of inhibitory receptors on the surface of lymphoma cells can have a tumour-suppressive effect (Boice et al., 2016). In Waldenström's macroglobulinemia, secreted PD-1 ligands inhibit T cell function (Jalali et al., 2018), but other mechanisms of immune evasion have not been studied.

1.5 The cell cycle and DNA damage response

As mentioned above, some of the most common translocations in multiple myeloma involve the cell cycle regulator genes *CCND1* and *CCND3*, which are important for driving cell cycle progression (Gabrea et al., 1999; Shaughnessy et al., 2001). Additionally, cell cycle checkpoint and DNA repair pathway genes are frequently mutated in multiple myeloma (Walker et al., 2015). Multiple myeloma cells are also dependent on the cell cycle positive regulator E2F1, which binds to the majority of active promoters in the MM1.S cell line (Fulciniti et al., 2018). In DLBCL, there are frequent copy number alterations in the cell cycle inhibitor genes *CDKN2A*, *RB* and *TP53* (Monti et al., 2012). Furthermore, therapies targeting cell cycle regulators are currently

in clinical trials for both multiple myeloma and DLBCL (Otto & Sicinski, 2017). Thus, investigating perturbations of cell cycle regulators and transcriptional mechanisms underlying these perturbations may serve to increase our understanding of Waldenström's macroglobulinemia and multiple myeloma disease biology.

The cell cycle is an ordered series of events including cell growth, which lead to cell division. There are four main cell cycle phases: G1, where the cells expand and prepare for division; S, where the cells replicate their DNA; G2, where the cells ensure accurate replication has taken place and prepare for cell division; and M, where the cells undergo mitosis and separate into two daughter cells. Each of these phases are controlled by progression mediators and cell-cycle inhibitory checkpoints. Beginning in G1, the cyclin-dependant kinases (CDKs) CDK4 and CDK2 phosphorylate the cell cycle inhibitor Rb, to prevent it binding to the E2F1 transcription factor (Harbour et al., 1999; Kato et al., 1993; Tsutsui et al., 1999; van den Heuvel & Harlow, 1993). E2F1 transcriptionally activates a wave of gene expression to drive the cells into S phase (Johnson et al., 1993; Takahashi et al., 2000). Before the cells can commit to enter S phase, they must first ensure that they have a sufficient nutrient supply and size, as well as that they are not carrying DNA lesions. The G1/S checkpoint can stall the cell cycle in G1 to allow the cells time to correct any of these problems. The transcription factor p53 is the main regulator of this checkpoint, and functions to activate the CDK inhibitor p21 (encoded by CDKN1A) (el-Deiry et al., 1993). In G2, the CDC2 kinase (encoded by CDK1) drives progression to mitosis via a multitude of phosphorylation events. CDC2 requires the activity of the CDC25 phosphatase to initiate mitosis (Izumi & Maller, 1993; Kumagai & Dunphy, 1991). However, the cells at this point again require scrutiny to ensure the absence of DNA damage following replication, as well as size and nutrient requirements. The G2/M checkpoint is largely regulated by the kinase CHK1, which targets the CDC25 phosphatase for inhibition (Furnari et al., 1997). However, p53 can also inhibit progression to mitosis (Agarwal et al., 1995; St Clair et al., 2004). Once mitosis is underway, another checkpoint, the mitotic spindle assembly checkpoint is necessary to ensure correct attachment of kinetochores to the spindle microtubules before cell division. The mitotic checkpoint complex comprising MAD2, BUBR1, BUB3 and CDC20 blocks activation of the anaphase promoting complex, and thereby prevents cell cycle progression (Lara-Gonzalez et al., 2012).

A large number of DNA lesions occur during each cell cycle, and also frequently in non-cycling cells. This can be due to mistakes in DNA

replication, faulty actions of topoisomerases, and environmental factors such as radiation or reactive oxygen species (Lieber & Karanjawala, 2004). The main pathways of DNA repair for DSBs are non-homologous end joining (NHEJ) and homologous recombination. Homologous recombination relies on the presence of a homologous region in the sister chromatid, and so can only take place during the S or G2 phases (San Filippo et al., 2008). Whereas NHEJ can occur at any phase of the cell cycle and while inaccurate, is the main choice for DSB repair (Lieber, 2008). For other forms of DNA damage, there are multiple repair pathways, which are activated depending of the kind of damage. These include base excision repair, nucleotide excision repair, mismatch repair, and interstrand crosslink repair amongst others (Ciccia & Elledge, 2010).

Understanding the regulation of cell cycle progression and inhibition, and DNA repair genes may be key to uncovering novel treatments in multiple myeloma and Waldenström's macroglobulinemia.

1.6 Transcriptional regulation

Transcriptional regulation is an essential mechanism underlying development, differentiation, and disease states. The development of B cells and plasma cells is driven by the integration of external signals through transcriptional mechanisms. Perturbations in transcriptional regulation are also strong drivers in multiple myeloma and Waldenström's macroglobulinemia. Understanding the mechanisms of transcriptional regulation in multiple myeloma and Waldenström's macroglobulinemia may help us to uncover novel factors in the pathogenesis and maintenance of these diseases.

1.6.1 Fundamentals of transcription initiation

Transcription is the mechanism by which DNA is transcribed to RNA, which can then have its own function or be translated into proteins. In eukaryotes, transcription is performed by at least three enzymes termed RNA polymerases (RNA pol) (Roeder & Rutter, 1969, 1970). RNA pol I is mainly responsible for transcribing ribosomal RNA (rRNA), while RNA pol III mainly transcribes transfer RNA (tRNA), 5S rRNA and pri-miRNAs. RNA pol II on the other hand, is responsible for transcribing protein coding genes, enhancer RNAs (eRNAs), long non-coding (lnc)RNAs and pri-miRNAs, amongst others (Vannini & Cramer, 2012). While RNA pol I and III have similar structures, RNA pol II contains an additional C-terminal domain which is affected by

post-translational modifications to influence capping and slicing of transcripts, among other functions (Hsin & Manley, 2012).

The identification of a method for in vitro transcription by RNA polymerase II (RNA pol II) (Anthony Weil et al., 1979) led to the discovery of general transcription factors (GTFs) that are important for eukaryotic RNA pol II transcription, TFIIA , -B, -D, -E, -F and -H (Matsui et al., 1980). While all the GTFs contribute to transcription initiation, only TFIIB and the TBP subunit of TFIID are strictly required (Luse, 2013). However, recent evidence contradicts this, and suggests that all GTFs are indeed required for RNA pol II transcription except the TAF subunits of TFIID (Petrenko et al., 2019). Although, this has so far only been demonstrated in a single study in yeast. Transcription of genes by RNA pol II requires the presence of a promoter sequence (Corden et al., 1980). Promoters are genetic elements that are present directly upstream of the transcription start site and have the ability to recruit the transcriptional machinery. There are a few core promoter sequences common to a large proportion of promoters, including the TATA box (Breathnach & Chambon, 1981), the initiator element (Smale & Baltimore, 1989), and the downstream promoter element (Burke & Kadonaga, 1997) to name a few, however many promoters also function in the absence of known core promoter elements (Roy & Singer, 2015). Indeed, many factors including the presence of sequence-specific transcription factor binding motifs and DNA accessibility also influence the initiation of transcription from promoters. Furthermore, the orientation and spacing of promoter elements can dictate their specificity and function (Näär et al., 1991). Promoter elements typically serve as binding sites for the TFIID transcription factor complex (Parker & Topol, 1984; Sawadogo & Roeder, 1985), which contains the TBP and TAF proteins (Burley & Roeder, 1996). The formation of the pre-initiation complex (PIC) begins with binding of TFIID, then TFIIA to the core promoter sequence, followed by TFIIB to stabilise the complex. RNA pol II together with TFIIF is then recruited followed by TFIIE and TFIIH (Buratowski et al., 1989; He et al., 2013). However, other protein complexes can also function in transcription initiation, including SAGA (Baptista et al., 2017). Members of the TFIID complex can carry out various enzymatic activities including that of a histone acetyltransferase (Mizzen et al., 1996), a bromodomain (Jacobson et al., 2000), a PHD finger capable of recognising histone methylation (van Ingen et al., 2008), and a ubiquitin conjugater (Pham & Sauer, 2000). Whereas, TFIIH has subunits with helicase and kinase activity (Schaeffer et al., 1993; Tirode et al., 1999). Through these mechanisms, the PIC affects chromatin structure and

promoter accessibility. After recruitment of the PIC to the core promoter elements, RNA pol II transcribes 20-30 nucleotides of RNA (Rasmussen & Lis, 1993) and then is paused by the negative elongation factor (NELF) and DSIB (Yamaguchi et al., 1999). This pause is lifted by the P-TEFb complex, which phosphorylates RNA pol II (Yamaguchi et al., 1999), NELF (Fujinaga et al., 2004) and DSIB (Kim & Sharp, 2001), initiating transcriptional elongation. RNA pol II pausing allows for priming of promoters so that transcription can be initiated rapidly upon receiving the right signal, rather than waiting for the PIC to be assembled.

1.6.2 Histone modifications and transcriptional regulation

One of the key mechanisms of transcriptional regulation is modification to the chromatin without changes to the DNA sequence itself. DNA is wrapped around nucleosomes in units of 146 base pairs (bp) in a superhelix structure (Luger et al., 1997). The nucleosome comprises two sets of the four core histones H2A, H2B, H3 and H4 (Kornberg, 1974; Thomas & Kornberg, 1975a, 1975b). The histones bear N-terminal tails, short amino acid chains, which can be modified post-translationally. Histone modifications can influence the structure and binding affinities of histones (Tessarz & Kouzarides, 2014), as well as affecting the accessibility of DNA to the transcriptional machinery (Zentner & Henikoff, 2013).

Chromatin accessibility plays a crucial role in transcriptional regulation. In addition to core promoter sequences and transcription factors, the position of nucleosomes can influence the recruitment and positioning of the PIC and RNA pol II (Rhee & Pugh, 2012). During cellular differentiation, where cells can be pushed towards an entirely different lineage and large transcriptional changes are taking place, there are enormous changes to the positioning of nucleosomes, with active promoters having nucleosome-depleted regions, and inactive promoters often being present in nucleosome-dense regions (Teif et al., 2012).

The most well studied histone modifications include methylation and acetylation on lysine or arginine residues, however in addition, serines and threonines can be phosphorylated, and lysines ubiquitinated and SUMOylated to name a few (Peterson & Laniel, 2004). Histone lysine acetylation was described early on as a mechanism for increasing DNA accessibility, and therefore transcriptional activation (Lee et al., 1993; Shogren-Knaak et al., 2006). Histone acetylation increases DNA accessibility by neutralising the positive charge of histone lysine residues, and weakening the histone-DNA interactions (Hong et al., 1993; Zentner & Henikoff, 2013).

As DNA is negatively charged and histone lysine residues are positively charged they will attract one another. Thus, neutralising the positive charge of the histone lysine residue by acetylation will weaken this interaction. Depending on the residue, histone methylation can mark either repressed or active chromosomal regions. Histone 3 lysine 4 tri-methylation (H3K4me3) is common at active promoters, and yet the inhibition of enzymes that deposit this mark leads to only minor changes in transcription in both mammalian cells (Clouaire et al., 2012) and yeast (Lenstra et al., 2011). This suggests that transcriptional activation is not a direct effect of H3K4me3. Instead, H3K4me3 may promote activation by preventing the spread of repressive histone methylation such as histone 3 lysine 27 tri-methylation (H3K27me3) (Schmitges et al., 2011). Similarly, H3K27me3 can prevent deposition of the activating H3K27 acetylation (H3K27Ac) (Ferrari et al., 2014).

Histone marks are recognised by a variety of factors, known as “readers”. For example, bromodomain and PHD proteins recognise histone acetylation (Dhalluin et al., 1999; Zeng et al., 2010). Whereas, histone methylation is recognised by several factors including PHD, chromodomain proteins, WD40, Tudor and more (Yun et al., 2011). The presence of repressive histone marks such as H3K9me3 may help to stabilise histones on DNA by recruitment of recognition factors (Zentner & Henikoff, 2013). For example, in yeast, the Swi6 protein recognises and binds to the H3K9me3 mark, and influences the positioning of nucleosomes to assemble heterochromatin (Canzio et al., 2011). The H3K36me3 mark, which is typically present on the gene bodies of actively transcribed genes also plays a stabilising role in preventing histone exchange and the incorporation of acetylated histones over coding regions of actively transcribed genes in order to maintain the accuracy of RNA pol II (Venkatesh et al., 2012).

1.6.3 Transcription factors

A fundamental of cell biology is in the question of what drives the activation of a particular gene or set of genes to determine cellular states. Integrating transcription initiation with chromatin states, genome architecture, and extrinsic signals are the class of proteins known as transcription factors. They are frequently seen as “master regulators” of cell states and transitions through their ability to cause a complete cellular reprogramming, even being able to induce pluripotent stem cells from adult cells (Takahashi & Yamanaka, 2006). Moreover, a large analysis of cancer-related proteins found transcription factors to be one of the most highly overrepresented protein classes, highlighting their importance in various cancers (Furney et

al., 2006). Transcription factors are proteins that either bind directly to DNA through sequence specific recognition (Lambert et al., 2018; Vaquerizas et al., 2009), with the specific sequence they recognise referred to as a motif, or indirectly, via protein-protein interactions.

Just as histone modifications serve as a major marker of transcriptional cell states, transcription factors function as the major regulators. Recent evidence shows a two-way relationship between transcription factors and histone modifications. Transcription factors are one of the main mechanisms for recruiting histone modifiers to specific sites in the genome (Demers et al., 2007; Kurland & Tansey, 2008; Lambert et al., 2018; Sripathy et al., 2006), and transcription factor binding profiles are highly predictive of histone modifications (Benveniste et al., 2014). Interestingly, the landscape of histone modifications can also influence the binding of specific families of transcription factors, possibly through maintenance of chromatin structure and DNA accessibility (Xin & Rohs, 2018).

Remarkably, some transcription factors can bind to sites containing their motifs even in nucleosome-dense regions, and actually function cooperatively to cause changes in nucleosome positioning (Mirny, 2010; Polach & Widom, 1996). Factors that can bind to inaccessible and nucleosomal DNA and open it up are known as pioneer factors (Iwafuchi-Doi & Zaret, 2014). This can occur through interactions with ATP-dependent chromatin remodellers (Rippe et al., 2007; Wang et al., 2014) or independently (Cirillo et al., 2002). They can recognise their motifs within nucleosome-bound chromatin and also bind directly to nucleosomes, opening the nucleosomal DNA for other transcription factors to bind and transcription initiation to take place (Cirillo et al., 2002; Soufi et al., 2015).

In concert with their role of directly binding to DNA, transcription factors can also function as multi-domain proteins with enzymatic activity, but mostly function through their recruitment of co-factors. Common interactions include those of transcription factors with RNA pol II and PIC members, recruiting them to promoter regions (Cujec et al., 1997; Gill et al., 1994; Horikoshi et al., 1988). Transcription factors can also relieve RNA pol II pausing, for example, the transcription factors MYC and NFκB recruit P-TEFb to achieve this (Barboric et al., 2001; Nowak et al., 2008; Rahl et al., 2010). As mentioned above, transcription factors can also recruit chromatin remodelling complexes to open or close chromatin for transcriptional activation or silencing (Cosma et al., 1999; Schultz et al., 2001). Interestingly, the motif sequence and chromatin state surrounding binding sites can influence the activity of the

transcription factor, changing the protein structure and determining its co-factors for activating or repressive activity (Ernst et al., 2016; Hall et al., 2002; Leung et al., 2004; Meijsing et al., 2009).

One of the most important roles transcription factors play to influence transcription is in the commissioning and recruitment of enhancers to promoter regions (Spitz & Furlong, 2012).

1.6.4 Transcriptional enhancers

Transcriptional enhancers are regulatory units of the genome that function *in cis* to interact with promoter regions and induce transcriptional activity from any position, even very distal, upstream or downstream of transcription start sites (Banerji et al., 1981). Enhancers are hubs for binding of transcription factors, enriched for multiple transcription factor motifs, and typically require this binding to become activated (Long et al., 2016). Although for certain genes, contact with an enhancer, even in the absence of normally essential transcription factors is sufficient to initiate transcription (Deng et al., 2012). To delineate enhancers from promoters, assays can be used to show that the putative enhancer can influence promoter-driven gene transcription, but is insufficient to drive gene transcription in the absence of a promoter (Heintzman et al., 2007). However, recent evidence shows that some enhancers can also act as weak promoters, and some promoters can act as strong enhancers. It has been suggested that a somewhat unique feature of enhancers is that their directionality has little effect on their function, whereas changing the orientation and position of a promoter often disrupts its function (Mikhaylichenko et al., 2018; Näär et al., 1991). Similar to promoters, enhancers can be in a closed conformation, blocked by inaccessible chromatin or nucleosomes, or can be accessible. Using recruitment of co-factors such as histone modifiers, chromatin remodellers and the basal transcriptional machinery, transcription factors can cause changes in chromatin architecture to influence enhancer accessibility (Spitz & Furlong, 2012). Most importantly, tethering of enhancers to promoters is orchestrated by sequence-specific transcription factors that determine the specificity of enhancer-promoter interactions (van Arensbergen et al., 2014; Zabidi et al., 2014).

Interestingly, the presence of transcription factors on enhancer and promoter regions is often not indicative of active transcription or enhancer activity from these sites (Whitfield et al., 2012). Moreover, the chromatin state indicated by the presence of histone modifications and DNA accessibility is also indicative of only a small proportion of transcriptionally active enhancer

elements (Kwasnieski et al., 2014). Instead, the combinatorial action of specific sets of transcription factors on enhancers is predictive of their activity (Grossman et al., 2017). Transcription factors can also link enhancers to promoters through interactions with PIC members (Koch et al., 2011), as well as other factors such as the protein complex Mediator. Mediator binds to enhancer regions in complex with the ring-shaped protein cohesin, which physically connects enhancers to promoter regions (Kagey et al., 2010).

Differential activation of enhancers allows for precise developmental-state and/or tissue-specific gene expression, and provides an expansive repertoire of gene expression control (Banerji et al., 1983; Bonn et al., 2012; Gillies et al., 1983; Heintzman et al., 2009). Enhancers not classified as inactive can be either active or poised for activity. Active enhancers induce transcription from matched promoter regions, whereas poised enhancers display the open chromatin and transcription factor occupancy of active enhancers without the induction of transcription (Creyghton et al., 2010). Additionally, active and poised enhancers bear specific histone marks, which are commonly used to identify them. The presence of H3K4me1 and the absence of H3K4me3 marks for active and poised enhancers, whereas promoters are marked by high H3K4me3 and sometimes also by H3K4me1 (Heintzman et al., 2009; Heintzman et al., 2007). Active enhancers are marked by H3K27Ac (Creyghton et al., 2010), whereas poised or inactive enhancers are marked by H3K27me3 (Rada-Iglesias et al., 2010). In comparison, inactive enhancers are often hidden in closed and nucleosome-dense chromatin regions without the presence of enhancer-identifying histone marks. They require the binding of transcription factors and significant chromatin reorganisation to become poised or active. During cellular reprogramming from fibroblasts to induced pluripotent stem cells, enhancers are reset, with H3K4me1 marks redistributed to match the profile of embryonic stem cells (Creyghton et al., 2010). All enhancers are enriched for transcription factor binding motifs, but they may be differentially commissioned in different cell types and during transitions. For example, the histone lysine demethylase LSD1 interacts with the chromatin remodelling NuRD complex and removes H3K4me1 to decommission active enhancers during embryonic stem cell differentiation (Whyte et al., 2012). It is unclear whether H3K4me1 simply acts as a substrate for LSD1 to recruit the NuRD complex and cause changes in the chromatin structure, or if the removal of this mark has functional consequences itself. Active enhancers are hypersensitive to DNase I digestion (Xi et al., 2007) and have bi-directionally transcribed enhancer RNA (eRNA) (Kim et al., 2010), which facilitates the release of

NELF to relieve RNA pol II pausing (Schaukowitch et al., 2014). eRNAs can also contribute to DNA looping of enhancers and promoters by binding to Mediator (Hsieh et al., 2014; Lai et al., 2013), however this likely not the case at all loci (Schaukowitch et al., 2014).

The underlying mechanism by which enhancers influence transcriptional activation is not yet known. Proposed mechanisms include a tracking and transcription method, whereby the enhancer bound to RNA pol II and TBP slides across DNA transcribing short RNAs until it reaches its target promoter to deliver RNA pol II to the transcription start site (TSS) (Zhu et al., 2007). Another proposed model is that enhancers form “transcription factories” that recruit high levels of transcriptional activators and the basal transcriptional machinery to drive transcription from genes that are brought into close spatial proximity of the factories through chromatin architecture changes (Kolovos et al., 2012).

Taken together, transcription factors orchestrate the transcriptional circuitry of the cell, causing and maintaining changes in chromatin architecture and accessibility, recruiting and regulating the basal transcriptional machinery, and activating or decommissioning enhancers to drive and maintain cell states.

1.7 Transcriptional regulation of B cell development

Commitment to the B cell lineage requires the presence of specific transcription factors. Common lymphoid progenitors (CLPs) can give rise to B cells, T cells and NK cells (Kondo et al., 1997). The transcription factors E2a and Ebf are necessary for the development of mouse pro- and pre-B cells from CLPs (Lin & Grosschedl, 1995; Zhuang et al., 1994). However in the mouse, the cells cannot move past the pro-B cell stage without the induction of the Pax5 transcription factor, but instead move along the trajectory of other haematopoietic lineages (Nutt et al., 1999). Deletion of Pax5 in mature mouse B cells leads to de-differentiation into progenitors, which are able to differentiate into functional T cells (Cobaleda et al., 2007). Thus, Pax5 is the key determinant of the B cell lineage. Pax5 functions through direct binding to DNA in mouse B cells, but only a small proportion of Pax5 binding sites correlate with direct transcriptional activation (Revilla-I-Domingo et al., 2012). Instead, the major function of Pax5 in mouse B cells is in orchestrating global changes in genome architecture by binding to and directing anchor regions to form new DNA structures, independent of transcription (Johanson et al., 2018). This is likely to occur via interactions with chromatin remodellers. For

example, Pax5 interacts with the chromatin architecture regulator CTCF in mouse pro-B cells (Medvedovic et al., 2013).

Pax5 is also active later in B cell maturation, activating many of the transcription factors necessary for the maturation process. In mouse B cells these include Irf4, Irf8, Bach2, and Spib (Schebesta et al., 2007). The transcription factors Irf4 and Irf8 direct the differentiation towards immature B cells from pre-B cells in mice (Lu et al., 2003). During antigen stimulation of mouse B cells, Pax5 is necessary for the transcription of essential members of the BCR signaling pathway (Schebesta et al., 2007). Without Pax5, BCR signaling does not take place. Furthermore, PAX5 inhibits expression of plasma cell transcription factors BLIMP1 and XBP1, and inhibits plasma cell differentiation in chicken (Nera et al., 2006), mouse (Delogu et al., 2006), and human B cells (Reimold et al., 1996). Low levels of Irf4, activated downstream of Pax5 are necessary for transcriptional activation of Bcl6 and Aid induction of SHM and CSR in mouse B cells (Ochiai et al., 2013; Sciammas et al., 2006). So too is the transcriptional repressor Bach2 (Muto et al., 2004). Meanwhile Spib is necessary for germinal center maintenance in mice (Su et al., 1997).

Bcl6 is one of the major regulators of the germinal center reaction, without which germinal centers are not formed in mice (Fukuda et al., 1997; Ye et al., 1997). It is a zinc finger transcriptional repressor that functions through the recruitment of co-factors such as histone deacetylases (HDACs) and co-repressors (Dhordain et al., 1997; Fujita et al., 2004; Lemercier et al., 2002; Mendez et al., 2008; Wong & Privalsky, 1998; Zhang et al., 2001). BCL6 represses expression of cell cycle inhibitors such as p27kip1, p21, and p53 (Phan & Dalla-Favera, 2004; Phan et al., 2005; Shaffer et al., 2000), as well as DNA damage sensors ATR and CHEK1 in human B cells (Ranuncolo, S. M. et al., 2007; Ranuncolo, S. M. et al., 2008), and Blimp1 in mouse germinal center B cells (Tunyaplin et al., 2004). BCL6 also indirectly induces transcription of the *MYC* gene, most likely through repression of *PRDM1* in human cell lines (Shaffer et al., 2000).

The dramatic changes that take place during B cell activation are underpinned by a vast array of changes to the cells' transcriptome and genomic architecture. Early on it was observed that the addition of antigen to naïve B cells led to large increases in transcriptional activity (Pogo et al., 1966), and the levels of RNA pol (Jaehning et al., 1975). Indeed, the quantity of mRNA in the cell increases by approximately 10-fold in the 24 h following antigen stimulation of mouse naïve B cells. This increase comprises the

entire mouse naïve B cell transcriptome, with non-specific transcriptional amplification (Kouzine et al., 2013). The vast majority of these genes are already occupied by RNA pol II in mouse naïve B cells, and their activation is dependent upon increased promoter accessibility mediated by Tfiih, which has dramatically increased expression following B cell activation (Kouzine et al., 2013). Additionally, the transcription factor Myc is essential to this process. Myc is rapidly induced by antigen stimulation of mouse naïve B cells (Kelly et al., 1983), and Myc activates the amplification of the transcriptome non-specifically during B cell activation, and in embryonic stem cells of mice (Nie et al., 2012). The transcriptional amplification is associated with increases in active histone marks and decreases in repressive marks. Chromatin decompaction occurs on a global scale, and Myc promotes an almost 2-fold increase in chromatin looping, changing the global chromatin architecture of the mouse B cell genome (Kieffer-Kwon et al., 2017). Thus, naïve B cells are primed for activation by RNA pol II on gene promoters, and upon receiving signals following antigenic stimulation, produce dramatic changes in chromatin architecture and transcriptional output. Taken together, the pathway of differentiation from common lymphoid progenitors to activated B cells relies on carefully orchestrated transcription factor networks and extensive reorganisation of chromatin architecture, with Pax5 driving activation of the key factors. A summary of important transcription factors driving B and plasma cell fates is depicted in Figure 2.

1.8 BLIMP1 and transcriptional regulation of plasma cell development

BLIMP1, encoded by the *PRDM1* gene is activated by a number of mechanisms. Firstly, BLIMP1 is activated downstream of pattern recognition receptors such as TLRs which signal through the adaptor molecule MYD88 and downstream effector NFκB in mice (Genestier et al., 2007; Lin et al., 2006; Morgan et al., 2009; Pasare & Medzhitov, 2005) and in human cells (Capolunghi et al., 2008; Douagi et al., 2009). Secondly, BLIMP1 is activated by interleukins IL-2, IL-5, IL-10 and IL-21 as shown in mice (Ozaki et al., 2004; Turner et al., 1994) and human cells (Choe & Choi, 1998; Ding et al., 2013; Le Gallou et al., 2012; Messika, Eric J. et al., 1998). These can work in concert with CD40 and BCR signalling. However, in the absence of IL-2 and IL-5, and in the presence of IL-4, Blimp1 is instead repressed to allow for CSR to take place in mouse B cells (Knödel et al., 2001). STAT3 is activated downstream of IL-2, IL-10 and IL-21 and transcriptionally activates BLIMP1 in human B cells (Diehl et al., 2008). Also, the transcription factor Irf4 activates

Blimp1 expression in the mouse (Sciammas et al., 2006), and binds in cooperation with Stat3 to the *Prdm1* gene (Kwon et al., 2009). Furthermore, the AP-1 transcription factor also transcriptionally activates BLIMP1 in human B cells (Vasanwala et al., 2002). AP-1 is a protein complex comprising several families of factors including Jun, Fos, ATF and Maf, with diverse roles including proliferation, transformation and cell death (Shaulian, 2010). At the B cell to plasma cell transition in mice, the *Prdm1* locus undergoes extensive chromatin reorganisation, with a dramatic increase in the number of interactions between this locus and surrounding regions (Johanson et al., 2018). This is likely to represent increased activation of enhancers and *Prdm1* transcription. Essentially, the mechanisms that activate BLIMP1 tie in with initiation of the B cell to plasma cell switch. However, recent evidence demonstrates that Blimp1 is also expressed early in B cell development to prevent the production of auto-reactive immunoglobulins in mice. This is driven by the PI3K pathway (Setz et al., 2018).

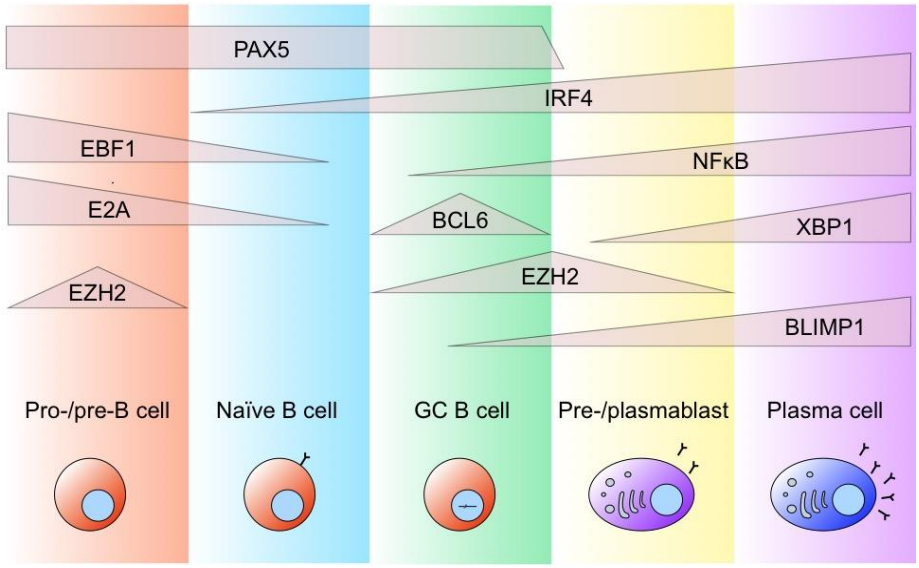

Figure 2: Key transcription factors driving B cell and plasma cell differentiation

During early B cell development, the B cell identity factor PAX5 is activated along with EBF1, E2A and EZH2. The expression of IRF4 slowly increases from low levels in naïve B cells to high levels in plasma cells. BCL6 is expressed during the germinal centre reaction along with EZH2, which is also expressed in the pre-plasmablast and plasmablast stages. NFκB has increasing expression during plasma cell differentiation, along with BLIMP1 and XBP1.

BLIMP1 is a zinc-finger transcription factor with a proline rich region and a PR/SET domain, with very high similarity between mouse and human (Huang, 1994; Keller, A D & Maniatis, T, 1991; Tunyaplin et al., 2000). The PR/SET domain of BLIMP1 is highly conserved and has similarity to other PR/SET domain proteins (Buyse et al., 1995; Tunyaplin et al., 2000). However, while most PR/SET domain proteins use this domain to catalyse lysine methylation (Dillon et al., 2005), BLIMP1 does not have methyltransferase activity. It binds to chromatin through recognition of a sequence-specific DNA motif (A/C)AG(T/C)GAAAG(T/C)(G/T) (Keller, A. D. & Maniatis, T., 1991; Kuo & Calame, 2004). While only two of the five zinc fingers are required for binding to chromatin (Keller & Maniatis, 1992), both the zinc fingers and proline rich region are required for transcriptional repression. The proline rich region is necessary for interactions with co-repressors (Ren et al., 1999; Yu et al., 2000). Without intrinsic enzymatic activity, BLIMP1 carries out its functions by recruiting co-factors to chromatin. These include co-repressor Groucho family proteins (Ren et al., 1999),

histone lysine methyltransferase G9a (Győry et al., 2004), arginine methyltransferase PRMT5 (Ancelin et al., 2006), histone lysine demethylases LSD1 (Su et al., 2009), and histone deacetylases HDAC1 and HDAC2 (Yu et al., 2000). More recently, the histone lysine methyltransferase Ezh2 was also shown to be a Blimp1 interaction partner in mouse plasmablasts (Minnich et al., 2016). Beyond histone modifiers, proteins that influence chromatin structure also interact with BLIMP1. The chromatin remodeller Aiolos interacts with BLIMP1 in multiple myeloma cells (Hung et al., 2016), and Blimp1 also interacts with several chromatin remodelling complexes including BAF, NuRD, NCoR, and SIN3 in mouse plasmablasts (Minnich et al., 2016). This raises an interesting possibility that BLIMP1 may be participating in large-scale chromatin architecture changes along the lines of PAX5 or MYC.

BLIMP1 primarily functions as a transcriptional repressor, although it has also been demonstrated to work as an activator (Minnich et al., 2016). Key B cell identity genes including *BCL6*, *MYC*, *ID3*, *PAX5* and *CIITA* are repressed by BLIMP1 in human cells (Lin et al., 2002; Piskurich et al., 2000; Shaffer et al., 2002). In addition, Blimp1 inhibits CSR by directly repressing *Aicda* (encoding AID) in mouse plasmablasts (Minnich et al., 2016). Meanwhile, important plasma cell functions are activated by Blimp1. These include the unfolded protein response, with the transcription factors Xbp1 and Atf6 activated by Blimp1 in mouse plasma cells (Shaffer et al., 2004; Tellier et al., 2016). XBP1 is activated downstream of ATF6 to initiate the unfolded protein response and increase protein synthesis (Shaffer et al., 2004; Yoshida et al., 2001). Blimp1 also stimulates antibody secretion, by activating immunoglobulin transcripts and *Ell2* in mouse plasma cells (Minnich et al., 2016). Blimp1 is activated early during the B cell to plasma cell differentiation process in mice, and the levels of Blimp1 expression increase as it progresses (Kallies et al., 2004). Whether BLIMP1 is required for the maintenance of long-lived bone marrow plasma cells is controversial. One study found that the inactivation of Blimp1 leads to a loss of both newly- and previously-formed plasma cells in mice (Shapiro-Shelef et al., 2005). In a contradictory result, another study found that inactivation of Blimp1 in mature mouse bone marrow plasma cells leads to a loss of antibody secreting ability but these plasma cells are able to survive (Tellier et al., 2016). Another reported function of BLIMP1 is in repressing cell cycle progression in order to promote differentiation of mature non-dividing plasma cells. This occurs through transcriptional repression of positive cell cycle regulator genes *CDK1*, *CDK2*, *PLK1* and *E2F1*, as well as DNA replication/repair genes

PCNA, *XRCC6*, *XRCC5* and *MCM2* in human plasma cells (Shaffer et al., 2002).

The question of BLIMP1's role in the development of antibody-secreting cells is complicated. Early on it was shown that high levels of antibody secretion cannot take place in the absence of BLIMP1 (Savitsky & Calame, 2006; Shapiro-Shelef et al., 2003). However, when mouse activated B cells begin the differentiation process towards plasma cells, *Pax5* is one of the first B cell genes to be silenced. It has been proposed that the reduction of Pax5 is the defining feature of antibody secreting cells, as the repression of Pax5 expression can occur in the absence of Blimp1. These B cells are then able to form pre-plasmablasts secreting low levels of antibody in the absence of Blimp1. However, fully differentiated plasma cells require Blimp1 (Kallies et al., 2007). Irf4 expression is also necessary for plasma cell formation in mice (Klein et al., 2006). The dose of Irf4 determines its function, whereby lower levels drive earlier B cell differentiation and activation of *Bcl6*, and higher levels drive plasma cell differentiation and *Bcl6* repression in mice (Ochiai et al., 2013; Sciammas et al., 2006) and *BCL6* repression in humans (Saito et al., 2007). IRF4 interacts with various factors including PU.1 (Brass et al., 1996; Perkel & Atchison, 1998) and STAT6 (Gupta et al., 1999) in human B cells, and the AP-1 complex in mouse T cells (Li et al., 2012). Another transcription factor Oct2 (encoded by *Pou2f2*) contributes to plasma cell differentiation via regulation of the IL-5 receptor in mouse activated B cells (Emslie et al., 2008). Finally, in a similar situation to what occurs during differentiation into mature B cells and during B cell activation, large changes to chromatin accessibility also take place during mouse plasma cell differentiation (Scharer et al., 2018).

Plasma cell differentiation is a tightly controlled process, regulated not only by activation of BLIMP1, but also by repression. Expression of Blimp1 at the wrong point in time can inhibit the germinal centre response, and lead to premature terminal differentiation and apoptosis or auto-antibody production (Bönelt et al., 2018; Lin et al., 1997; Messika, E. J. et al., 1998; Setz et al., 2018). Bcl6 is a major repressor of Blimp1, which directly binds to and represses the *Prdm1* gene in the mouse (Tunyaplin et al., 2004) as well as repressing AP-1 function (Vasanwala et al., 2002). Additionally, the transcription factor PAX5 also binds to and represses transcription of the human *PRDM1* gene, while Bach2 directly represses mouse *Prdm1* (Mora-López et al., 2007; Ochiai et al., 2006). In addition to transcriptional regulation, BLIMP1 is also regulated at a post-transcriptional level. The RNA-binding protein Zfp36l1 binds to the *Prdm1* transcript and promotes its

degradation to prevent plasma cell differentiation in mouse B cells (Nasir et al., 2012). On the protein level, Blimp1 is marked by removable SUMO-1. When SUMO-1 is removed by Senp1, it prevents the proteasomal degradation of Blimp1 in mouse plasmacytoma cells (Shimshon et al., 2011). However another study found that SUMOylation of BLIMP1 by PIAS1 was necessary for its interaction with HDAC2 and transcriptional repression during human plasma cell differentiation (Ying et al., 2012). During *C. elegans* development, the $SCF^{DRE-1/FBXO11}$ complex leads to ubiquitination and degradation of the BLMP-1 protein (Horn et al., 2014). Additionally, Hrd1 binds to Blimp1 and catalyses its ubiquitination to enhance MHC class II expression in mouse dendritic cells (Yang et al., 2014). A more recent study found that not only SUMO1-SENP1, but also SUMO2/3-SENP6 regulated degradation of BLIMP1 in human cell lines. They also found that BLIMP1 degradation was regulation by both SUMOylation-dependent and -independent ubiquitination (Wang et al., 2017). Thus, many factors ensure precise timing and control for the presence of BLIMP1 on a transcriptional, post-transcriptional and post-translational level. Taken together, BLIMP1 is the key player in a carefully regulated and precisely timed process, which orchestrates the differentiation from an activated B cell to a mature plasma cell.

1.9 EZH2

The polycomb group (PcG) of proteins comprise different protein complexes known for maintenance of cell identity (Aranda et al., 2015). Here, we focus on the PcG protein EZH2, which catalyses methylation of H3K27 as a subunit of the polycomb repressive complex 2 (PRC2) (Cao et al., 2002). EZH2 has highest specificity for the deposition of H3K27me2 and me3, although knock-out of EZH2 is also associated with a decrease in H3K27me1 (Shen et al., 2008). In the PRC2 complex, EZH2 works with the key proteins, SUZ12 and EED, which are necessary for the methyltransferase activity (Cao & Zhang, 2004; Montgomery et al., 2005; Pasini et al., 2004). EED functions through recognition of H3K27 methylation (Xu et al., 2010), and together with SUZ12 maintains the integrity of the PRC2 complex (Cao & Zhang, 2004; Pasini et al., 2004). Knock-out of either SUZ12 or EED leads to loss of EZH2 (Montgomery et al., 2005; Pasini et al., 2004). Other PRC2 subunits include RbAp48 and AEBP2 (Cao et al., 2002; Cao & Zhang, 2004). RbAp48 recognises the histone H3 N-terminus when H3K4me3 and H3K36me2/3 are not present (Schmitges et al., 2011). AEBP2 modulates the structure of PRC2 to facilitate RbAp48 activity (Kasinath et al., 2018). EZH2 mediated

deposition of H3K27 tri-methylation (H3K27me3) is most commonly associated with gene repression, although EZH2 can also place di-methylation. An EZH2 homologue, EZH1 can replace EZH2 in the PRC2 complex, and the two have overlapping, yet non-redundant roles. EZH1 is expressed in dividing and non-dividing cells, whereas EZH2 is only expressed in dividing cells, and EZH1 has lower histone methyltransferase activity compared to EZH2 (Margueron et al., 2008). EZH2 has also been proposed to act independently of PRC2 activity. It can interact with the androgen receptor in prostate cancer, as well as with E2F1 in both prostate cancer and DLBCL to activate gene transcription (Xu et al., 2016; Xu, K. et al., 2012). In addition, EZH2 has functions outside of its methyltransferase activity, with SWI/SNF tumours primarily dependent on its non-catalytic role in stabilising the PRC2 complex (Kim et al., 2015).

While EZH2 is necessary for embryonic development (Carroll et al., 2001), it also plays an essential role later on in early B cell development, regulating IgH rearrangement (Su et al., 2003). As B cells enter their resting state, EZH2 expression is lowered, and then again increased following antigen recognition and germinal centre activation (van Galen et al., 2004). EZH2 is necessary for formation of the germinal centre and promotes proliferation by repressing tumour suppressor and cell-cycle inhibitor genes (Béguelin et al., 2013; Velichutina et al., 2010). It is also necessary for class switch recombination and somatic hypermutation (Béguelin et al., 2013). Furthermore, in the mouse Ezh2 maintains the germinal centre B cell transcriptional program by repressing the *Prdm1* promoter (Caganova et al., 2013). As the B cells progress towards plasma cells, EZH2 expression is again lowered, with lower expression in tonsilar plasma cells compared to activated B cells, and then even lower expression in bone marrow plasma cells (Zhan et al., 2003). However, a recent study demonstrated that EZH2 is highly upregulated in pre-plasmablasts during the B cell to plasma cell transition where it represses B cell and plasma cell genes, and maintains proliferation (Herviou et al., 2019). When Ezh2 is knocked out prior to antigenic stimulation, there is a defect in production of antibody secreting cells (Guo et al., 2018), but enzymatic inhibition of Ezh2 applied simultaneously with antigen stimulation results in enhanced plasma cell differentiation (Scharer et al., 2018). One thing to consider is that turnover of histone marks takes some time to come into effect, and so the activity of Ezh2 in the second study may not have been lost until after the pre-plasmablast stage. Thus, the difference here likely arises from the timing of EZH2 loss, whereby EZH2 is required for the pre-plasmablast and

plasmablast stages, but must be repressed in mature plasma cells. Hence, EZH2 undergoes waves of expression changes during the B cell to plasma cell differentiation process.

1.10 Transcriptional and epigenetic drivers of DLBCL, Waldenström's macroglobulinemia and multiple myeloma

B cell malignancies can arise from different stages of B cell to plasma cell development, and these diseases frequently rely on transcription factors that maintain the cell identity at each differentiation stage. For example, hyper-activating translocations of *BCL6*, the master regulator of GC B cells, prevents the cells from differentiating into plasma cells and can lead to DLBCL (Cattoretti et al., 2005). NFκB is essential for the maintenance of germinal centre B cells and for driving the differentiation to plasma cells (Heise et al., 2014). A frequent characteristic of activated B cell type (ABC)-DLBCL is the constitutive activation of NFκB through activating mutations in upstream signal transducers that lead to its activation. These include BCR components (Davis et al., 2010), signal transducer CARD11 (Lenz et al., 2008), and MYD88 (Ngo et al., 2010). Activation of NFκB functions in cooperation with the loss of *PRDM1*, driving pro-survival programs and preventing terminal plasma cell differentiation (Calado et al., 2010). Beyond transcription factors, some of the most frequently inactivated genes are those encoding the histone and non-histone acetyltransferases CREBBP and EP300, mutated in approximately 39% of DLBCL (Pasqualucci et al., 2011a). Also, the gene encoding the histone methyltransferase MLL2, which is responsible for deposition of the H3K4me3 mark, is genetically inactivated in around a third of DLBCLs (Morin et al., 2011; Pasqualucci et al., 2011b). While the wider implications of these losses are not fully known, inactivation of CREBBP and EP300 leads to altered acetylation and functions of the BCL6 and p53 proteins (Pasqualucci et al., 2011a). Meanwhile, inactivation of MLL2 is associated with transcription stress and genome instability, leading to the increased accumulation of mutations (Kantidakis et al., 2016).

Multiple myeloma relies on the expression of a number of transcription factors normally expressed in B cells and plasma cells. These include IRF4, which drives myeloma, plasma cell and activated B cell transcriptional programs in myeloma cells, including the MYC transcription factor (Shaffer et al., 2008). Myeloma cells also rely on the activation of the NFκB and STAT3 transcription factors (Bharti et al., 2004; Catlett-Falcone et al., 1999). XBP1, which regulates the unfolded protein response, is also necessary for driving

myeloma pathogenesis (Carrasco et al., 2007). Epigenetic mechanisms are also essential for driving myeloma progression. The histone lysine demethylase KDM3A activates *IRF4* by removing H3K9 methylation, thus maintaining myeloma cells (Ohguchi et al., 2016). Inhibition of the histone methyltransferase DOT1L leads to decreased myeloma cell survival through repression of IRF4 target genes (Ishiguro et al., 2019). Furthermore, loss of the H3K27 demethylase UTX drives the malignant phenotype in multiple myeloma (Ezponda et al., 2017). Supporting the importance of aberrant histone modifications in multiple myeloma, the histone deacetylase (HDAC) inhibitor panobinostat has been in use for the treatment of relapsed/refractory myeloma since 2015, and other more specific HDAC inhibitors are currently being investigated (Harada et al., 2016).

Waldenström's macroglobulinemia is also dependant on aberrant transcriptional programs. The B cell transcription factor SPIB prevents plasmacytic differentiation of Waldenström's macroglobulinemia cells (Zhou et al., 2014), and inhibiting activation of NFκB leads to cell death in Waldenström's macroglobulinemia (Leleu et al., 2008). A recent study found that the B cell transcription factors BACH2 and CIITA were transcriptionally repressed in symptomatic Waldenström's macroglobulinemia compared to asymptomatic Waldenström's macroglobulinemia (Herbaux et al., 2016). In a large proteomic screen, the transcription factors STAT3, PAX5, the E2F1-binding partner TFDP1, and the MYC-interaction partner MAX were all overexpressed in Waldenström's macroglobulinemia compared to normal bone marrow (Hatjiharissi et al., 2007). While epigenetic mechanisms have largely gone unstudied in Waldenström's macroglobulinemia, the gene encoding H3K4 demethylase KDM1B was found to be associated with bone marrow involvement in Waldenström's macroglobulinemia (Hunter et al., 2016). Furthermore, perturbations of histone acetylation are present in Waldenström's macroglobulinemia (Roccaro et al., 2010).

Overall, transcriptional and epigenetic programs are central drivers of the malignant phenotype and survival of B/plasma cell malignancies such as DLBCL, multiple myeloma and Waldenström's macroglobulinemia. Further investigation into mechanisms of transcriptional regulation in Waldenström's macroglobulinemia and multiple myeloma is likely to provide novel insights into the molecular pathogenesis and maintenance of these diseases.

1.11 BLIMP1 and EZH2 in DLBCL, Waldenström's macroglobulinemia and myeloma

A frequent genetic alteration in ABC-DLBCL is the loss of *PRDM1* (Pasqualucci et al., 2006), which also prevents plasma cell differentiation. When BLIMP1 is expressed in DLBCL it functions as a tumour suppressor, driving terminal differentiation and apoptosis (Calado et al., 2010; Mandelbaum et al., 2010; Pasqualucci et al., 2006). Conversely, in multiple myeloma, BLIMP1 is thought to be necessary for malignant plasma cell survival (Hung et al., 2016; Lin et al., 2007). In a mouse model of plasmacytoma, loss of BLIMP1 prevented plasmacytoma formation (D'Costa et al., 2009). However, in a contradictory result, a more recent study found inactivating mutations of the *PRDM1* gene in 4% of multiple myeloma patients (Lohr et al., 2014). Although it has not been examined in great detail, studies suggest that abnormal expression of BLIMP1 could influence multiple myeloma cells. Analyses of B cells from myeloma patients showed BLIMP1 may be expressed early to drive premature plasma cell differentiation (Borson et al., 2002). Furthermore, in plasma cell leukaemia, where the cells have lost expression of normal B/plasma cell factors such as SPIB and POU2F2, BLIMP1 is still expressed (Nagy et al., 2002). In Waldenström's macroglobulinemia, BLIMP1 is expressed in a subset of lymphoplasmacytic cells (Roberts et al., 2013; Zhou et al., 2014), consistent with its role in promoting antibody secretion (Minnich et al., 2016; Savitsky & Calame, 2006; Shapiro-Shelef et al., 2003). Despite the interesting conundrum of BLIMP1 playing opposing roles in DLBCL and multiple myeloma, its role has not been studied in Waldenström's macroglobulinemia, which derives from a cell possibly somewhere in between the germinal centre or memory B cell and plasma cell stages.

While EZH2 has important roles in development and differentiation, it is also frequently overexpressed in cancer, and was found to be a bona fide oncogene (Kleer et al., 2003). EZH2 has frequent heterozygous gain of function mutations in DLBCL (McCabe et al., 2012a; Morin et al., 2010; Ryan et al., 2011; Sneeringer et al., 2010; Yap et al., 2011), and inhibition of EZH2 catalytic activity has shown efficacy against EZH2-mutant lymphomas (Knutson et al., 2014; Knutson et al., 2012; McCabe et al., 2012b; Qi et al., 2012), with the inhibitor tazemetostat showing antitumour activity in patients with refractory B cell non-hodgkin lymphoma (Italiano et al., 2018). One of the mechanisms by which EZH2 inhibition affects DLBCL is in lifting the repression of plasma cell genes including PRDM1 and IRF4, and inducing plasma cell differentiation (Béguelin et al., 2013). In multiple myeloma, while

few genes have been found differentially expressed between MGUS and malignant myeloma cells, EZH2 is one of the most significantly differentially expressed, with increased expression in myeloma plasma cells (Zhan et al., 2002). Profiling EZH2 expression across the span of myeloma development showed that EZH2 expression increases with disease progression (Zhan et al., 2003), and high EZH2 is associated with poor patient outcomes (Pawlyn et al., 2017). EZH2 is necessary for the growth-factor independence of IL-6 independent myeloma cell lines, and is induced by IL-6 in dependent cell lines. Furthermore, knock-down of EZH2 expression or reduced EZH2 enzymatic activity leads to inhibition of myeloma cell growth (Croonquist & Van Ness, 2005). EZH2 target genes bear the H3K27me3 mark and show low expression in myeloma and MGUS plasma cells (Kalushkova et al., 2010). A more recent study suggested that MMSET overexpression, which is common in myeloma with the IgH translocation to the MMSET/FGFR3 locus, is responsible for redistribution of EZH2 binding in the genome (Popovic et al., 2014). While mutations in EZH2 are not common in myeloma, there are frequent mutations in the H3K27 demethylase UTX (KDM6A) (van Haaften et al., 2009).

Testing of EZH2 catalytic inhibition in myeloma cell lines has shown inhibition of proliferation and induction of apoptosis via effects on the cell cycle in a subset of cell lines (Hernando et al., 2016; Pawlyn et al., 2017; Rastgoo et al., 2018b). The response to EZH2 inhibition can be somewhat predicted by the mutation status in the *ARID1A* gene, where *ARID1A*-mutant cancers are dependant on EZH2 expression when mutations in the Ras pathway are absent (Bitler et al., 2015; Kim et al., 2015). Interestingly, mutations in *ARID1A* are present in 17% of Waldenström's macroglobulinemia patients (Hunter et al., 2014), suggesting that EZH2 inhibition could have efficacy in these cancers. Furthermore, perturbations in the regulation of histone modifications contribute to Waldenström's macroglobulinemia pathogenesis (Roccaro et al., 2010). Given the role of EZH2 in DLBCL and multiple myeloma, as well as the interplay between EZH2 and *ARID1A*, and the role of epigenetic regulation in pathogenesis, it is surprising that EZH2 has not been investigated in Waldenström's macroglobulinemia.

An interaction between BLIMP1 and EZH2 was first suggested in mouse primordial germ cells, where BLIMP1 and EZH2 were bound to many of the same sites on a genome-wide scale (Kurimoto et al., 2015; Magnúsdóttir et al., 2013). This interaction was later confirmed in mouse plasmablasts, where BLIMP1 recruits EZH2 to chromatin to control the spread of the H3K27me3

mark (Minnich et al., 2016). Using EZH2 KO in mouse B cells, another study demonstrated severe defects in the formation of antibody-secreting cells in response to a T-independent viral antigen. They also found EZH2 expression to be necessary for the repression of a large proportion of BLIMP1 targets (Guo et al., 2018). While not all of the above studies were available during the original conception of the project, they lend support to the idea that BLIMP1 may be recruiting EZH2 to chromatin in malignant antibody-secreting cells where they are both expressed, such as in Waldenström's macroglobulinemia and multiple myeloma.

1.12 Transcriptional enhancers and regulation of cell states in MGUS/myeloma

Enhancer chromatin states are much more cell-type specific than chromatin states at promoters (Heintzman et al., 2009). Furthermore, within the genome, there are typically multiple enhancers with similar activity towards the same target gene (The et al., 2012). A recent study has demonstrated that this redundancy can promote robustness of gene expression and maintain the phenotype when one enhancer is decommissioned through loss of function mutations (Osterwalder et al., 2018). In multiple myeloma, dysregulation of enhancers is known as a contributing mechanism in the disease pathology. For example, translocation of the IgH locus to several genes as discussed above puts these genes under the strong control of the *IgH* enhancers, which drives their overexpression. *MYC* translocations are very common in myeloma, and result in *MYC* being put under control of several highly active enhancers to drive proliferation (Affer et al., 2014). Given the role of MYC in orchestrating enormous architectural changes in the chromatin during B cell activation (Kieffer-Kwon et al., 2017), it is likely that MYC overexpression is a driver for enhancer perturbation in myeloma. A variant in an enhancer of *ELL2*, which leads to decreased enhancer activity is associated with a genetic predisposition to multiple myeloma (Li et al., 2017), and in Waldenström's macroglobulinemia a variant in a potential enhancer for *IRF4* leads to increased enhancer activity and disease susceptibility (McMaster et al., 2018). Inhibition of the bromodomain protein BRD4 leads to selective deactivation of enhancers associated with critical oncogenic driver genes in myeloma, termed "super-enhancers" (Lovén et al., 2013). Super-enhancers are clusters of enhancers with particularly high occupancy of Mediator and other transcriptional activators, although there are no consistently defined criteria for classifying them (Pott & Lieb, 2014). B-cell specific enhancers bear DNA hypermethylation in multiple myeloma, and the

progression from MGUS to myeloma is associated with an increase in hypomethylated CpGs (Agirre et al., 2015). Enhancer profiling in primary myeloma cells identified a large number of enhancers that were activated in myeloma compared to normal plasma cells and memory B cells. It demonstrated large changes in regulatory circuits from normal plasma cells to myeloma cells without equally large gene expression changes (Jin et al., 2018).

Taken together, the evidence suggests a role for enhancers in promoting MGUS to myeloma progression. Enhancers may promote robustness of a pro-survival phenotype, even after the loss of external signals, such as in advanced stage myeloma. They could promote escape from signals that keep oncogenic growth in check, and they are one of the few mechanisms that can support a phenotypic change in the absence of large transcriptional changes.

2 Aims

Transcriptional regulation plays an important role in the pathogenesis and maintenance of Waldenström's macroglobulinemia and multiple myeloma. The transcription factor BLIMP1 is essential for plasma cell differentiation and multiple myeloma, yet its role has been critically unexplored in Waldenström's macroglobulinemia. The BLIMP1 interaction partner EZH2 has also not been studied in relation to Waldenström's macroglobulinemia, although it is a factor in DLBCL and multiple myeloma. Investigation into the interplay of BLIMP1 and EZH2 could provide insight into the mechanisms of Waldenström's macroglobulinemia disease biology.

Enhancers are central to the transcriptional architecture of multiple myeloma and undergo profound changes during the transformation from normal plasma cells. Despite this, enhancers have not been examined for changes at the MGUS to myeloma transition. Studying the differential activation of enhancers between MGUS and myeloma could help to further our understanding of the molecular mechanisms underlying this transformation.

Specific Aims:

1. To determine if BLIMP1 plays a role in Waldenström's macroglobulinemia cells
2. To investigate the possible interplay of BLIMP1 and EZH2 in Waldenström's macroglobulinemia
3. To identify pathways regulated by BLIMP1 and EZH2 in Waldenström's macroglobulinemia
4. To identify transcriptional enhancer regulatory networks underlying the transition from MGUS to multiple myeloma

3 Materials and methods

3.1 Molecular Cloning

3.1.1 PiggyBac artificial miRNA constructs

For knock-down (KD) of BLIMP1 and EZH2, we designed artificial miRNA sequences to target the *PRDM1* and *EZH2* transcripts using the RNAiDesigner tool (Thermo Fisher). We cloned the miRNA sequences into the pPB-hCMV*1-miR plasmid, containing a tetracycline-inducible CMV promoter (Hackett et al., 2013). We generated plasmids containing the *PRDM1-miR#1*, *PRDM1-miR#2* and *EZH2-miR#1* miRNAs using the method described for cloning miRNAs below. The non-targeting control *(NT)-miR* sequence was obtained from from Hackett et al. (Hackett et al., 2013). The *EZH2-miR#2* plasmid was generated using site-directed mutagenesis as described below. The mature miR RNAi sequences are marked in bold below (Table 1).

Table 1: Artificial miRNA sequences for RNAi

Name	Sequence (5'-3')
PRDM1-miR#1	G**TACACTTCTCTTCAAACTCAG**GTTTTGGCCAC TGACTGACCTGAGTTTAGAGAAGTGTACA
PRDM1-miR#2	G**TTACTCATCACTCCAATAACC**GTTTTGGCCAC TGACTGACGGTTATTGGTGATGAGTAACA
EZH2-miR#1	G**TTTACACGCTTCCGCCAACAA**GTTTTGGCCAC TGACTGACTTGTTGGCAAGCGTGTAAACA
EZH2-miR#2	G**TACTGAAGCAACTGCATTCAG**GTTTTGGCCA CTGACTGACCTGAATGCTTGCTTCAGTACA
Non-targeting (*NT-miR*)	**AAATGTACTGCGCGTGGAGAC**GTTTTGGCCAC TGACTGACGTCTCCACGCAGTACATTT

3.1.2 Cloning of miRNAs

For annealing, we diluted the miRNA oligonucleotides to 100µM concentration with nuclease-free water (#AM9937, Thermo Fisher Scientific), Then 1µL of forward and reverse oligonucleotides for each miRNA were mixed together with 43µL of nuclease-free water and 5µL of CutSmart Buffer. We incubated the mixture in a heat block at 95˚C for 3 min. The block was then switched off and the samples were allowed to cool slowly to room temperature inside the heat block overnight. We phosphorylated the ends of the annealed miRNA templates using T4 Polynucleotide Kinase, using 2µL of the miRNA templates.

The pPB-hCMV*1-miR plasmid (#43860, Addgene) was digested for 4h at 37˚C in CutSmart buffer with BsgI (#R0559S, New England Biolabs) and 80µM S-adenosylmethionine (#B9003S, New England Biolabs). It was then run on a 1% agarose gel, excised and purified using the Monarch® DNA gel extraction kit. In order to dephosphorylate the cut ends of the backbone, approximately 1.2µg of the digested backbone in 17µL volume was combined with 1µL Antarctic Phosphatase (#M0289, New England Biolabs) and 2µL Antarctic Phosphatase reaction buffer (#B0289, New England Biolabs). The sample was incubated at 37˚C for 30 min and then heat inactivated at 80˚C for 2 min. We combined 3µL of the phosphorylated miRNA template with 2µL of the dephosphorylated backbone and then added 5µL of Instant Sticky-End Ligase master mix and mixed well by pipetting. For a negative control, only the backbone was used in the ligation reaction. The ligation reaction was stored on ice before transformation.

3.1.3 Site Directed Mutagenesis

We used site directed mutagenesis for the insertion of miRNA sequences, as well as for introducing mutations in the coding sequences of BLIMP1 and EZH2 overexpression constructs to render them resistant to the targeting miRNAs. We generated the pPB-EZH2-miR2 plasmid using site directed mutagenesis of the pPB-hCMV*1-miR backbone. The FUW-PRDM1 miRNA-resistant mutants were constructed by PCR from the FUW-PRDI-BFI-GFP plasmid (Kuo, 2005; Magnúsdóttir et al., 2007). We first derived the EZH2 miRNA-resistant mutants by mutagenesis PCR using the pCMVHA-hEZH2 plasmid (#24230**,** Addgene) as a template, then incorporated the *EZH2* cDNA via Gibson assembly (see below) into the FUGW backbone (Lois et al., 2002).

We performed PCR using 0.1 ng of the plasmid backbone DNA with Phusion® High-Fidelity DNA Polymerase (#M0530, New England Biolabs). See Table 2 for reaction setup, Table 3 for primer sequences and Table 4 for cycling conditions. For those PCR reactions with multiple products, such as for the *PRDM1-miR#1*-mutant, we excised the appropriately sized band from the agarose gel and purified it with the Monarch® DNA gel extraction kit (#T1020, New England Biolabs). We digested the PCR products for 2 h at 37˚C with 1µL DpnI (#R0176S, New England Biolabs) in CutSmart Buffer (#B7204S, New England Biolabs) and then heat inactivated them for 20 min at 80˚C. We then combined the sample (~0.1 pmol) with 1mM ATP (#P0756, New England Biolabs), PNK buffer (#B0201, New England Biolabs) and 1µL T4 polynucleotide kinase (#M0201S, New England Biolabs) and incubated it for 30 min at 37˚C and 20 min at 65˚C. From this sample, we combined 5µL with 5µL of the Instant Sticky-End Ligase master mix (#M0370S, New England Biolabs) and mixed well by pipetting before transformation.

Table 2: PCR reaction setup

Reagent	**Concentration per reaction**
5x HF buffer (#B0518S, New England Biolabs)	1x
10mM dNTPs (#R0191, Thermo Fisher Scientific)	0.2mM
10µM Fwd primer	0.5µM
10µM Rev Primer	0.5µM
Phusion polymerase (#M0535L, New England Biolabs)	0.4 units
Nuclease-free water (#AM9937, Ambion)	to 20µL after adding template

Table 3: Primers used for site-directed mutagenesis

Primer name	**Sequence**	**Ta**	**Extension time**
EZH2-miR2-pPB_Fwd	cactgactgacctgaatgcttgcttcagtaCAGGACACAAGGCCTGTT	61˚C	2 min
EZH2-miR2-pPB_Rev	gccaaaacctgaatgcagttgcttcagtacAGCATACAGCCTTCAGCAA		
FUW-PRDM1-miR1-mut_Fwd	gaaaaatgcaCATACATTGTGAACGACCAC	72˚C	4 min 30 s
FUW-PRDM1-miR1-mut_Rev	ctcgaattccgCCTCTGTCCACAGAGTCA		
EZH2-miR2-mut-Fwd	ggcaagtgttCCCATAATGTATTCTTGGTC	51˚C	3 min 30 s
EZH2-miR2-mut-Rev	acggcgtttaaAGTCTTTAATGGGATGAC		

Table 4: PCR Cycles

Temperature	**Time**	
98˚C	30 sec	
98˚C	10 sec	x35 cycles
Ta	15 sec	
72˚C	extension time	
72˚C	5 min	
4˚C	hold	

3.1.4 Gibson Assembly

We used Gibson assembly for the construction of FUW-EZH2-GFP. First, we prepared the FUGW plasmid backbone via restriction digest with AgeI (#R0552, New England Biolabs) in Buffer 1.1 (#B7201, New England Biolabs). We then excised it from a 1% agarose gel and purified it using the Monarch® DNA gel extraction kit. We amplified the EZH2-miR2-mutant insert sequence from the pCMVHA-hEZH2-miR2-mut produced earlier by mutagenesis using Phusion DNA polymerase as above, with primer sequences listed in Table 5. We excised bands from the gel and purified as above. Using a ~1:3 molar ratio of backbone:insert, we combined 18.28 fmol of the digested backbone with 54.83 fmol of the insert in 2.5µL volume. We added an equal volume of the 2x Gibson Assembly master mix (#E2611, New England Biolabs) to the DNA and mixed well by pipetting. We also included a negative control that contained only the backbone without the insert. We incubated the samples for 15 min at 50˚C in a PCR machine and then on ice before transformation.

Table 5: Primer sequences used for Gibson assembly

Primer name	Sequence	Ta	Extension time
FUGW-EZH2-GFP_fwd	gtcgactctagaggatccccgggtaATGGGCCAGACTGGGAAG	64˚C	1 min
FUGW-EZH2-GFP_Rev	tcgcccttgctcaccatggtggcgagAGGGATTTCCATTTCTCTTTCG		

3.1.5 Transformation

We transformed the above cloning reactions into NEB 10-beta Competent *E. coli*. The NEB 10-beta cells were thawed on ice and aliquoted 60µL per tube for each transformation. We added 3µL of the samples from ligation or Gibson assembly reactions to the bacterial cells and mixed by gently flicking the tube. We incubated the tubes on ice for 30 min, then heat shocked for exactly 30 sec at 42˚C in a water bath. The tubes were incubated on ice for 5 minutes without mixing. We transferred the samples to culture tubes with 950µL SOC media and incubated at 37˚C for 1 h. Following the incubation, we spread 100µL of the culture over an LB agar plate with 100µg/mL ampicillin (#A0839, Applichem) and incubated at 37˚C overnight. For formulations of media and agar see Table 6.

Table 6: Media for bacterial culture

SOC media (1L)	LB Media (1L)	LB Agar
20g Bacto Tryptone (#211705, BD Biosciences)	10g Bacto Tryptone	10g Bacto Tryptone
5g Bacto Yeast Extract (#212750, BD Biosciences)	5g Bacto Yeast Extract	5g Bacto Yeast Extract
0.5g NaCl (#31434, Sigma)	10g NaCl	10g NaCl
20mM Glucose		15g Bacto Agar (#214010, BD Biosciences)

3.1.6 Miniprep by alkaline lysis

Using previously transformed bacterial culture plates, we inoculated one colony into each culture tube containing 3mL LB media with 100µg/mL ampicillin and incubated 16-18 h overnight. We then centrifuged the cultures for 30 min at maximum speed in a tabletop centrifuge. We removed the media and resuspended the cells in 100µL of Solution I. We added 200µL of freshly prepared Solution II to each tube and gently inverted 6-8 times. Then, we added 150µL of ice-cold Solution III to each tube and inverted 6-8 times. See Table 7 for solution composition. We incubated the samples on ice for 5 min, then centrifuged at maximum speed for 5 min at 4˚C. We transferred the supernatant to a fresh tube and discarded the pellet. We precipitated the plasmid DNA from the supernatant with 2 volumes of 96% ethanol (#A8075, Applichem), incubated it for 2 min at room temperature, then centrifuged at maximum speed for 4 min at 4˚C. We aspirated the supernatant and washed the pellet with 500µL freshly prepared 70% ethanol. We air dried the pellets and resuspended in 50µL TE buffer with 20µg/mL RNase A (#EN0531, Thermo Fisher Scientific).

Table 7: Solutions for alkaline lysis

Solution I	Solution II	Solution III
50mM Glucose (#G-5400, Sigma)	0.2N NaOH (#106482, Merck)	3M Potassium Acetate (#104820, Merck)
25mM Tris HCl pH 8 (#15504-020, Invitrogen)	1% SDS (#L4390, Sigma)	11.5mL Glacial Acetic Acid (#27225, Fluka, Honeywell)
10mM EDTA pH 8 (#ED, Sigma)		Up to 100mL with water

3.1.7 Midiprep Plasmid preparation

Using previously transformed bacterial culture plates, we inoculated one colony into each culture tube containing 3mL LB media with 100µg/mL ampicillin and incubated it for 8h at 37˚C. We diluted the culture 1:10000 in 100mL LB media with 100µg/mL ampicillin and incubated for 16-22h overnight, with longer incubation times for the viral transfer plasmids. For isolation of large quantities of plasmid from these cultures, we used the GeneJet Plasmid Midiprep Kit (#K0481, Thermo Fisher Scientific). We carried out the protocol according to the manufacturer's instructions, and the DNA concentration of the isolated plasmids was then measured on the Nanodrop 1000 spectrophotometer (Thermo Fisher Scientific).

3.2 Cell culture

3.2.1 Waldenström's macroglobulinemia and multiple myeloma cell lines

We maintained the RPCI-WM1 (a gift from Asher A. Chanan-Khan, Department of Cancer Biology, Mayo Clinic), BCWM.1 (a gift from Steven P. Treon, Bing Center for Waldenström's Macroglobulinemia, Dana-Farber Cancer Institute) and OPM-2 (#ACC50, Leibniz Institute DSMZ) cell lines in RPMI media (#SH30255.FS, Hyclone, GE Healthcare Biosciences) supplemented with 10% foetal bovine serum (FBS) (#SV30160.03, Hyclone, GE Healthcare Biosciences, Denmark). We maintained the U266 cell line (#TIB-196, ATCC) in RPMI media with 15% FBS. The MWCL1 (a gift from Stephen M. Ansell, Division of Hematology, Department of Internal Medicine, Mayo Clinic) and NCI-H929 (#ACC163, Leibniz Institute DSMZ) cell lines

were maintained in RPMI media supplemented with 10% FBS as well as 1mM sodium pyruvate (#SH30239.01, Hyclone GE Healthcare Biosciences) and 50µM beta-mercaptoethanol (#0482, VWR). We subcultured the cells three times per week and incubated all the cell lines at 37˚C with 5% CO_2 in a humid environment.

3.2.2 Electroporation of cell lines

We generated stable cells with inducible *PRDM1-miR#2* and *EZH2-miR#1* by Amaxa nucleofection using the 4D-Nucleofector® X Kit L (#V4XC-2024, Lonza) with the DY-100 program on the 4D-Nucleofector X-Unit (#AAF-1002X, Lonza).

All other electroporations were carried out using the following method. We suspended the cells at a density of 1 x 10^6 cells in 80µL culture media, mixed them with 10µg plasmid DNA, and transferred them to a 4mm electroporation cuvette (#Z706094, Sigma). We electroporated the cells at 220V, 350µF using the Gene Pulser XCell (Bio-Rad), then transferred them to a 6-well cell culture plate in a total of 3mL media. We measured the transfection efficiency by electroporation with pAcGFP1-N1 (Clonetech, Takara, USA), with green fluorescent protein (GFP) expression assessed after 24h and 48h.

3.2.3 Construction of knock-down (KD) cell lines

We generated the knock-down cell lines via electroporation as above with piggyBac plasmids containing our miRNA as described above (4.55µg), using the piggyBac transposon system with the piggyBac transposase (pPyCAG-pBase, 4.55µg), the reverse-tetracycline transactivator (pPB-rtTA, 0.45µg) and a tetracycline-inducible enhanced GFP (EGFP) (pPBhCMV*1-EGFP-pA, 0.45µg). For induction of miRNA expression, we used doxycycline hyclate (dox, #sc-211380, Santa Cruz Biotechnology) diluted in sterile water at a concentration of 0.2 µg/mL for the RPCI-WM1 and OPM-2 cell lines, and at a concentration of 0.5 µg/mL for the MWCL1 and BCWM.1 cell lines.

3.2.4 Antibiotic selection of stable cell lines

We selected the inducible KD cell lines described above using G418 Disulfate solution (#A6798, Applichem). We applied G418 to the cells 48h following electroporation at a concentration of 1 mg/mL for the RPCI-WM1, MWCL1 and BCWM.1 cell lines, and at 0.5 mg/mL for the OPM-2 cell line.

3.2.5 Lentivirus production

We cultured HEK293T cells (#ACC635, DSMZ) in DMEM (#SH30243.FS, Hyclone, GE Healthcare Biosciences), supplemented with 10% FBS, subcultured by trypsinisation with 1x trypsin (#SV30037.01, Hyclone, GE Healthcare Biosciences) three times per week. We seeded the HEK293T cells at a density of 5.8 x 10^6 cells per plate in 3 x 100mm round cell culture dishes, 24h prior to transfection. Immediately before transfection, we removed the media from the cells and replaced it with 5mL fresh DMEM with 10% FBS per plate. We mixed a total of 5µg plasmid DNA per 100mm plate together with the following molar ratio:

Table 8: Plasmids used for lentivirus production

Plasmid	**Size (bp)**	**Molar ratio**
psPAX2 (#12260, Addgene)	10668	1.3
pMD2.G (#12259, Addgene)	5822	0.72
transfer plasmid		1.64

We topped up the plasmid mixtures to a final volume of 486µL with serum-free DMEM, then added 14µL of FuGene HD transfection reagent (#E2311, Promega). We mixed the plasmid-FuGene well by pipetting at least 10 times, then incubated 10 min at room temperature. The mixture was then gently added dropwise to the HEK293T cells in the 100mm plate. We incubated the cells for 24h at 37˚C. Then the supernatant was removed and replaced with 10mL DMEM with 10% FBS. We incubated the cells for another 24h and the viral supernatant was then harvested 48h after transfection, and replaced with 10mL fresh DMEM with 10% FBS. We centrifuged the viral supernatant at 2000 rpm for 3 min to pellet debris. The supernatant was then passed through a 0.45µm PVDF syringe filter (#sc-358814, Santa Cruz Biotechnology), and stored at 4˚C. At 72h post transfection, we harvested the viral supernatant, centrifuged it and filtered it as above. We then combined the supernatants from the 48h and 72h time points and transferred 15mL at a time to Amicon 100kDa ultracentrifugal filter unit (#UFC910008, Millipore). We centrifuged the filter unit at 1000 x*g* for 10 minutes, then discarded the flow-through and the filter was topped up with more viral supernatant. This process was repeated until almost all the viral supernatant had passed through, and ~1mL remained in filter. We transferred the viral concentrate

from the filter to a fresh 15mL tube and washed the filter twice with 1mL fresh RPMI with 10% FBS, with each wash being combined with the viral concentrate for a final volume of 3mL. The viral concentrate was snap-frozen in liquid nitrogen and stored at -80˚C.

Table 9: Viral transfer plasmids

Viral transfer plasmid	Citation
FUGW	(Lois et al., 2002).
FUW-PRDI-BFI-EGFP	(Kuo, 2005; Magnúsdóttir et al., 2007)
FUW-EZH2-EGFP	Cloned from (Lois et al., 2002) and #24230**,** Addgene.

3.2.6 Viral spinoculation of suspension cell lines

We suspended the cells in 100µL culture media and mixed with concentrated viral supernatant (typically 100-250µL). We added polybrene to a final concentration of 8µg/mL and mixed well by gently pipetting. We centrifuged the cells with virus at 800 x*g* for 30 min, then resuspended in supernatant and transferred to cell culture flasks. We topped up the flasks with RPMI with 10% FBS. Transduction efficiency was assessed after 72 h.

3.2.7 Drug treatments

We diluted tazemetostat (EPZ-6438, #S7128, Selleckchem) in DMSO (#A3672, Applichem) to 15.7mM concentration, then further diluted in cell culture medium for treatments. DMSO was used as a vehicle control, which we diluted in cell culture medium to the same extent as tazemetostat.

3.2.8 Proteasome inhibition

For proteasome inhibition experiments, we added MG-132 (#sc-201270, Santa Cruz Biotechnology) dissolved in DMSO to cells 20 h after dox induction at a final concentration of 5µM and incubated for 4 h before harvesting. DMSO diluted to the same extent was used as the vehicle control.

3.3 Isolation of human cells

Plasma cells were isolated from human bone marrow aspirates via two separate methods. Icelandic bone marrow aspirates were obtained from Landspitali University Hospital from MGUS and multiple myeloma patients who provided informed consent (ethical approval VSN: b2014050002/03.11). Swedish samples comprising already-isolated $CD138^+$ cells from bone marrow aspirates were obtained from Karolinska Institute from MGUS and multiple myeloma patients who provided informed consent (ethical approval: #2005/206-31/3 and #2013/1353-32).

3.3.1 Isolation of CD138+ cells from human bone marrow using density gradient centrifugation

We diluted bone marrow aspirate 1:5 using phosphate buffered saline (PBS) with 2mM EDTA and layered it over Histopaque-1077 (#10771, Sigma-Aldrich) and then centrifuged the cells at 500 x*g* at room temperature for 30 min without brake. We collected the peripheral blood mononuclear cell layer, washed two times in PBS with 2mM EDTA and 0.5% BSA, and filtered through a 30µm pre-separation filter (#130-041-407, Miltenyi Biotech). We then isolated the CD138+ cells using anti-CD138 conjugated microbeads (# 130-051-301, Miltenyi Biotech) according to the manufacturer's protocol using LS positive selection columns (#130-042-401, Miltenyi Biotech). We assessed the cells for purity by flow cytometry using the BD FACS Calibur instrument. Gating on forward scatter (FSC) and side scatter (SSC) was used to exclude debris, and the percentage of $CD138^+$ cells was assessed compared to an unstained sample and non-enriched PBMCs by staining with anti-CD138-PerCP-Cy5.5 (#341087, BD Biosciences). In order to obtain more detailed information on the myeloma cells, we also performed staining using anti-CD38-APC (#340439, BD Biosciences) and anti-CD56-PE (#340363, BD Biosciences), with gating set by comparison to an unstained sample.

3.3.2 Isolation of CD138+ cells from human bone marrow using whole blood isolation kit

We diluted the bone marrow aspirate with an equal volume of RPMI media, then passed it through a pre-separation filter as above. We centrifuged the cells at 445 x*g* for 10 minutes at room temperature without brake. We then resuspended the cell pellet in 1 volume of PBS with 2mM EDTA and 0.5% BSA. The cells were magnetically labelled with Whole Blood and Bone Marrow CD138 MicroBeads, human (#130-105-961, Miltenyi Biotech) and

isolated according to the manufacturer's protocol using the Whole Blood Column Kit (#130-093-545, Miltenyi Biotech). We assessed the cells for purity by flow cytometry using the BD FACS Calibur instrument as described above.

3.3.3 Isolation of NK cells

We isolated NK cells from buffy coats from healthy human volunteers, who all provided informed consent. The samples were provided by the Icelandic Blood Bank (ethical approval: #06-068). We isolated peripheral blood mononuclear cells by density gradient centrifugation with Histopaque-1077 as above, then the NK cells were purified by negative enrichment using the NK cell isolation kit (#130-092-657, Miltenyi Biotech) according to the manufacturer's instructions. We cultured the NK cells overnight in RPMI media supplemented with 10% FBS and 10ng/mL IL-2. We carried out analysis for purity during the degranulation assay as described below.

3.4 Flow Cytometric Analyses

3.4.1 Annexin V apoptosis assay

We assessed apoptosis of the RPCI-WM1 KD cell lines 48h after dox induction using APC Annexin V (#550474, BD Biosciences) together with Annexin V binding buffer (#556454, BD Biosciences). Staining was carried out according to the manufacturer's instructions, using 5 µL Annexin V per sample with 10^5 cells and assessed using the MACSQuant analyser (Miltenyi Biotec), with gating set by comparison to an unstained sample used to determine the percentage of Annexin V positive cells.

3.4.2 NK cell degranulation assay

We co-cultured NK cells with pre-treated RPCI-WM1 cells at a 10:1 ratio, with anti-CD107a-PE (H4A3, BioLegend) added to the co-culture media. For the positive control, NK cells in co-culture with RPCI-WM1 cells were treated with 2.5µg/mL phorbol 12-myristate 13-acetate (#ab120297, Abcam) and 0.5µg/mL ionomycin (#ab120370, Abcam). After 1h of co-culture, we added 2µM monensin (#ab120499, Abcam) to every sample and incubated for an additional 4h. We stained the cells with anti-CD56-APC (CMSSB, EBioscience), fixed with 1% paraformaldehyle (PFA) and analysed on the Sony SH800S flow cytometer. NK cells were gated according to FSC and SSC properties and the GFP-positive RPCI-WM1 cells were excluded. The percentage of $CD56^+CD107a^+$ cells was determined by comparison to an unstained control, with the percentage of $CD56^+$ cells denoting the purity of the NK cells.

3.4.3 Cell cycle analysis

RPCI-WM1 cells with inducible miRNAs that had been treated with dox 48h earlier were harvested from culture and washed in PBS, then resuspended in 200µL PBS and kept on ice. The cells were vortexed at a low speed and 5mL of methanol was slowly added to the suspension, which was then incubated on ice for 20 min. We centrifuged the cells and washed twice in ice-cold PBS, then resuspended in PBS with 60µg/mL propidium iodide and 50µg/mL RNase I. Analysis was carried out using the BD FACS Calibur instrument. Gating on FSC and SSC was used to exclude debris, and the cell cycles phases were gated according to the locations of the G0/G1 and G2/M peaks.

3.4.4 Flow cytometric data analysis

Data from flow cytometry experiments were analysed using FlowJo v10.

3.5 Viability and reduction assays

3.5.1 Viability count

We determined the percentage of live cells by mixing 10µL volume of cell culture with equal volume of Trypan Blue Solution, 0.4% (#15250061, Gibco). Live and dead cells were counted under a phase-contrast microscope, with live cells identified by exclusion of Trypan blue.

3.5.2 Resazurin Assay

In order to assess the metabolic capability of the cells, we used the resazurin assay. Resazurin is a colourimetric/fluorometric dye which changes colour in response to oxidation-reduction reactions occurring in live cells. As mitochondrial metabolism takes place, resazurin is reduced by dehydrogenase enzymes to resorufin, with a corresponding colour change. The protocol is as follows. We prepared a concentrated stock (250x) solution of resazurin by dissolving 1g of resazurin sodium salt (#sc-206037, Santa Cruz Biotechnology) in 100mL sterile PBS. We prepared the working (10x) solution by combining 200µL of stock solution with 4.8mL of sterile PBS. The fully reduced form of resazurin, resorufin was prepared by autoclaving a mixture of 10% volume of 10x resazurin solution with cell culture media. For measurement of reduction, we added 10x resazurin solution to cell culture at a final concentration of 1x in a 96-well plate 5h before the assay end-point. Resorufin was used as a positive control and resazurin solution mixed with media without cells was used as a negative control. Absorbance was measured at 595nm and 570nm. Per cent reduction was normalised relative to resorufin. The percentage reduction of resazurin was calculated according to the following formula:

$$\text{Percentage reduction of resazurin} = \frac{(O2 \times A1) - (O1 \times A2)}{(R1 \times N2) - (R2 \times N1)} \times 100$$

Where O1 = molar extinction coefficient (E) of oxidized resazurin at 570 nm (80586); O2= E of oxidized resazurin at 595 nm (117216); R1 = E of reduced resazurin (Red) at 570 nm (155677); R2= E of reduced resazurin at 595 nm (14652); A1 = absorbance of test wells at 570 nm; A2 = absorbance of test wells at 595 nm; N1 = absorbance of negative control well (media plus resazurin but no cells) at 570 nm; N2 = absorbance of negative control well (media plus resazurin but no cells) at 595 nm.

3.5.3 Cytotoxicity Assay

We co-cultured NK cells with pre-treated RPCI-WM1 cells at a 20:1 ratio for 4h. Cytotoxicity was assessed by measurement of the adenylate kinase activity in the culture medium using the ToxiLight assay (#LT07-217, Lonza). Luminescence was measured using a Modulus microplate reader (Promega). We normalised the values to wells containing pre-treated RPCI-WM1 cells without NK cells, and present them as relative luminescence units (RLU).

3.6 Protein Expression Analyses

3.6.1 Cell lysis for immunoblotting

We harvested the cells, then resuspended them in 1mL PBS and centrifuged 5 min at 800 x*g*. We removed the PBS and resuspended the cells in 30µL 1x protein sample buffer (60mM Tris #15504-020, Invitrogen, pH 6.8, 2% SDS #L4390, Sigma, 10% glycerol, 0.01% bromophenol blue, 1.25% β-mercaptoethanol) per 10^6 cells. We incubated the cell lysate for 5 min at 95˚C, then cooled and stored it at -20˚C. Before immunoblotting, we added benzonase nuclease (#sc-202391, Santa Cruz Biotechnology) to cell lysates at a 1:100 dilution and incubated 20 min at room temperature. Typically, lysate from $0.5\text{-}1 \times 10^6$ cells was loaded onto each lane.

3.6.2 Histone Extraction

Histone extracts were prepared using the protocol from Abcam (https://www.abcam.com/protocols/histone-extraction-protocol-for-western-blot). We harvested the cells and washed in PBS, then resuspended the pellets in triton extraction buffer (TEB: 0.5% triton-X-100, 2mM

phenylmethylsulfonyl fluoride, 0.2% NaN_3 in PBS), and incubated on ice for 10 min with occasional mixing. We pelleted the nuclei and washed in TEB, then resuspended in 0.2N HCl and incubated overnight at 4˚C. We pelleted the debris and the supernatant containing the histones was neutralised with 1/10 volume 2M NaOH. Protein sample buffer was added to histone extracts before gel electrophoresis. Typically, histone extract from 2×10^5 cells was loaded onto each lane.

3.6.3 SDS-Polyacrylamide gel electrophoresis (PAGE)

SDS-PAGE and immunoblotting were based on a previously described protocol (Burnette, 1981). We prepared polyacrylamide gels by mixing the following reagents:

Table 10: SDS-PAGE gel

8% Resolving gel		**5% Stacking gel**	
Reagent	**Volume (mL) in 10mL**	**Reagent**	**Volume (mL) in 4mL**
40% Acrylamide (#01709, Sigma)	2	40% Acrylamide	0.5
Lower Tris Buffer	2.5	Upper Tris Buffer	1
10% APS (#A3678, Sigma)	0.1	10% APS	0.04
TEMED (#15524-010, Invitrogen)	0.008	TEMED	0.004
MilliQ H20	5.39	MilliQ H20	2.46

Lower Tris Buffer: 1.5M Tris, 0.4% SDS, pH 8.8 with HCl (#30721, Sigma).
Upper Tris Buffer: 0.5M Tris, 0.4% SDS, pH 6.8 with HCl.

SDS-PAGE gels were assembled in Mini-PROTEAN® Tetra Vertical electrophoresis system (#1658004, Bio-Rad) and filled with running buffer (0.192M glycine #15527-013, Invitrogen, 25mM Tris, 0.1% SDS). We loaded the colour pre-stained protein standard (#P7712S, New England Biolabs) into the gel for size comparison. We loaded the protein lysates in sample buffer into wells of the SDS-PAGE gel and subjected them to electrophoresis at 80V

until the proteins had passed through the upper stacking gel. The voltage was then increased to 120V and run until the dye front reached the bottom of the gel.

3.6.4 Immunoblotting

We equilibrated the gels 10 min in 1x transfer buffer (0.192M glycine, 25mM Tris, 0.05% SDS, 20% methanol #106009, Merck), then assembled them with PVDF membrane (#10600021, GE Healthcare Biosciences) between sponges and filter paper and transferred the proteins to the membrane at 90 V for 90 min using the wet electrophoretic transfer system (#1703930, Bio-Rad). We blocked the membranes for 1h at room temperature in blocking buffer comprising TBST (20mM Tris, 150mM NaCl, 0.1% Tween-20 #P1379, Sigma, pH 7.6) with 5% BSA (#A1391, Applichem GmbH). We incubated the membrane overnight at 4˚C with primary antibodies diluted in blocking buffer. See Table 11 for antibody dilutions. We washed the membrane 3 x 10 min in TBST before application of the secondary antibody, diluted 1:15000 in blocking buffer. We incubated the membrane for 1h at room temperature with the secondary antibody, then again washed it 3 x 10 min with TBST. BLIMP1 was visualised by enhanced chemiluminescence using goat anti-rabbit IgG-HRP secondary antibody (#sc-2004, Santa Cruz Biotechnology) on the ImageQuant LAS 4000 (GE Healthcare Biosciences) following addition of western blotting Luminol reagent (#sc-2048, Santa Cruz Biotechnology). All other proteins were visualised by fluorescence detection using the IRDye800CW goat anti-mouse IgG (#925-32210, LiCor Biosciences GmbH) on the LiCor Odyssey instrument (LiCor Biosciences GmbH). Quantitation of immunoblots was carried out by densitometry using the ImageJ software package (Schneider et al., 2012).

Table 11: Antibodies used for immunoblotting

Antibody	Product Details	Quantity used in 5 mL (µg or µL if conc. unknown)	Dilution
α-BLIMP1	C14A4 Rabbit mAb #9115, Cell Signaling Technology	5 µL	1:1000
α-EZH2	Mouse mAb #612666, BD Biosciences	1.25 µg	1:1000
α-ACTIN	Mouse mAb #MAB1501, Millipore	1 µL	1:5000
α-H3	Rabbit polyclonal #ab1791, Abcam	5 µg	1:1000
α-H3K27me2/3	Mouse mAb #39536, Active motif	5 µg	1:1000

3.6.5 Immunofluorescence

We centrifuged ~1 x 10^5 cells onto glass slides (#KG VA11310, Kittel Glass) using the Cyto-Tek® 2500 Cytocentrifuge (Sakura Finetek Europe) at 800 rpm for 3 min. We encircled the sample using a PAP pen (#ab2601, Abcam), then fixed the sample for 10 min at room temperature in fixation solution: 4% formaldehyde (#28906, Thermo Fisher Scientific), 0.1% triton X-100 (#T-9284, Sigma) in PBS. We washed the sample 2 x 5 min in PBS, then incubated for 1 h at room temperature in blocking solution: 0.1% triton X-100, 1% BSA, 10% goat serum (#16210064, Gibco) in PBS. We incubated the sample overnight at 4˚C with primary antibodies diluted 1:100 in PBS with 0.25% BSA. The same antibodies were used as described above for immunoblotting. We washed the samples 3 x 5 min in PBS then incubated for 1 h at room temperature with secondary antibodies (Goat anti-mouse IgG H + L Alexa Fluor 546, #A11030, Thermo Fisher Scientific; and Goat anti-rabbit IgG H + L Alexa Fluor 647 #A21244, Thermo Fisher Scientific) diluted 1:1000 in blocking solution. We washed the samples 2 x 5 min with PBS, then nuclei were stained with DAPI (#sc-3598, Santa Cruz Biotechnology) at a 1:5000 dilution of 5mg/mL stock solution. We mounted coverslips onto the slides

using UltraCruz® Aqueous Mounting Medium (#sc-516212, Santa Cruz Biotechnology) and sealed them with Marabu FixoGum glue. The samples were visualised by confocal microscopy using the FV 1200 Laser Scanning Microscope (Olympus).

3.7 RNA Expression Analyses

3.7.1 RNA Isolation

We lysed cell pellets in TRIsure™ reagent (#BIO-38032, Bioline GmbH), and then stored them at -80˚C. At the time of isolation, we allowed the TRIsure™ cell suspensions to thaw for 15 min at room temperature, and then processed them according to the manufacturer's instructions, with only change being that the RNA pellet was washed 2 x in 75% ethanol (#A8075, Applichem) rather than just once.

3.7.2 cDNA Synthesis

We diluted 2µg RNA in nuclease-free water to a total volume of 16.5µL and mixed with 1.5µL dNTP mix (10mM, #R0191, Thermo Fisher Scientific), and 1.5µL Random Primer 6 (100µM, #S1230S, New England Biolabs). We heated the samples at 65˚C for 5 min then cooled them on ice. We used the GoScript Reverse Transcriptase system (#A5001, Promega) to synthesise cDNA. We prepared a master mix by combining 6µL 5x reaction buffer, 1.5µL 25mM $MgCl_2$, and 1.5µL murine RNase inhibitor (#M0314S, New England Biolabs) per reaction. Minus-RT controls were prepared by mixing 9µL of master mix with the samples and then transferring 9µL of this to a fresh tube. We added GoScript Reverse Transcriptase at a volume of 0.5µL to each sample tube, except the –RT samples. The samples were then heated at 25˚C for 5 min, 42˚C for 2 h, 70˚C for 15 min, and then stored at -20˚C. The cDNA samples were diluted 1:50 with nuclease-free water for qPCR.

3.7.3 Quantitative reverse-transcription PCR (RT-qPCR)

We performed RT-qPCR using the SensiFAST SYBR Lo-Rox Kit (#BIO-94020, Bioline GmbH). For each reaction, we combined 10µL of the SYBR reagent with 0.1µM forward primer, 0.1µM reverse primer, 4.6µL nuclease-free water and 5µL of diluted cDNA in a 20µL reaction. The cDNA quantity per well was ~6.84ng. Reactions were carried out and data was analysed using the 7500 Real-Time PCR system (Applied Biosystems). The cycling conditions were as follows:

1. 95˚C – 10 min
2. 95˚C – 15 sec
3. 60˚C – 1 min
4. Repeat steps 2-3, 39x
5. 95˚C – 15 sec (Steps 5-8 are for generating a melt curve)
6. 60˚C – 1 min
7. 95˚C – 30 sec
8. 60˚C – 15 sec

Relative quantitation was calculated according to the Pfaffl method (Pfaffl, 2001), with *ACTB* and *PPIA* used as reference genes, using the following formula:

$$\text{ratio} = \frac{(E_{target})^{\Delta CP_{target}(control-sample)}}{(E_{ref})^{\Delta CP_{ref}(control-sample)}}$$

Where *E* is the amplification factor of the primer pair, and *ΔCP* is the difference in Ct values. The ratio for the gene of interest was calculated as the geometric mean of the ratios normalised to each reference genes. See Table 12 for primer sequences. In order to determine primer efficiencies, standard curves were prepared using 10-fold dilutions of appropriate cDNA. Primer amplification factors were calculated as $10^{-1/\text{slope of standard curve}}$.

Table 12: Primers used for RT-qPCR

Primer	Sequence	Amplification factor
PRDM1_fwd	GGTACACACGGGAGAAAAGC	1.99
PRDM1_rev	GAGATTGCTGGTGCTGCTAA	
EZH2_fwd	ACATCCTTTTCATGCAACACC	2.08
EZH2_rev	GCTCCCTCCAAATGCTGGTA	
STAT1_fwd	CTGTGCGTAGCTGCTCCTT	1.91
STAT1_rev	GAGTCAAGCTGCTGAAGTTCG	
TFEC_fwd	ACATGGGGCTTACAAGTGCT	1.94
TFEC_rev	TCAATGAGGTTGTGGTTGTCC	
POU2F2_fwd	ACTCATGTTGACGGGCAGC	1.94
POU2F2_rev	GGTAGCAGGAACTGAGCAGG	
MICA_fwd	ACATTCCATGTTTCTGCTGTTGC	1.92
MICA_rev	GACCTGCAGGCTCACGA	
LGALS9_fwd	TCAATGGGACCGTTCTCAGC	1.99
LGALS9_rev	GAGGGTTGAAGTGGAAGGCA	
BCL2L11_fwd	CCTCGGCGCCCTTTCTT	1.93
BCL2L11_rev	AGGTTGCTTTGCCATTTGGTC	
CASP4_fwd	TGCTGTTTACAAGACCCACG	1.97
CASP4_rev	AGAGCCCATTGTGCTGTCTC	
OAS2_fwd	CAGGAACCCGAACAGTTCCC	1.92
OAS2_rev	AGGACAAGGGTACCATCGGA	
PIK3CD_fwd	TGTACGCCGTGATCGAGAAA	1.91
PIK3CD_rev	CGGTCTTAAGCTGGTCCTTGT	

RCAN3_fwd RCAN3_rev	GCGCGAATAGAACTCCACGA GCGGCAGGAGATAGGACTTG	1.98
ZFP36L1_fwd ZFP36L1_rev	GTCTGCCACCATCTTCGACT TTTCTGTCCAGCAGGCAACC	2.02
CIITA_fwd CIITA_rev	CATCCTTGGGGAAGCTGAGG CTGTGAGCTGCCTTGGGG	2.02
TNFRSF14_fwd TNFRSF14_rev	GCAGTGCCAAATGTGTGACC CCTGGACGATGCAGAAGTGG	1.94
HAVCR2_fwd HAVCR2_rev	GGCTCTTATCTTCGGCGCT GGGAGGTTGGCCAAAGAGAT	2.06
CDKN1A_fwd CDKN1A_rev	ACTCTCAGGGTCGAAAACGG GCGGATTAGGGCTTCCTCTT	1.92
PPIA_fwd PPIA_rev	CATCTGCACTGCCAAGACTGA TGGCCTCCACAATATTCATGC	1.89
ACTIN_fwd ACTIN_rev	AGGCACCAGGGCGTGAT GCCCACATAGGAATCCTTCTGAC	1.93

3.8 Statistical analyses

Graphs represent the mean of three biological replicates unless stated otherwise. Error bars represent standard deviation. We carried out statistical analyses on the above experiments using the student's two-tailed t-test, with a p-value ≤ 0.05 deemed significant.

3.9 Chromatin Immunoprecipitation (ChIP)

3.9.1 Histone ChIP

For immunoprecipitation (IP) of histone modifications, we used 1 x 10^7 cells per IP. All buffers in this protocol contained 1mM phenylmethylsulfonyl fluoride, 1% Protease Inhibitor Cocktail (#P8340, Sigma Aldrich) and for the H3K27Ac mark, 5mM sodium butyrate. Using 25µL Protein A Dynabeads

(#10001D, Invitrogen) per ChIP sample, we combined the beads and washed 3x with dilution buffer (0.01% SDS, 1.1% Triton X-100, 1.2mM EDTA, 16.7mM Tris pH 8, 167mM NaCl) using the Dynamag-2 magnet (#12321D, Thermo Fisher Scientific). We resuspended the beads in 200µL dilution buffer per ChIP and transferred to separate tubes. We added the antibodies and incubated the tubes for 6 h at 4˚C with rotation. See Table 14 for antibodies.

We suspended the cells at a final concentration of 1 x 10^6 cells per mL in PBS, then crosslinked with 0.4% formaldehyde (#28906, Thermo Fisher Scientific) for 10 min at room temperature. We quenched the reaction with 125mM glycine for 5 min at room temperature. We resuspended the pellets in 5mL ChIP lysis buffer (10mM Tris pH 8, 10mM NaCl, 0.2% NP-40) per 3 x 10^7 cells and incubated on ice for 10 min then centrifuged at 4000 rpm for 5 min at 4˚C. The pellet was resuspended in sonication buffer (10mM Tris pH 8, 10mM EDTA, 1% SDS) at a density of 5 x 10^6 nuclei per 100µL. We sonicated the samples in volumes of 100µL per tube in the Bioruptor® Standard (#UCD-200, Diagenode), pulsing three times for 5 min on high with 30 sec on, 30 sec off. Using 20µL Protein A Dynabeads per ChIP, we combined the beads and washed 3x with dilution buffer before adding to the sonicated lysate. We incubated this mixture for 1 h at 4˚C on rotation to pre-clear the sample. The antibody-beads mixture prepared earlier was washed 1x in dilution buffer. We removed the pre-cleared lysate from the beads added it to the antibody-beads mixture, and then incubated overnight at 4˚C with rotation.

We removed the supernatant from the beads, and then washed them for 5 min at 4˚C with low-salt buffer (20mM Tris pH 8, 0.1% SDS, 1% triton X-100, 2mM EDTA, 150mM NaCl), high-salt buffer (as for low-salt buffer but with 500mM NaCl), and then LiCl buffer (10mM Tris pH 8, 250mM LiCl, 1% NP-40, 1% sodium deoxycholate, #30970, Sigma, 1mM EDTA). We washed the beads briefly in TE buffer with 50mM NaCl and then resuspended them in 100µL elution buffer (50mM Tris pH 8, 10mM EDTA, 1% SDS). We eluted the sample from the beads at 68˚C for 15 min and then transferred it to a fresh tube and topped up to 500µl with elution buffer. For reverse crosslinking, we mixed the sample with 0.2M NaCl and incubated overnight at 65˚C. The samples were treated with 0.2 µg/µL RNase A (#EN0531, Thermo Fisher Scientific) for 1 h at 37˚C, then with 0.2 µg/µL proteinase K (#P8107S, New England Biolabs) for 2h at 55˚C. We used Phenol-chloroform extraction with Phenol:chloroform:IAA (#AM9732, Thermo Fisher Scientific) and Chloroform (#372978, Sigma) to purify the ChIP DNA in phase-lock tubes (#733-2478,

VWR). The DNA was mixed with 1 µL glycogen (#R0561, Thermo Fisher Scientific), 0.2M NaCl, then combined with 1ml ethanol and incubated at -80˚C overnight. We Precipitated the DNA by centrifugation at maximum speed for 30 min at 4˚C. The pellet was washed 1x in 70% ethanol, then allowed to dry and resuspended in 0.1 x TE buffer.

3.9.2 Transcription factor ChIP

The following protocol was used for ChIP of BLIMP1 and EZH2. Transcription factor ChIP was performed as previously described (Boyer et al., 2005; Magnúsdóttir et al., 2013; Magnúsdóttir et al., 2007) with the following modifications: 1. Cells were crosslinked as above with 0.4% formaldehyde for BLIMP1 ChIP, but 1% formaldehyde was used for EZH2 ChIP. 2. Cell number was 3 x 10^7 per sample for BLIMP1 ChIP, whereas for EZH2 ChIP, 2 x 10^7 cells were used per sample. 3. Nuclei were sonicated with 1 x 10^7 cells per tube in 300µL volume for 6 min for 0.4% crosslinked cells, and for 7 min for 1% crosslinked cells. 4. The volume of beads per sample was 50µL. 5. Sonication was performed using the Epishear™ probe sonicator (#53052, Active Motif) at 25% output with cycles of 15 s on, 30 s off. Assessment of each ChIP experiment was carried out using ChIP-qPCR using 0.01% of the input DNA, and a 1% of the ChIP DNA per reaction. The enrichment in known target regions was compared to negative control regions to confirm if the ChIP was a technical success.

Table 13: Antibodies used for transcription factor ChIP

Name	**Details**	**Quantity Used per IP**
Rabbit polyclonal antiserum recognising the C-terminal region of BLIMP1 (Kuo & Calame, 2004)	Clone CLU-267	60 µL
Anti-EZH2	D2C9, #5246, Cell Signaling Technology	40 µL

3.9.3 Low-cell number histone ChIP

This protocol was carried out as with the histone ChIP protocol above with minor changes. Fewer cells (1 x 10^5) were used per ChIP with 12.5µL protein

A Dynabeads. Cells were lysed directly in sonication buffer (1mL per 5 x 10^5 cells) and incubated on ice for 5 min. The sample was centrifuged at 2000 rpm for 5 min at 4˚C, then the supernatant was discarded and the pellet was resuspended in 100µL dilution buffer. The remainder of the protocol was continued as above, with immunoprecipitation performed overnight in 0.2ml PCR tubes in 160µL volume. Following washing and elution in 50µL elution buffer, we incubated the sample with 1µg/µL proteinase K for 2 h at 42˚C then reverse crosslinked at 68˚C for 6 h. We did not perform RNase A digestion. See Table 14 for antibodies used. For the optimisations, we performed ChIP-qPCR using the primers listed in Table 15. For calculating the ChIP-qPCR results as per cent input, we used the following formulas:

$$input\ adj = Ct^{input} - log_2(dilution\ factor)$$

$$\Delta Ct = Ct^{sample} - Ct^{input\ adj}$$

$$\%\ input = E^{-(\Delta Ct)} \times 100\%$$

Where, the dilution factor is the dilution factor for the input, i.e. if 1% input was used, the dilution factor is 100; E = the primer amplification factor. Our % input for each ChIP sample was then divided by the % input for the histone H3 ChIP, so it was normalised to histone density.

For ChIP libraries, we calculated fold enrichment relative to H3 using the following formula:

$$fold\ enrichment = E^{-(sample\ Ct\ -\ H3\ Ct)}$$

Amplification factors for ChIP-qPCR primers were determined as described above for RT-qPCR, using genomic input DNA as a template.

Table 14: Antibodies used for histone ChIP. Quantities are given in µL where antibody concentrations are not known.

Name	Catalogue number	Quantity Used
Anti-H3K27me3	Mouse mAb, #ab6002, Abcam	5µg – Histone ChIP 0.25µg – Low-cell number
Anti-Histone H3	Rabbit mAb, D2B12 #4620S, Cell Signaling Technology	3µL – Histone ChIP 0.25µL – Low-cell number
Anti-H3K4me1	Rabbit mAb, D1A9 #5326, Cell Signaling Technology	5µL – Histone ChIP 0.25µL – Low-cell number
Anti-H3K4me3	Rabbit mAb, C42D8 #9751, Cell Signaling Technology	5µL – Histone ChIP 0.25µL – Low-cell number
Anti-H3K27Ac	Rabbit polyclonal, #ab4729, Lot# GR276934-1, Abcam	5µg – Histone ChIP 0.25µg – Low-cell number

Table 15: Primers used for ChIP-qPCR

Primer	Sequence	Amp factor
Actin_AG_fwd Actin_AG_rev	AGTGTGGTCCTGCGACTTCTAAG CCTGGGCTTGAGAGGTAGAGTGT	1.98
hMYC_PROM_FW hMYC_PROM_Rev	CCTCCCATATTCTCCCGTCTAGCACCTT TTTGCGCCCTGTGGCGCCGGTTTGCA	2.08
hPRDM1_PROM_FW hPRDM1_PROM_Rev	GGACAGAGGCTGAGTTTGAAGA CGCCATCAGCACCAGAATC	2.11
hPRDM1_SuperEn1_FW hPRDM1_SuperEn1_Rev	GGGTTAGGGGAAGGAATGTT GTGTGGGAACATGATGCTTG	1.78
hPRDM1_SuperEn2_FW hPRDM1_SuperEn2_Rev	ATTACGGGCAGCTAAAGCAA CCAGCTCAGGATGGAGAAAG	1.97
hXBP1_SuperEn_Fw hXBP1_SuperEn_Rev	TTGCTGTGCAAACAATAGCC GGGCCTTCAGGTGCTATTTA	1.95
hTYRi4_Fw hTYRi4_Rev	CCATTCTGCCAATGGAATTT AAGAACAGCATGCACACAGG	2.02
hPRDM16_PROM_FW hPRDM16_PROM_Rev	CCGCCAAGCTACTCTGTTTT AAGGCAAGTGGCTCTTTCAA	2.07

3.10 Illumina® Sequencing Library Preparation

3.10.1 PolyA RNAseq Library Preparation

We isolated total RNA using TRI-reagent (#AM9738, Thermo Fisher Scientific) according to the manufacturer's instructions, then treated with HL-dsDNase (#70800-201, ArcticZymes) in the presence of 2.85mM $MgCl_2$ for

10 min at 37˚C. We purified the RNA using the RNeasy MinElute Cleanup Kit (#74204, Qiagen) according to the manufacturer's instructions. RNA quantity and quality were assessed first using the Nanodrop 1000 spectrophotometer, then using the RNA 6000 Nano kit (#50671511, Agilent) with the 2100 Bioanalyzer Instrument (#G2939BA, Agilent). We prepared RNAseq libraries using the NEBNext® Ultra™ Directional RNA Library Prep Kit for Illumina® (#E7420S, New England Biolabs) in combination with the NEBNext® Poly(A) mRNA Magnetic Isolation Module (#E7490S, New England Biolabs), NEBNext® Multiplex Oligos for Illumina® (Index Primers Set 1) (#E7335S, New England Biolabs) and NEBNext® Multiplex Oligos for Illumina® (Index Primers Set 2) (#E7500S, New England Biolabs). We carried out the protocol according to the manufacturer's instructions, with 15 cycles of PCR.

3.10.2 Total RNAseq Library Preparation

We suspended the cell pellet (typically 1 x 10^5 – 5 x 10^5 cells) in TRI-reagent (#AM9738, Thermo Fisher Scientific) and stored at -80˚C. On day of isolation, we allowed the samples to reach room temperature and then processed them with 0.2 volumes of chloroform, shook them vigorously for 30 seconds and allowed them to rest at room temperature for 2 min. The samples were centrifuged 12000 x*g* for 15 minutes at 4˚C and the upper aqueous phase was transferred to a fresh tube. An equal volume of 70% ethanol was added to this sample and mixed well. This sample was added to pre-conditioned column from the Arcturus PicoPure RNA Isolation Kit (#KIT0204, Thermo Fisher Scientific). We centrifuged the column for 2 min at 100 x*g* and discarded the flow-through. This was repeated until the entire sample had been processed through the column. The remainder of the protocol was carried out according to the manufacturer's instructions, without the DNase I treatment. RNA quantity and quality were measured as above using the Nanodrop 1000 spectrophotometer and the 2100 Bioanalyzer instrument. The total RNA was then used for library preparation with the Ovation® Universal RNA-seq System (#0343, NUGen Technologies Inc.). As a part of the procedure, ribosomal RNAs and immunoglobulin transcripts were depleted. The protocol was carried out according to the manufacturer's instructions, with the only exception being that fragmentation was performed with the Bioruptor® Standard (#UCD-200, Diagenode) using 4 x 5 minutes sonication with 30 sec on, 30 sec off. We performed library amplification over 15 PCR cycles.

3.10.3 Preparation and assessment of Serapure beads

We prepared Serapure beads using 1mL of SeraMag SpeedBeeds (#09-981-123, Fisher Scientific). SeraMag SpeedBeads were placed in a 1.5mL microcentrifuge tube and placed on a magnet. The supernatant was removed and the beads were washed off the magnet with 1mL TE buffer (10mM Tris pH8, 1mM EDTA). The tube containing the beads was returned to the magnet and supernatant was removed. The beads were washed again as before, then fully resuspended in 1mL TE buffer away from the magnet. We prepared a PEG-8000 solution by mixing 9g PEG-8000 in solution with 1M NaCl, 10mM Tris pH8, 1mM EDTA, and 0.055% (v/v) tween-20 to a total 49mL volume. We then added the previously prepared beads in TE buffer to the PEG-8000 solution and mixed well. Various volumes of Serapure beads were tested for their ability to purify the GeneRuler DNA ladder mix (#SM0331, Thermo Fisher Scientific), compared to AMPure XP beads (#A63880, Beckman Coulter).

3.10.4 Whole-genome amplification of ChIP DNA

We performed whole genome amplification (WGA) of ChIP DNA using components of the GenomePlex Single Cell Whole Genome Amplification Kit (#WGA4, Sigma) according to the protocol used in (Ng et al., 2013). The ChIP DNA was suspended in 5µL nuclease free water and mixed with 1µL of the library preparation buffer and 0.5µL stabilisation solution. The mixture was incubated for 2 min at 95˚C, then quickly chilled on ice-water. We combined the mixture with 0.5µL of the library synthesis enzyme mix and incubated it with the following temperature program:

1. 16˚C for 20 min
2. 24˚C for 20 min
3. 37˚C for 20 min
4. 75˚C for 5 min
5. Hold at 4˚C

We then combined the ChIP DNA mixture with 25µL NEB HiFi HotStart Q5 PCR master mix (#M0543S, New England Biolabs), 5µM BpmI-primer (CCGGCCCTGGAGTGTTGGGTGTGTTTGG) and 15.5µL nuclease free water to a final volume of 50µL. The ChIP DNA was then amplified using the program shown in Table 16.

Table 16: WGA cycling conditions

Temperature	Time	
98˚C	3 min	
98˚C	10 sec	x 5 cycles
65˚C	30 sec	
72˚C	1 min	
72˚C	7 min	
4˚C	Hold	

We purified the amplified ChIP DNA using 2.7x volumes of pre-prepared Serapure beads. Adaptor digestion was then performed to remove WGA adaptors from the amplified DNA prior to sequencing library preparation. We mixed the additional BpmI oligos (BpmI_2top_GG: ATGCTCAGCTGGAGGG, BpmI_2btm: CTCCAGCTGAGCAT) at a final concentration of 43nM with 4µL of 10x T4 DNA ligase reaction buffer (#B0202S, New England Biolabs) and 2µL T4 polynucleotide kinase (#M0201S, New England Biolabs) for phosphorylation. This mixture was incubated at 37˚C for 30 min.

In a fresh tube containing 50µL of the previously purified and amplified ChIP DNA, we mixed 6µL of NEB buffer 3 (#B7003S, New England Biolabs) with 0.6µL of BSA (#B9000S, New England Biolabs) and 4µL of the BpmI restriction enzyme (#R0565S, New England Biolabs). This mixture was incubated at 37˚C for 2 h. We then purified the digested DNA using 2.7x volumes of Serapure beads and eluted in 40µL 10mM Tris pH8. We added the previously phosphorylated BpmI oligo mix (2.5µL) to the ChIP DNA along with 5µL of 10x T4 DNA ligase reaction buffer and 5µL of T4 DNA ligase (#M0202S, New England Biolabs). We incubated this mixture at 16˚C for 2 h to allow the ligation reaction to take place. The ligation reaction was then purified using 2.7x volumes of Serapure beads and eluted in 50µL 10mM Tris pH8. We then mixed the ligated ChIP DNA with 6µL NEB buffer 3, 0.6µL of BSA, and 4µL of BpmI and incubated overnight at 37˚C for complete digestion and removal of adaptors. Finally, we purified the digested ChIP DNA once again using 2.7x volumes of Serapure beads.

3.10.5 ChIPseq Library Preparation

We prepared Sequencing libraries from ChIP DNA using the NEBNext® Ultra™ DNA Library Prep Kit for Illumina® (#E7370S, New England Biolabs) with the Multiplex Oligos for Illumina as described above. We first quantified the ChIP DNA using the Qubit dsDNA HS Assay Kit (#Q32854, Thermo Fisher Scientific) with Qubit Assay Tubes (#Q32856, Thermo Fisher Scientific) in the Qubit Fluorometer (Thermo Fisher Scientific). We normalised the ChIP DNA quantities to 2ng per library. The libraries were prepared according to the manufacturer's instructions, with minor modifications. The NEBNext Adaptor for Illumina was diluted 20x in 10mM Tris HCl pH 8, and adaptor ligation was carried out for 60 min rather than 15 min. Enrichment of adaptor ligated DNA was carried out over 12 PCR cycles. Following PCR amplification, we performed size-selection with 0.6 volumes of AMPure XP beads to remove larger fragments. Libraries were then cleaned up 2x with 0.9 volumes of AMPure XP beads.

3.10.6 Sequencing Library Quantification

We assessed the sequencing libraries for quantity and size distribution using the High Sensitivity DNA Kit (#5067-4626, Agilent) with the 2100 Bioanalyzer. Further library quantification was carried out using the Universal library quantification kit for Illumina (#KK4824, KAPA, Roche Sequencing) according the manufacturer's protocol. Library concentrations were normalised to 10nM prior to sequencing.

3.10.7 Illumina Sequencing

For the polyA RNAseq samples as well as the transcription factor and histone ChIPseq samples, sequencing was carried out according to the following method. Samples were pooled together at equimolar ratios and clustered on paired-end (PE) flowcells using a cBot instrument (Illumina). The v4 SBS sequencing kits were used to perform sequencing to the Illumina HiSeq 2500 with a readlength of 2x125 cycles plus a 6 base index read. Primary processing was carried out using HiSeq Control Software (Illumina) and Real Time Analysis software (Illumina). Reads were demultiplexed and FASTQ files were generated using scripts from Illumina (bcl2fastq v.1.8).

For the total RNAseq and low-cell number histone ChIPseq samples, sequencing was carried out according to a second method. Samples were pooled together at equimolar ratios and clustered on paired-end (PE) HiSeq X version 2.5 flowcells, using a cBot instrument (Illumina). The v2.5 SBS sequencing kits were used for sequencing with a readlength of 2x125 cycles

plus a 6 base index read. Primary processing was carried out using HiSeq Control Software (Illumina) and Real Time Analysis software (Illumina). Reads were demultiplexed and FASTQ files were generated using scripts from Illumina (bcl2fastq2).

3.11 Bioinformatics Analyses

3.11.1 PolyA RNAseq data analysis

We assessed the read quality using FastQC. (https://www.bioinformatics.babraham.ac.uk/projects/fastqc/) with the default parameter settings. We then trimmed the RNAseq raw reads using Trim Galore (https://www.bioinformatics.babraham.ac.uk/projects/trim_galore/) with the setting for paired-end reads used along with default settings. We performed the initial genome alignment using STAR aligner (Dobin et al., 2013), aligning trimmed reads to the hg38 genome with default settings plus the addition of a command to generate sorted bam files from the aligned reads. The sorted bam files were converted to wig files in STAR using the "inputAlignmentsFromBAM" mode with the setting for stranded RNAseq, so that they could be visualized on the UCSC genome browser. The trimmed reads were then pseudoaligned to the Ensembl hg38 transcriptome and quantified using Kallisto with the "—rf-stranded" command added into the default settings (Bray et al., 2016). We performed differential expression analysis using the likelihood ratio test in Sleuth (Pimentel et al., 2017), on a gene level, with a q-value of 0.05, and a $\log_2$ fold-change of ±0.3 as a significance cutoff. Volcano plots were produced using the ggplot2 package in R (Wickham, 2016). We tested overlapping genes for significance using Fisher's exact test in the GeneOverlap package in R (http://shenlab-sinai.github.io/shenlab-sinai/). Gene set enrichment analysis (GSEA) using the Hallmarks collection of gene sets was run in pre-ranked mode using a list of all detected genes (Liberzon et al., 2015; Subramanian et al., 2005). The rank value was calculated as $-\log_{10}$(q-value) × (sign of fold change), and the genes were ranked with the highest value at the top of the list. We used the classic enrichment statistic setting with 1000 permutations, a maximum size of 5000, minimum size of 15, and the "meandiv" normalisation mode. Heatmaps of RNAseq data were prepared using the heatmap.2 function in the gplots package in R (Gregory R. Warnes, 2017). For the B cell and apoptosis gene sets, we performed clustering using the hclust function "complete linkage" method, with the dendrogram produced for the rows. All scripts and codes can be found in Appendix I.

3.11.2 ChIPseq data analysis

Raw ChIPseq reads were assessed for quality and trimmed as above using FastQC and Trim Galore with the default settings. The trimmed reads were aligned to the hg38 genome using Bowtie2 using the default settings (Langmead & Salzberg, 2012). Sam files were merged and converted to bam files using Samtools (Li et al., 2009). We first tried MACS1.4 for peak calling and to produce wig files using the "-w -S" command with otherwise default parameters, however were unhappy with the peak calling for the H3K27me3 mark, so we moved to using MACS2 instead. We called peaks using MACS2 with q-value cutoffs of 0.01, 0.001 and 0.0001 with the "BAMPE" command for paired-end sequences and otherwise default settings (Zhang et al., 2008). We used the WigToBigWig program from UCSC to convert wig files to BigWig files which were then visualised by loading into the UCSC genome browser (Kent et al., 2002).The peaks were filtered using a list of regions containing centromeres and amplification artefacts (see Appendix Table II) with the BedOps package in order to avoid considering sequencing artefacts as peaks in downstream analyses (Reynolds et al., 2012). The DiffBind package in R was used to combine biological replicates into peak lists, such that only peaks called in both replicates were retained (Ross-Innes et al., 2012; Stark, 2011). Enrichment over BLIMP1 peaks was calculated and mapped using Deeptools (Ramírez et al., 2016). Firstly, we generated a matrix of ChIPseq signal enrichment over BLIMP1 binding sites using a bed file containing the binding sites with a BigWig file generated from MACS1.4 using two ChIPseq replicates in combination. We then plotted a heatmap and profile for these computed regions. We tested overlapping regions for significance using the hypergeometric test in the ChIPPeakAnno package in R (Zhu et al., 2010). Overlapping genes were tested for significance using Fisher's exact test in the GeneOverlap package in R (http://shenlab-sinai.github.io/shenlab-sinai/). De novo motif enrichment analysis was performed using MEME ChIP with the input comprising fasta files generated from the regions specified in our peak lists (Machanick & Bailey, 2011). We used the human and mouse HOCOMOCO v11 set of motifs to search for enrichment, with default settings (Kulakovskiy et al., 2018). All scripts and codes can be found in Appendix I.

4 Data availability

Raw RNAseq and ChIPseq data are available at http://www.ebi.ac.uk/arrayexpress/experiments/E-MTAB-7739 under the accession code: E-MTAB-7739.

Differentially expressed genes from RNAseq experiments as well as peak and gene lists for ChIPseq experiments are attached as additional files, listed as additional file tables 1-16:

Table 1: Differentially expressed genes - BLIMP1 KD RNAseq in RPCI-WM1

Table 2: Differentially expressed genes - Tazemetostat RNAseq in RPCI-WM1

Table 3: BLIMP1 peaks in RPCI-WM1

Table 4: Genes assigned to BLIMP1 peaks in RPCI-WM1

Table 5: H3K27me3 peaks in RPCI-WM1

Table 6: Genes assigned to H3K27me3 peaks in RPCI-WM1

Table 7: BLIMP1 peaks in OPM-2

Table 8: Genes assigned to BLIMP1 peaks in OPM-2

Table 9: BLIMP1 peaks in NCI-H929

Table 10: Genes assigned to BLIMP1 peaks in NCI-H929

Table 11: H3K27me3 peaks in OPM-2

Table 12: Genes assigned to H3K27me3 peaks in OPM-2

Table 13: H3K27me3 peaks in NCI-H929

Table 14: Genes assigned to H3K27me3 peaks in NCI-H929

Table 15: EZH2 peaks in NCI-H929

Table 16: Genes assigned to EZH2 peaks in NCI-H929

5 Results

5.1 BLIMP1 promotes Waldenström's macroglobulinemia cell survival

BLIMP1 is expressed in at least a subset of WM lymphoplasmacytic cells (Roberts et al., 2013; Zhou et al., 2014). However, it has contrasting roles as a tumour suppressor in DLBCL and a pro-survival factor in multiple myeloma (Calado et al., 2010; Lin et al., 2007; Mandelbaum et al., 2010; Pasqualucci et al., 2006). Because WM is likely derived from a stage somewhere in between the cellular origins of DLBCL and myeloma, we were interested to investigate if BLIMP1 may also play a role in the disease. We began by comparing the expression of BLIMP1 in the WM cell lines RPCI-WM1, MWCL-1 and BCWM.1 to the multiple myeloma cell line OPM-2 by immunofluorescence staining (Figure 3A). BLIMP1 was present in all of the cell lines tested, and had more uniform expression across individual cells in the OPM-2 and RPCI-WM1 cell lines, with 93% and 88% of the cells respectively expressing high BLIMP1 levels. In contrast, the MWCL-1 and BCWM.1 cell lines showed a variable pattern of expression, with 43% and 22% of cells with high BLIMP1 expression, repectively. In order to determine the role of BLIMP1 in WM, we generated RPCI-WM1 cells with stable doxycycline (dox)-inducible overexpression of two artificial miRNAs targeting the *PRDM1* transcript (*PRDM1-miR#1* and *PRDM1-miR#2*), and a non-targeting control miRNA (*NT-miR*). Both *PRDM1*-targeting miRNAs induced a significant decrease in BLIMP1 protein expression in the RPCI-WM1 cell line following 48h of dox induction (Figure 3B). In addition, we generated MWCL-1 cells with stable overexpression of the *PRDM1-miR#1* and *NT-miR*, and found that the *PRDM1-miR#1* led to a significant knock-down (KD) of BLIMP1 protein, albeit to a lesser extent than seen for the RPCI-WM1 cell line (Figure 3C).

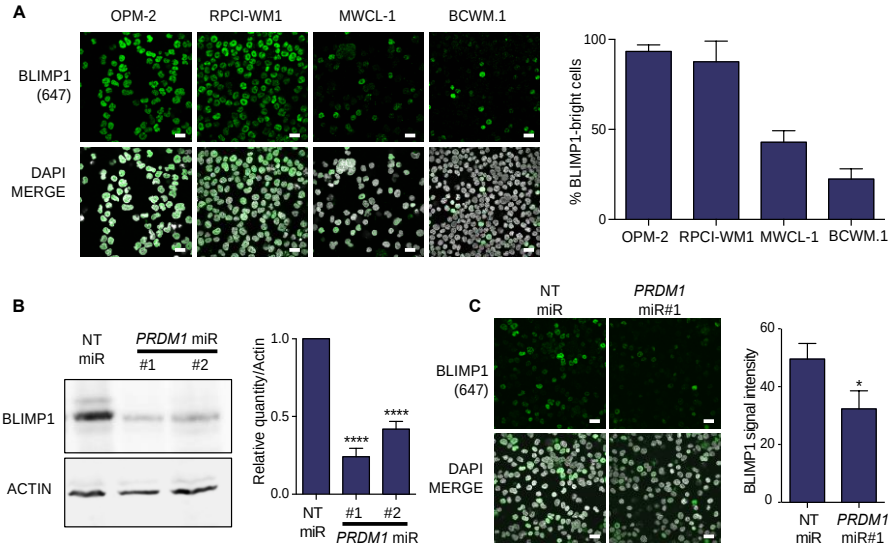

Figure 3: BLIMP1 is expressed in WM cells

(A) BLIMP1 expression in myeloma cell line OPM-2 and in WM cell lines RPCI-WM1, MWCL-1 and BCWM.1 as detected by immunofluorescence staining, with bar graph representing percentage of BLIMP1^{bright} cells. Scale bars represent 20µm. **(B)** Immunoblot of BLIMP1 expression following 48h dox induction of RPCI-WM1 cells expressing *NT-miR*, *PRDM1-miR#1* or *PRDM1-miR#2*, with bar graph representing the quantity of BLIMP1 relative to actin; ****p < 0.0001. **(C)** Immunofluorescence staining of BLIMP1 following 48h dox induction in MWCL-1 cells expressing *NT-miR*, *PRDM1-miR#1* or *PRDM1-miR#2*, with cell profiler quantification; *p = 0.0228.

Following BLIMP1 KD, we observed a decrease in the survival of both cell lines, with 62% of RPCI-WM1 cells and 71% of MWCL-1 cells viable following 48h of dox induction (Figure 4A). The proportion of apoptotic cells was also significantly increased following BLIMP1 KD in the RPCI-WM1 cell line, with an increase of 2.64-fold for *PRDM1-miR#1* (p = 0.0004) and 2.25-fold for *PRDM1-miR#2* (p = 0.0071) (Figure 4B). There was trend towards increased apoptosis in the MWCL-1 cell line, although this was not statistically significant (Figure 4C).

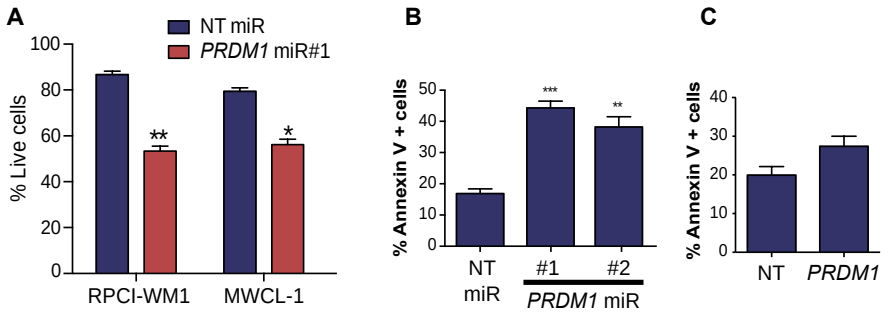

Figure 4: BLIMP1 promotes viability of WM cells

(A) Percentage of live cells as determined by Trypan blue exclusion assay in the RPCI-WM1 and MWCL-1 cell lines. RPCI-WM1, **p = 0.0019; MWCL-1, *p = 0.0162. **(B)** Annexin V staining of dox-induced RPCI-WM1 cells with NT-miR, *PRDM1-miR#1* or *PRDM1-miR#2*; ***p = 0.0004; **p = 0.0071. **(C)** Annexin V staining of dox-induced MWCL-1 cells with NT-miR or *PRDM1-miR#1*; p = 0.0572.

To test the specificity of the *PRDM1-miR#1*, we then performed genetic complementation using lentiviral ectopic expression of a *PRDM1-miR#1*-resistant BLIMP1-EGFP or EGFP alone (Lois et al., 2002) (Figure 5A). Ectopic expression of BLIMP1 was able to rescue the effects of BLIMP1 KD on cell death compared to the EGFP alone, with a significant increase in the proportion of live cells following 2 days and 5 days of dox induction (Figure 5B). This was also demonstrated by an increase in the reduction capability of the cells with *PRDM1-miR#1* transduced with BLIMP1-EGFP (Figure 5C). This demonstrates that the cell-death effects of the *PRDM1-miR#1* are not due to an off-target effect, and verifies the specificity of the miRNA. In summary, the above results demonstrate that BLIMP1 promotes the survival of WM cells, potentially through the repression of apoptosis.

5.2 BLIMP1 maintains EZH2 protein levels

Earlier work in primordial germ cells showed an overlap in the binding sites of BLIMP1 and EZH2 (Kurimoto et al., 2015; Magnúsdóttir et al., 2013), and more recently in mouse plasmablasts, BLIMP1 and EZH2 were shown to physically interact (Minnich et al., 2016). Due to this evidence, we wanted to study the interplay of the two factors in WM. First, we tested the levels of EZH2 following BLIMP1 KD, and surprisingly observed a marked decrease in the EZH2 protein (Figure 6A). This was replicated in the multiple myeloma cell line OPM-2 with the *PRDM1-miR#1* (Figure 6B). To ensure that the loss of EZH2 was not an off-target effect of the miRNA, we performed genetic complementation as above using lentiviral ectopic expression of BLIMP1-EGFP and observed an increase in the level of EZH2 protein compared to BLIMP1 KD cells transduced with EGFP alone (Figure 6C).

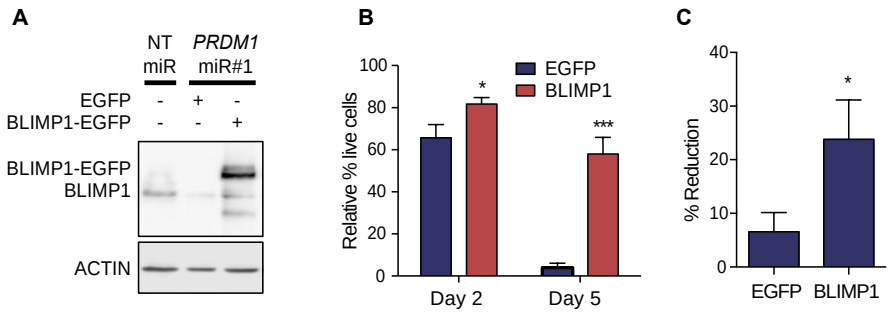

Figure 5: Restoring BLIMP1 levels rescues the cell death phenotype of BLIMP1 KD

(A) Immunoblot depicting lentiviral ectopic expression of EGFP or BLIMP1-EGFP in the RPCI-WM1 *PRDM1-miR#1* cells, next to the RPCI-WM1 *NT-miR* cells. **(B)** The percentage of live RPCI-WM1 *PRDM1-miR#1* cells with ectopic EGFP or BLIMP1-EGFP expression determined by the Trypan blue exclusion assay normalised to the percentage of live cells following transduction of RPCI-WM1 *NT-miR* cells with EGFP or BLIMP1-EGFP. Day 2, p = 0.0165; Day 5, p = 0.0003. **(C)** Per cent reduction as measured by resazurin assay for RPCI-WM1 *PRDM1-miR#1* cells with EGFP or BLIMP1-EGFP, five days after dox induction. p = 0.0208. All p-values as determined by student's two-tailed t-test. All graphs plotted as mean of three independent experiments, with error bars representing standard deviation.

Next, we were interested in the mechanism behind the loss of EZH2 with BLIMP1 KD. We performed qPCR to test the expression of *PRDM1* and *EZH2* following BLIMP1 KD. In the RPCI-WM1 cell line, we observed somewhat of an increase in the *PRDM1* transcript levels, which fits with the model of BLIMP1 autoregulation, whereby BLIMP1 binds within intron 2 of the *PRDM1* gene for transcriptional repression, and BLIMP1 knock-out leads to increased production of the *Prdm1* transcript (Kallies et al., 2006; Magnúsdóttir et al., 2007), although this was highly variable (Figure 7A). Interestingly, *EZH2* mRNA levels were not decreased following BLIMP1 KD in the RPCI-WM1 cells (Figure 7A). This indicates that BLIMP1 KD does not affect *EZH2* steady state mRNA levels. In the OPM-2 cell line, there appeared to be a trend towards decrease in the transcript levels of *EZH2*, however this was not statistically significant (p = 0.067) (Figure 7B). In order to determine if BLIMP1 is affecting EZH2 levels via the proteasome, we treated the RPCI-WM1 *NT-miR* or *PRDM1-miR#1* cells with the proteasome inhibitor MG-132 for 4h following 20h of dox induction (Figure 7C). While the result was complicated by EZH2 being decreased by proteasome inhibition in the *NT-miR* cells, when we looked at the ratio of EZH2 comparing MG-132 treated cells to the vehicle control, we observed an increase in the relative EZH2 levels (Figure 7D). This suggested that proteasome inhibition is able to restore the loss of EZH2 induced by BLIMP1 KD. Thus, BLIMP1 is likely maintaining EZH2 in the RPCI-WM1 cell line by inhibition of its proteasomal degradation

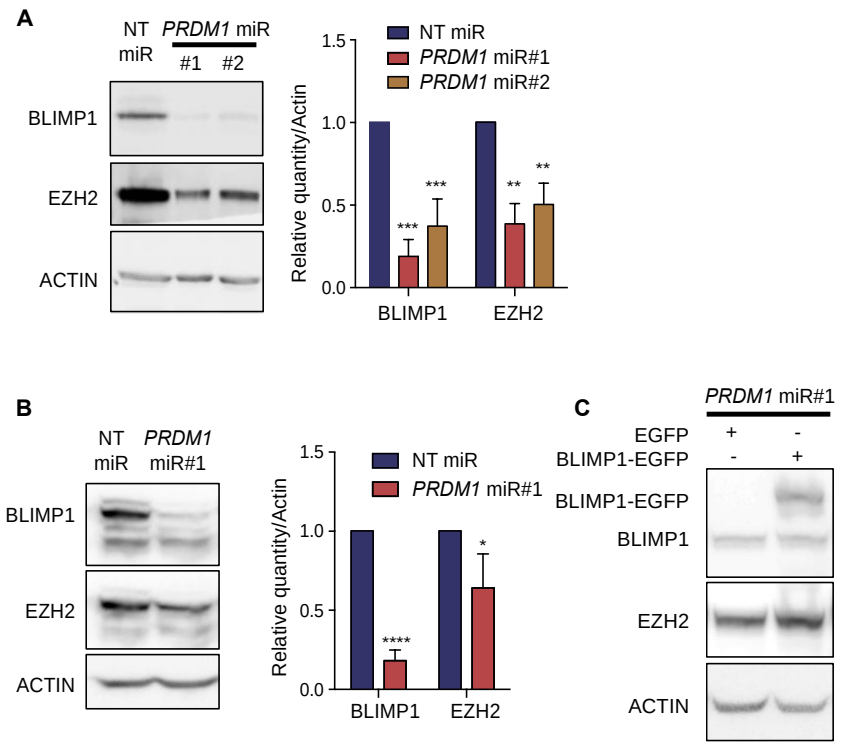

Figure 6: BLIMP1 maintains EZH2 protein levels

(A) Immunoblot of BLIMP1 and EZH2 expression following 48h dox-induction of RPCI-WM1 cells expressing *NT-miR*, *PRDM1-miR#1* or *PRDM1-miR#2*, with quantification of signal relative to actin in bar plot; ***p = 0.0002; ***p = 0.001; **p = 0.0027. **(B)** Immunoblot of BLIMP1 and EZH2 expression following 48h dox-induction of OPM-2 cells expressing *NT-miR* or *PRDM1-miR#1*, with quantification of signal relative to actin in bar plot; ****p < 0.0001; *p = 0.016. **(C)** Immunoblot of BLIMP1 and EZH2 expression following 24h dox-induction of RPCI-WM1 cells expressing *PRDM1-miR#1*, transduced with EGFP or BLIMP1-EGFP.

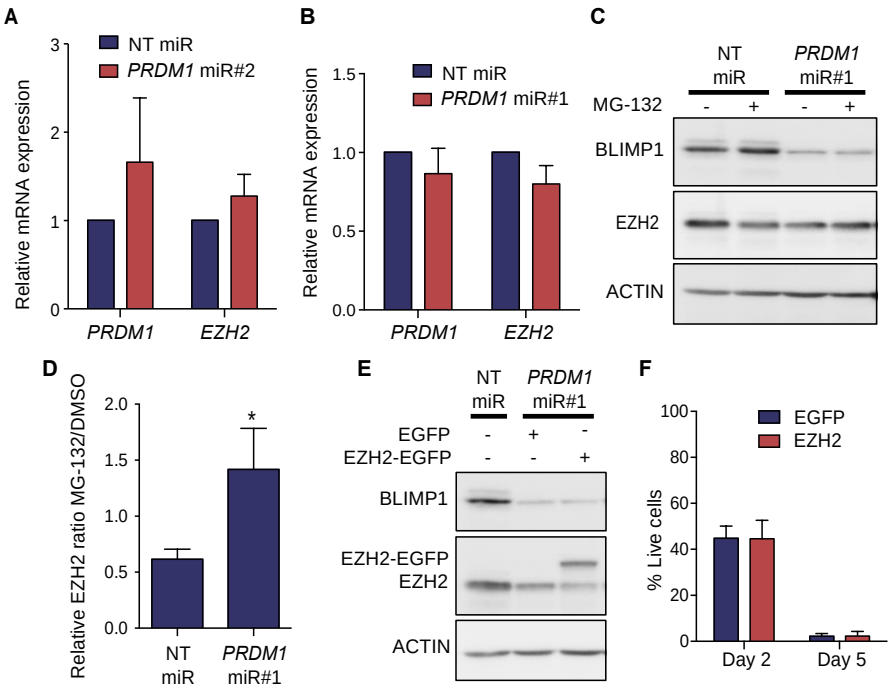

Figure 7: BLIMP1 maintains EZH2 via the proteasome

(A) RT-qPCR results depicting relative mRNA expression of *PRDM1* and *EZH2* normalised to *PPIA* and *ACTB* in the RPCI-WM1 cell line and **(B)** in the OPM-2 cell line. **(C)** Immunoblot of BLIMP1 and EZH2 expression following 24h dox-induction of RPCI-WM1 cells expressing *NT-miR* or *PRDM1-miR#1* treated with DMSO or 5µM MG-132 for 4h. **(D)** The ratio of EZH2 expression relative to actin for cells treated with MG132 divided by DMSO for RPCI-WM1 *NT-miR* and *PRDM1-miR#1* cells as in Fig. 7C; p = 0.0214. **(E)** Immunoblot of BLIMP1 and EZH2 expression following 48h dox-induction of RPCI-WM1 *NT-miR* cells or *PRDM1-miR#1* cells transduced with EGFP or EZH2-EGFP. **(F)** Percentage of live cells as determined by Trypan blue exclusion assay in the RPCI-WM1 *PRDM1-miR#1* cells transduced with EGFP or EZH2-EGFP.

.

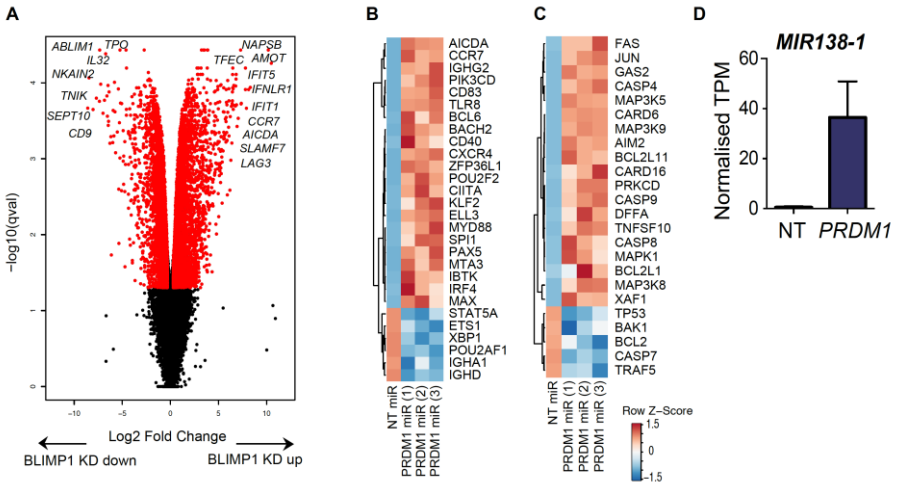

Figure 8: BLIMP1 KD induces large transcriptional changes

(A) RNAseq results for 48h dox-induced RPCI-WM1 cells comparing *PRDM1-miR#2* to *NT-miR*. Values are plotted as $\log_2$ fold change vs. $-\log_{10}$(qvalue). Red indicates those genes with a q-value ≤ 0.05 and a $\log_2$ fold change ≤ -0.3 or ≥ 0.3. Heat maps depicting the Z-score of the $\log_2$ fold change comparing *PRDM1-miR#2* to *NT-miR* for three independent replicates looking at **(B)** B cell genes and **(C)** apoptosis genes. **(D)** Graph of RNAseq results depicting normalised transcripts per million (TPM) values for *miR138-1* in RPCI-WM1 cells with *NT-miR* and *PRDM1-miR#2*. All RNAseq experiments were performed as three biological replicates.

Because EZH2 can function to prevent apoptosis in cancer cells (Wu et al., 2009), we wanted to test if the repression of cell death by BLIMP1 was mediated through maintenance of EZH2. We performed a genetic complementation experiment using lentiviral ectopic expression of EZH2-EGFP or EGFP alone in the cells with BLIMP1 KD (Figure 7E). We found that restoring the level of EZH2 in the RPCI-WM1 cells with BLIMP1 KD did not lead to increased cell viability following 2 days and 5 days of dox induction (Figure 7F). Thus, the pro-survival effect of BLIMP1 is not due to its maintenance of EZH2.

5.3 BLIMP1 KD induces large transcriptional changes

We next sought to delve deeper into the molecular mechanisms driving the cell death phenotype and reduction of EZH2 following BLIMP1 KD. We were also interested to examine the effects on known BLIMP1 transcriptional targets, and to identify novel targets. To achieve this, we performed transcriptome profiling of the RPCI-WM1 cells comparing *NT-miR* and

PRDM1-miR#2 following 48h of miR induction with dox. We used a q-value cutoff of 0.5 and a $\log_2$ fold-change cutoff of ±0.3 to identify 7831 differentially expressed genes (Figure 8A), 4260 of which were induced and 3571 of which were repressed by BLIMP1 KD. The significantly differentially expressed genes are presented in Additional file Table 1.

Because BLIMP1 is known to repress the B cell transcriptional program during plasma cell differentiation (Kallies et al., 2004; Minnich et al., 2016; Shaffer et al., 2002; Shapiro-Shelef et al., 2003), we wanted to test if this was also taking place in WM, where there is a disruption in the differentiation process. Known BLIMP1 targets comprising B cell identity genes including *CIITA* (Chen et al., 2007; Piskurich et al., 2000), *PAX5* (Lin et al., 2002), *SPIB* and *BCL6* (Shaffer et al., 2002) showed significantly increased expression following BLIMP1 KD (Figure 8B). The expression of other BLIMP1 targets including *MYC* (Lin et al., 1997) and *ID3* (Shaffer et al., 2002) was not changed, but the gene encoding the MYC interaction partner MAX was increased following BLIMP1 KD.

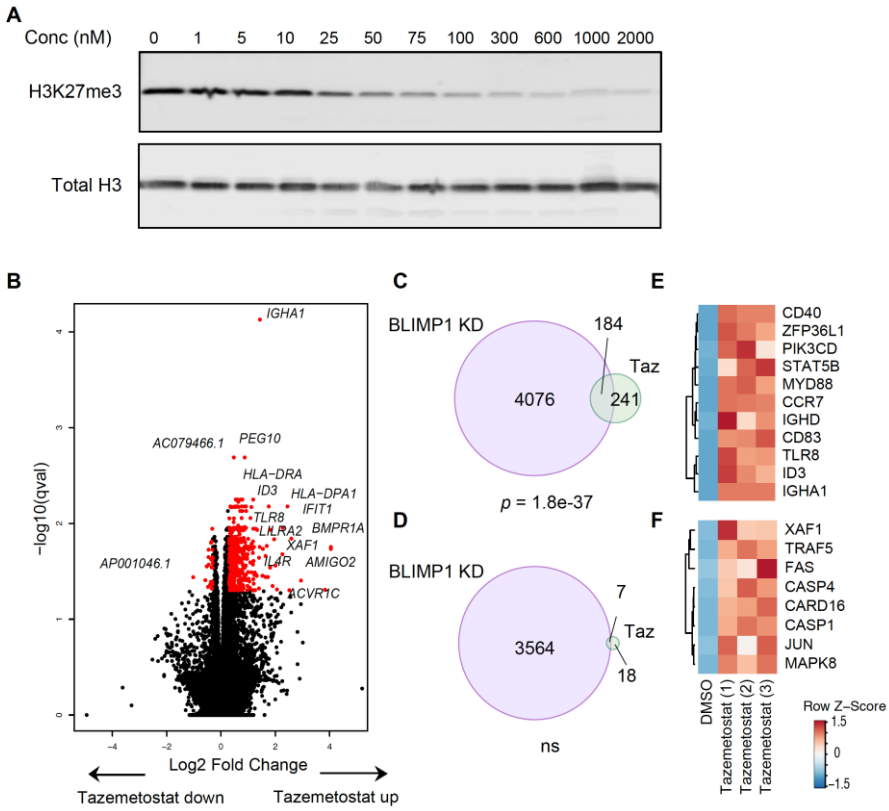

Figure 9: BLIMP1 and EZH2 share many transcriptional targets

(A) Western blot of histone extracts from RPCI-WM1 cells treated with varying concentrations of tazemetostat for 48h. H3K27me3 and total H3 were detected by antibody staining. **(B)** RNAseq results for RPCI-WM1 cells treated for 48h with 300nM tazemetostat compared to vehicle control (DMSO). **(C)** Overlapping genes with increased expression following *PRDM1* KD or tazemetostat treatment. **(D)** Overlapping genes with decreased expression following *PRDM1* KD or tazemetostat treatment. Overlaps tested using Fisher's exact test. Heat maps depicting the Z-score of the $\log_2$ fold change comparing tazemetostat treatment to DMSO for three independent replicates looking at **(E)** B cell genes and **(F)** apoptosis genes. All RNAseq experiments were performed as three biological replicates.

Surprisingly the gene encoding the transcription factor *IRF4*, which is necessary for survival of multiple myeloma cells (Shaffer et al., 2008), and has been shown to be activated downstream of BLIMP1 (Minnich et al., 2016), was actually induced downstream of BLIMP1 KD here, indicating that it is repressed by BLIMP1. This shows an interesting contradiction between the regulation of *IRF4* by BLIMP1 in the RPCI-WM1 cell line compared to

mouse plasmablasts. Interestingly, the gene encoding the inhibitor of BTK, *IBTK* was induced by BLIMP1 KD (Figure 8B). This could be a mechanism for BLIMP1 to maintain BTK activity, which is a target of the effective WM drug Ibrutinib (Gertz, 2019). In summary, BLIMP1 is repressing the majority of its known B cell targets, with some exceptions in the RPCI-WM1 cell line. In order to understand the apoptosis-promoting effect of BLIMP1 KD, we next examined the expression of apoptosis mediators. Consistent with our earlier results, many of these genes had significantly increased expression following BLIMP1 KD, including *MAP3K5* (*ASK1*), *XAF1*, *CASP4*, *CASP8*, *FAS*, *DFFA*, *JUN* and *BCL2L11* (*BIM*) (Figure 8C). Interestingly, we also observed a significant increase in expression of *miR-138-1* (Figure 8D), which is known to target *EZH2* in several cancers (Liang et al., 2014; Zhang et al., 2013; Zhu et al., 2016). This could be another mechanism by which BLIMP1 maintains EZH2 protein levels, in contrast to our results using the proteasome inhibitor. Futher experiments would be needed to determine if *miR-138-1* also contributes to the maintenance of EZH2 by BLIMP1. Thus, BLIMP1 KD leads to many significant transcriptional changes in the RPCI-WM1 cell line, which point to different biological roles.

5.4 BLIMP1 and EZH2 share transcriptional targets and regulate overlapping pathways

In order to address Aim 2 of the project, investigating the possible interplay of BLIMP1 and EZH2 in WM, we sought to investigate the overlapping transcriptional targets of BLIMP1 and EZH2 in WM. First, we treated RPCI-WM1 cells with a range of concentrations of the EZH2 inhibitor tazemetostat to test if the H3K27me3 mark could be depleted within 48 h. Indeed, 48 h of treatment resulted in dose-dependent decreases in H3K27me3 (Figure 9A). RPCI-WM1 cells were then treated with 300 nM tazemetostat, or DMSO prior to transcriptome profiling. Using a q-value cutoff of 0.05 and a $\log_2$ fold-change cutoff of ±0.3 as above, we identified 450 differentially expressed genes comparing tazemetostat treatment to DMSO. This included 425 induced genes and 25 repressed genes. The list of significantly differentially expressed genes can be found in Additional file Table 2. However, there was a smaller amplitude of change compared to the changes seen with BLIMP1 KD (Figure 9B). Most of the differentially expressed genes following tazemetostat treatment had a $\log_2$ fold change within ±2, whereas the $\log_2$ fold change of differentially expressed genes following BLIMP1 KD was frequently greater than ±2. Next, we compared those genes that had significantly increased expression following BLIMP1 KD to those genes with significantly increased expression following tazemetostat treatment. There was a statistically significant overlap of 184 genes between these two groups,

as determined by Fisher's exact test ($p = 1.8 \times 10^{-37}$) (Figure 9C). However, for genes repressed in the two groups, there was very little overlap, and this was not statistically significant, in line with the small number of genes repressed by tazemetostat treatment (Figure 9D). Fewer B cell genes were induced by tazemetostat treatment than by BLIMP1 KD, but those affected included *PIK3CD*, *CCR7* and *ID3* (Figure 9E). PIK3CD and ID3 are important for B cell responses (Clayton et al., 2002; Pan et al., 1999), while CCR7 is important for homing of B cells within secondary lymphoid organs (Förster et al., 1999). We also checked the expression of apoptosis mediators, but were not expecting to see many changes, as restoring EZH2 did not rescue the cell death phenotype of BLIMP1 KD (Figure 7F). Surprisingly, while fewer genes were induced by tazemetostat than by BLIMP1 KD, there were still a number of apoptosis mediators, including *XAF1*, *CASP4*, *FAS* and *JUN* (Figure 9F).

To address the third aim of the project, identifying pathways regulated by BLIMP1 and EZH2, and to expand our understanding of the factors' overlap, we performed gene set enrichment analysis (GSEA) using the Hallmarks collection of gene sets (Liberzon et al., 2015; Subramanian et al., 2005) and identified enriched gene sets with BLIMP1 KD and tazemetostat treatment. For BLIMP1 KD, the sets relating to the interferon (IFN) and tumour necrosis factor alpha (TNFα) responses, apoptosis, and the inflammatory response were positively enriched, implying they are repressed by BLIMP1 (Figure 10A). Negatively enriched gene sets, induced by BLIMP1, included the unfolded protein response, mTORC1 signalling, and oxidative phosphorylation, all previously reported as being activated downstream of BLIMP1 (Price et al., 2018; Tellier et al., 2016). Interestingly, the most significantly negatively enriched sets were those of the G2/M checkpoint and E2F targets (Figure 10A). This implies a role for BLIMP1 in regulation of the cell cycle and possibly the DNA damage response, with DNA repair also being significantly negatively enriched. Upon tazemetostat treatment, many of the positively enriched gene sets were overlapping with those of BLIMP1 KD, including the IFN and TNFα responses, and apoptosis (Figure 10B). However, given the smaller amplitude of changes seen with tazemetostat treatment, the changes to these pathways are likely to be much more subtle than for BLIMP1 KD. Similarly, all of the significantly depleted gene sets were also depleted upon BLIMP1 KD. Thus, there is a large overlap in pathways targeted by BLIMP1 and EZH2 in the RPCI-WM1 cell line, and these are likely to have biological significance in WM.

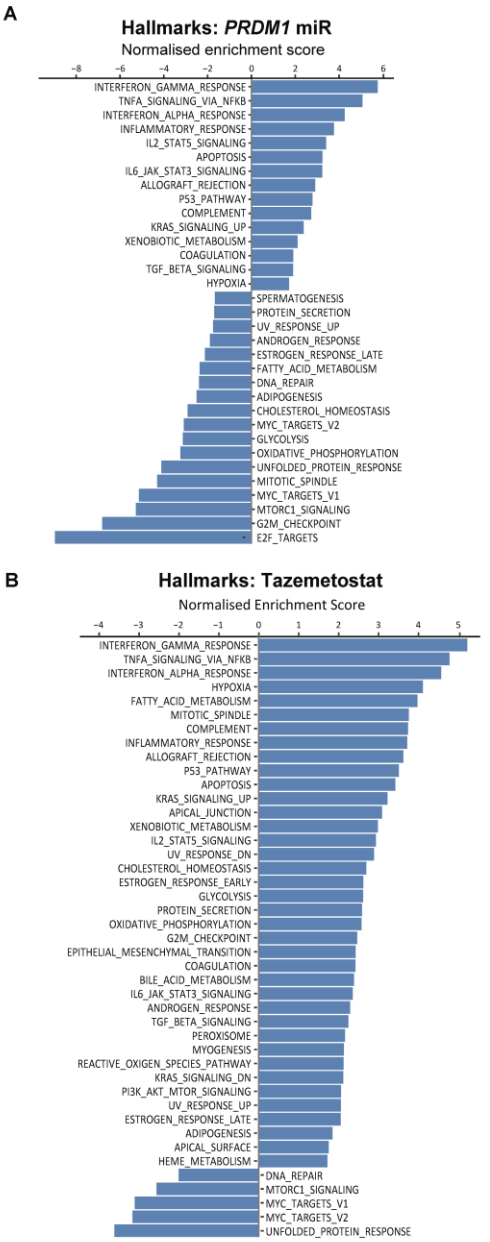

Figure 10: BLIMP1 and EZH2 transcriptionally regulate overlapping pathways

Bar plots depicting normalised enrichment score for Hallmarks gene sets identified using GSEA pre-ranked with FDR-corrected p-value ≤ 0.05 for **(A)** *PRDM1-miR#1* compared to *NT-miR* and **(B)** tazemetostat treatment compared to DMSO.

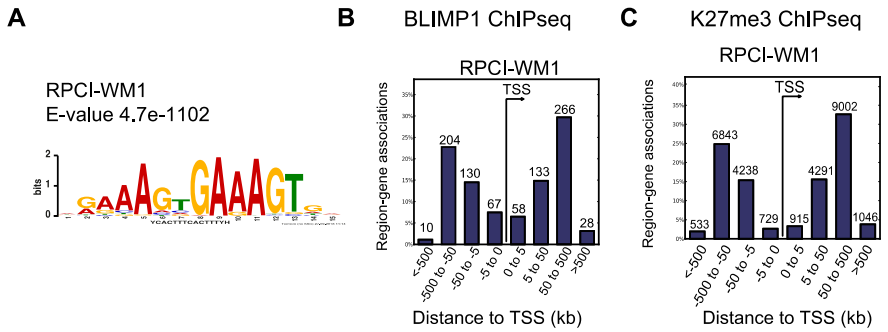

Figure 11: Characteristics of the BLIMP1 and H3K27me3 ChIPseq in the RPCI-WM1 cell line

(A) De-novo motif enrichment analysis of the BLIMP1 ChIPseq in the RPCI-WM1 cell line, showing the most highly enriched motif. E = 4.7e-1102. Distances of peaks to TSS plotted as the number of peaks within each distance bin for **(B)** the BLIMP1 ChIPseq and **(C)** the H3K27me3 ChIPseq in the RPCI-WM1 cell line.

5.5 BLIMP1 binds to a set of H3K27me3 marked genes at a distance from the mark

We were interested to investigate the overlap of BLIMP1 and the mark deposited by EZH2, H3K27me3 in WM, as this has previously been reported in mouse plasmablasts, along with the physical interaction of BLIMP1 and EZH2 (Minnich et al., 2016). To this end, we performed ChIPseq for BLIMP1 and the H3K27me3 mark in the RPCI-WM1 cell line. We identified 505 BLIMP1 binding sites assigned to 841 genes (Additional file Tables 3-4) and 14813 H3K27me3 peaks assigned to 4198 genes (Additional file Tables 5-6). Firstly, we performed motif enrichment analysis and identified the previously reported BLIMP1 motif as highly significantly enriched (Figure 11A). This gave us confidence in our BLIMP1 ChIPseq results. We also examined the distribution of BLIMP1 and the H3K27me3 mark in relation to transcription start sites (TSS) and found the highest enrichment of peaks at a distance of ±50-500 kb from the TSS for both BLIMP1 (Figure 11B) and H3K27me3 (Figure 11C).

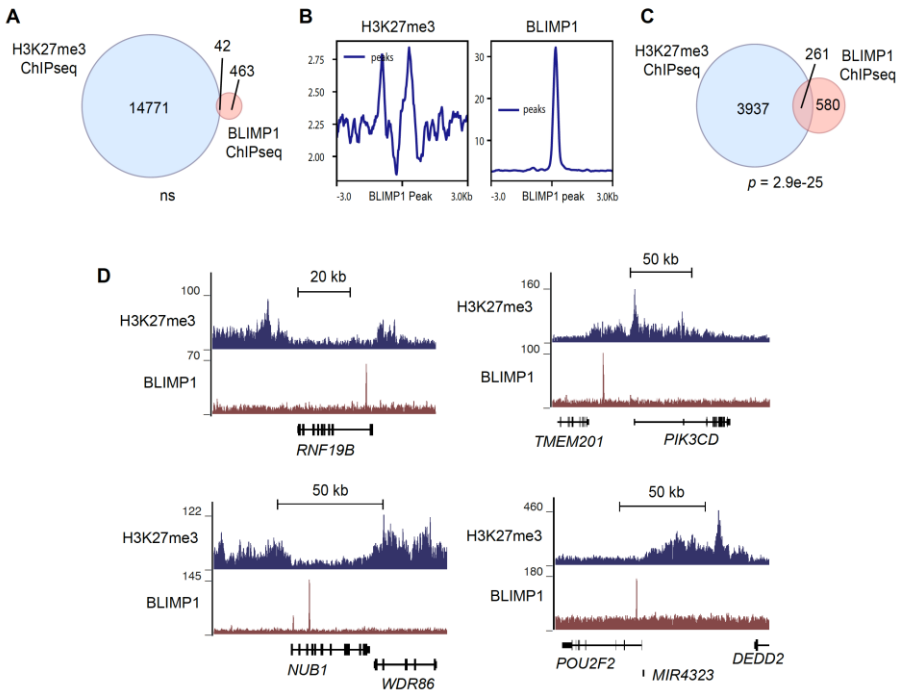

Figure 12: BLIMP1 binds at a distance to H3K27me3 in the RPCI-WM1 cell line

(A) Venn diagram of H3K27me3 and BLIMP1 peaks extended ±10kb, showing overlaps in these regions. (ns) not significant as determined by hypergeometric test. Called peaks determined by overlap from peak calling from two independent experiments. **(B)** Enrichment of signal from ChIPseq tracks ±3kb from the centre of BLIMP1 binding sites. Data depicts representative experiment of two biological replicates. **(C)** Venn diagram of genes assigned to H3K27me3 and BLIMP1 peaks showing overlapping genes. p= 2.9e-25 as determined by Fisher's exact test. **(D)** ChIPseq tracks for H3K27me3 and BLIMP1 in the RPCI-WM1 cell line. Data represents combination of reads from two independent experiments.

Surprisingly, when we extended the binding sites by 10 kb to either side, we saw very little overlap between BLIMP1 and H3K27me3 (Figure 12A), indicating that the factors are rarely binding within 10kb of one another. Using the raw ChIPseq signals, we checked for enrichment of H3K27me3 over BLIMP1 binding sites, and did observe some level of enrichment (Figure 12B). However, because few called peaks were present in proximity to each other, this enrichment could be due to background levels of H3K27me3. We next looked at the genes assigned to BLIMP1 binding sites and the H3K27me3 mark. On the gene level, there was a statistically significant degree of overlap (Figure 12C). This indicates that BLIMP1 and EZH2 may

be binding to the same genes, but at distant sites. We then investigated the genes marked by the presence of both BLIMP1 and H3K27me3. These included *RNF19B*, encoding NKLAM, which activates STAT1 (Lawrence & Kornbluth, 2016), the B cell genes *POU2F2* and *PIK3CD*, and the IFN responsive cell growth inhibitor NUB1 (Kito et al., 2001) (Figure 12D).

We wanted to extend our study to determine if the factors may be binding to nearby loci in multiple myeloma cells. We therefore performed ChIPseq for BLIMP1 and H3K27me3 in the OPM-2 and NCI-H929 multiple myeloma cell lines. We were also able to perform ChIPseq for EZH2 in the NCI-H929 cell line. We identified 572 peaks assigned to 892 genes for BLIMP1 in the OPM-2 cell line (Additional file Tables 7-8) and 520 peaks assigned to 830 genes for BLIMP1 in the NCI-H929 cell line (Additional file Tables 9-10). We identified 5138 peaks assigned to 2606 genes for H3K27me3 in the OPM-2 cell line (Additional file Tables 11-12) and 2789 peaks assigned to 2403 genes for H3K27me3 in the NCI-H929 cell line (Additional file Tables 13-14). For EZH2, there were 697 peaks assigned to 716 genes in the NCI-H929 cell line (Additional file Tables 15-16). We performed motif enrichment analysis for the BLIMP1 ChIP in the OPM-2 and NCI-H929 cell lines, and found the previously described BLIMP1 motif to be highly enriched in both cell lines (Figure 13A). Interestingly, while the BLIMP1 ChIPseq in both OPM-2 and NCI-H929 showed a very similar distribution to RPCI-WM1 (Figure 13B), the H3K27me3 mark showed more peaks present at sites closer to the TSS in both myeloma cell lines compared to the RPCI-WM1 cells (Figure 13C). In addition, the EZH2 ChIPseq in the NCI-H929 cell line showed a large proportion of peaks within 0-5 kb of the transcription start site (Figure 13D), indicating that more EZH2 peaks are present at gene promoters than BLIMP1 peaks.

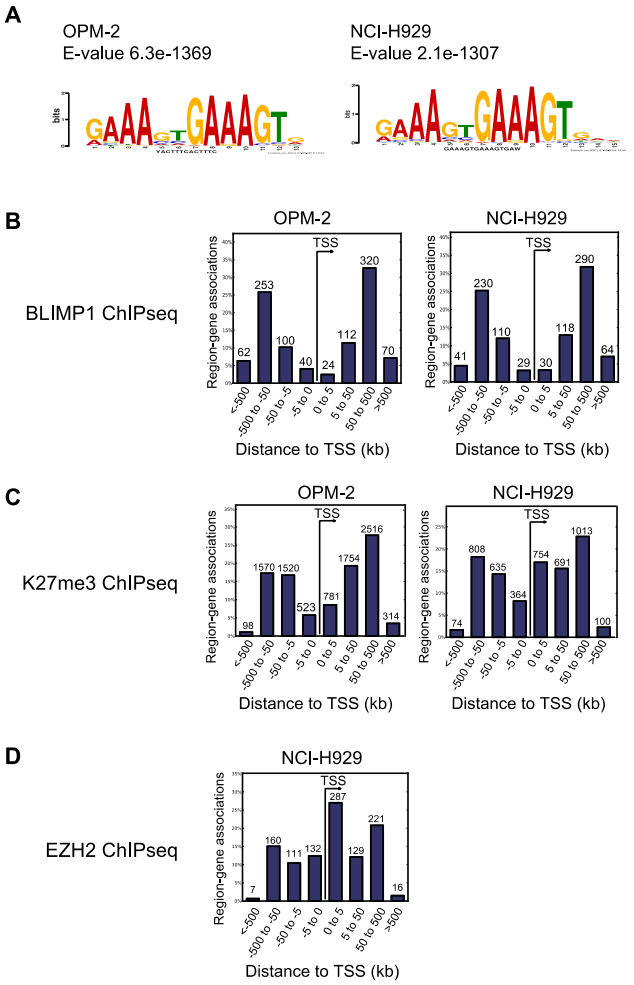

Figure 13: Characteristics of the BLIMP1, H3K27me3 and EZH2 ChIPseq experiments in the OPM-2 and NCI-H929 cell lines

(A) De-novo motif enrichment analysis for BLIMP1 ChIPseq in the OPM-2 and NCI-H929 cell lines showing the most highly enriched motif. Distances of peaks to TSS plotted as the number of peaks within each distance bin for **(B)** the BLIMP1 ChIPseq, **(C)** the H3K27me3 ChIPseq, and **(D)** the EZH2 ChIPseq in the OPM-2 and NCI-H929 cell lines. All ChIPseq experiments were performed as two biologic replicates.

Next, we tested the overlaps of BLIMP1 with H3K72me3 and EZH2 and interestingly, there appeared to be even less overlap in binding of the factors within 10 kb of one another for both the OPM-2 and NCI-H929 cell lines compared to RPCI-WM1 (Figure 14A). In the NCI-H929 cell line, there were almost no overlapping sites at all between BLIMP1 and EZH2 (Figure 14B). When comparing genes bound by BLIMP1 or marked by H3K27me3, we observed a higher degree of overlap, but this was only statistically significant for the NCI-H929 cell line (Figure 14C). However, there was not a significant overlap in genes bound by BLIMP1 or EZH2 in the NCI-H929 cell line (Figure 14D). We also investigated the overall signal enrichment for H3K27me3 and EZH2 over BLIMP1 binding sites in NCI-H929 cells, but observed only a small level of enrichment for H3K27me3, and potentially no enrichment for EZH2 (Figure 14E). Taken together, our results suggest that BLIMP1 is unlikely to be recruiting EZH2 to chromatin in WM or multiple myeloma, and that the factors may instead work in parallel, by binding to and regulating the same genes. Furthermore, the large overlap in transcriptional targets of BLIMP1 KD and tazemetostat may also be due to BLIMP1 maintaining the levels of the EZH2 protein.

5.6 A subset of BLIMP1 and H3K27me3 marked genes are transcriptional targets of BLIMP1 KD and tazemetostat

As a further line of inquiry, we decided to examine the overlap in genes bound by BLIMP1 or marked by H3K27me3 with those that were differentially expressed with BLIMP1 KD or tazemetostat treatment. This should provide us with an indication of possible direct targets of BLIMP1 or EZH2. Approximately one third of genes bound by BLIMP1 were transcriptionally induced by BLIMP1 KD, indicating that these are potential direct targets of transcriptional repression by BLIMP1 (Figure 15A). This also suggests that the presence of BLIMP1 at these sites is actively maintaining repression. In contrast, around half that number had decreased expression with BLIMP1 KD and were bound by BLIMP1, which could potentially be direct targets of transcriptional activation (Figure 15B). For those genes marked by H3K27me3, only a small proportion was induced by tazemetostat (Figure 15C). This suggests that for the vast majority of H3K27me3 marked genes, a decrease in H3K27me3 is insufficient for transcriptional activation. They could instead rely on other transcription factors or require the activity of histone acetyltransferases to become active. Finally, the overlap of genes repressed by tazemetostat treatment with H3K27me3-marked genes was not statistically significant (Figure 15D). Thus, while the direct binding of BLIMP1 appears to be maintaining transcriptional repression for around one third of bound genes, the presence of the H3K27me3 mark represents only a small subset of genes transcriptionally affected by tazemetostat treatment.

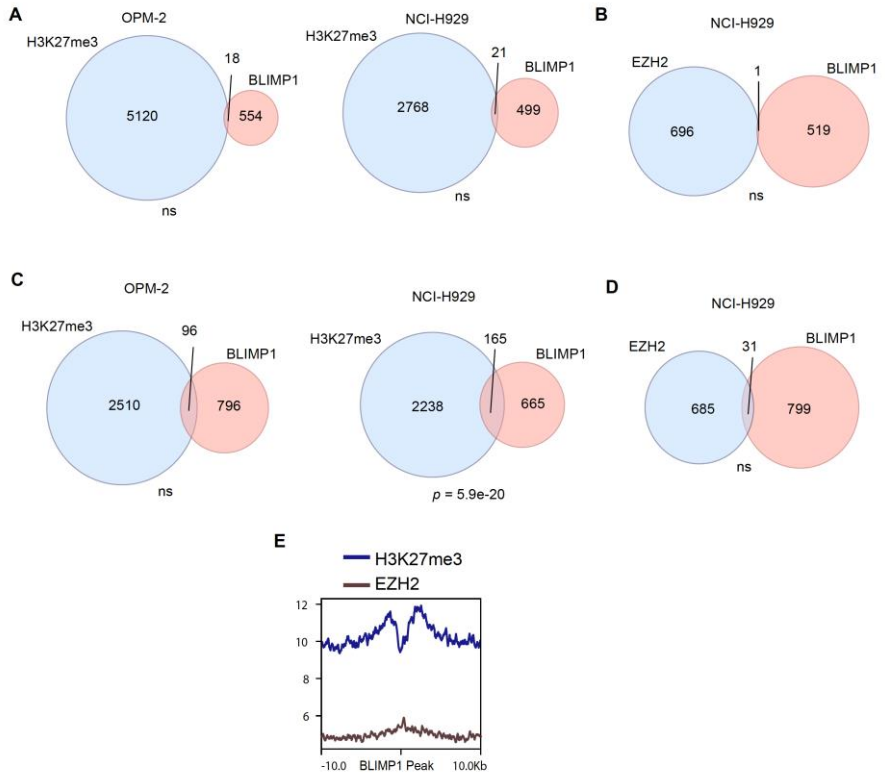

Figure 14: BLIMP1 binds at distal sites to H3K27me3 and EZH2 in multiple myeloma cell lines

(A) Venn diagrams of H3K27me3 and BLIMP1 peaks extended ±10kb, showing overlaps in these regions in the OPM-2 and NCI-H929 cell lines. (ns) not significant as determined by hypergeometric test. **(B)** Venn diagram of EZH2 and BLIMP1 peaks extended ±10kb, showing overlaps in these regions in the NCI-H929 cell line. (ns) not significant as determined by hypergeometric test. **(C)** Venn diagrams of overlapping genes assigned to peaks for H3K27me3 or BLIMP1 in the OPM-2 and NCI-H929 cell lines. Significance determined by Fisher's exact test. OPM-2, ns, not significant; NCI-H929, p = 5.9e-20. **(D)** Venn diagram of overlapping genes assigned to peaks for EZH2 or BLIMP1 in the NCI-H929 cell lines. (ns) not significant, as determined by Fisher's exact test. **(E)** Enrichment of signal from ChIPseq tracks ±10kb from the centre of BLIMP1 binding sites in the NCI-H929 cell line.

5.7 BLIMP1 represses transcription of immune surveillance and signalling molecule genes in concert with EZH2

In our GSEA, we observed that the most significantly enriched gene sets for both BLIMP1 KD and tazemetostat treatment were related to immune signalling mechanisms (Figure 10A-B). In addition, the gene set for allograft rejection was enriched in both analyses. This set includes genes that are induced during transplant rejection, which involves the activity of immune cells in targeting transplanted organs and tissues. The enrichment of this gene set upon inhibition or knock-out has been shown to link to immune evasion mechanisms (Alag et al., 2019; Goel et al., 2017; Xiong et al., 2019). These results led us to hypothesise that KD of BLIMP1 or EZH2 inhibition may affect the expression of molecules that mediate immune surveillance mechanisms. As such, we investigated the differentially expressed genes in these sets, and found a significant increase in expression of at least 34 genes relating to immune surveillance and signalling following BLIMP1 KD. These included genes coding for stimulatory T cell ligands ICOSLG and TNFSF9, as well as stimulatory NK cell ligands such as MICA, CD48 and CLEC2B (Figure 16A) (Pardoll, 2012; Vivier et al., 2008). Interestingly, while genes coding for MHC class I molecules HLA-A and HLA-B were decreased with BLIMP1 KD, those coding for MHC class II molecules HLA-DMA and HLA-DMB had increased expression with BLIMP1 KD. In addition to stimulatory molecules, a number of genes encoding inhibitory ligands and also some of their receptors were induced following BLIMP1 KD, implying they are repressed by BLIMP1. These included genes encoding LGALS3 and LAG3, TNFRSF14 and BTLA, as well as LGALS9 and HAVCR2 (Figure 16A). The gene encoding inhibitory receptor LILRB1 (also known as CD85j) was also repressed by BLIMP1. Repression of LILRB1 is a mechanism by which myeloma cells evade immune surveillance (Lozano et al., 2018). The inhibitory PD-L2 ligand gene *PDCDLG2* was also repressed by BLIMP1, however it is important to note that the gene encoding the PD-1 receptor, which can have an inhibitory effect on B cells was expressed to a comparable level in the RPCI-WM1 cell line. In addition to ligands that can stimulate and inhibit T or NK cells, a number of receptors for IFN and TNF were repressed by BLIMP1, and so too were downstream effectors of IFN signalling (Figure 16A).

We next examined the expression of these genes following tazemetostat treatment, and found around half of them to be repressed by EZH2. Fewer genes encoding stimulatory ligands were induced by tazemetostat, but a number of inhibitory ligand genes were induced without the genes for their receptors also being induced (Figure 16B).

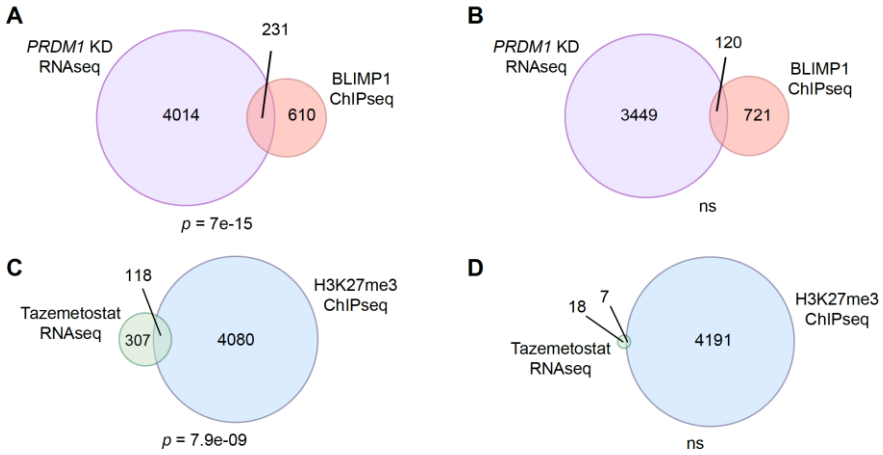

Figure 15: A subset of BLIMP1 and H3K27me3 marked genes are transcriptional targets

(A) Venn diagram depicting the overlap in genes with significantly increased expression following BLIMP1 KD and genes assigned to BLIMP1 binding sites. p= 7e-15, as determined by Fisher's exact test. **(B)** Venn diagram depicting the overlap in genes with significantly decreased expression following BLIMP1 KD and genes assigned to BLIMP1 binding sites. (ns) not significant as determined by Fisher's exact test. **(C)** Venn diagram depicting genes with significantly increased expression following tazemetostat treatment overlapping with genes assigned to H3K27me3 peaks. p= 7.9e-9, as determined by Fisher's exact test. **(D)** Venn diagram depicting genes with significantly decreased expression following tazemetostat treatment overlapping with genes assigned to H3K27me3 peaks. (ns) not significant, as determined by Fisher's exact test.

Interestingly, genes encoding MHC class I molecules were also induced by tazemetostat, in contrast to what we observed for BLIMP1 KD. However, a proportionally high number of downstream signalling effector molecule genes were induced by tazemetostat, similarly to what we saw with BLIMP1 KD (Figure 16B).

Taken together, BLIMP1 is largely repressing the expression of genes encoding activating ligands, inhibitory ligands and their receptors, as well as receptors and downstream signalling molecules. All of these are likely to affect the stimulation of NK cells and T cells, as well as the response of WM cells to these immune effector cells. However, the changes induced by tazemetostat are unlikely to affect the WM cells' interaction with NK and T cells in the same way as BLIMP1 KD. The signalling molecules whose encoding genes are differentially expressed with BLIMP1 KD are depicted in in Figure 17.

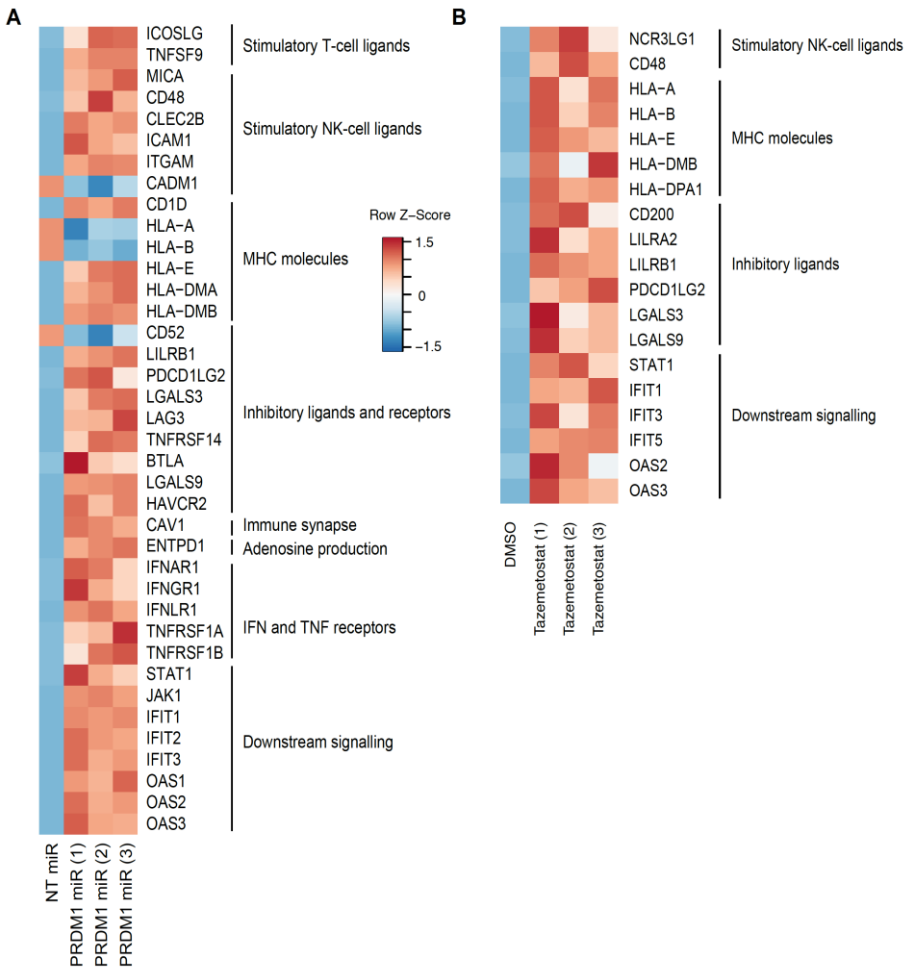

Figure 16: BLIMP1 and EZH2 repress transcription of immune surveillance and signalling molecule genes

(A) Heat map showing z-score of the log2 fold change for *PRDM1-miR#2* compared to *NT-miR* and in RPCI-WM1 cells with three independent replicates looking at genes involved in stimulation of T and NK cells, MHC molecules, inhibitory ligands and receptors, IFN and TNF receptors and downstream signalling. **(B)** Heat map showing the z-score of the $\log_2$ fold change for tazemetostat compared to DMSO in RPCI-WM1 cells with three independent replicates looking at genes involved in stimulation of NK cells, MHC molecules, inhibitory ligands, and downstream signalling.

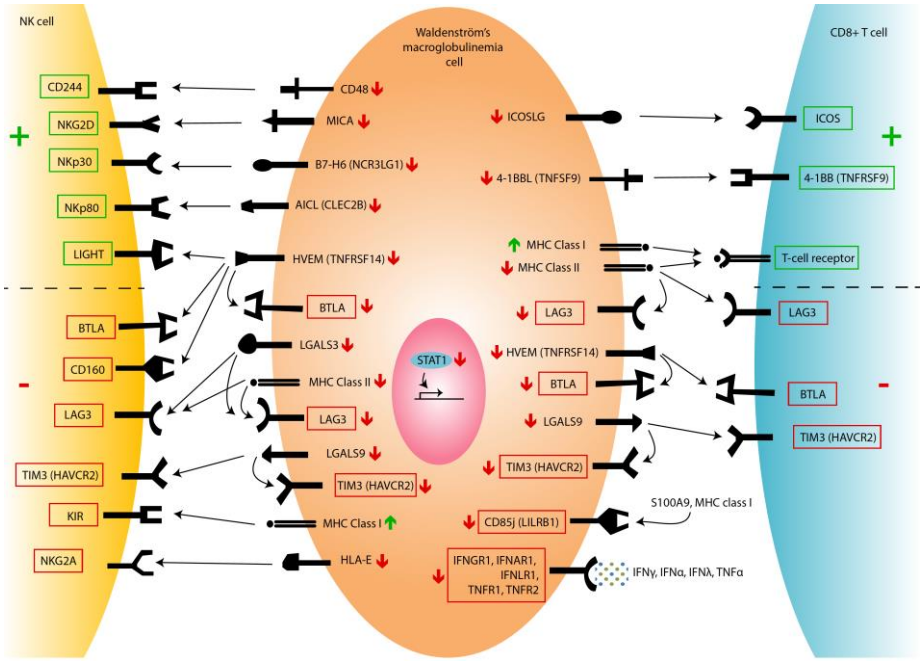

Figure 17: Immune surveillance and signalling molecules transcriptionally regulated by BLIMP1.

The green "+" symbol represents stimulatory receptors, and the red "-" symbol represents inhibitory ligands. Red ↓ arrows indicate that the genes encoding these molecules are repressed by BLIMP1, whereas green ↑ arrows indicate that the genes encoding these molecules are activated by BLIMP1. Receptor names are surrounded by boxes, whereas ligands are not.

5.8 BLIMP1 regulates a subset of immune signalling targets through EZH2

In order to understand the direct effects of BLIMP1 and EZH2 on the transcriptional changes associated with evasion from immune surveillance, we examined the ChIPseq data for the RPCI-WM1 cell line, and observed the H3K27me3 mark to be present without BLIMP1 over a number of immune signalling genes including *HLA-B*, *MICA*, *LILRB1*, *NCR3LG1* and *TNFRSF1A* (Figure 18A). On the other hand, BLIMP1 was present in proximity to the H3K27me3 mark over downstream signalling genes *IFIT2* and *STAT1* (Figure 18B). We were interested to determine which targets of BLIMP1 were repressed via BLIMP1 maintaining EZH2 expression, and which targets were repressed independently of EZH2. In order to do this, we ectopically expressed EZH2-EGFP or EGFP in cells with BLIMP1 KD, as in Figure 7E. We then performed RT-qPCR on cDNA derived from these cells, compared to cDNA derived from cells expressing the *NT-miR*. Our results demonstrated that the majority of BLIMP1 targets tested did not have their repression restored by EZH2 (Figure 18C). Interestingly, all of the genes repressed by restoring EZH2 levels related to B cell development and immune signalling. *RCAN3*, which codes for an inhibitor of cytokine signalling in T cells (Mulero et al., 2007) and *ZFP36L1*, which is important for germinal centre B cells (Galloway et al., 2016) showed some level of repression when EZH2 was ectopically expressed. So too did the immune inhibitory molecule genes *TNFRSF14* and *HAVCR2*. Taken together, BLIMP1 represses a subset of its target genes through maintaining EZH2 levels.

5.9 BLIMP1 and EZH2 confer evasion from NK cell mediated cytotoxicity

Given the transcriptional changes related to immune surveillance as described above, we sought to determine if these changes would affect the interactions between WM cells and NK cells. Firstly, to determine the effect of BLIMP1 KD or EZH2 inhibition in the RPCI-WM1 cells on the NK cells, we performed a degranulation assay. This assay involves staining for the CD107a molecule which is expressed at the surface of NK cells when cytotoxic granules are released, and measures the activity of NK cells (Alter et al., 2004). We co-cultured NK cells isolated from human blood with the RPCI-WM1 cells and stained for CD107a. Following 5 h of co-culture, there was an increase in degranulating NK cells ($CD56^+CD107a^+$) when cultured with the *PRDM1-miR#1* RPCI-WM1 cells compared to the *NT-miR* (Figure 19A). In contrast, there was no change in the degranulation of NK cells co-

cultured with DMSO or tazemetostat-treated RPCI-WM1 cells. These results were reflected in experiments from four donors as quantified in Figure 19B. In addition to the effect on the NK cells, we were also interested in the effect of BLIMP1 KD or EZH2 inhibition on the RPCI-WM1 cells' responses to NK cell mediated cytotoxicity. In order to examine this, NK cells were co-cultured with RPCI-WM1 cells for 4 h, and cytolysis was assessed by measuring the adenylate kinase activity in the cell culture media. The levels of cytolysis were normalised to those of wells containing RPCI-WM1 cells with the relevant miRNAs or treatments without NK cells. Interestingly the results demonstrated an increase in NK cell mediated cytotoxicity for RPCI-WM1 cells with BLIMP1 KD, and for those treated with tazemetostat (Figure 19C). In accordance with our transcriptomic data, BLIMP1 KD leads to both increased NK cell degranulation and increased cytotoxic effect against RPCI-WM1 cells. In contrast, EZH2 inhibition does not affect NK cell activation, but increases the sensitivity of the RPCI-WM1 cells to killing by NK cells. This is likely to be due to increased expression of downstream signalling from IFNs. Thus, BLIMP1 and EZH2 confer evasion from NK cell mediated cytotoxicity, with BLIMP1 likely performing this through effects on both the NK cells and RPCI-WM1 cells, whereas EZH2 affects only the RPCI-WM1 cells' responses.

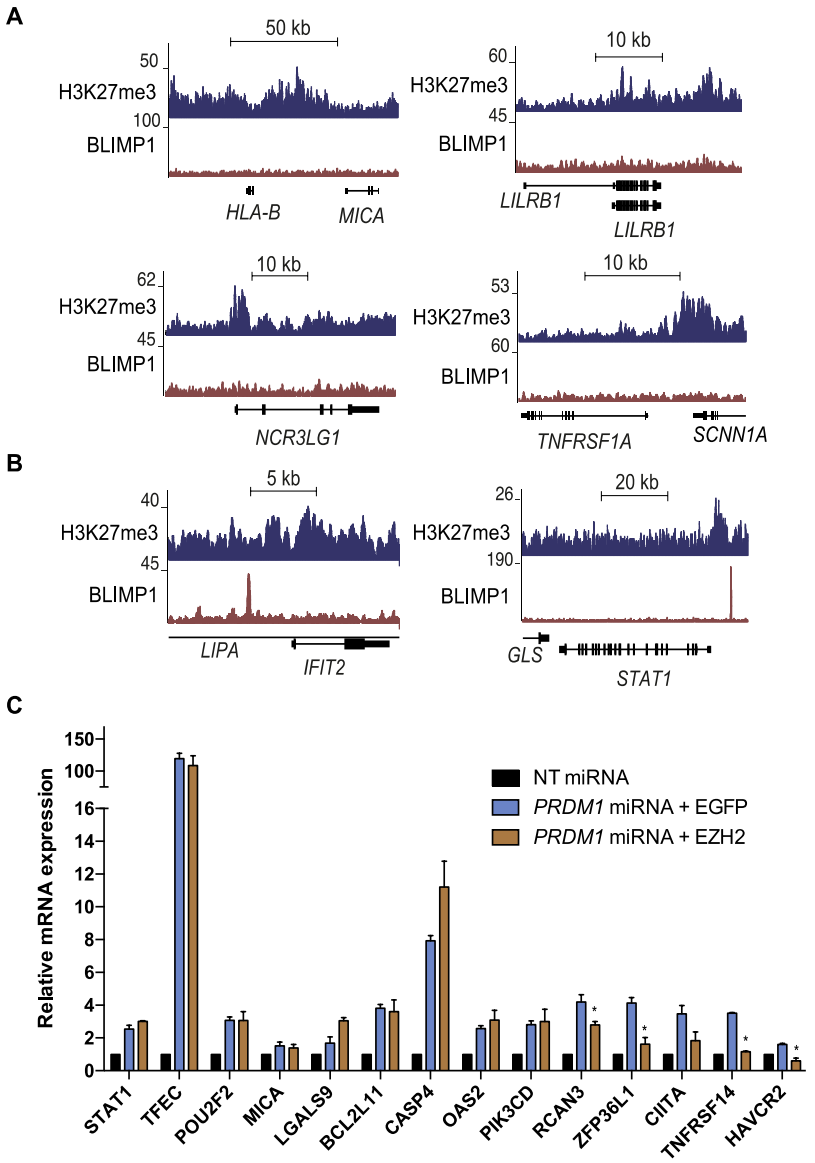

Figure 18: BLIMP1 regulates a subset of targets through EZH2

ChIPseq tracks for H3K27me3 and BLIMP1 in the RPCI-WM1 cell line over **(A)** the immune surface molecule genes *HLA-B, MICA, LILRB1, NCR3LG1, TNFRSF1A*, or **(B)** the downstream signalling genes, *IFIT2* and *STAT1*. Data represents combination of reads from two independent experiments. **(C)** RT-qPCR from three independent experiments depicting relative mRNA expression comparing RPCI-WM1 cells with *NT-miR*, and *PRDM1-miR#1* transduced with EGFP or EZH2-EGFP.

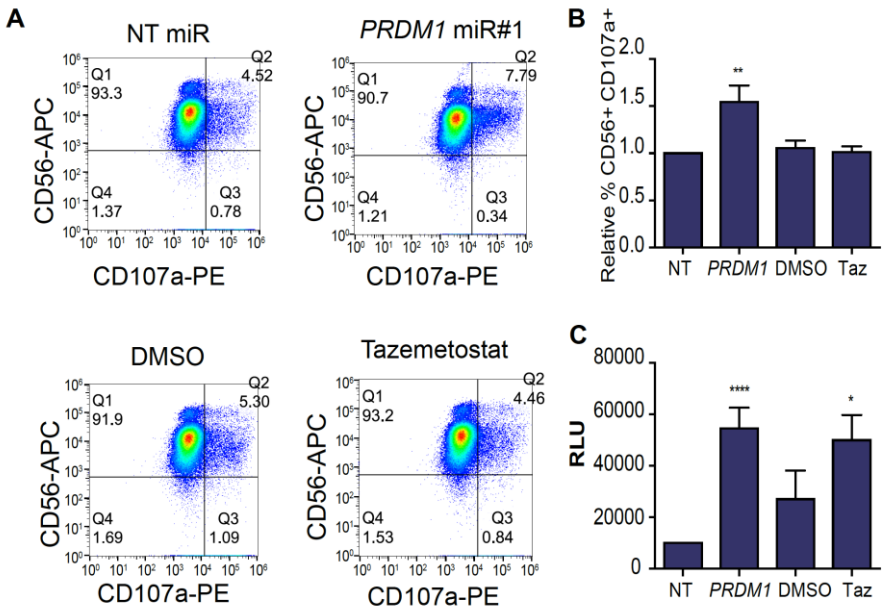

Figure 19: BLIMP1 and EZH2 confer evasion from NK cell mediated cytotoxicity

(A) Percentage $CD56^{+}CD107a^{+}$ cells (Q2) representing degranulating NK cells, as determined by flow cytometry following co-culture with RPCI-WM1 cells with *NT-miR* or *PRDM1-miR#1*, or RPCI-WM1 cells treated with DMSO or Tazemetostat. One representative experiment is displayed. **(B)** Relative quantification of the degranulation assay **p = 0.0088. **(C)** Cytotoxicity depicted in relative luminescence units (RLU), as measured by adenylate kinase activity in the culture media following 4 h co-culture of NK cells with RPCI-WM1 cells with *NT-miR* or *PRDM1-miR#1*, or RPCI-WM1 cells treated with DMSO or 1µM Tazemetostat. Cells were co-cultured at the effector:target ratio of 20:1. ****p = 3.1×10^{-5}; *p = 0.02. Results of the degranulation and cytotoxicity assays from four individual donors, performed in two pairs on two separate occasions.

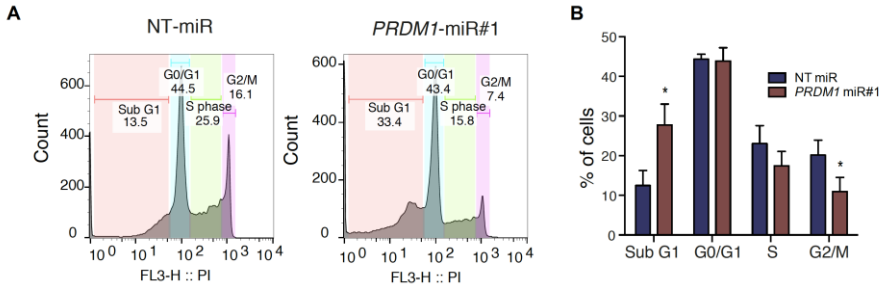

Figure 20: BLIMP1 KD induces cell cycle arrest

(A) Histogram plots of methanol-fixed propidium iodide-stained cells depicting the cell cycle phases. **(B)** Quantification of three independent experiments as depicted in A. Sub G1 **p* = 0.015; G2/M **p* = 0.038, as determined by the student's two-tailed t-test. The bar graph depicts the mean with standard deviation.

5.10 BLIMP1 regulates the cell cycle and DNA repair in Waldenström's macroglobulinemia

5.10.1 BLIMP1 KD induces cell cycle arrest

BLIMP1 is known to have a role in repressing positive cell cycle regulators during the B cell to plasma cell transition (Shaffer et al., 2002). As part of our early characterisation of the BLIMP1 KD cells, we checked if BLIMP1 KD would result in changes to the cell cycle in the RPCI-WM1 cell line. We performed propidium iodide staining on methanol-fixed cells. Propidium iodide is a fluorescent DNA intercalating agent, which can be used to determine cell cycle phases based off the quantities of DNA. Using this method, we observed some notable changes when comparing the *NT-miR* cells to the *PRDM1-miR#1* cells. The proportion of cells in the G2/M phase was significantly decreased, and a significantly larger proportion of cells was now in the Sub-G1 phase, representing apoptotic cells (p = 0.015) (Figure 20A-B). Although the proportion of cells in S phase was not significantly decreased with BLIMP1 KD, there was a trend towards a decrease, indicating fewer cells may be undergoing DNA replication, but were instead being driven towards apoptosis. The ratio of cells in G2/M:S was consistently lower following BLIMP1 KD (0.65) compared to the *NT-miR* cells (0.92), with on average a 30% reduction in the ratio. The G2/M:S ratio signifies the rate of cells passing through S phase into G2 and M phases. A lower ratio indicates fewer cells in G2/M compared to S, and suggests that the cells are passing faster through G2/M, either into G1 or directly into the apoptotic sub G1 phase.

5.10.2 BLIMP1 maintains expression of positive cell cycle regulators

The results of the GSEA suggested effects of BLIMP1 KD on regulators of the cell cycle, with the 'G2/M checkpoint' and 'E2F targets' sets having the strongest negative enrichment with BLIMP1 KD (Figure 10A). As we had already observed an effect on apoptosis (Figure 4B), but without direct binding of BLIMP1 to apoptosis genes, we hypothesized that BLIMP1 KD may be inducing apoptosis via inhibition of the cell cycle. To further investigate this, we looked into the genes that were differentially expressed with BLIMP1 KD compared to the *NT-miR* in the RPCI-WM1 cells, and observed decreased expression of positive cell cycle regulators (Figure 21A). These included the transcription factor encoding genes *E2F1* and *LIN54*. E2F1 is a positive regulator of the cell cycle, responsible for activating the transcriptional wave that drives the G1-S transition (Johnson et al., 1993; Takahashi et al., 2000). LIN54 is a subunit of the DREAM/LINC complex that binds to the *CDK1* promoter, and is necessary for cell cycle progression (Schmit et al., 2009). The cyclin dependent kinase (CDK) encoding genes, *CDK1* (encoding CDC2)*, CDK2*, *CDK4*, and the cyclin genes *CCNA2*, *CCNB2* and *CCNE2* (Figure 21A) were decreased with BLIMP1 KD. However, the cyclin genes *CCNE1* and *CCND1* had increased expression, indicating they are repressed by BLIMP1. CDC2 is necessary for the G2-M transition, phosphorylating a myriad of targets necessary for mitosis (Blethrow et al., 2008), and is the only CDK completely necessary for the cell cycle (Santamaría et al., 2007; van den Heuvel & Harlow, 1993). CKD4 and CDK2 phosphorylate Rb during G1 phase to prevent inhibition of E2F1 and allow entry into S phase (Harbour et al., 1999; Kato et al., 1993; Tsutsui et al., 1999; van den Heuvel & Harlow, 1993). The CDKs rely on interaction with cyclin proteins to carry out their functions. CDC2 interacts primarily with cyclin B, but also with cyclin A and others (Draetta et al., 1989; Santamaría et al., 2007), CDK4 interacts with cyclin D (Kato et al., 1993), and CDK2 interacts with cyclin E (Harbour et al., 1999). The genes encoding key CDK phosphatase CDC25, which activates the CDKs for cell cycle progression (Hoffmann et al., 1994; Jinno et al., 1994) followed the trend of decreased expression with BLIMP1 KD. So too did the chromatin assembly factor gene *TLK1* (Silljé & Nigg, 2001) and E2F target/MYC cofactor gene *ATAD2* (Ciró et al., 2009; Koo et al., 2016) (Figure 21A). A number of origin recognition complex genes *ORC3*, *ORC6* and *CDC6* (Méndez & Stillman, 2000), *CDC45*, and pre-replication complex members, *MCM2-7* and *MCM10* (Labib et al., 2000; Wohlschlegel et al., 2002; Zou et al., 1997) were also maintained by

BLIMP1, with decreased expression following BLIMP1 KD (Figure 21A). The origin recognition complex is required for recruiting the pre-replication complex to sites of replication initiation to ensure timely DNA replication (Méndez & Stillman, 2000). The mitosis regulators *AURKA* (Mori et al., 2007), *AURKB* (Liu et al., 2009; Welburn et al., 2010), and genes encoding kinetochore proteins CENP-O, -P, -Q and -U (Pesenti et al., 2018) were also decreased with BLIMP1 KD (Figure 19A). Additionally, a number of anaphase-promoting complex subunit genes (Reddy et al., 2007) showed decreased expression following BLIMP1 KD (Figure 19A). Interestingly, the gene encoding the RNA-binding protein ZFP36L1 was induced with BLIMP1 KD (Figure 21A), indicating it is repressed by BLIMP1. ZFP36L1 plays an important role in facilitating V(D)J recombination by binding to the 3'UTRs of cell cycle mRNAs to promote their degradation and initiate cell quiescence (Galloway et al., 2016). Taken together, BLIMP1 is maintaining expression of positive cell cycle regulators in the RPCI-WM1 cell line.

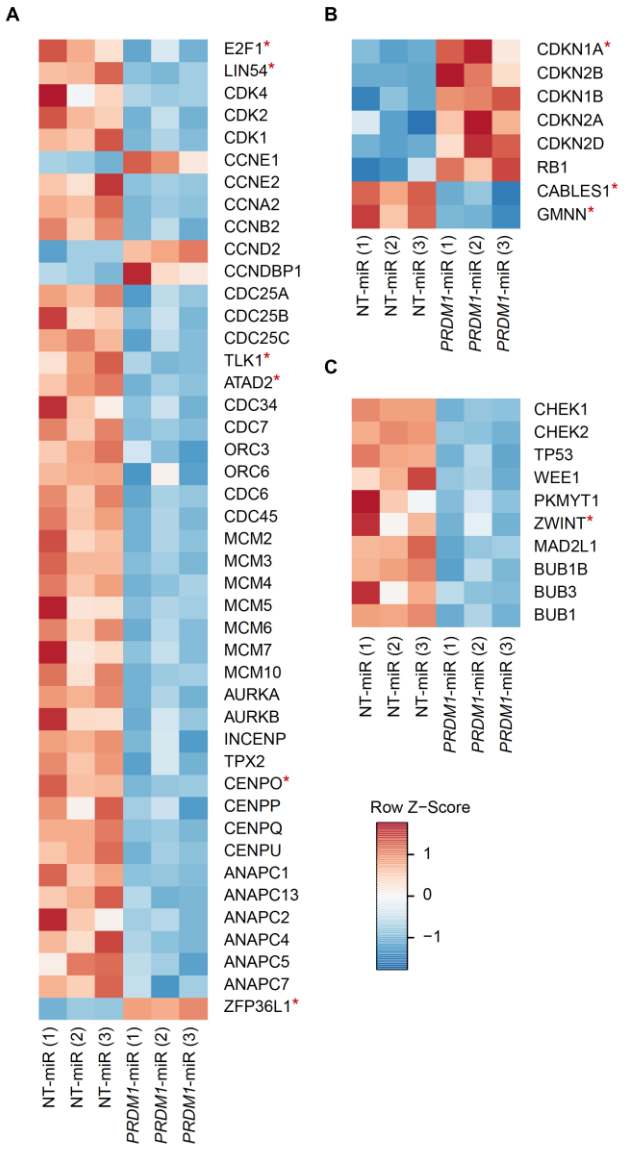

Figure 21: BLIMP1 KD affects expression of cell cycle and checkpoint genes

(A) Heatmap depicting z-scores of normalised transcript per million (TPM) values for cell cycle genes in RPCI-WM1 cells comparing *NT-miR* to *PRDM1-miR#2*. **(B)** Heatmap depicting z-scores of normalised TPM values for G1/S checkpoint genes. **(C)** Heatmap depicting z-scores of normalised TPM values for G2/M and mitotic spindle checkpoint genes. Genes marked with a red * bear BLIMP1 binding sites.

5.10.3 Increased expression of G1/S checkpoint genes following BLIMP1 KD

As we had observed significant changes in the cell cycle profiles of RPCI-WM1 cells following BLIMP1 KD, we decided to investigate the expression of negative regulators of the cell cycle. First, we examined the expression of G1/S checkpoint genes and found many of the key checkpoint regulators to have higher expression following BLIMP1 KD (Figure 21B). These included *CDKN1A* (encoding p21), *CDKN2A* (encoding p16INK4A), and *RB1*. p21 is a strong inhibitor of CDKs, including CDK2 and CDC2 (Xiong et al., 1993), p16INK4A is an inhibitor of CDK4/6 (Lukas et al., 1995), and RB1 inhibits E2F1 by binding to it and preventing its activating role (Flemington et al., 1993; Helin et al., 1993; Hiebert et al., 1992). Conversely, the p21 stabiliser *CABLES1* (Shi et al., 2014) and the replication initiation inhibitor *GMNN* (Wu et al., 2014) were maintained by BLIMP1. In general, the trend appeared to be increased expression of the main G1/S checkpoint enforcer genes following BLIMP1 KD. Although these repressed genes were expressed when BLIMP1 was present, BLIMP1 KD led to an increase in their expression, indicating that BLIMP1 may be preventing hyper-activation of the G1/S checkpoint.

5.10.4 BLIMP1 maintains G2/M and mitotic spindle checkpoint genes

The G2/M checkpoint is essential for detection of DNA damage and halting entry into mitosis. As the GSEA set “G2M checkpoint” was one of the most significantly depleted with BLIMP1 KD (Figure 10A), we sought to look further into the specific genes within this set. The genes encoding key enforcers of the G2/M checkpoint here include *CHK1* (Liu et al., 2000) and *CHK2* (Hirao et al., 2000; Matsuoka et al., 1998), both of which show decreased expression upon BLIMP1 KD (Figure 21C). The gene *TP53*, encoding the crucial transcription factor p53 (Innocente et al., 1999), which regulates both the G2/M and G1/S checkpoints (Agarwal et al., 1995; Kuerbitz et al., 1992) also has decreased expression following BLIMP1 KD. p53 transcriptionally activates *CDKN1A* (el-Deiry et al., 1993) and inhibits *CDC25C*, which is necessary for entry into mitosis (St Clair et al., 2004). Furthermore the transcripts encoding the WEE1 and PKMYT1 kinases, responsible for inhibiting CDC2 (Heald et al., 1993; Mueller et al., 1995) were decreased upon BLIMP1 KD (Figure 21C). While some of the genes mentioned above in relation to the G1/S checkpoint such as *CDKN1A* also have an effect on the G2/M checkpoint, in general, genes enforcing the G2/M checkpoint appear to have their expression maintained in the presence of BLIMP1.

The mitotic spindle assembly checkpoint is essential for ensuring correct chromosomal segregation before cytokinesis can take place. Investigation into spindle checkpoint enforcer genes led us to find that the main regulators of this checkpoint, *ZWINT* (Wang et al., 2004)*, MAD2L1, BUB1B, BUB3* (Sudakin et al., 2001) and *BUB1* (Perera et al., 2007) show decreased expression following BLIMP1 KD (Figure 21C). Thus, the presence of BLIMP1 may be maintaining expression of both G2/M and mitotic spindle checkpoint genes.

5.10.5 BLIMP1 binds directly to cell cycle regulator genes

In order to determine if the transcriptional effects on cell cycle regulators were a direct effect of BLIMP1, we next looked into the binding of the BLIMP1 protein in our ChIPseq data. Indeed, a number of the differentially expressed genes mentioned above bore BLIMP1 binding sites. While BLIMP1 has traditionally been thought of as a transcriptional repressor, recent evidence has painted a role for BLIMP1 in direct transcriptional activation (Minnich et al., 2016). A number of the positive cell cycle regulator genes bound by BLIMP1 appear to be induced by it, rather than repressed, as their expression decreased with BLIMP1 KD. These included the transcription factor genes *E2F1* and *LIN54*, and the chromatin assembly factor gene *TLK1* (Figure 22A). Whereas, the cell cycle inhibitor genes, *ZFP36L1* and *CDKN1A* were repressed by BLIMP1 binding (Figure 22B). Therefore, transcriptional activation of cell cycle progression genes and transcriptional repression of certain cell cycle inhibitor genes is likely a direct result of BLIMP1 binding.

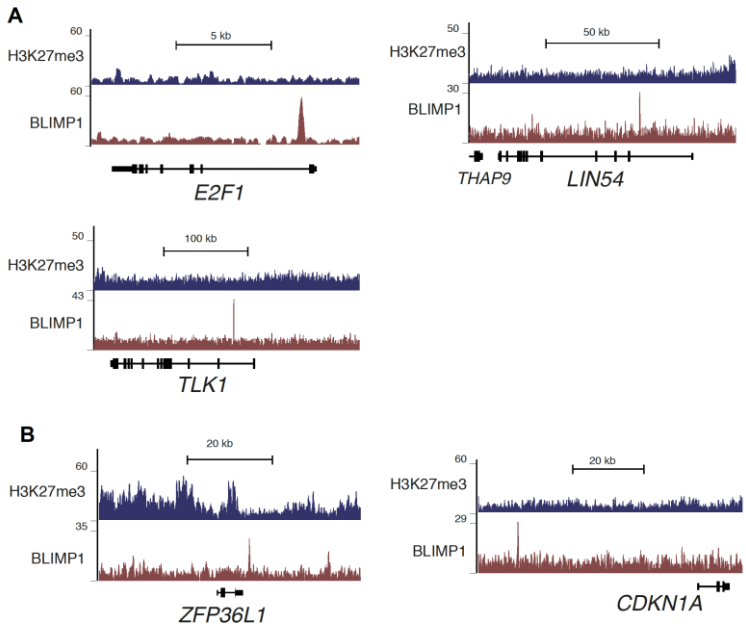

Figure 22: BLIMP1 binds directly to cell cycle regulators

(A) ChIPseq tracks for BLIMP1 and H3K27me3 showing BLIMP1 binding to the positive cell cycle regulator genes, *E2F1*, *LIN54* and *TLK1* in the RPCI-WM1 cell line. **(B)** ChIPseq tracks for BLIMP1 and H3K27me3 showing BLIMP1 binding to the cell cycle inhibitor genes *ZFP36L1* and *CDKN1A* in the RPCI-WM1 cell line.

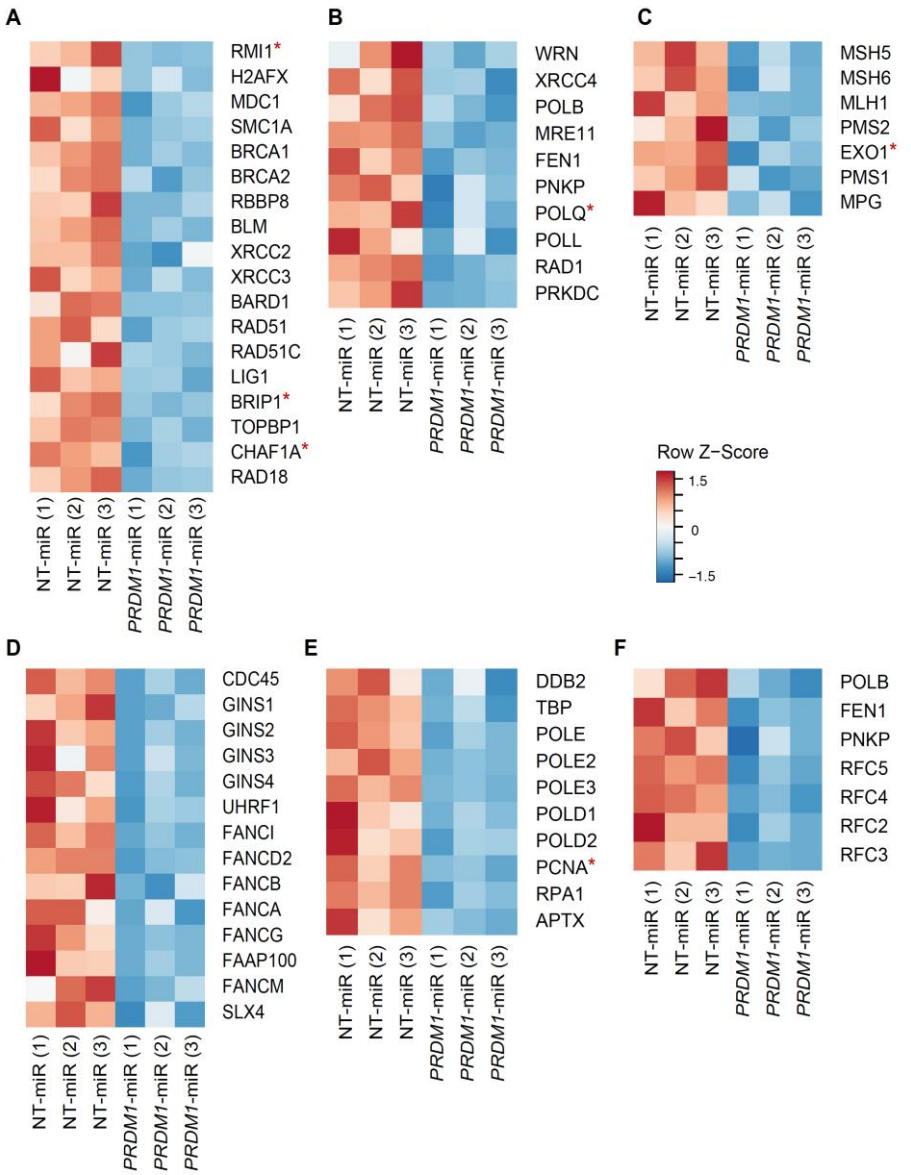

Figure 23: BLIMP1 maintains expression of DNA repair pathway genes

Genes involved in the following pathways show decreased expression following induction of *PRDM1-miR#2*, compared to the *NT-miR* in the RPCI-WM1 cell line: **(A)** Homologous recombination, **(B)** Non-homologous end joining, **(C)** Mismatch repair, **(D)** Interstrand crosslink repair, **(E)** Nucleotide excision repair, and **(F)** Base excision repair. Genes marked with a red * bear BLIMP1 binding sites.

Put together, BLIMP1 KD is affecting the cell cycle in RPCI-WM1 cells, possibly by arresting the cells in G1, which fits with the expression increases in G1/S checkpoint genes, and the expression decreases in the G2/M and mitotic spindle checkpoint genes. Furthermore, KD of BLIMP1 is likely to be inhibiting commitment to division, which takes place during G1, as there was a possible decrease in the number of cells in S phase and decreased expression of G1 progression regulator genes such as *CDK4* and *CDK2*. The ability of the cells to pass through the G2 and M phases is also likely to be affected, due to the decreased expression of the genes encoding the essential kinase CDC2, cyclin B, and the crucial phosphatase CDC25. Furthermore, the decrease in the G2/M:S ratio seen with BLIMP1 KD indicates that the cells are possibly exiting the G2/M phases faster, either to initiate apoptosis or enter G1. Thus, transcriptional control by direct binding of BLIMP1 and indirect mechanisms contribute to maintenance of cell cycle progression in the RPCI-WM1 cell line, with BLIMP1 KD leading to cell cycle arrest.

5.10.6 BLIMP1 maintains expression of genes essential to DNA repair pathways

Since BLIMP1 KD had a striking effect on positive cell cycle regulator genes, checkpoint enforcer genes, and the cell cycle itself, we hypothesised that DNA repair pathway genes may also be affected. The purpose of cell cycle checkpoints is to ensure the absence of DNA damage, and if needed, give the cells a chance to repair any damage before progression to the next stage in the cycle. The DNA damage response is activated at these checkpoints if damage is detected, and can lead to DNA repair. Thus, changes in expression of checkpoint regulators are likely to lead to changes in DNA repair genes.

When we investigated the differentially expressed genes with BLIMP1 KD compared to the *NT-miR* cells, we found that genes from six main DNA repair pathways as reviewed in (Ciccia & Elledge, 2010), showed decreased expression with BLIMP1 KD, and thus were maintained by BLIMP1. These pathways included homologous recombination (Figure 23A), non-homologous end joining (NHEJ) (Figure 23B), mismatch repair (Figure 23C), interstrand crosslink repair (Figure 23D), nucleotide excision repair (Figure 23E), and base excision repair (Figure 23F). However, the genes within each category listed above often play a role in multiple DNA repair pathways as well as in DNA replication. An alternative explanation to that of positive regulation by BLIMP1 could also be that changes in the distribution of the

cells in different phases of the cell cycle could also lead to fewer cells with active DNA repair taking place. For example, homologous recombination only takes place in the S and G2 phases, so a decrease in the proportion of cells in these phases could lead to lower overall expression of homologous recomination genes. Furthermore, many of the genes involved in DNA repair pathways are also important for DNA replication, so fewer cells in S phase could lead to lower expression of these genes. However, we cannot rule out the possibility of BLIMP1 postively regulating these genes without further experiments. As BLIMP1 has not been previously studied in relation to DNA damage repair, the finding of BLIMP1 maintaining expression of DNA repair pathways could be a highly novel result.

5.10.7 BLIMP1 binds to DNA repair genes

As we observed such dramatic changes in DNA repair pathway genes following BLIMP1 KD, we sought to determine whether BLIMP1 was binding to any of these genes for possible direct transcriptional activation. Indeed, a small proportion of DNA repair genes were bound by BLIMP1. The homologous recombination genes *RMI1*, *BRIP1* and *CHAF1A* were bound by BLIMP1 (Figure 24A). RMI1 is responsible for dissolution of homologous recombination intermediates (Cejka et al., 2010; Wu et al., 2006). BRIP1 (also known as BACH1) is a BRCA1 interaction partner and DNA helicase, essential for homologous recombination (Cantor et al., 2004; Litman et al., 2005). CHAF1A is a subunit of the chromatin assembly factor-1 (CAF-1), and plays a role both in homologous recombination (Baldeyron et al., 2011), and to assemble nucleosomes during nucleotide excision repair (Mello et al., 2002). The genes *EXO1*, *PCNA* and *POLQ* are also bound by BLIMP1 (Figure 24B). EXO1 has an integral role in processing of DNA double-strand breaks (Mimitou & Symington, 2008; Zhu et al., 2008). While PCNA is an essential factor in DNA replication, functioning as a sliding clamp processivity factor for DNA polymerases (Bravo et al., 1987; Yao et al., 1996), it is also crucial for DNA repair (Shivji et al., 1992; Umar et al., 1996). DNA polymerase theta (Pol-θ, encoded by *POLQ*) is important for translesion synthesis past sites of base damage, and plays a role in alternative NHEJ (Mateos-Gomez et al., 2015) and base excision repair (Yoshimura et al., 2006). Taken together, we provide evidence for the first time of BLIMP1 maintaining expression of DNA repair pathway genes and directly binding to the genes encoding key players in DNA repair.

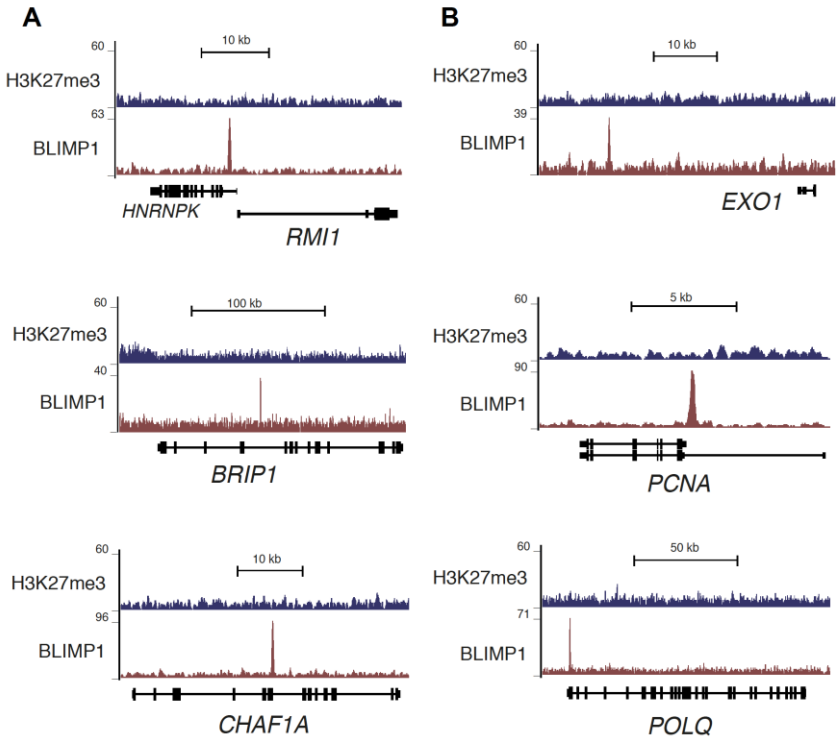

Figure 24: BLIMP1 binds directly to DNA repair genes

(A) ChIPseq tracks of BLIMP1 and H3K27me3 in the RPCI-WM1 cell line over *RMI1*, *BRIP1* and *CHAF1A*. **(B)** ChIPseq tracks of BLIMP1 and H3K27me3 in the RPCI-WM1 cell line over *EXO1*, *PCNA* and *POLQ*.

5.11 Optimisations of a low-cell number ChIP and RNAseq protocol

5.11.1 Establishment of a procedure for low-cell number ChIPseq from plasma cells

As part of Aim 4 of the project, identifying transcriptional enhancer networks underlying the transition from MGUS to multiple myeloma, we first sought to identify transcriptional enhancers using ChIPseq. In the earlier sections of this thesis, ChIPseq was performed for histone marks using 1×10^7 cells per IP**.** However, here we needed to perform ChIP using cells from patients. Isolations of $CD138^+$ cells from bone marrow aspirates typically yielded only 10^6 cells per patient, or even fewer (Table 17). To overcome this scarcity of ChIP input material, we optimized the histone ChIP protocol for use with 10^5 cells per IP. To begin with, we used the U266 myeloma cell line and tested enrichment of the histone marks H3K4me1, H3K4me3, H3K27Ac and H3K27me3 over expected enhancer or promoter regions compared to negative control regions. We tested for H3K4me1 as it marks enhancer regions, H3K4me3 as it marks promoter regions, and H3K27Ac as it marks for active enhancers and promoters (Creyghton et al., 2010; Heintzman et al., 2009; Heintzman et al., 2007). The H3K27me3 modification marks for poised or repressed promoters and enhancers (Rada-Iglesias et al., 2010). For the active marks (H3K4me1, H3K4me3 and H3K27Ac), the negative control regions were intron 4 of the *TYR* gene, and the promoter region of *PRDM16*. These regions were selected because while they are regulatory elements, bound by transcription factors or bearing active histone marks in other types of cells, neither of these genes is known to be expressed in plasma cells. Several antibody quantities per IP were tested. We started by testing 3 µg of antibody per ChIP, but found little enrichment over background (Figure 25A-D). Next, we tested 0.5 µg and again found not a great deal of enrichment over background (Figure 26A-D). Finally, we tested 0.25 µg and found it to show the largest enrichments over control regions (Figure 27A-D). To determine the validity of the assay, we set the criteria for a successful ChIP experiment as having an enrichment over a negative control region of at least 5-fold for the H3K4me1, H3K4me3, and H3K27Ac marks. For the H3K27me3 mark, we set the criteria to a 3-fold enrichment. This was lower because the H3K27me3 mark is known to have a wider and less sharp distribution. The ChIP experiments showed high levels of H3K4me1 over the *PRDM1* promoter, two *PRDM1* enhancer regions, and an *XBP1* enhancer (Figure 27A). H3K4me1 marks enhancer and sometimes promoter regions (Heintzman et al., 2007).

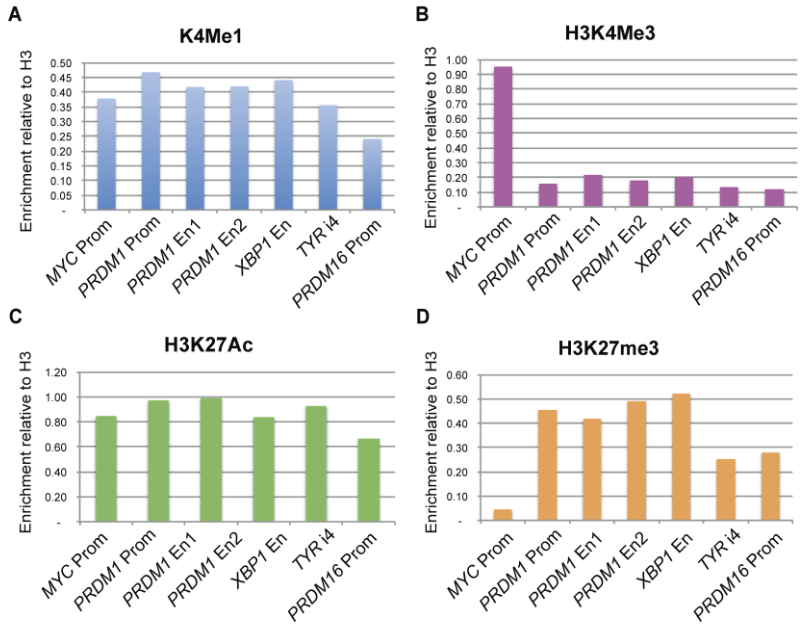

Figure 25: Testing of low-cell number ChIP using 3 µg of antibody per ChIP.

ChIP-qPCR results in the U266 cell line using 10^5 cells per ChIP for the following histone marks: **(A)** H3K4me1, **(B)** H3K4me3, **(C)** H3K27Ac, **(D)** H3K27me3. Values represent per cent input enrichment relative to ChIP-qPCR for histone H3.

The H3K4me3 mark, which marks promoters but not enhancers (Heintzman et al., 2007), was highly enriched over the *MYC* promoter (Figure 27B). The H3K27Ac mark is present on active promoters and enhancers (Creyghton et al., 2010), and here we observed it highest on the strong MYC promoter, and lowest over the negative control region of *TYR* intron 4 (Figure 27C). The H3K27me3 mark, which marks inactive or poised promoters and enhancers (Barski et al., 2007; Rada-Iglesias et al., 2010), was lowest over the *MYC* promoter region (Figure 27D). While earlier experiments had failed to show differences between positive and negative control regions, following our optimisation, we were able to clearly demarcate active and inactive promoter and enhancer regions. Thus, we were able to establish a procedure for performing ChIP using 10^5 plasma cells per IP.

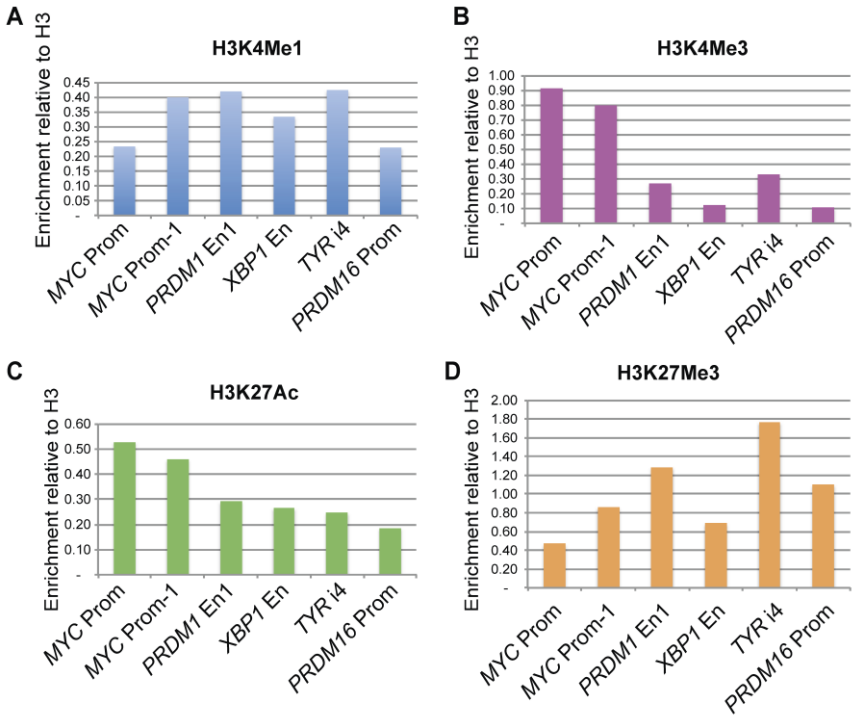

Figure 26: Testing of low-cell number ChIP using 0.5 µg of antibody per ChIP

ChIP-qPCR results in the U266 cell line using 10^5 cells per ChIP for the following histone marks: **(A)** H3K4me1, **(B)** H3K4me3, **(C)** H3K27Ac, **(D)** H3K27me3. Values represent per cent input enrichment relative to ChIP-qPCR for histone H3.

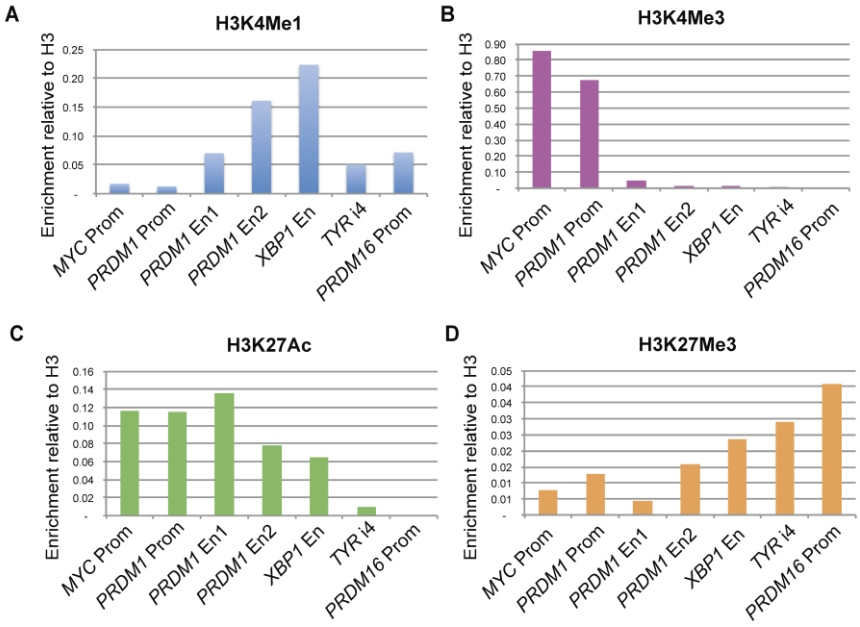

Figure 27: Establishment of a low-cell number ChIP protocol using 0.25µg antibody per ChIP

ChIP-qPCR results in the U266 cell line using 10^5 cells per ChIPwith 0.25 µg antibody for the following histone marks: **(A)** H3K4me1, **(B)** H3K4me3, **(C)** H3K27Ac, **(D)** H3K27me3. Values represent per cent input enrichment relative to ChIP-qPCR for histone H3.

Table 17: Cell quantities obtained from $CD138^+$ cell isolations

Patient diagnosis	**Number of cells**
Myeloma	1×10^5
Myeloma	4.4×10^5
Myeloma	2.4×10^5
Myeloma	5.1×10^5
Myeloma	2×10^6
Myeloma	1×10^6
Myeloma	5×10^5
Myeloma	8.5×10^5
MGUS	0.8×10^4
Myeloma	1.8×10^6
MGUS	1×10^5
Myeloma	18×10^6
Myeloma	4.92×10^5
SMM	2.87×10^6
Myeloma	5×10^5
Myeloma	1.95×10^5
Myeloma	2×10^3
Myeloma	1.1×10^4
Myeloma	6.3×10^4
Myeloma	2×10^4
Myeloma	5.8×10^6
Myeloma	1.63×10^5
MGUS	1.43×10^5
Myeloma	1.5×10^5

Myeloma	1.5×10^5
Myeloma	7×10^4
Myeloma	1.3×10^6
MGUS	1.2×10^6
Myeloma	3.4×10^4

The second task in establishing the procedure was to generate sequencing libraries using less than 2 ng of ChIP DNA, which was lower than the minimum 5 ng specified in ChIPseq library preparation kit protocols. We attempted to use a whole-genome amplification (WGA) method as used in (Ng et al., 2013), whereby the ChIP DNA was subjected to 5 cycles of PCR amplification using the Sigma single cell WGA kit. Because the WGA adaptors would cause problems in the sequencing run, we included a primer containing a BmpI restriction site during the amplification step. Following amplification, the adaptors were removed by BmpI restriction digest. Because this was insufficient to remove all of the remaining adaptors, the fragments were re-ligated to oligos containing an additional BmpI restriction site then subjected to a second restriction digest. This method provided us with sufficient quantities of ChIP DNA for library preparation, but did not seem ideal as it forced us to use additional PCR cycles. We had been attempting to use an in-house preparation of solid phase reversible immobilisation (SPRI) beads for purifying the WGA and ChIP DNA libraries (DeAngelis et al., 1995; Fisher et al., 2011). However, these beads provided much lower yields than could be obtained from the commercial Agencourt XP beads (Figure 28). Because the WGA and restriction digest protocol required many rounds of purification using SPRI beads, it was beyond our budget to use the Agencourt XP beads for every sample with this procedure.

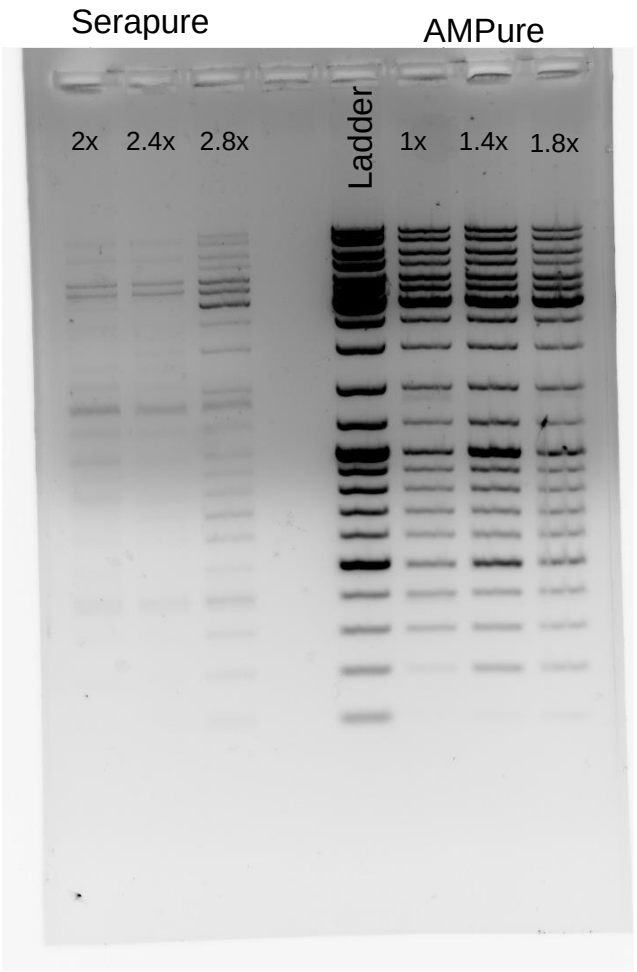

Figure 28: Testing of an in-house preparation of SPRI beads compared to a commercial preparation.

The in-house preparation (Serapure) provided much lower yields for DNA purification than the commercial preparation (AMPure). Serapure and AMPure SPRI beads were used at varying volume ratios relative to the volume of DNA ladder. Even the highest ratios of Serapure beads were unable to reproduce the yield of the lowest ratio of AMPure beads.

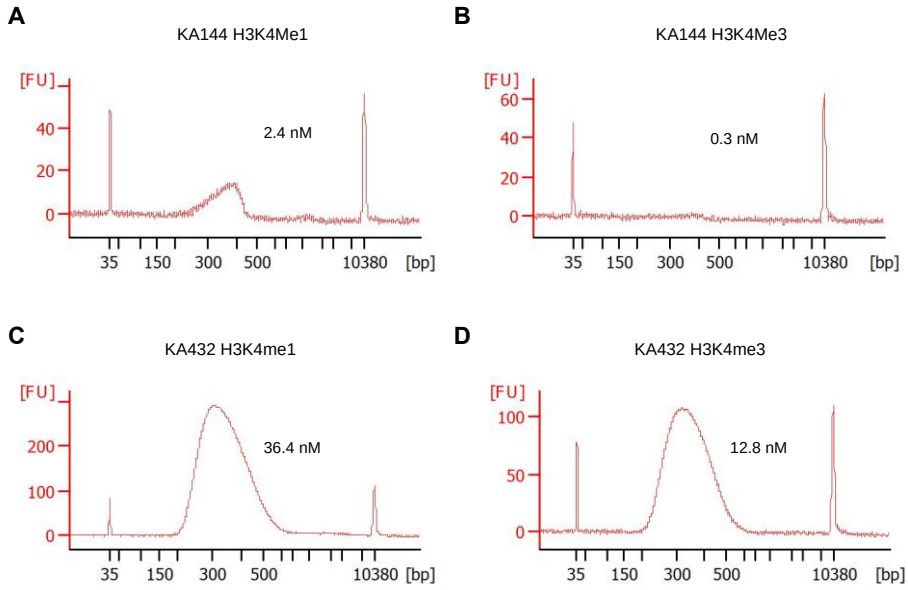

Figure 29: Quantities of ChIPseq library DNA

Bioanalyzer graphs depicting the size distribution and concentrations of ChIPseq library DNA following use of the standard procedure for library generation for the **(A)** H3K4me1 and **(B)** H3K4me3 ChIP experiments. Below are bioanalyzer graphs depicting the size distribution and concentrations of ChIPseq library DNA following use of the optimised protocol with increased adaptor ligation time for the **(C)** H3K4me1 and **(D)** H3K4me3 ChIP experiments.

In attempting to solve the above problems, we hypothesised that using the DNA library preparation kit without the pre-WGA procedure may come close to providing us with sequenceable quantities of ChIPseq libraries. When first attempting the library preparation procedure, we were unable to generate sufficient quantities of library DNA (Figure 29A-B). We did not want to over-amplify our libraries by increasing the number of PCR cycles above the recommended level, as over-amplification of a PCR reaction can lead to rehybridisation of PCR products, interfering with primers and extension, and leading to a decrease in the amplification rate of abundant PCR products (Mathieu-Daude et al., 1996). Instead, we hypothesised that an

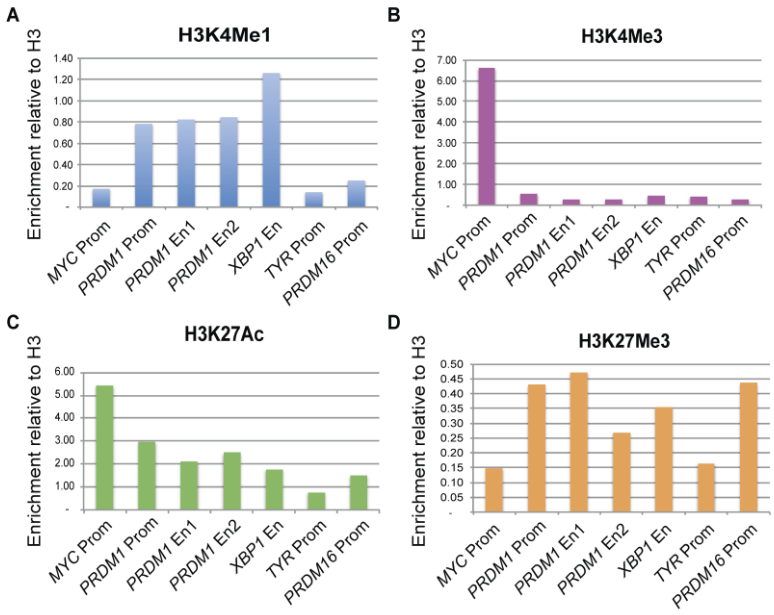

Figure 30: Low-cell number ChIPseq library generation

Low-cell number ChIPseq libraries were generated from 10^5 cells per ChIP using $CD138^+$ cells from myeloma patient bone marrow aspirate. qPCR was used to assess the libraries for enrichment over selected genomic regions for the following histone marks: **(A)** H3K4me1, **(B)** H3K4me3, **(C)** H3K27Ac, **(D)** H3K27me3. Values represent the enrichment relative to a ChIPseq library for histone H3.

increased incubation time for the adaptor ligation step may result in higher yields, and indeed using 1 h rather than the recommended 15 min led to successful generation of ChIPseq libraries with sufficient quantities for sequencing (Figure 29C-D).

To test if the enrichment of positive control regions was maintained over negative regions, we diluted the ChIPseq libraries 1:100 and subjected them to qPCR using the same primers as above, normalising to a ChIPseq library for histone H3. To demonstrate the effectiveness of this procedure, we then performed ChIP, sequencing library generation and qPCR in a patient myeloma sample, and observed a strong enrichment for the H3K4me1 mark over enhancer regions, but not over promoters or negative control regions

(Figure 30A). The H3K4me3 mark was highly enriched over the *MYC* and *PRDM1* promoter regions, but not enhancers (Figure 30B). The H3K27ac and H3K27me3 marks showed inverse enrichment, with the *MYC* and *PRDM1* promoters high for H3K27ac, but low for H3K27me3, and the repressed regions, *TYR* intron 4 and the *PRDM16* promoter showing low H3K27ac and high H3K27me3 (Figure 30C-D). Interestingly, the second *PRDM1* enhancer and *XBP1* enhancer were marked with both H3K27ac and H3K27me3, which could be indicative of heterogeneity within the pool of cells. Thus, the sequencing library generation procedure was able to maintain the representation of histone mark distribution seen with ChIP-qPCR. Together, these results demonstrate establishment of a working protocol for low-cell number ChIPseq library generation.

5.11.2 Validation of targeted transcript depletion in RNAseq library generation

The next component of Aim 4 of the project involved total RNAseq to identify differentially expressed eRNAs and other transcripts between MGUS and myeloma $CD138^+$ cells. We decided to use total RNAseq rather than a poly(A) isolation protocol because eRNAs are frequently non-polyadenylated. Standard protocols for total RNAseq involve depletion of ribosomal RNAs (rRNA) which make up a very large proportion of all transcripts in the cell (Zhao et al., 2014). A unique feature of plasma cells however, is that more than 70% of the transcriptome comprises transcripts of immunoglobulins (Shi et al., 2015), which plasma cells secrete as the antibody-producing factories of the body. In order to improve the sequencing depth for transcripts of interest, we performed an additional depletion of immunoglobulin transcripts along with rRNAs during our total RNAseq library preparation. This involved use of primer sequences targeted to the immunoglobulin transcripts, followed by elongation to form double-stranded reverse adaptors, and then

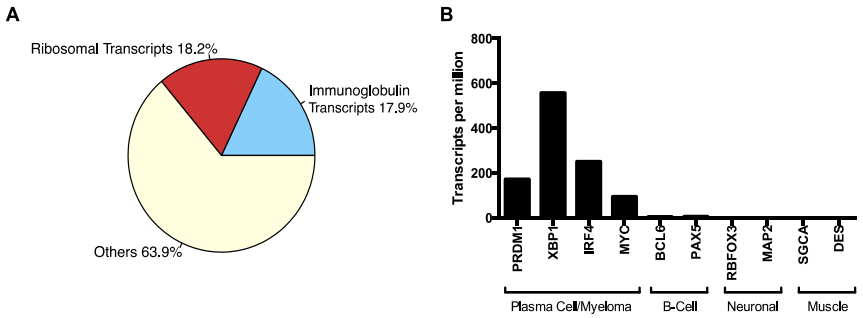

Figure 31: Efficacy of total RNAseq library preparation from CD138$^+$ cells from a myeloma patient bone marrow aspirate.

(A) Percentages of ribosomal and immunoglobulin transcripts following targeted depletion, compared to other annotated transcripts. **(B)** Transcript abundances in transcripts per million for plasma cell/myeloma genes, B cell genes, neuronal genes and muscle genes in the RNAseq sample.

cleavage of the double-stranded adaptors, so that the targeted transcripts were not able to be amplified during the subsequent PCR step. Because we did not have primers targeting other transcripts, they were not marked by double-stranded reverse adaptors and so did not have their adaptors cleaved prior to the PCR step. Following library preparation, we performed shallow sequencing to an approximate depth of 5 million reads per sample to test the percentage of rRNAs and immunoglobulin transcripts. Our results demonstrated that after depletion, the majority (63.9%) of transcripts detected were not ribosomal nor immunoglobulin RNAs (Figure 31A).

Since we were in possession of the shallow sequencing data, we then decided to examine the expression of myeloma plasma cell genes to validate the CD138$^+$ cell isolation and the total RNAseq library preparation. Promisingly, the plasma cell identity genes *PRDM1*, *XBP1* and *IRF4*, as well as the myeloma oncogene *MYC* were all highly expressed (Figure 31B). Contrastingly, there was very little expression of the B cell genes *BCL6* and *PAX5*, and no expression of the neuronal genes *RBFOX3* and *MAP2* or the muscle genes *SGCA* and *DES*. This confirmed the identity of the cells used in library preparation, and validated the procedure as maintaining expected gene expression profiles. Thus, we were able to confirm effective generation

of total RNAseq libraries depleted of ribosomal and immunoglobulin transcripts.

Taken together, our optimisations have established effective procedures for ChIPseq and total RNAseq using small quantities of material such as is obtained from bone marrow aspirates. The procedures described above have now been used for ChIPseq and RNAseq on bone marrow plasma cells from MGUS and myeloma patients. However, due to time constraints, we have not yet analysed the sequencing data from these experiments.

6 Technical hurdles and considerations

6.1 Off-target effects of EZH2 KD

Initially, we wanted to test the inhibition of EZH2 not only through catalytic inhibition, but also using the same piggyBac system that was used to generate the cells with BLIMP1 KD. We created two RPCI-WM1 cell lines harbouring inducible miRNAs targeting *EZH2* and generated single cell clones of these cells. These were termed *EZH2-miR#1*, *EZH2-miR#2-B10* and *EZH2-miR#2-G7*. Two clones were used for the *EZH2-miR#2* because they showed varying levels of EZH2 KD, and so were deemed valuable as a tool to see the effects of different quantities of EZH2. Both miRNAs produced a decrease in the amount of EZH2 protein, but the *EZH2-miR#2-G7* clone had the biggest decrease (Figure 32A). All of the clones examined led to an increase in apoptosis following 48h of induction (Figure 32B).

We next sought to rescue the effect of EZH2 KD by lentiviral ectopic expression of EZH2. We had received EZH2 lentiviral overexpression plasmids with a pLenti-CMV-Hygro backbone as used in (Xu, K. et al., 2012) as a kind gift from Kexin Xu. The EZH2 was fused to a haemagglutinin (HA) tag. When we tried to generate lentivirus using this plasmid, we failed to see any surviving cells following hygromycin selection. Furthermore, we failed to see any HA staining following transduction of RPCI-WM1 cells. This was attempted many times, with the idea of opmtimising the virus production. However, we also used a pLenti-CMV-EGFP-Hygro plasmid obtained from Addgene with the same method for lentivirus production. When this virus was used to transduce RPCI-WM1 cells, we observed very high transduction efficiency, with all cells surviving hygromycin selection.

At this point, we were running out of time and so decided to send our *EZH2-miR#2-B10* clone out for RNAseq before completing the rescue experiment. We found a highly significant correlation between the gene expression changes induced by this miRNA and those induced by the *PRDM1-miR#2* (Figure 32C). This suggested that BLIMP1 and EZH2 were likely targeting many of the same genes. During this time, we decided to clone the EZH2 cDNA from the pLenti-CMV-Hygro lentiviral plasmid into the FUGW backbone, which was previously used for ectopic expression of BLIMP1. We generated an *EZH2-miR#2*-resistant mutant EZH2-EGFP cDNA in this backbone. Using lentivirus produced with this plasmid, we were

successfully able to express miR-resistant EZH2-EGFP in the RPCI-WM1 *EZH2-miR#2* cells. (Figure 33A). This did not lead to any difference in the cell death phenotype following 2 days and 5 days of EZH2 KD compared to EGFP alone (Figure 33B). Thus, we concluded that the *EZH2-miR#2* was most likely causing cell death in the RPCI-WM1 cell line through an off-target effect. We had earlier attempted to rescue the EZH2 KD by ectopic expression of BLIMP1 (Figure 33C), and interestingly, we observed an increase in cell viability compared with cell expressing EGFP alone (Figure 33D). This, combined with the highly significant correlation between EZH2 and BLIMP1 target genes (Figure 32C), suggested that the *EZH2-miR#2* might have been targeting the *PRDM1* transcript or a factor that affects BLIMP1 expression. In light of this, we did not continue our RNAseq analyses or continue using these cells, but instead focused on treating the cells with the EZH2 inhibitor, tazemetostat.

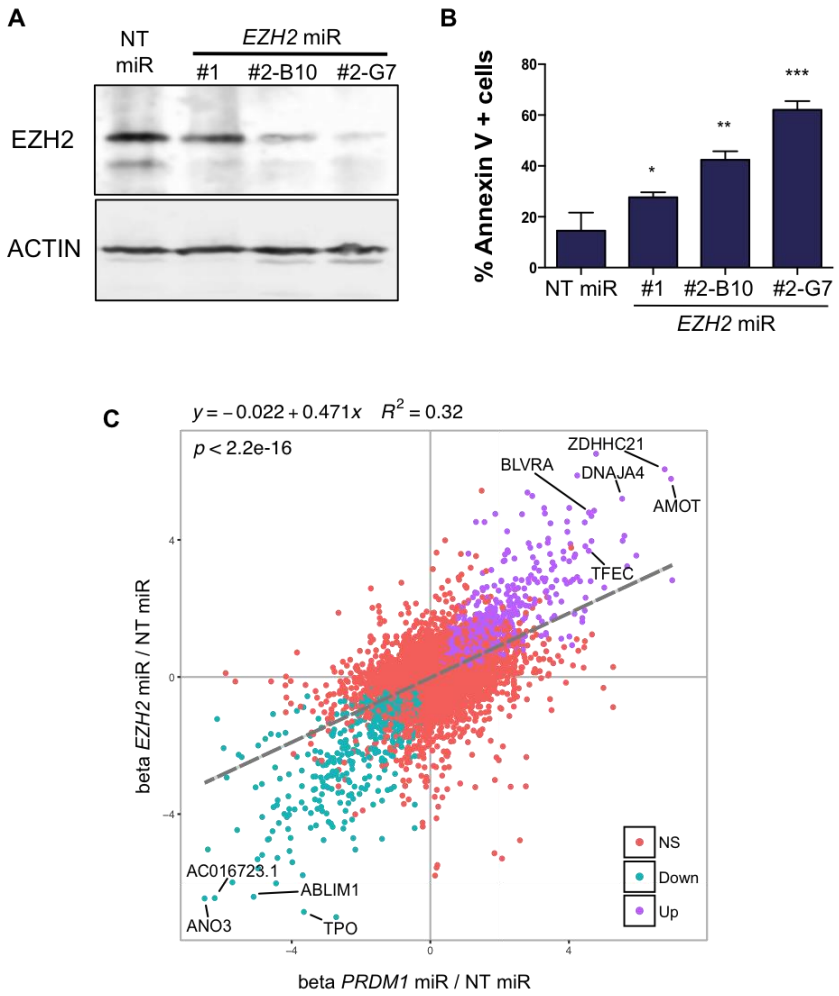

Figure 32: Profiling of the EZH2 miRs

(A) Western blot depicting the quantity of EZH2 following 48 h induction of the *NT-miR*, *EZH2-miR#1*, *EZH2-miR#2-B10* or *EZH2-miR#2-G7* RPCI-WM1 cells. **(B)** Annexin V staining depicting the percentage of apoptotic cells following 48 h induction of the RPCI-WM1 cells with the *NT-miR*, *EZH2-miR#1*, *EZH2-miR#2-B10* or *EZH2-miR#2-G7*. **(C)** Scatterplot depicting the beta values derived from the Wald test in Sleuth. The beta values represent the effect size of the $\log_e$-transformed values The x-axis depicts the beta values of *PRDM1-miR#2* compared to the *NT-miR* and the y-axis depicts the beta values of the *EZH2-miR#2-B10* compared to the *NT-miR*, all following 48 h of induction with dox. The blue dots represent genes with a statistically significant decrease in expression in both conditions, whereas the purple dots represent genes with a statistically significant increase in expression in both conditions. The red dots represent those genes that did not have statistically singificant changes in both conditions. The linear regression of these beta values shows a statistically significant correlation; $R^2 = 0.32$, $p < 2.2e\text{-}16$.

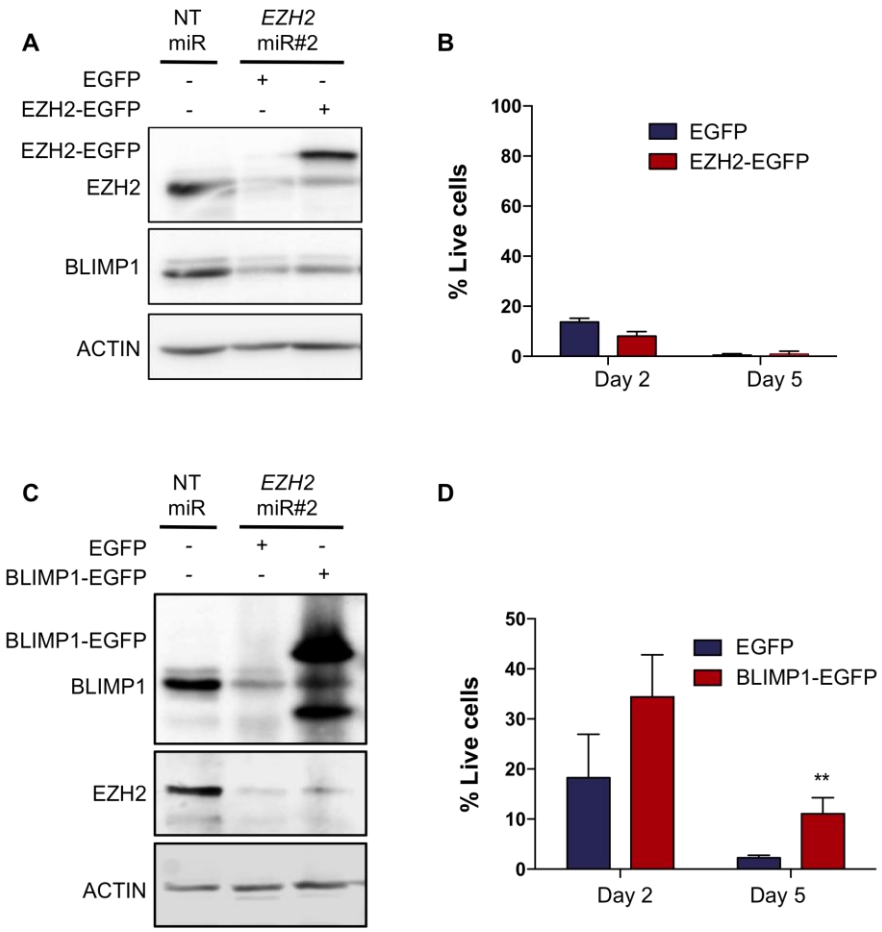

Figure 33: Restoring EZH2 expression does not rescue the cell death phenotype

(A) Western blot depicting ectopic expression of EGFP or EZH2-EGFP in RPCI-WM1 cells with *EZH2-miR#2-G7* compared to the *NT-miR*. **(B)** Percentage of live cells as determined by trypan blue exclusion assay following 2 days or 5 days of induction of *EZH2-miR#2-G7* with ectopic expression of EGFP or EZH2-EGFP. **(C)** Western blot depicting ectopic expression of EGFP or BLIMP1-EGFP in RPCI-WM1 cells with *EZH2-miR#2-G7* compared to the *NT-miR*. **(D)** Percentage of live cells as determined by trypan blue exclusion assay following 2 days or 5 days of induction of *EZH2-miR#2-G7* with ectopic expression of EGFP or BLIMP1-EGFP.

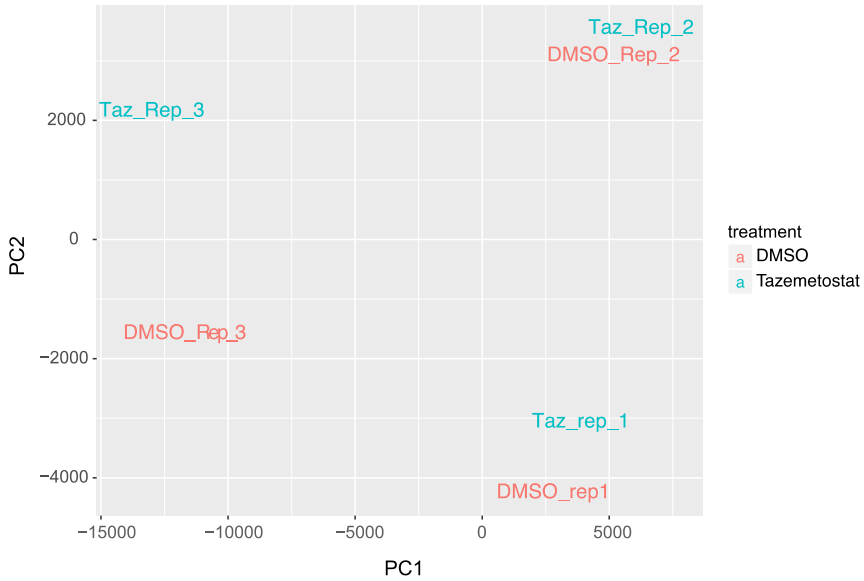

Figure 34: Principle component analysis of DMSO and tazemetostat-treated RNAseq samples, showing individual replicates

6.2 Alternative methods needed for Tazemetostat RNAseq analysis

Following RNAseq for RPCI-WM1 cells treated with tazemetostat or the DMSO vehicle control, we failed to see separation of the samples based on treatment using principle component analysis (Figure 34). Additionally, a basic wald test and likelihood ratio test using Sleuth provided almost no differentially expressed genes. Further investigation led us to realize that the samples were clustering based on the day that the libraries were prepared rather than the treatment. But fortunately, we had designed our experimental setup such that one replicate for every sample was prepared on each separate day, essentially in batches for each replicate. All samples were given separate indexes and sequenced together in a multiplexed pool on an individual lane so that lane effects would not be present. In this way, if we took the batch into account as another covariate in the analysis it would allow us to see through the batch effect. This was very effective, allowing us to uncover 450 differentially expressed genes comparing tazemetostat to DMSO in the RPCI-WM1 cell line (Figure 9B). For the R script used, please see Appendix I.

6.3 Isolation of CD138+ cells from human bone marrow

A major hurdle in the project was in the difficulty of isolating a pure population of $CD138^+$ cells with a yield high enough to be used for ChIPseq and RNAseq library generation. Our initial protocol involved positive selection using anti-CD138 conjugated microbeads. The purity resulting from this method was often very low, but varied from patient to patient, with a maximum of 99%, and a minimum of 6% (Table 18). We consulted with the labs of Minal Patek (Memorial Sloan Kettering Cancer Center) and Sigurður Yngvi Kristinsson (Karolinska Institute and the University of Iceland) who had been isolating $CD138^+$ cells on a large scale. We found that they did not continue with plasma cell isolation from samples that had fewer than 20×10^6 mononuclear cells following density gradient centrifugation. However, due to the average diagnoses of myeloma patients in Iceland, being only around 12 cases per year, we could not afford to discard samples if we were to complete the project in the allotted time frame.

Table 18: Purity of multiple myeloma and MGUS samples collected in Iceland purified using the anti-CD138 microbeads

Sample	Purity
Myeloma	89%
Myeloma	75%
MGUS	too few cells
Myeloma	30%
MGUS	30%
Myeloma	97%
Myeloma	93%
SMM	70%
Myeloma	83%
Myeloma	65%
Myeloma	6%

Myeloma	too few cells
Myeloma	too few cells
Myeloma	67%
Myeloma	90%
Myeloma	99%
Myeloma	89%
MGUS	56%
Myeloma	26%

In order to try to improve the purity of our $CD138^+$ cell isolations, we moved to using a plasma cell isolation kit from Miltenyi, which first involved depletion of non-plasma cells, followed by positive selection using anti-CD138 microbeads. This method appeared to improve the purity, but was very time consuming (Table 19). In our search, we were then introduced to the CD138 whole blood isolation kit, which involves purification of $CD138^+$ cells directly from whole blood or bone marrow without the density gradient centrifugation step. This cut down on the time of the procedure dramatically and appeared to give a good yield and purity (Table 20), but by this stage we were running out of time for increasing our sample collection. Instead, we then contacted collaborators in Sweden who supplied us with 8 MGUS patient samples that had already been purified. Unfortunately, two of these samples had very low quality RNA following isolation, likely due to being stored as cell pellets at -80˚C for more than five years. We were finally able to generate ChIPseq and RNAseq libraries for seven Icelandic multiple myeloma patient samples and seven MGUS samples, one Icelandic and six Swedish. Because of the small number of samples, we also decided to include ChIPseq and RNAseq libraries for the multiple myeloma cell lines OPM-2 and NCI-H929. The libraries have now been sequenced and the data is awaiting analysis. Having the vast majority of MGUS samples from Sweden, and all of the myeloma samples from Iceland is a potential caveat of this project due to the genetic differences in these populations.

Table 19: Purity of multiple myeloma samples isolated using the plasma cell isolation kit with depletion of non-plasma cells

Sample	Purity
Myeloma	33%
Myeloma	93%
Myeloma	95%

Table 20: Purity of MGUS and multiple myeloma samples isolated using the CD138 whole blood isolation kit

Sample	Purity
MGUS	87%
Myeloma	34%

6.4 Technical hurdles as learning opportunities

The technical hurdles described above absorbed large amounts of time during this PhD project, but served as important learning opportunities. The first hurdle demonstrated the importance of performing rescue experiments for any RNA interference or knock-out experiment. In addition, using more than two targeting miRNAs may have saved us the time of profiling cells with an off-target effect. The second hurdle was fortunately not too difficult to overcome due to our careful experimental design early on. This highlights the extreme importance of batch design, as batch effects can be a heavily confounding variable (Auer & Doerge, 2010).

The third hurdle gave us the opportunity to learn about the difficulty of using freshly collected human patient material and the challenges associated with needing to utilise every sample from a newly diagnosed patient in the country. The small population of Iceland, while providing us with a unique situation from a genomic perspective, creates additional challenges due to the scarcity of patient material. This is something that needs to be taken into account for future projects. Furthermore, the challenges associated with setting up isolation protocols in a location where they have not previously been performed in this way need to be taken into account when planning the time line of a project.

7 Discussion

Transcriptional regulation is a central process in development and disease, driving cell identities and differentiation, as well as malignant transformation. Antibody secreting malignancies such as Waldenström's macroglobulinemia and multiple myeloma are suitable disease models for studying transcriptional regulation, as both are derived from the B cell differentiation process with its multitude of changes in transcriptional control and chromatin architecture. It is interesting to study these diseases in relation to their cells of origin and to consider the transformative events in the context of the normal genetic and transcriptional changes that occur during differentiation.

In this study I present novel evidence of BLIMP1 functioning as a pro-survival factor in Waldenström's macroglobulinemia cell lines. I show for the first time that BLIMP1 maintains EZH2 protein levels. Highlighting the interplay of the two factors, I demonstrate a large overlap in transcriptional targets. Although an interaction has been shown between these proteins in mouse plasmablasts (Minnich et al., 2016), I find here that the majority of their co-operation results from binding to distinct sites on the same genes as well as through BLIMP1 maintaining EZH2 protein levels. Interestingly, both BLIMP1 and EZH2 inhibit NK cell mediated cytotoxicity against Waldenström's macroglobulinemia cells through effects on NK cell activation and promoting resistance to killing by NK cells. Furthermore, BLIMP1 KD leads to cell cycle arrest, and large transcriptional changes in genes relating to the cell cycle, checkpoint enforcers, and the DNA damage response. In addition, I present the development of procedures for ChIPseq and total RNAseq from low numbers of cells derived from patient bone marrow aspirates. These techniques can be used for the identification of transcriptional enhancers.

7.1 BLIMP1 as a pro-survival factor in Waldenström's macroglobulinemia

BLIMP1 has long been considered a tumour suppressor in the context of DLBCL (Calado et al., 2010; Mandelbaum et al., 2010; Pasqualucci et al., 2006), and yet it has been described as a necessary survival factor for multiple myeloma (Hung et al., 2016; Lin et al., 2007). In an interesting contradiction, inactivating mutations in the *PRDM1* gene have been found in

some myeloma patients (Lohr et al., 2014). This has led to speculation that BLIMP1 could act as a tumour suppressor in this context as well (Nutt et al., 2015). However, the inactivating mutations in *PRDM1* are almost exclusively heterozygous events (Lohr et al., 2014). Thus, there is likely to be some BLIMP1 expression remaining in these cells. This is in line with the frequent heterozygous deletions in the 6q region, containing *PRDM1* in Waldenström's macroglobulinemia (Schop et al., 2002; Schop et al., 2006). Although *PRDM1* is not the most frequently lost gene with 6q deletions, with loss of other genes such as *HIVEP2* and *ARID1B* being more common (Hunter et al., 2014), *PRDM1* is still commonly lost, and deletions within 6q are likely to be a secondary event following malignant transformation (Schop et al., 2006). Indeed, the loss of 6q has been shown to correlate with the $MYD88^{L265P}$ mutation in Waldenström's macroglobulinemia (Kim et al., 2014). Intriguingly, *PRDM1* is transcriptionally activated downstream of MYD88 and TLRs in B cells (Capolunghi et al., 2008; Douagi et al., 2009; Genestier et al., 2007; Lin et al., 2006; Morgan et al., 2009; Pasare & Medzhitov, 2005), and transcriptomic analyses from Waldenström's macroglobulinemia patients show *PRDM1* expression to positively correlate with the presence of the $MYD88^{L265P}$ mutation (Hunter et al., 2016). To explain this apparent contradiction, of both heterozygous *PRDM1* deletion and *PRDM1* expression correlating with $MYD88^{L265P}$, it is useful to consider the effect of BLIMP1 expression at different stages of B cell differentiation. Just as described for IRF4 in B cells (Ochiai et al., 2013; Saito et al., 2007; Sciammas et al., 2006), graded expression of BLIMP1 defines different stages of antibody-secreting cell differentiation (Kallies et al., 2004). Low to intermediate levels of BLIMP1 are expressed in plasmablasts to support antibody secretion, but at levels low enough that the cells retain proliferative capacity and the ability to migrate (Kabashima et al., 2006; Nutt et al., 2007). Conversely, high levels of BLIMP1 have been reported to inhibit the cell cycle (Shaffer et al., 2002). I propose a model whereby *PRDM1* is activated downstream of $MYD88^{L265P}$ in Waldenström's macroglobulinemia, and in order to maintain proliferative capacity, the cells that lose one copy of *PRDM1* are positively selected for, as those with high BLIMP1 expression cease cycling. Furthermore, loss of other loci within the 6q region could impact on *PRDM1* transcription by inactivating enhancer regions or causing changes to the chromatin structure around this gene. The remaining copy of *PRDM1* could produce low to intermediate BLIMP1 protein levels and provide a survival advantage, supporting antibody secretion without inhibiting proliferation. Thus, the heterozygous loss of *PRDM1* does not necessitate a function as a tumour suppressor.

7.1.1 BLIMP1 maintenance of cell cycle progression and DNA repair pathways

The repression of pro-apoptosis genes by BLIMP1 is a likely mechanism for promoting cell survival. However, the absence of BLIMP1 binding to these genes indicates that this is not a primary effect of BLIMP1. Instead, maintaining expression of positive cell cycle regulator genes such as *E2F1* and repressing G1/S checkpoint enforcer genes such as *CDKN1A* may prevent apoptosis. Whether BLIMP1 is indeed inducing transcriptional activation of *E2F1* is an interesting question. It would be highly informative to conduct experiments such as in Minnich et al., 2016, where Blimp1 was ectopically expressed fused to the oestrogen receptor, and could be induced to translocate to the nucleus through the addition of 4-hydroxytamoxifen. The authors added cycloheximide to inhibit translation, then induced the nuclear translocation of Blimp1. Under these conditions, they were able to measure direct transcriptional targets that were not mediated through secondary transcriptional effects. It is also interesting to consider the graded expression of BLIMP1 conferring different functions in relation to regulation of the cell cycle. I propose that low levels of BLIMP1 may actually positively regulate the cell cycle, whereas higher levels inhibit it. This is also relevant in relation to the overlapping targets of BLIMP1 and EZH2, and BLIMP1 maintenance of EZH2 protein levels, with EZH2 most well known as a driver of proliferation. Surprisingly here, I did not observe EZH2 inhibition to induce changes in cell cycle progression genes.

A highly relevant question is whether BLIMP1 is in fact maintaining expression of genes involved in DNA repair pathways. While I did see extensive gene expression changes, this could be more due to the changed distribution of the RPCI-WM1 cells in each phase of the cell cycle. The homologous recombination and mismatch repair pathways do not take place in the G1 phase (Hustedt & Durocher, 2016), and so it follows that if most of the cells are arrested in G1, there will be decreased expression of these repair pathway genes. However, genes involved in other pathways such as NHEJ are expressed throughout the cell cycle and also show decreased expression following BLIMP1 KD. While more experiments would be needed to understand more precisely what is occurring, it appears that BLIMP1 could be maintaining expression of DNA repair genes, and possibly even though direct binding and activation. Again, conducting experiments to determine direct targets of transcriptional activation by BLIMP1 would provide useful insight into this situation. If it is indeed the case that BLIMP1 is maintaining DNA repair pathway activation, it is interesting to speculate that the loss of

BLIMP1 might lead to the accumulation of DNA damage, and that BLIMP1 might be induced in response to DNA damage. Indeed, in human skin cells, *PRDM1* is one of the few genes activated early on in response to ionising radiation (Albrecht et al., 2012). Furthermore, a polymorphism affecting the expression of the *PRDM1* gene confers increased susceptibility to radiation therapy induced secondary malignant neoplasms. This variant decreases BLIMP1 expression and prevents BLIMP1 activation in response to ionising radiation (Best et al., 2011). Recent preliminary data from our lab indicate that DNA double strand breaks accumulate in the RPCI-WM1 cell line upon BLIMP1 KD. Together, these data support the concept of BLIMP1 playing an important role in DNA repair.

As an alternative to direct regulation by BLIMP1, the repression of BCL6 by BLIMP1 could also be the main mechanism behind BLIMP1's role in regulation of cell cycle and DNA repair genes. BCL6 represses the DNA damage sensor ATR, and the G2/M checkpoint driver CHEK1 in B cells (Ranuncolo, Stella Maris et al., 2007; Ranuncolo, Stella M. et al., 2008). This is a normal mechanism for allowing the processes of SHM and CSR to take place in germinal centre B cells. I could speculate that perhaps low levels of BLIMP1 are induced by the DNA damage taking place during these processes. BLIMP1 could then function to repress BCL6 and activate DNA repair mechanisms, which also play a role in SHM and CSR, and subsequently drive the cell towards a more differentiated plasmablast-like state.

Overall, BLIMP1 regulating the cell cycle and DNA repair pathways in Waldenström's macroglobulinemia could be a good example of how cancer cells can utilise the conventional roles of a transcription factor in cell differentiation to promote a malignant phenotype.

7.1.2 BLIMP1 promoting escape from immune surveillance

The evasion from immune surveillance promoted by BLIMP1 can be seen as another survival mechanism in Waldenström's macroglobulinemia. BLIMP1 has long been studied in relation to transcriptional repression of immune signalling mechanisms, such as the *IFN-β* promoter and *CIITA* (Chen et al., 2007; Keller, A D & Maniatis, T, 1991; Piskurich et al., 2000; Tooze et al., 2006). However, this was always discussed as an aspect of its role in B cell biology, rather than a mechanism for evading the immune system. Crosstalk between NK cells and B cells occurs under normal circumstances to promote immunoglobulin secretion and class switching following B cell activation, as well as to influence the presentation of antigen by B cells to T cells (Yuan et

al., 2010). B cells can also activate NK cells to increase cytokine production via direct cell-cell interactions (Gao et al., 2006). It therefore follows that as BLIMP1 represses the B cell transcriptional program and B cell immune signalling, it also represses the transcription of genes relating to B cell-NK cell interactions.

MHC class I is important for managing the balance between activation and inhibition of NK cells, providing a strong inhibitory signal. While BLIMP1 has previously been shown to repress MHC class I pathway genes, but not the MHC class I molecule-encoding genes themselves (Doody et al., 2007; Mould et al., 2015), in the present study, I found it to be activating or maintaining expression of the MHC class I genes *HLA-A* and *HLA-B*. This could represent a perturbation of BLIMP1's normal role in repressing the MHC class I antigen presentation pathway, instead maintaining MHC class I molecule expression in order to maintain NK cell immune tolerance in Waldenström's macroglobulinemia. The expression of MHC class II molecules on B cells is an integral part of their role as professional APCs, and MHC class II repression by BLIMP1 is a normal part of plasma cell differentiation (Piskurich et al., 2000). However, loss of MHC class II could also lead to impaired recognition by T cells. Thus, BLIMP1 may be avoiding killing by both NK cells and T cells through modulation of MHC class I and II genes in Waldenström's macroglobulinemia cells.

Repression of activating ligands by BLIMP1 indicates that BLIMP1 is likely leading the Waldenström's macroglobulinemia cells to "hide" from the NK cells. This is evidenced by the increased degranulation of the NK cells following BLIMP1 KD. In this way, Waldenström's macroglobulinemia cells expressing BLIMP1 are able to avoid activating the NK cells, and thus escape immune-mediated killing. At the same time, Waldenström's macroglobulinemia cells expressing BLIMP1 are likely evading cell death signals from the NK cells by repressing expression of IFN and TNF receptors as well as downstream responder genes such as *STAT1*. NK cells perform their cytotoxic activities both by releasing cytotoxic granules and apoptosis-inducing cytokines, as well as directly through the Fas Ligand and TNF-related apoptosis-inducing ligand (Morvan & Lanier, 2015). Hand-in-hand with the repression of responses to inhibitory cytokines, is the repression of apoptosis mediators themselves. As discussed above, BLIMP1 suppresses apoptosis in Waldenström's macroglobulinemia cells, which can be seen as another mechanism of immune escape, through de-sensitisation to apoptosis-inducing signals.

In addition to modulating T or NK cell activation, B cells and plasma cells themselves bear inhibitory checkpoint receptors, which when stimulated with ligand can lead to cell death and altered interactions with immune effector cells. These checkpoints are frequently lost in DLBCL and multiple myeloma as a mechanism for promoting survival (Boice et al., 2016; Lozano et al., 2018). As well as inhibitory checkpoint receptors, many of their corresponding ligands were also expressed on the RPCI-WM1 cells following BLIMP1 KD. Recent studies have shown that *in cis* interactions of inhibitory receptors and ligands can lead to inhibition of *trans* interactions between target and effector cells (Claus et al., 2016; Zhao et al., 2018). Through expressing the receptors alongside the ligands, the RPCI-WM1 cells could be activating inhibitory signalling *in cis*, as well as preventing engagement of inhibitory receptors on NK cells or T cells. Thus, BLIMP1 promotes Waldenström's macroglobulinemia cell survival through multiple methods relating to escape from immune surveillance. This demonstrates how BLIMP1 makes use of its normal roles in plasma cells to provide a survival advantage to cancer cells.

Using only one cell line for the immune evasion experiments is however, a weakness of this project. To increase the scope of the project, using other Waldenström's macroglobulinemia cell lines and multiple myeloma cell lines as well as cells from patients would be extremely useful. It would be interesting to extend these results even beyond B cell malignancies by looking at the effects of BLIMP1 KD on immune evasion in other cancers where BLIMP1 is expressed, such as in breast cancer or pancreatic cancer (Chiou et al., 2017; Sciortino et al., 2017).

Taken together, the graded expression of BLIMP1 and the developmental stage at which it is expressed are likely the keys to its tumour suppressor verses pro-survival role. Our results demonstrate that BLIMP1 affects apoptosis, the cell cycle, DNA repair and immune evasion to maintain Waldenström's macroglobulinemia cell survival. It would be worthwhile to inhibit BLIMP1 in Waldenström's macroglobulinemia patient tumour cells to confirm these mechanisms.

It is useful to keep in mind that the use of cell lines and not primary patient material has limited the scope of our study. I cannot say that our results apply generally in Waldenström's macroglobulinemia due to this. Furthermore, it would have been good to use more than one cell line in the RNAseq and ChIPseq analyses. For the RNAseq analyses this may have been possible, but I had technical difficulties in generating and culturing MWCL-1 and

BCWM.1 cell lines with BLIMP1 KD. Even though this was an inducible miRNA, the induction was often present even without the addition of doxycycline, and so I often observed a large amount of cell death very quickly, and upon subsequent passages was no longer able to observe an inducible KD. This was particularly a problem for the BCWM.1 cell line where I was not able to generate a stable cell line with inducible BLIMP1 KD. Outside of the project's time constraints it would be good to produce such cells using another method, such as a lentiviral inducible system, or an inducible CRISPR-Cas9 system. If these methods could provide us with a more precisely inducible system we could have avoided the miRNA expression in the absence of doxycycline, and possibly achieved a good KD of BLIMP1 in the BCWM.1 cell line. If this method could then be applied to Waldenström's macroglobulinemia patient lymphoplasmacytic cells, it would go a long way towards increasing our understanding of BLIMP1's role in Waldenström's macroglobulinemia.

7.2 The interplay of BLIMP1 and EZH2

7.2.1 BLIMP1 and EZH2 in Waldenström's macroglobulinemia and multiple myeloma – relation to B cell development

Considering the co-expression of BLIMP1 and EZH2 in the same cell can underscore the roles these factors are playing, as both have highly specific expression in B cell and plasma cell ontogeny. Pre-plasmablasts and plasmablasts are perhaps the only B cell stage where these two factors are co-expressed (Herviou et al., 2019; Jourdan et al., 2011; Kallies et al., 2004). While Waldenström's macroglobulinemia and myeloma cells do not have all of the characteristics of pre-/plasmablasts, it follows that these malignant cells may have hijacked the transcriptional apparatus of this differentiation stage to maintain proliferation. I would conjecture that Waldenström's macroglobulinemia could arise from a pre-plasmablast-like cell, with both proliferative and antibody-secreting capacity. These pre-plasmablast-like cells likely differentiated from memory B cells or other B cells, which had previously undergone SHM outside of the germinal centre, which could explain the phenotype of expressing somatically hypermutated but not class switched immunoglobulins.

The co-expression of both B cell and plasma cell transcription factors in Waldenström's macroglobulinemia, including PAX5, SPIB, BLIMP1, IRF4, and the spliced form of XBP1 (Zhou et al., 2014) represents an expression profile in conflict with the most well-known expression patterns for these

factors, which would typically not be co-expressed (Nutt et al., 2015). However, following stimulation of memory B cells, both pre-plasmablasts and those B cells which do not lose expression of CD20 to form pre-plasmablasts exhibit co-expression of B cell and plasma cell transcription factor genes (Jourdan et al., 2011). Although both B cell and plasma cell transcription factors are co-expressed in Waldenström's macroglobulinemia, that does not rule out a role for BLIMP1 in repressing transcription of B cell genes such as *PAX5* and *BCL6*. Indeed, my results did demonstrate increased expression of *PAX5* and *BCL6* following BLIMP1 KD. Instead, BLIMP1 may be partially suppressing the expression of these genes, keeping them at a low enough level to support antibody secretion. Meanwhile, the expression of PAX5 may be simultaneously promoted by other B cell transcription factors such as TCF3 (E2A), SPI1 (PU.1) and IKZF1 (IKAROS), which are all highly expressed on an mRNA level in the RPCI-WM1 cell line. TCF3 is also known to be expressed in activated and germinal centre B cells in mice, likely playing a role in maintaining PAX5 expression (Kwon et al., 2008). It is interesting to speculate that some perturbed factors in Waldenström's macroglobulinemia could maintain the chromatin architecture needed for the expression of B cell factors, while at the same time allowing for plasma cell gene expression. For example, the DNA methyltransferases Dnmt3a and Dnmt3b were recently implicated in the regulation of chromatin architecture, functioning to dampen plasma cell differentiation (Barwick et al., 2018). Factors such as these and others may contribute to the feedback mechanisms dampening the effects of constitutive MYD88 signalling and holding the cells in an "in-between" stage of differentiation. Taken together, the co-expression of B cell and plasma cell transcription factors in Waldenström's macroglobulinemia likely occurs as a finely tuned balancing act between inhibition and activation.

A recent study demonstrated that ectopically expressing BLIMP1 early in B cell development leads to increased plasma cell differentiation in the absence of germinal centre B cells (Bönelt et al., 2018). Interestingly, these plasma cells express higher levels of IgM, but not IgG. This also shows some similarities to Waldenström's macroglobulinemia cells, suggesting that the early expression of BLIMP1 in Waldenström's macroglobulinemia, due to for example, $MYD88^{L265P}$, could lead to a more differentiated antibody-secreting phenotype. In support of this idea, *SDC1*, which encodes the plasma cell marker CD138, has higher mRNA expression in Waldenström's $CD19^{+}$ cells compared to healthy donor B cells (Hunter et al., 2016).

Another possibility is that Waldenström's macroglobulinemia cells comprise a spectrum of cells at different stages of differentiation, with some cells acting as tumour initiating cells, capable of replenishing the tumour following treatment. The assortment of cells at different differentiation stages is evidenced by the heterogeneity of BLIMP1 expression in the MWCL1 and BCWM.1 cell lines. It would be highly informative in the future to conduct an experiment where the cells would be sorted for BLIMP1 or CD138 expression and profiled for the expression of B cell markers such as CD19 and CD20, a well as other properties such as levels of antibody secretion, proliferation rate, responses to currently used therapies, and their ability to be maintained in culture. I would hypothesise that the cells with high BLIMP1 expression may have different properties to those with low BLIMP1. For example, in multiple myeloma, there exists a cellular subset resembling pre-plasmablasts that express the un-spliced form of XBP1. They are resistant to bortezomib, and capable of recapitulating tumours following treatment (Leung-Hagesteijn et al., 2013). In Waldenström's macroglobulinemia, the cells with low BLIMP1 expression may comprise the more proliferative or treatment-resistant compartment, perhaps the tumour initiating cells, which can later differentiate to express higher levels of BLIMP1 and secrete high levels of antibody.

Interestingly, in mouse plasmablasts and pre-plasmablasts, EZH2 binds to cell cycle and DNA repair genes in the absence of the H3K27me3 mark (Herviou et al., 2019). I observed some of these same genes to be induced following BLIMP1 KD, but not EZH2 inhibition in our RNAseq data. This raises the interesting idea of the differences in the role of EZH2 as a histone methyltransferase verses its role independent of this activity. It was previously shown that in some cancers dependant on EZH2 expression, the catalytic activity of EZH2 was somewhat dispensable for their survival (Kim et al., 2015). I could speculate that BLIMP1 maintaining EZH2 protein levels drives its histone methyltransferase-independent activity to positively regulate the cell cycle and DNA repair mechanisms. If this occurred independently of EZH2's catalytic activity, we would not observe these changes following tazemetostat treatment, as tazemetostat only inhibits the catalytic activity of EZH2.

The physical interaction of Blimp1 and Ezh2 demonstrated in mouse plasmablasts showed only a very small proportion of the endogenous Ezh2 protein was precipitated with Blimp1 (Minnich et al., 2016). Furthermore, our ChIPseq for BLIMP1 and H3K27me3 suggested that if the proteins are co-binding to chromatin in these cells, it is indeed a very small fraction of the endogenous proteins, as there were very few regions bound by both BLIMP1

and H3K27me3 within 10 kb of one another. In fact, I observed a similar enrichment of H3K27me3 over BLIMP1 binding sites in the RPCI-WM1 cell line, as seen in mouse plasmablasts (Minnich et al., 2016). However, I believe this to be more likely a reflection of general histone density, rather than due to the specific recruitment of EZH2 by BLIMP1. The presence of H3K27me3 is a hallmark of transcriptionally inactive regulatory elements (Barski et al., 2007), and BLIMP1 typically functions as a transcriptional repressor, bound to inactive regions of the genome. There is typically a depletion of nucleosomes in the immediate vicinity of sequence-specific transcription factor binding sites (Li et al., 2007). Thus, even if BLIMP1 is not recruiting EZH2 to chromatin to deposit H3K27me3, there could be a slight enrichment of H3K27me3 on either side of BLIMP1 binding sites due to the repressed state of most of these regions. Alternatively, it is also possible that the co-expression of these factors without their physical interaction could be an underlying pathogenic feature of Waldenström's macroglobulinemia and high-risk multiple myeloma. It would be interesting to generate BLIMP1 and EZH2 deletion mutants to identify which specific portions of the proteins are necessary for their interaction, and to examine the effects of disrupting the interaction in plasmablasts.

Using only one Waldenström's macroglobulinemia cell line for ChIPseq was a weakness in our project. For the ChIPseq analyses, I wanted to only look at the binding sites of endogenous BLIMP1 rather than using overexpression, as the level of BLIMP1 expression can have a huge influence on its function. In light of this, it would be technically very challenging to perform ChIPseq for BLIMP1 in the MWCL-1 and BCWM.1 cell lines because of their low BLIMP1 expression. Although, in the absence of time constraints, a project on optimising BLIMP1 ChIPseq in other Waldenström's macroglobulinemia cell lines or even in patient tumour samples could provide us with extremely valuable insights into the function of this protein.

7.2.2 The maintenance of EZH2 by BLIMP1

The observation of BLIMP1 maintaining EZH2 protein levels is a highly novel result. This could explain the results of a recent study which found that knock-out of EZH2 induced the activation of BLIMP1 transcriptional targets (Guo et al., 2018). These targets could simply be repressed by BLIMP1 through the maintenance of EZH2. It also explains the transcriptional changes overlapping between BLIMP1 KD and EZH2 inhibition, beyond the mechanism of the two factors binding to the same genes.

A question that was raised during the study was whether BLIMP1 maintains EZH2 levels through inhibition of the proteasome or through *miR-138*. Inhibition of the proteasome by BLIMP1 is the more likely candidate, as when I combined BLIMP1 KD with proteasomal inhibition it led to a restoration of EZH2 levels. However, BLIMP1 KD induced *miR-138* expression from a previously undetectable level and *miR-138* is well known to target EZH2 (Liang et al., 2014; Rastgoo et al., 2018a; Zhang et al., 2013; Zhu et al., 2016). It would be useful to further investigate the role of *miR-138* targeting EZH2 downstream of BLIMP1 by knocking out *miR-138* and then inducing BLIMP1 KD to confirm that inhibition of the proteasome by BLIMP1 was the main mechanism by which it maintains EZH2 levels.

One way in which BLIMP1 may be inhibiting the proteasome to maintain EZH2 is via mTOR. Protein degradation via both autophagy and the ubiquitin-proteasome system is activated when mTORC1 is inhibited (Zhao et al., 2015). The mTOR pathway is regulated by Blimp1 in mouse plasmablasts (Tellier et al., 2016), and in our results mTORC1 signalling was negatively enriched with BLIMP1 KD. Furthermore, the mTOR inhibitor, everolimus has recently demonstrated activity in clinical trials for relapsed and primary Waldenström's macroglobulinemia (Ghobrial, Irene M. et al., 2013; Treon et al., 2017b). BLIMP1 also activates the unfolded protein response, which interacts with mTOR signalling in plasma cells (Goldfinger et al., 2011; Shaffer et al., 2004; Tellier et al., 2016), and was also negatively enriched in our results with both BLIMP1 KD and EZH2 inhibition. These pathways are likely to play a role in the degradation of EZH2, and may be of clinical significance to Waldenström's macroglobulinemia, however further studies are needed to elucidate this mechanism.

Our RT-qPCR in RPCI-WM1 cells with BLIMP1 KD and ectopic expression of EZH2 showed a number of BLIMP1 targets that were regulated through EZH2. It was interesting to note that these all related to B cell and immune signalling processes. Surprisingly some genes that were significantly activated by tazemetostat such as *STAT1* did not have their repression reinstated by restoring EZH2 levels. Perhaps changes in the cells due to EZH2 overexpression prior to inducing BLIMP1 KD led to changes in the regulation of these genes. Another surprising result was that some genes such as *TNFRSF14* were activated following BLIMP1 KD, and then had their repression restored by ectopic expression of EZH2, but did not have significantly increased expression following tazemetostat treatment. This leads us to conjecture that the non-catalytic activity of EZH2 could be causing repression of *TNFRSF14*. However, another aspect to consider is the rate of

turnover of the H3K27me3 mark, and the small amplitude of gene expression changes induced by tazemetostat. It is likely that while tazemetostat was insufficient to completely activate genes such as *TNFRSF14*, using a higher dosage or treating for a longer period of time may have done so.

One conundrum is that the half-life of H3K27me3 was shown to be approximately 1 day using tazemetostat in non-Hodgkin lymphoma cells, and yet the effects of tazemetostat on cell growth take around 7 days in EZH2-WT cells (Brach et al., 2017; Knutson et al., 2014). It is likely that other mechanisms such as the actions of transcription factors, DNA methylation, or HDACs leads to sustained repression of many EZH2 targets in EZH2 WT cells. This is in line with the large number of regions marked by H3K27me3 compared with the small number of differentially expressed genes following tazemetostat treatment in the RPCI-WM1 cell line. In hindsight, it might have been better to treat the cells with tazemetostat at a higher concentration before RNAseq to have a better chance of identifying more targets. Although most studies have also used longer time periods for tazemetostat treatment, I wanted our treatment to be comparable to the induction of BLIMP1 KD, and so could not extend it.

I also did not observe tazemetostat to induce cell death in the RPCI-WM1 cell line. However, I did see a small level of activation of some apoptosis-promoting genes. This was not to the same extent as observed for BLIMP1 KD, and fewer genes were activated. Instead, this could represent apoptosis priming of the RPCI-WM1 cell line by EZH2 inhibition. This priming could lead to the sensitisation of the RPCI-WM1 cells to NK cell mediated cytotoxicity, similar to what has been shown for EZH2 inhibition in melanoma cells, where the response to cytotoxic T cells is dependent on the T cell production of IFN-γ (Zingg et al., 2017).

The RNA-binding factor encoding gene *ZFP36L1* is another interesting target repressed by BLIMP1 via EZH2 that we can consider in relation to the regulation of cell cycle progression. It is expressed during early B cell development to promote quiescence and allow the V(D)J recombination process to take place (Galloway et al., 2016). EZH2 is also expressed around this time (Su et al., 2003), and so it follows that EZH2 may cause repression of *ZFP36L1* to allow the cells to continue cycling. It would be of interest to further investigate the repression of *ZFP36L1* in B cell and other cancers, where it could perhaps function as a tumour suppressor. In fact, this role was recently proposed in myelofibrosis (Martínez-Calle et al., 2019), but I believe it may have a similar role in many cancers.

Taken together, BLIMP1 and EZH2 have a complex interplay in Waldenström's macroglobulinemia, and their continued co-expression in the same cell could represent a harnessing of the pre-/plasmablast transcriptional program.

A weakness in the RNAseq analyses was that using the GSEA program for identifying enriched gene sets with tazemetostat treatment may have provided us with some false positives. For GSEA input, I used a list of all detected genes, not just those that were differentially expressed. This provided us with high levels of sensitivity for detecting pathways affected by BLIMP1 KD, where there was a large amplitude of change and a huge number of differentially expressed genes. However, with tazemetostat, the smaller amplitude of change and fewer differentially expressed genes meant that some of the enriched gene sets may not have reflected actual changes. In accordance with this, it is always good to regard these kinds of analyses sceptically, and use them only as a stepping-stone for future hypothesis generation.

A highly worthwhile experiment would be to treat cultured Waldenström's macroglobulinemia patient cells with DMSO or tazemetostat for RNAseq. This would be very useful as a validation method for our transcriptional targets of EZH2 in Waldenström's macroglobulinemia and might present additional novel targets.

7.3 Implications for future work

The results of our project can serve to inform future studies in relation to the roles of BLIMP1 and EZH2 in Waldenström's macroglobulinemia and multiple myeloma.

I have demonstrated a possible role for BLIMP1 in maintaining survival in Waldenström's macroglobulinemia cells. It is very difficult to target BLIMP1 due to its lack of intrinsic enzymatic activity, however it could be effective to target signalling pathways upstream of BLIMP1 activation. While targeting of the MYD88 signalling pathway has been investigated in depth, perhaps inhibition of other pathways upstream of BLIMP1 activation such as PI3K or JAK/STAT signalling could be utilised. Further investigation into mechanisms of BLIMP1 activation in Waldenström's macroglobulinemia would therefore be very useful. BLIMP1 can also be linked to current treatments through its possible maintenance of BTK activity via the transcriptional repression of the BTK inhibitor gene *IBTK*. Ibrutinib, which targets BTK, is currently one of the

most effective Waldenström's macroglobulinemia therapeutics (Treon et al., 2015).

I have also demonstrated a mechanism for increasing susceptibility of Waldenström's macroglobulinemia cells to immune surveillance through BLIMP1 KD or EZH2 inhibition. It would be interesting to further investigate the apoptosis- and immune surveillance-sensitising roles of tazemetostat in Waldenström's macroglobulinemia and other EZH2-WT cancers, given that tazemetostat is now in clinical trials for non-Hodgkin lymphoma (Italiano et al., 2018). Also, given the reliance of some *ARID1A*-mutated cancers on EZH2, it would be interesting to test the use of tazemetostat on *ARID1A*-mutated Waldenström's macroglobulinemia, which comprises around 17% of Waldenström's macroglobulinemia patients (Hunter et al., 2014).

Future investigation into the role of BLIMP1 in the regulation of the cell cycle and DNA repair could have lasting implications for its role in other cancers where it is expressed, as well as for its role in normal biology. BLIMP1 is essential for the development of many cells and tissues in the body including the placenta (Vincent et al., 2005), primordial germ cells (Ohinata et al., 2005), and the epidermis (Magnúsdóttir et al., 2007) to name a few. In addition, inactivation of BLIMP1 later during embryonic development leads to severe developmental abnormalities (Robertson et al., 2007). Thus, further investigation of BLIMP1's role in the regulation of cell cycle and DNA repair mechanisms could provide insight into its roles in these cells and tissues.

7.4 Profiling of transcriptional enhancers and disease insights

In the years since the conception of this project, the profiling of enhancers has now been used effectively to identify disease risk and treatable features of cancers that were not previously identified by genome sequencing or transcriptome profiling (Mack et al., 2017; Ooi et al., 2016; Wong et al., 2017). This demonstrates the validity of our aim. Furthermore, enhancer profiling has recently been performed in multiple myeloma to identify transcriptional regulatory networks underlying the disease state (Jin et al., 2018). However, that study lacked an investigation of the MGUS stage compared to malignant myeloma, which I felt was the most salient question.

The technical difficulties I encountered in collecting patient bone marrow extracts from the Landspitali university hospital, and in isolating $CD138^+$ cells with sufficient yield and purity was the major setback of this project. If I was

beginning this project again it would be best to begin with a complete collection of patient samples already selected for CD138 expression, and move directly from optimising the ChIPseq and RNAseq methods into processing the samples and sequencing, without spending any time on the cell isolations. This would have provided us with enough time to complete the data analysis.

In the most ideal situation, I would not only be profiling enhancers in newly diagnosed MGUS and myeloma patient cells, but would have access to a collection of patient-matched MGUS and myeloma samples. If this was available, I could then examine the patient-specific changes that took place during the malignant transformation. This could allow us to identify novel predictive markers for progression from MGUS to myeloma, and these would have very important implications for clinical practice.

One weakness in our methodology is that profiling of eRNAs is notoriously difficult to achieve by looking at steady-state RNA through total RNAseq due to their instability. Instead, sequencing of nascent transcripts is now the preferred option (Core et al., 2014). However, this method had not yet been developed at the time when the project was initially conceived. In the most ideal situation, it may have been beneficial to opt for nascent transcript sequencing rather than total RNAseq for our eRNA profiling. However, the standard protocols for such methods require starting material of 1×10^7 cells (Gardini, 2017), which would not be feasible using patient MGUS and myeloma samples. Nonetheless, the profiling of histone marks should still provide us with a sufficient amount of information to identify enhancers. Although, we will not be confident of the activation of these enhancers unless we can also identify transcribed eRNAs. Meanwhile, the total RNAseq may produce additional novel data regarding the transcriptomes of MGUS and myeloma cells. Importantly, the years of work spent on this project led to the development of effective tools for profiling of enhancers from low numbers of cells and could be highly useful for future studies.

8 Conclusions

Mechanisms of transcriptional regulation are essential for maintaining cell states and driving cell state transitions. In this thesis I present evidence that transcriptional regulation by the factors BLIMP1 and EZH2 maintains the malignant phenotype in Waldenström's macroglobulinemia cells. I furthermore present the development of a procedure for profiling of transcriptional enhancers in small numbers of cells from MGUS and multiple myeloma patient material. Taken together, this thesis presents a body of work that builds upon some key questions, including that of the role of BLIMP1 and EZH2 in Waldenström's macroglobulinemia, and their interplay in the disease. I hope the results of this thesis will create opportunities for future exploration into these mechanisms.

References

Abeykoon, J. P., Paludo, J., King, R. L., Ansell, S. M., Gertz, M. A., LaPlant, B. R., Halvorson, A. E., Gonsalves, W. I., Dingli, D., Fang, H., Rajkumar, S. V., Lacy, M. Q., He, R., Kourelis, T., Reeder, C. B., Novak, A. J., McPhail, E. D., Viswanatha, D. S., Witzig, T. E., Go, R. S., Habermann, T. M., Buadi, F. K., Dispenzieri, A., Leung, N., Lin, Y., Thompson, C. A., Hayman, S. R., Kyle, R. A., Kumar, S. K., & Kapoor, P. (2018). MYD88 mutation status does not impact overall survival in Waldenstrom macroglobulinemia. *Am J Hematol, 93*(2), 187-194.

Affer, M., Chesi, M., Chen, W. D., Keats, J. J., Demchenko, Y. N., Tamizhmani, K., Garbitt, V. M., Riggs, D. L., Brents, L. A., Roschke, A. V., Van Wier, S., Fonseca, R., Bergsagel, P. L., & Kuehl, W. M. (2014). Promiscuous MYC locus rearrangements hijack enhancers but mostly super-enhancers to dysregulate MYC expression in multiple myeloma. *Leukemia, 28*, 1725.

Agarwal, M. L., Agarwal, A., Taylor, W. R., & Stark, G. R. (1995). p53 controls both the G2/M and the G1 cell cycle checkpoints and mediates reversible growth arrest in human fibroblasts. *Proceedings of the National Academy of Sciences, 92*(18), 8493.

Agirre, X., Castellano, G., Pascual, M., Heath, S., Kulis, M., Segura, V., Bergmann, A., Esteve, A., Merkel, A., Raineri, E., Agueda, L., Blanc, J., Richardson, D., Clarke, L., Datta, A., Russiñol, N., Queirós, A. C., Beekman, R., Rodríguez-Madoz, J. R., José-Enériz, E. S., Fang, F., Gutiérrez, N. C., García-Verdugo, J. M., Robson, M. I., Schirmer, E. C., Guruceaga, E., Martens, J. H. A., Gut, M., Calasanz, M. J., Flicek, P., Siebert, R., Campo, E., Miguel, J. F. S., Melnick, A., Stunnenberg, H. G., Gut, I. G., Prosper, F., & Martín-Subero, J. I. (2015). Whole-epigenome analysis in multiple myeloma reveals DNA hypermethylation of B cell-specific enhancers. *Genome Research, 25*(4), 478-487.

Alag, A., Conover, C. A., Lau, C., Oxvig, C., Sotillo, E., Shern, J. F., Khan, J., Maris, J. M., Lorette, J., Fazli, L., Pollak, M., Meltzer, P., Xu, P., Noer, P. R., Sorensen, P. H., Jones, R., Heitzeneder, S., Sindiri, S., & Mackall, C. L. (2019). Pregnancy-Associated Plasma Protein-A (PAPP-A) in Ewing Sarcoma: Role in Tumor Growth and Immune Evasion.

Albrecht, H., Durbin-Johnson, B., Yunis, R., Kalanetra, K. M., Wu, S., Chen, R., Stevenson, T. R., & Rocke, D. M. (2012). Transcriptional response of ex vivo human skin to ionizing radiation: comparison between low- and high-dose effects. *Radiation research, 177*(1), 69-83.

Alexanian, R., Dimopoulos, M. A., Delasalle, K., & Barlogie, B. (1992). Primary dexamethasone treatment of multiple myeloma. *Blood, 80*(4), 887.

Allen, C. D., Okada, T., Tang, H. L., & Cyster, J. G. (2007). Imaging of germinal center selection events during affinity maturation. *Science, 315*(5811), 528-531.

Alt, F. W., Yancopoulos, G. D., Blackwell, T. K., Wood, C., Thomas, E., Boss, M., Coffman, R., Rosenberg, N., Tonegawa, S., & Baltimore, D. (1984). Ordered rearrangement of immunoglobulin heavy chain variable region segments. *Embo j, 3*(6), 1209-1219.

Alter, G., Malenfant, J. M., & Altfeld, M. (2004). CD107a as a functional marker for the identification of natural killer cell activity. *Journal of Immunological Methods, 294*(1), 15-22.

Ancelin, K., Lange, U. C., Hajkova, P., Schneider, R., Bannister, A. J., Kouzarides, T., & Surani, M. A. (2006). Blimp1 associates with Prmt5 and directs histone arginine methylation in mouse germ cells. *Nature Cell Biology, 8*, 623.

Ansell, S. M., Hodge, L. S., Secreto, F. J., Manske, M., Braggio, E., Price-Troska, T., Ziesmer, S., Li, Y., Johnson, S. H., Hart, S. N., Kocher, J. P. A., Vasmatzis, G., Chanan-Kahn, A., Gertz, M., Fonseca, R., Dogan, A., Cerhan, J. R., & Novak, A. J. (2014). Activation of TAK1 by MYD88 L265P drives malignant B-cell Growth in non-Hodgkin lymphoma. *Blood cancer journal, 4*(2), e183-e183.

Anthony Weil, P., Luse, D. S., Segall, J., & Roeder, R. G. (1979). Selective and accurate initiation of transcription at the ad2 major late promotor in a soluble system dependent on purified rna polymerase ii and dna. *Cell, 18*(2), 469-484.

Aranburu, A., Ceccarelli, S., Giorda, E., Lasorella, R., Ballatore, G., & Carsetti, R. (2010). TLR Ligation Triggers Somatic Hypermutation in Transitional B Cells Inducing the Generation of IgM Memory B Cells. *The Journal of Immunology, 185*(12), 7293.

Aranda, S., Mas, G., & Di Croce, L. (2015). Regulation of gene transcription by Polycomb proteins. *Science Advances, 1*(11), e1500737.

Auer, P. L., & Doerge, R. W. (2010). Statistical Design and Analysis of RNA Sequencing Data. *Genetics, 185*(2), 405.

Avbelj, M., Wolz, O.-O., Fekonja, O., Benčina, M., Repič, M., Mavri, J., Krüger, J., Schärfe, C., Delmiro Garcia, M., Panter, G., Kohlbacher, O., Weber, A. N. R., & Jerala, R. (2014). Activation of lymphoma-associated MyD88 mutations via allostery-induced TIR-domain oligomerization. *Blood, 124*(26), 3896.

Avet-Loiseau, H., Attal, M., Moreau, P., Charbonnel, C., Garban, F., Hulin, C., Leyvraz, S., Michallet, M., Yakoub-Agha, I., Garderet, L., Marit, G., Michaux, L., Voillat, L., Renaud, M., Grosbois, B., Guillerm, G., Benboubker, L., Monconduit, M., Thieblemont, C., Casassus, P., Caillot, D., Stoppa, A.-M., Sotto, J.-J., Wetterwald, M., Dumontet, C., Fuzibet, J.-G., Azais, I., Dorvaux, V., Zandecki, M., Bataille, R., Minvielle, S., Harousseau, J.-L., Facon, T., & Mathiot, C. (2007). Genetic abnormalities and survival in multiple myeloma: the

experience of the Intergroupe Francophone du Myélome. *Blood, 109*(8), 3489.
Bachanova, V., & Burns, L. J. (2012). Hematopoietic cell transplantation for Waldenstrom macroglobulinemia. *Bone Marrow Transplant, 47*(3), 330-336.
Bahlis, N. J., & Lazarus, H. M. (2006). Multiple myeloma-associated AL amyloidosis: is a distinctive therapeutic approach warranted? *Bone Marrow Transplantation, 38*, 7.
Bajénoff, M., Egen, J., Koo, L. Y., Laugier, J. P., Brau, F., Glaichenhaus, N., & Germain, R. N. (2006). Stromal Cell Networks Regulate Lymphocyte Entry, Migration, and Territoriality in Lymph Nodes. *Immunity, 25*(6), 989-1001.
Bajénoff, M., Granjeaud, S., & Guerder, S. (2003). The Strategy of T Cell Antigen-presenting Cell Encounter in Antigen-draining Lymph Nodes Revealed by Imaging of Initial T Cell Activation. *The Journal of Experimental Medicine, 198*(5), 715-724.
Baldeyron, C., Soria, G., Roche, D., Cook, A. J. L., & Almouzni, G. (2011). HP1α recruitment to DNA damage by p150CAF-1 promotes homologous recombination repair. *The Journal of Cell Biology, 193*(1), 81.
Banerji, J., Olson, L., & Schaffner, W. (1983). A lymphocyte-specific cellular enhancer is located downstream of the joining region in immunoglobulin heavy chain genes. *Cell, 33*(3), 729-740.
Banerji, J., Rusconi, S., & Schaffner, W. (1981). Expression of a β-globin gene is enhanced by remote SV40 DNA sequences. *Cell, 27*(2, Part 1), 299-308.
Baptista, T., Grünberg, S., Minoungou, N., Koster, M. J. E., Timmers, H. T. M., Hahn, S., Devys, D., & Tora, L. (2017). SAGA Is a General Cofactor for RNA Polymerase II Transcription. *Molecular Cell, 68*(1), 130-143.e135.
Barboric, M., Nissen, R. M., Kanazawa, S., Jabrane-Ferrat, N., & Peterlin, B. M. (2001). NF-κB Binds P-TEFb to Stimulate Transcriptional Elongation by RNA Polymerase II. *Molecular Cell, 8*(2), 327-337.
Barski, A., Cuddapah, S., Cui, K., Roh, T.-Y., Schones, D. E., Wang, Z., Wei, G., Chepelev, I., & Zhao, K. (2007). High-Resolution Profiling of Histone Methylations in the Human Genome. *Cell, 129*(4), 823-837.
Barwick, B. G., Scharer, C. D., Martinez, R. J., Price, M. J., Wein, A. N., Haines, R. R., Bally, A. P. R., Kohlmeier, J. E., & Boss, J. M. (2018). B cell activation and plasma cell differentiation are inhibited by de novo DNA methylation. *Nature Communications, 9*(1), 1900.
Basso, K., & Dalla-Favera, R. (2015). Germinal centres and B cell lymphomagenesis. *Nature Reviews Immunology, 15*, 172.
Batista, F. D., & Harwood, N. E. (2009). The who, how and where of antigen presentation to B cells. *Nat Rev Immunol, 9*(1), 15-27.
Bauer, S., Groh, V., Wu, J., Steinle, A., Phillips, J. H., Lanier, L. L., & Spies, T. (1999). Activation of NK Cells and T Cells by NKG2D, a Receptor for Stress-Inducible MICA. *Science, 285*(5428), 727.

Béguelin, W., Popovic, R., Teater, M., Jiang, Y., Bunting, Karen L., Rosen, M., Shen, H., Yang, Shao N., Wang, L., Ezponda, T., Martinez-Garcia, E., Zhang, H., Zheng, Y., Verma, Sharad K., McCabe, Michael T., Ott, Heidi M., Van Aller, Glenn S., Kruger, Ryan G., Liu, Y., McHugh, Charles F., Scott, David W., Chung, Young R., Kelleher, N., Shaknovich, R., Creasy, Caretha L., Gascoyne, Randy D., Wong, K.-K., Cerchietti, L., Levine, Ross L., Abdel-Wahab, O., Licht, Jonathan D., Elemento, O., & Melnick, Ari M. (2013). EZH2 Is Required for Germinal Center Formation and Somatic EZH2 Mutations Promote Lymphoid Transformation. *Cancer Cell, 23*(5), 677-692.

Benveniste, D., Sonntag, H.-J., Sanguinetti, G., & Sproul, D. (2014). Transcription factor binding predicts histone modifications in human cell lines. *Proceedings of the National Academy of Sciences, 111*(37), 13367.

Bergsagel, P. L., Chesi, M., Nardini, E., Brents, L. A., Kirby, S. L., & Kuehl, W. M. (1996). Promiscuous translocations into immunoglobulin heavy chain switch regions in multiple myeloma. *Proceedings of the National Academy of Sciences of the United States of America, 93*(24), 13931-13936.

Bernal, M., Garrido, P., Jiménez, P., Carretero, R., Almagro, M., López, P., Navarro, P., Garrido, F., & Ruiz-Cabello, F. (2009). Changes in activatory and inhibitory natural killer (NK) receptors may induce progression to multiple myeloma: Implications for tumor evasion of T and NK cells. *Human Immunology, 70*(10), 854-857.

Best, T., Li, D., Skol, A. D., Kirchhoff, T., Jackson, S. A., Yasui, Y., Bhatia, S., Strong, L. C., Domchek, S. M., Nathanson, K. L., Olopade, O. I., Huang, R. S., Mack, T. M., Conti, D. V., Offit, K., Cozen, W., Robison, L. L., & Onel, K. (2011). Variants at 6q21 implicate PRDM1 in the etiology of therapy-induced second malignancies after Hodgkin's lymphoma. *Nature medicine, 17*(8), 941-943.

Bharti, A. C., Shishodia, S., Reuben, J. M., Weber, D., Alexanian, R., Raj-Vadhan, S., Estrov, Z., Talpaz, M., & Aggarwal, B. B. (2004). Nuclear factor–κB and STAT3 are constitutively active in CD138⁺ cells derived from multiple myeloma patients, and suppression of these transcription factors leads to apoptosis. *Blood, 103*(8), 3175.

Bitler, B. G., Aird, K. M., Garipov, A., Li, H., Amatangelo, M., Kossenkov, A. V., Schultz, D. C., Liu, Q., Shih, I.-M., Conejo-Garcia, J. R., Speicher, D. W., & Zhang, R. (2015). Synthetic lethality by targeting EZH2 methyltransferase activity in ARID1A-mutated cancers. *Nature Medicine, 21*, 231.

Blank, C., Kuball, J., Voelkl, S., Wiendl, H., Becker, B., Walter, B., Majdic, O., Gajewski, T. F., Theobald, M., Andreesen, R., & Mackensen, A. (2006). Blockade of PD-L1 (B7-H1) augments human tumor-specific T cell responses in vitro. *Int J Cancer, 119*(2), 317-327.

Blethrow, J. D., Glavy, J. S., Morgan, D. O., & Shokat, K. M. (2008). Covalent capture of kinase-specific phosphopeptides reveals Cdk1-cyclin B

substrates. *Proceedings of the National Academy of Sciences, 105*(5), 1442.

Blimark, C. H., Turesson, I., Genell, A., Ahlberg, L., Björkstrand, B., Carlson, K., Forsberg, K., Juliusson, G., Linder, O., Mellqvist, U.-H., Nahi, H., & Kristinsson, S. Y. (2018). Outcome and survival of myeloma patients diagnosed 2008–2015. Real-world data on 4904 patients from the Swedish Myeloma Registry. *Haematologica, 103*(3), 506.

Boice, M., Salloum, D., Mourcin, F., Sanghvi, V., Amin, R., Oricchio, E., Jiang, M., Mottok, A., Denis-Lagache, N., Ciriello, G., Tam, W., Teruya-Feldstein, J., de Stanchina, E., Chan, W. C., Malek, S. N., Ennishi, D., Brentjens, R. J., Gascoyne, R. D., Cogne, M., Tarte, K., & Wendel, H.-G. (2016). Loss of the HVEM tumor suppressor in lymphoma and restoration by modified CAR-T cells. *Cell, 167*(2), 405-418.e413.

Bönelt, P., Wöhner, M., Minnich, M., Tagoh, H., Fischer, M., Jaritz, M., Kavirayani, A., Garimella, M., Karlsson, M. C. I., & Busslinger, M. (2018). Precocious expression of Blimp1 in B cells causes autoimmune disease with increased self - reactive plasma cells. *The EMBO Journal*, e100010.

Bonn, S., Zinzen, R. P., Girardot, C., Gustafson, E. H., Perez-Gonzalez, A., Delhomme, N., Ghavi-Helm, Y., Wilczyński, B., Riddell, A., & Furlong, E. E. M. (2012). Tissue-specific analysis of chromatin state identifies temporal signatures of enhancer activity during embryonic development. *Nature Genetics, 44*, 148.

Bonnert, T. P., Garka, K. E., Parnet, P., Sonoda, G., Testa, J. R., & Sims, J. E. (1997). The cloning and characterization of human MyD88: a member of an IL-1 receptor related family 1. *FEBS Letters, 402*(1), 81-84.

Borson, N. D., Lacy, M. Q., & Wettstein, P. J. (2002). Altered mRNA expression of Pax5 and Blimp-1 in B cells in multiple myeloma. *Blood, 100*(13), 4629.

Boyer, L. A., Lee, T. I., Cole, M. F., Johnstone, S. E., Levine, S. S., Zucker, J. P., Guenther, M. G., Kumar, R. M., Murray, H. L., Jenner, R. G., Gifford, D. K., Melton, D. A., Jaenisch, R., & Young, R. A. (2005). Core Transcriptional Regulatory Circuitry in Human Embryonic Stem Cells. *Cell, 122*(6), 947-956.

Brach, D., Johnston-Blackwell, D., Drew, A., Lingaraj, T., Motwani, V., Warholic, N. M., Feldman, I., Plescia, C., Smith, J. J., Copeland, R. A., Keilhack, H., Chan-Penebre, E., Knutson, S. K., Ribich, S. A., Raimondi, A., & Thomenius, M. J. (2017). EZH2 Inhibition by Tazemetostat Results in Altered Dependency on B-cell Activation Signaling in DLBCL. *Molecular Cancer Therapeutics, 16*(11), 2586.

Brack, C., Hirama, M., Lenhard-Schuller, R., & Tonegawa, S. (1978). A complete immunoglobulin gene is created by somatic recombination. *Cell, 15*(1), 1-14.

Branagan, A. R., Santos, D., Anderson, K. C., Tournhilac, O., Treon, S. P., & Hunter, Z. (2004). Paradoxical increases in serum IgM and viscosity

levels following rituximab in Waldenstrom's macroglobulinemia. *Annals of Oncology, 15*(10), 1481-1483.
Brass, A. L., Kehrli, E., Eisenbeis, C. F., Storb, U., & Singh, H. (1996). Pip, a lymphoid-restricted IRF, contains a regulatory domain that is important for autoinhibition and ternary complex formation with the Ets factor PU.1. *Genes & Development, 10*(18), 2335-2347.
Bravo, R., Frank, R., Blundell, P. A., & Macdonald-Bravo, H. (1987). Cyclin/PCNA is the auxiliary protein of DNA polymerase-δ. *Nature, 326*(6112), 515-517.
Bray, N. L., Pimentel, H., Melsted, P., & Pachter, L. (2016). Near-optimal probabilistic RNA-seq quantification. *Nature biotechnology, 34*(5), 525.
Breathnach, R., & Chambon, P. (1981). Organization and Expression of Eucaryotic Split Genes Coding for Proteins. *Annual Review of Biochemistry, 50*(1), 349-383.
Buratowski, S., Hahn, S., Guarente, L., & Sharp, P. A. (1989). Five intermediate complexes in transcription initiation by RNA polymerase II. *Cell, 56*(4), 549-561.
Burke, T. W., & Kadonaga, J. T. (1997). The downstream core promoter element, DPE, is conserved fromDrosophila to humans and is recognized by TAFII60 of Drosophila. *Genes & Development, 11*(22), 3020-3031.
Burley, S. K., & Roeder, R. G. (1996). BIOCHEMISTRY AND STRUCTURAL BIOLOGY OF TRANSCRIPTION FACTOR IID (TFIID). *Annual Review of Biochemistry, 65*(1), 769-799.
Burnet, F. M. (1957). A modification of Jerne's theory of antibody production using the concept of clonal selection. *Australian J Sci, 20*(3), 67-69.
Burnette, W. N. (1981). “Western Blotting”: Electrophoretic transfer of proteins from sodium dodecyl sulfate-polyacrylamide gels to unmodified nitrocellulose and radiographic detection with antibody and radioiodinated protein A. *Analytical Biochemistry, 112*(2), 195-203.
Buyse, I. M., Shao, G., & Huang, S. (1995). The retinoblastoma protein binds to RIZ, a zinc-finger protein that shares an epitope with the adenovirus E1A protein. *Proc Natl Acad Sci U S A, 92*(10), 4467-4471.
Caganova, M., Carrisi, C., Varano, G., Mainoldi, F., Zanardi, F., Germain, P.-L., George, L., Alberghini, F., Ferrarini, L., Talukder, A. K., Ponzoni, M., Testa, G., Nojima, T., Doglioni, C., Kitamura, D., Toellner, K.-M., Su, I. h., & Casola, S. (2013). Germinal center dysregulation by histone methyltransferase EZH2 promotes lymphomagenesis. *The Journal of Clinical Investigation, 123*(12), 5009-5022.
Calado, D. P., Zhang, B., Srinivasan, L., Sasaki, Y., Seagal, J., Unitt, C., Rodig, S., Kutok, J., Tarakhovsky, A., Schmidt-Supprian, M., & Rajewsky, K. (2010). Constitutive Canonical NF-κB Activation Cooperates with Disruption of BLIMP1 in the Pathogenesis of Activated B Cell-like Diffuse Large Cell Lymphoma. *Cancer Cell, 18*(6), 580-589.

Cantor, S., Drapkin, R., Zhang, F., Lin, Y., Han, J., Pamidi, S., & Livingston, D. M. (2004). The BRCA1-associated protein BACH1 is a DNA helicase targeted by clinically relevant inactivating mutations. *Proceedings of the National Academy of Sciences of the United States of America, 101*(8), 2357.

Canzio, D., Chang, E. Y., Shankar, S., Kuchenbecker, K. M., Simon, M. D., Madhani, H. D., Narlikar, G. J., & Al-Sady, B. (2011). Chromodomain-mediated oligomerization of HP1 suggests a nucleosome-bridging mechanism for heterochromatin assembly. *Molecular cell, 41*(1), 67-81.

Cao, R., Wang, L., Wang, H., Xia, L., Erdjument-Bromage, H., Tempst, P., Jones, R. S., & Zhang, Y. (2002). Role of Histone H3 Lysine 27 Methylation in Polycomb-Group Silencing. *Science, 298*(5595), 1039.

Cao, R., & Zhang, Y. (2004). SUZ12 Is Required for Both the Histone Methyltransferase Activity and the Silencing Function of the EED-EZH2 Complex. *Molecular Cell, 15*(1), 57-67.

Capolunghi, F., Cascioli, S., Giorda, E., Rosado, M. M., Plebani, A., Auriti, C., Seganti, G., Zuntini, R., Ferrari, S., Cagliuso, M., Quinti, I., & Carsetti, R. (2008). CpG Drives Human Transitional B Cells to Terminal Differentiation and Production of Natural Antibodies. *The Journal of Immunology, 180*(2), 800.

Carbone, E., Neri, P., Mesuraca, M., Fulciniti, M. T., Otsuki, T., Pende, D., Groh, V., Spies, T., Pollio, G., Cosman, D., Catalano, L., Tassone, P., Rotoli, B., & Venuta, S. (2005). HLA class I, NKG2D, and natural cytotoxicity receptors regulate multiple myeloma cell recognition by natural killer cells. *Blood, 105*(1), 251.

Carrasco, D. R., Sukhdeo, K., Protopopova, M., Sinha, R., Enos, M., Carrasco, Daniel E., Zheng, M., Mani, M., Henderson, J., Pinkus, G. S., Munshi, N., Horner, J., Ivanova, E. V., Protopopov, A., Anderson, K. C., Tonon, G., & DePinho, R. A. (2007). The Differentiation and Stress Response Factor XBP-1 Drives Multiple Myeloma Pathogenesis. *Cancer Cell, 11*(4), 349-360.

Carroll, D., Erhardt, S., Pagani, M., Barton, S. C., Surani, M. A., & Jenuwein, T. (2001). The Polycomb-Group Gene Ezh2 Is Required for Early Mouse Development. *Molecular and Cellular Biology, 21*(13), 4330.

Castillo, J. J., Olszewski, A. J., Cronin, A. M., Hunter, Z. R., & Treon, S. P. (2014). Survival trends in Waldenström macroglobulinemia: an analysis of the Surveillance, Epidemiology and End Results database. *Blood, 123*(25), 3999.

Castillo, J. J., Olszewski, A. J., Kanan, S., Meid, K., Hunter, Z. R., & Treon, S. P. (2015). Overall survival and competing risks of death in patients with Waldenstrom macroglobulinaemia: an analysis of the Surveillance, Epidemiology and End Results database. *Br J Haematol, 169*(1), 81-89.

Catlett-Falcone, R., Landowski, T. H., Oshiro, M. M., Turkson, J., Levitzki, A., Savino, R., Ciliberto, G., Moscinski, L., Fernández-Luna, J. L., Nuñez, G., Dalton, W. S., & Jove, R. (1999). Constitutive Activation

of Stat3 Signaling Confers Resistance to Apoptosis in Human U266 Myeloma Cells. *Immunity, 10*(1), 105-115.
Cattoretti, G., Pasqualucci, L., Ballon, G., Tam, W., Nandula, S. V., Shen, Q., Mo, T., Murty, V. V., & Dalla-Favera, R. (2005). Deregulated BCL6 expression recapitulates the pathogenesis of human diffuse large B cell lymphomas in mice. *Cancer Cell, 7*(5), 445-455.
Cejka, P., Plank, J. L., Bachrati, C. Z., Hickson, I. D., & Kowalczykowski, S. C. (2010). Rmi1 stimulates decatenation of double Holliday junctions during dissolution by Sgs1–Top3. *Nature Structural &Amp; Molecular Biology, 17*, 1377.
Cerutti, A., Cols, M., & Puga, I. (2013). Marginal zone B cells: virtues of innate-like antibody-producing lymphocytes. *Nature Reviews Immunology, 13*, 118.
Challa-Malladi, M., Lieu, Y. K., Califano, O., Holmes, A. B., Bhagat, G., Murty, V. V., Dominguez-Sola, D., Pasqualucci, L., & Dalla-Favera, R. (2011). Combined genetic inactivation of beta2-Microglobulin and CD58 reveals frequent escape from immune recognition in diffuse large B cell lymphoma. *Cancer Cell, 20*(6), 728-740.
Chaudhuri, J., Tian, M., Khuong, C., Chua, K., Pinaud, E., & Alt, F. W. (2003). Transcription-targeted DNA deamination by the AID antibody diversification enzyme. *Nature, 422*(6933), 726-730.
Chauhan, D., Pandey, P., Ogata, A., Teoh, G., Treon, S., Urashima, M., Kharbanda, S., & Anderson, K. C. (1997). Dexamethasone induces apoptosis of multiple myeloma cells in a JNK/SAP kinase independent mechanism. *Oncogene, 15*, 837.
Chen, H., Gilbert, C. A., Hudson, J. A., Bolick, S. C., Wright, K. L., & Piskurich, J. F. (2007). Positive regulatory domain I-binding factor 1 mediates repression of the MHC class II transactivator (CIITA) type IV promoter. *Molecular Immunology, 44*(6), 1461-1470.
Chesi, M., Bergsagel, P. L., Shonukan, O. O., Martelli, M. L., Brents, L. A., Chen, T., Schröck, E., Ried, T., & Kuehl, W. M. (1998a). Frequent Dysregulation of the c-maf Proto-Oncogene at 16q23 by Translocation to an Ig Locus in Multiple Myeloma. *Blood, 91*(12), 4457.
Chesi, M., Nardini, E., Lim, R. S. C., Smith, K. D., Kuehl, W. M., & Bergsagel, P. L. (1998b). The t(4;14) Translocation in Myeloma Dysregulates Both FGFR3 and a Novel Gene, MMSET, Resulting in IgH/MMSET Hybrid Transcripts. *Blood, 92*(9), 3025.
Chiou, S.-H., Risca, V. I., Wang, G. X., Yang, D., Grüner, B. M., Kathiria, A. S., Ma, R. K., Vaka, D., Chu, P., Kozak, M., Castellini, L., Graves, E. E., Kim, G. E., Mourrain, P., Koong, A. C., Giaccia, A. J., & Winslow, M. M. (2017). BLIMP1 Induces Transient Metastatic Heterogeneity in Pancreatic Cancer. *Cancer Discovery, 7*(10), 1184.
Chitta, K. S., Paulus, A., Ailawadhi, S., Foster, B. A., Moser, M. T., Starostik, P., Masood, A., Sher, T., Miller, K. C., Iancu, D. M., Conroy, J., Nowak, N. J., Sait, S. N., Personett, D. A., Coleman, M., Furman, R. R., Martin, P., Ansell, S. M., Lee, K., & Chanan-Khan, A. A. (2013). Development and characterization of a novel human Waldenström

macroglobulinemia cell line: RPCI-WM1, Roswell Park Cancer Institute - Waldenström Macroglobulinemia 1. *Leukemia & lymphoma, 54*(2), 387-396.
Choe, J., & Choi, Y. S. (1998). IL-10 interrupts memory B cell expansion in the germinal center by inducing differentiation into plasma cells. *European Journal of Immunology, 28*(2), 508-515.
Choe, K. N., & Moldovan, G.-L. (2017). Forging Ahead through Darkness: PCNA, Still the Principal Conductor at the Replication Fork. *Molecular Cell, 65*(3), 380-392.
Chretien, M.-L., Corre, J., Lauwers-Cances, V., Magrangeas, F., Cleynen, A., Yon, E., Hulin, C., Leleu, X., Orsini-Piocelle, F., Blade, J.-S., Sohn, C., Karlin, L., Delbrel, X., Hebraud, B., Roussel, M., Marit, G., Garderet, L., Mohty, M., Rodon, P., Voillat, L., Royer, B., Jaccard, A., Belhadj, K., Fontan, J., Caillot, D., Stoppa, A.-M., Attal, M., Facon, T., Moreau, P., Minvielle, S., & Avet-Loiseau, H. (2015). Understanding the role of hyperdiploidy in myeloma prognosis: which trisomies really matter? *Blood, 126*(25), 2713.
Ciccia, A., & Elledge, S. J. (2010). The DNA Damage Response: Making It Safe to Play with Knives. *Molecular Cell, 40*(2), 179-204.
Cirillo, L. A., Lin, F. R., Cuesta, I., Friedman, D., Jarnik, M., & Zaret, K. S. (2002). Opening of Compacted Chromatin by Early Developmental Transcription Factors HNF3 (FoxA) and GATA-4. *Molecular Cell, 9*(2), 279-289.
Ciró, M., Prosperini, E., Quarto, M., Grazini, U., Walfridsson, J., McBlane, F., Nucifero, P., Pacchiana, G., Capra, M., Christensen, J., & Helin, K. (2009). ATAD2 Is a Novel Cofactor for MYC, Overexpressed and Amplified in Aggressive Tumors. *Cancer Research, 69*(21), 8491.
Claus, M., Wingert, S., & Watzl, C. (2016). Modulation of natural killer cell functions by interactions between 2B4 and CD48 in cis and in trans. *Open Biology, 6*(5).
Clayton, E., Bardi, G., Bell, S. E., Chantry, D., Downes, C. P., Gray, A., Humphries, L. A., Rawlings, D., Reynolds, H., Vigorito, E., & Turner, M. (2002). A Crucial Role for the p110δ Subunit of Phosphatidylinositol 3-Kinase in B Cell Development and Activation. *The Journal of Experimental Medicine, 196*(6), 753.
Clouaire, T., Webb, S., Skene, P., Illingworth, R., Kerr, A., Andrews, R., Lee, J. H., Skalnik, D., & Bird, A. (2012). Cfp1 integrates both CpG content and gene activity for accurate H3K4me3 deposition in embryonic stem cells. *Genes Dev, 26*(15), 1714-1728.
Cobaleda, C., Jochum, W., & Busslinger, M. (2007). Conversion of mature B cells into T cells by dedifferentiation to uncommitted progenitors. *Nature, 449*(7161), 473-477.
Corden, J., Wasylyk, B., Buchwalder, A., Sassone-Corsi, P., Kedinger, C., & Chambon, P. (1980). Promoter sequences of eukaryotic protein-coding genes. *Science, 209*(4463), 1406.
Core, L. J., Martins, A. L., Danko, C. G., Waters, C. T., Siepel, A., & Lis, J. T. (2014). Analysis of nascent RNA identifies a unified architecture of

initiation regions at mammalian promoters and enhancers. *Nature Genetics, 46*, 1311.
Cosma, M. P., Tanaka, T., & Nasmyth, K. (1999). Ordered Recruitment of Transcription and Chromatin Remodeling Factors to a Cell Cycle– and Developmentally Regulated Promoter. *Cell, 97*(3), 299-311.
Creyghton, M. P., Cheng, A. W., Welstead, G. G., Kooistra, T., Carey, B. W., Steine, E. J., Hanna, J., Lodato, M. A., Frampton, G. M., Sharp, P. A., Boyer, L. A., Young, R. A., & Jaenisch, R. (2010). Histone H3K27ac separates active from poised enhancers and predicts developmental state. *Proceedings of the National Academy of Sciences, 107*(50), 21931.
Croonquist, P. A., & Van Ness, B. (2005). The polycomb group protein enhancer of zeste homolog 2 (EZH2) is an oncogene that influences myeloma cell growth and the mutant ras phenotype. *Oncogene, 24*, 6269.
Cujec, T. P., Cho, H., Maldonado, E., Meyer, J., Reinberg, D., & Peterlin, B. M. (1997). The human immunodeficiency virus transactivator Tat interacts with the RNA polymerase II holoenzyme. *Molecular and cellular biology, 17*(4), 1817-1823.
D'Costa, K., Emslie, D., Metcalf, D., Smyth, G. K., Karnowski, A., Kallies, A., Nutt, S. L., & Corcoran, L. M. (2009). Blimp1 is limiting for transformation in a mouse plasmacytoma model. *Blood, 113*(23), 5911-5919.
Davies, F. E., Raje, N., Hideshima, T., Lentzsch, S., Young, G., Tai, Y.-T., Lin, B., Podar, K., Gupta, D., Chauhan, D., Treon, S. P., Richardson, P. G., Schlossman, R. L., Morgan, G. J., Muller, G. W., Stirling, D. I., & Anderson, K. C. (2001). Thalidomide and immunomodulatory derivatives augment natural killer cell cytotoxicity in multiple myeloma. *Blood, 98*(1), 210.
Davis, R. E., Ngo, V. N., Lenz, G., Tolar, P., Young, R. M., Romesser, P. B., Kohlhammer, H., Lamy, L., Zhao, H., Yang, Y., Xu, W., Shaffer, A. L., Wright, G., Xiao, W., Powell, J., Jiang, J.-k., Thomas, C. J., Rosenwald, A., Ott, G., Muller-Hermelink, H. K., Gascoyne, R. D., Connors, J. M., Johnson, N. A., Rimsza, L. M., Campo, E., Jaffe, E. S., Wilson, W. H., Delabie, J., Smeland, E. B., Fisher, R. I., Braziel, R. M., Tubbs, R. R., Cook, J. R., Weisenburger, D. D., Chan, W. C., Pierce, S. K., & Staudt, L. M. (2010). Chronic active B-cell-receptor signalling in diffuse large B-cell lymphoma. *Nature, 463*, 88.
de Charette, M., & Houot, R. (2018). Hide or defend, the two strategies of lymphoma immune evasion: potential implications for immunotherapy. *Haematologica, 103*(8), 1256.
De Silva, N. S., & Klein, U. (2015). Dynamics of B cells in germinal centres. *Nature Reviews Immunology, 15*, 137.
DeAngelis, M. M., Wang, D. G., & Hawkins, T. L. (1995). Solid-phase reversible immobilization for the isolation of PCR products. *Nucleic acids research, 23*(22), 4742-4743.
Decker, T., Pasca di Magliano, M., McManus, S., Sun, Q., Bonifer, C., Tagoh, H., & Busslinger, M. (2009). Stepwise activation of enhancer and

promoter regions of the B cell commitment gene Pax5 in early lymphopoiesis. *Immunity, 30*(4), 508-520.
DeKoter, R. P., & Singh, H. (2000). Regulation of B lymphocyte and macrophage development by graded expression of PU.1. *Science, 288*(5470), 1439-1441.
Delbos, F., Aoufouchi, S., Faili, A., Weill, J.-C., & Reynaud, C.-A. (2007). DNA polymerase η is the sole contributor of A/T modifications during immunoglobulin gene hypermutation in the mouse. *The Journal of Experimental Medicine, 204*(1), 17.
Delbos, F., De Smet, A., Faili, A., Aoufouchi, S., Weill, J.-C., & Reynaud, C.-A. (2005). Contribution of DNA polymerase η to immunoglobulin gene hypermutation in the mouse. *The Journal of Experimental Medicine, 201*(8), 1191.
Delogu, A., Schebesta, A., Sun, Q., Aschenbrenner, K., Perlot, T., & Busslinger, M. (2006). Gene Repression by Pax5 in B Cells Is Essential for Blood Cell Homeostasis and Is Reversed in Plasma Cells. *Immunity, 24*(3), 269-281.
Demers, C., Chaturvedi, C.-P., Ranish, J. A., Juban, G., Lai, P., Morle, F., Aebersold, R., Dilworth, F. J., Groudine, M., & Brand, M. (2007). Activator-Mediated Recruitment of the MLL2 Methyltransferase Complex to the β-Globin Locus. *Molecular Cell, 27*(4), 573-584.
Deng, L., Wang, C., Spencer, E., Yang, L., Braun, A., You, J., Slaughter, C., Pickart, C., & Chen, Z. J. (2000). Activation of the IκB Kinase Complex by TRAF6 Requires a Dimeric Ubiquitin-Conjugating Enzyme Complex and a Unique Polyubiquitin Chain. *Cell, 103*(2), 351-361.
Deng, W., Lee, J., Wang, H., Miller, J., Reik, A., Gregory, P. D., Dean, A., & Blobel, G. A. (2012). Controlling long-range genomic interactions at a native locus by targeted tethering of a looping factor. *Cell, 149*(6), 1233-1244.
Dhalluin, C., Carlson, J. E., Zeng, L., He, C., Aggarwal, A. K., Zhou, M.-M., & Zhou, M.-M. (1999). Structure and ligand of a histone acetyltransferase bromodomain. *Nature, 399*, 491.
Dhordain, P., Albagli, O., Lin, R. J., Ansieau, S., Quief, S., Leutz, A., Kerckaert, J.-P., Evans, R. M., & Leprince, D. (1997). Corepressor SMRT binds the BTB/POZ repressing domain of the LAZ3/BCL6 oncoprotein. *94*(20), 10762-10767.
Di Noia, J., & Neuberger, M. S. (2002). Altering the pathway of immunoglobulin hypermutation by inhibiting uracil-DNA glycosylase. *Nature, 419*, 43.
Diehl, S. A., Schmidlin, H., Nagasawa, M., van Haren, S. D., Kwakkenbos, M. J., Yasuda, E., Beaumont, T., Scheeren, F. A., & Spits, H. (2008). STAT3-Mediated Up-Regulation of BLIMP1 Is Coordinated with BCL6 Down-Regulation to Control Human Plasma Cell Differentiation. *The Journal of Immunology, 180*(7), 4805.
Dillon, S. C., Zhang, X., Trievel, R. C., & Cheng, X. (2005). The SET-domain protein superfamily: protein lysine methyltransferases. *Genome Biology, 6*(8), 227.

Dimopoulos, M. A., Tedeschi, A., Trotman, J., Garcia-Sanz, R., Macdonald, D., Leblond, V., Mahe, B., Herbaux, C., Tam, C., Orsucci, L., Palomba, M. L., Matous, J. V., Shustik, C., Kastritis, E., Treon, S. P., Li, J., Salman, Z., Graef, T., & Buske, C. (2018). Phase 3 Trial of Ibrutinib plus Rituximab in Waldenstrom's Macroglobulinemia. *N Engl J Med, 378*(25), 2399-2410.

Dimopoulos, M. A., Terpos, E., Chanan-Khan, A., Leung, N., Ludwig, H., Jagannath, S., Niesvizky, R., Giralt, S., Fermand, J.-P., Bladé, J., Comenzo, R. L., Sezer, O., Palumbo, A., Harousseau, J.-L., Richardson, P. G., Barlogie, B., Anderson, K. C., Sonneveld, P., Tosi, P., Cavo, M., Rajkumar, S. V., Durie, B. G. M., & San Miguel, J. (2010). Renal Impairment in Patients With Multiple Myeloma: A Consensus Statement on Behalf of the International Myeloma Working Group. *Journal of Clinical Oncology, 28*(33), 4976-4984.

Dimopoulos, M. A., Trotman, J., Tedeschi, A., Matous, J. V., Macdonald, D., Tam, C., Tournilhac, O., Ma, S., Oriol, A., Heffner, L. T., Shustik, C., Garcia-Sanz, R., Cornell, R. F., de Larrea, C. F., Castillo, J. J., Granell, M., Kyrtsonis, M. C., Leblond, V., Symeonidis, A., Kastritis, E., Singh, P., Li, J., Graef, T., Bilotti, E., Treon, S., & Buske, C. (2017). Ibrutinib for patients with rituximab-refractory Waldenstrom's macroglobulinaemia (iNNOVATE): an open-label substudy of an international, multicentre, phase 3 trial. *Lancet Oncol, 18*(2), 241-250.

Ding, B. B., Bi, E., Chen, H., Yu, J. J., & Ye, B. H. (2013). IL-21 and CD40L Synergistically Promote Plasma Cell Differentiation through Upregulation of Blimp-1 in Human B Cells. *The Journal of Immunology*, 1201678.

Ditzel Santos, D., Ho, A. W., Tournilhac, O., Hatjiharissi, E., Leleu, X., Xu, L., Tassone, P., Neri, P., Hunter, Z. R., Chemaly, M. A., Branagan, A. R., Manning, R. J., Patterson, C. J., Moreau, A. S., Ciccarelli, B., Adamia, S., Kriangkum, J., Kutok, J. L., Tai, Y. T., Zhang, J., Pilarski, L. M., Anderson, K. C., Munshi, N., & Treon, S. P. (2007). Establishment of BCWM.1 cell line for Waldenstrom's macroglobulinemia with productive in vivo engraftment in SCID-hu mice. *Exp Hematol, 35*(9), 1366-1375.

Dobin, A., Davis, C. A., Schlesinger, F., Drenkow, J., Zaleski, C., Jha, S., Batut, P., Chaisson, M., & Gingeras, T. R. (2013). STAR: ultrafast universal RNA-seq aligner. *Bioinformatics, 29*(1), 15-21.

Dogan, I., Bertocci, B., Vilmont, V., Delbos, F., Megret, J., Storck, S., Reynaud, C. A., & Weill, J. C. (2009). Multiple layers of B cell memory with different effector functions. *Nat Immunol, 10*(12), 1292-1299.

Doody, G. M., Stephenson, S., McManamy, C., & Tooze, R. M. (2007). PRDM1/BLIMP-1 Modulates IFN-γ-Dependent Control of the MHC Class I Antigen-Processing and Peptide-Loading Pathway. *The Journal of Immunology, 179*(11), 7614.

Douagi, I., Gujer, C., Sundling, C., Adams, W. C., Smed-Sörensen, A., Seder, R. A., Karlsson Hedestam, G. B., & Loré, K. (2009). Human B

Cell Responses to TLR Ligands Are Differentially Modulated by Myeloid and Plasmacytoid Dendritic Cells. *The Journal of Immunology, 182*(4), 1991.

Draetta, G., Luca, F., Westendorf, J., Brizuela, L., Ruderman, J., & Beach, D. (1989). Cdc2 protein kinase is complexed with both cyclin A and B: evidence for proteolytic inactivation of MPF. *Cell, 56*(5), 829-838.

Durie, B. G., Hoering, A., Abidi, M. H., Rajkumar, S. V., Epstein, J., Kahanic, S. P., Thakuri, M., Reu, F., Reynolds, C. M., Sexton, R., Orlowski, R. Z., Barlogie, B., & Dispenzieri, A. (2017). Bortezomib with lenalidomide and dexamethasone versus lenalidomide and dexamethasone alone in patients with newly diagnosed myeloma without intent for immediate autologous stem-cell transplant (SWOG S0777): a randomised, open-label, phase 3 trial. *Lancet, 389*(10068), 519-527.

Early, P., Rogers, J., Davis, M., Calame, K., Bond, M., Wall, R., & Hood, L. (1980). Two mRNAs can be produced from a single immunoglobulin μ gene by alternative RNA processing pathways. *Cell, 20*(2), 313-319.

Ehlich, A., Schaal, S., Gu, H., Kitamura, D., Müller, W., & Rajewsky, K. (1993). Immunoglobulin heavy and light chain genes rearrange independently at early stages of B cell development. *Cell, 72*(5), 695-704.

el-Deiry, W. S., Tokino, T., Velculescu, V. E., Levy, D. B., Parsons, R., Trent, J. M., Lin, D., Mercer, W. E., Kinzler, K. W., & Vogelstein, B. (1993). WAF1, a potential mediator of p53 tumor suppression. *Cell, 75*(4), 817-825.

Emslie, D., D'Costa, K., Hasbold, J., Metcalf, D., Takatsu, K., Hodgkin, P. O., & Corcoran, L. M. (2008). Oct2 enhances antibody-secreting cell differentiation through regulation of IL-5 receptor alpha chain expression on activated B cells. *The Journal of experimental medicine, 205*(2), 409-421.

Ernst, J., Melnikov, A., Zhang, X., Wang, L., Rogov, P., Mikkelsen, T. S., & Kellis, M. (2016). Genome-scale high-resolution mapping of activating and repressive nucleotides in regulatory regions. *Nature Biotechnology, 34*, 1180.

Ezponda, T., Dupéré-Richer, D., Will, C. M., Small, E. C., Varghese, N., Patel, T., Nabet, B., Popovic, R., Oyer, J., Bulic, M., Zheng, Y., Huang, X., Shah, M. Y., Maji, S., Riva, A., Occhionorelli, M., Tonon, G., Kelleher, N., Keats, J., & Licht, J. D. (2017). UTX/KDM6A Loss Enhances the Malignant Phenotype of Multiple Myeloma and Sensitizes Cells to EZH2 inhibition. *Cell Reports, 21*(3), 628-640.

Fairfax, K. A., Kallies, A., Nutt, S. L., & Tarlinton, D. M. (2008). Plasma cell development: From B-cell subsets to long-term survival niches. *Seminars in Immunology, 20*(1), 49-58.

Fernández de Larrea, C., Kyle, R. A., Durie, B. G. M., Ludwig, H., Usmani, S., Vesole, D. H., Hajek, R., San Miguel, J. F., Sezer, O., Sonneveld, P., Kumar, S. K., Mahindra, A., Comenzo, R., Palumbo, A., Mazumber, A., Anderson, K. C., Richardson, P. G., Badros, A. Z.,

Caers, J., Cavo, M., LeLeu, X., Dimopoulos, M. A., Chim, C. S., Schots, R., Noeul, A., Fantl, D., Mellqvist, U. H., Landgren, O., Chanan-Khan, A., Moreau, P., Fonseca, R., Merlini, G., Lahuerta, J. J., Bladé, J., Orlowski, R. Z., & Shah, J. J. (2012). Plasma cell leukemia: consensus statement on diagnostic requirements, response criteria and treatment recommendations by the International Myeloma Working Group. *Leukemia, 27*, 780.

Ferrari, Karin J., Scelfo, A., Jammula, S., Cuomo, A., Barozzi, I., Stützer, A., Fischle, W., Bonaldi, T., & Pasini, D. (2014). Polycomb-Dependent H3K27me1 and H3K27me2 Regulate Active Transcription and Enhancer Fidelity. *Molecular Cell, 53*(1), 49-62.

Fisher, S., Barry, A., Abreu, J., Minie, B., Nolan, J., Delorey, T. M., Young, G., Fennell, T. J., Allen, A., Ambrogio, L., Berlin, A. M., Blumenstiel, B., Cibulskis, K., Friedrich, D., Johnson, R., Juhn, F., Reilly, B., Shammas, R., Stalker, J., Sykes, S. M., Thompson, J., Walsh, J., Zimmer, A., Zwirko, Z., Gabriel, S., Nicol, R., & Nusbaum, C. (2011). A scalable, fully automated process for construction of sequence-ready human exome targeted capture libraries. *Genome Biol, 12*(1), R1.

Flemington, E. K., Speck, S. H., & Kaelin, W. G. (1993). E2F-1-mediated transactivation is inhibited by complex formation with the retinoblastoma susceptibility gene product. *Proceedings of the National Academy of Sciences, 90*(15), 6914.

Fonseca, R., Abouzaid, S., Bonafede, M., Cai, Q., Parikh, K., Cosler, L., & Richardson, P. (2016). Trends in overall survival and costs of multiple myeloma, 2000–2014. *Leukemia, 31*, 1915.

Förster, R., Schubel, A., Breitfeld, D., Kremmer, E., Renner-Müller, I., Wolf, E., & Lipp, M. (1999). CCR7 Coordinates the Primary Immune Response by Establishing Functional Microenvironments in Secondary Lymphoid Organs. *Cell, 99*(1), 23-33.

Fujinaga, K., Irwin, D., Huang, Y., Taube, R., Kurosu, T., & Peterlin, B. M. (2004). Dynamics of human immunodeficiency virus transcription: P-TEFb phosphorylates RD and dissociates negative effectors from the transactivation response element. *Molecular and cellular biology, 24*(2), 787-795.

Fujita, N., Jaye, D. L., Geigerman, C., Akyildiz, A., Mooney, M. R., Boss, J. M., & Wade, P. A. (2004). MTA3 and the Mi-2/NuRD complex regulate cell fate during B lymphocyte differentiation. *Cell, 119*(1), 75-86.

Fukuda, T., Yoshida, T., Okada, S., Hatano, M., Miki, T., Ishibashi, K., Okabe, S., Koseki, H., Hirosawa, S., Taniguchi, M., Miyasaka, N., & Tokuhisa, T. (1997). Disruption of the Bcl6 Gene Results in an Impaired Germinal Center Formation. *The Journal of Experimental Medicine, 186*(3), 439.

Fulciniti, M., Lin, C. Y., Samur, M. K., Lopez, M. A., Singh, I., Lawlor, M. A., Szalat, R. E., Ott, C. J., Avet-Loiseau, H., Anderson, K. C., Young, R. A., Bradner, J. E., & Munshi, N. C. (2018). Non-overlapping Control of Transcriptome by Promoter- and Super-Enhancer-Associated

Dependencies in Multiple Myeloma. *Cell Reports, 25*(13), 3693-3705.e3696.
Furnari, B., Rhind, N., & Russell, P. (1997). Cdc25 Mitotic Inducer Targeted by Chk1 DNA Damage Checkpoint Kinase. *Science, 277*(5331), 1495.
Furney, S. J., Higgins, D. G., Ouzounis, C. A., & López-Bigas, N. (2006). Structural and functional properties of genes involved in human cancer. *BMC Genomics, 7*(1), 3.
Gabrea, A., Bergsagel, P. L., Chesi, M., Shou, Y., & Kuehl, W. M. (1999). Insertion of Excised IgH Switch Sequences Causes Overexpression of Cyclin D1 in a Myeloma Tumor Cell. *Molecular Cell, 3*(1), 119-123.
Galloway, A., Saveliev, A., Lukasiak, S., Hodson, D. J., Bolland, D., Balmanno, K., Ahlfors, H., Monzon-Casanova, E., Mannurita, S. C., Bell, L. S., Andrews, S., Diaz-Munoz, M. D., Cook, S. J., Corcoran, A., & Turner, M. (2016). RNA-binding proteins ZFP36L1 and ZFP36L2 promote cell quiescence. *Science, 352*(6284), 453-459.
Gao, N., Schwartzberg, P., Wilder, J. A., Blazar, B. R., & Yuan, D. (2006). B Cell Induction of IL-13 Expression in NK Cells: Role of CD244 and SLAM-Associated Protein. *The Journal of Immunology, 176*(5), 2758.
Gardini, A. (2017). Global Run-On Sequencing (GRO-Seq). *Methods in molecular biology (Clifton, NJ), 1468*, 111-120.
Gathings, W. E., Lawton, A. R., & Cooper, M. D. (1977). Immunofluorescent studies of the development of pre-B cells, B lymphocytes and immunoglobulin isotype diversity in humans. *Eur J Immunol, 7*(11), 804-810.
Geier, J. K., & Schlissel, M. S. (2006). Pre-BCR signals and the control of Ig gene rearrangements. *Seminars in Immunology, 18*(1), 31-39.
Genestier, L., Taillardet, M., Mondiere, P., Gheit, H., Bella, C., & Defrance, T. (2007). TLR Agonists Selectively Promote Terminal Plasma Cell Differentiation of B Cell Subsets Specialized in Thymus-Independent Responses. *The Journal of Immunology, 178*(12), 7779.
Georgopoulos, K., Bigby, M., Wang, J. H., Molnar, A., Wu, P., Winandy, S., & Sharpe, A. (1994). The Ikaros gene is required for the development of all lymphoid lineages. *Cell, 79*(1), 143-156.
Gertz, M. A. (2019). Waldenström macroglobulinemia: 2019 update on diagnosis, risk stratification, and management. *American Journal of Hematology, 94*(2), 266-276.
Ghobrial, I. M., Campigotto, F., Murphy, T. J., Boswell, E. N., Banwait, R., Azab, F., Chuma, S., Kunsman, J., Donovan, A., Masood, F., Warren, D., Rodig, S., Anderson, K. C., Richardson, P. G., Weller, E., & Matous, J. (2013). Results of a phase 2 trial of the single-agent histone deacetylase inhibitor panobinostat in patients with relapsed/refractory Waldenstrom macroglobulinemia. *Blood, 121*(8), 1296-1303.
Ghobrial, I. M., Gertz, M. A., & Fonseca, R. (2003). Waldenström macroglobulinaemia. *The Lancet Oncology, 4*(11), 679-685.
Ghobrial, I. M., Witzig, T. E., Gertz, M., LaPlant, B., Hayman, S., Camoriano, J., Lacy, M., Bergsagel, P. L., Chuma, S., DeAngelo, D., & Treon, S.

P. (2013). Long-term results of the phase II trial of the oral mTOR inhibitor everolimus (RAD001) in relapsed or refractory Waldenstrom Macroglobulinemia. *American Journal of Hematology, 89*(3), 237-242.

Ghobrial, I. M., Witzig, T. E., Gertz, M., LaPlant, B., Hayman, S., Camoriano, J., Lacy, M., Bergsagel, P. L., Chuma, S., DeAngelo, D., & Treon, S. P. (2014). Long-term results of the phase II trial of the oral mTOR inhibitor everolimus (RAD001) in relapsed or refractory Waldenstrom Macroglobulinemia. *Am J Hematol, 89*(3), 237-242.

Gill, G., Pascal, E., Tseng, Z. H., & Tjian, R. (1994). A glutamine-rich hydrophobic patch in transcription factor Sp1 contacts the dTAFII110 component of the Drosophila TFIID complex and mediates transcriptional activation. *Proceedings of the National Academy of Sciences of the United States of America, 91*(1), 192-196.

Gillies, S. D., Morrison, S. L., Oi, V. T., & Tonegawa, S. (1983). A tissue-specific transcription enhancer element is located in the major intron of a rearranged immunoglobulin heavy chain gene. *Cell, 33*(3), 717-728.

Goel, S., DeCristo, M. J., Watt, A. C., BrinJones, H., Sceneay, J., Li, B. B., Khan, N., Ubellacker, J. M., Xie, S., Metzger-Filho, O., Hoog, J., Ellis, M. J., Ma, C. X., Ramm, S., Krop, I. E., Winer, E. P., Roberts, T. M., Kim, H.-J., McAllister, S. S., & Zhao, J. J. (2017). CDK4/6 inhibition triggers anti-tumour immunity. *Nature, 548*, 471.

Goldfinger, M., Shmuel, M., Benhamron, S., & Tirosh, B. (2011). Protein synthesis in plasma cells is regulated by crosstalk between endoplasmic reticulum stress and mTOR signaling. *European Journal of Immunology, 41*(2), 491-502.

Gomez-Bougie, P., Wuillème-Toumi, S., Ménoret, E., Trichet, V., Robillard, N., Philippe, M., Bataille, R., & Amiot, M. (2007). Noxa Up-regulation and Mcl-1 Cleavage Are Associated to Apoptosis Induction by Bortezomib in Multiple Myeloma. *Cancer Research, 67*(11), 5418.

Goodman, A., Patel, S. P., & Kurzrock, R. (2016). PD-1–PD-L1 immune-checkpoint blockade in B-cell lymphomas. *Nature Reviews Clinical Oncology, 14*, 203.

Görgün, G., Samur, M. K., Cowens, K. B., Paula, S., Bianchi, G., Anderson, J. E., White, R. E., Singh, A., Ohguchi, H., Suzuki, R., Kikuchi, S., Harada, T., Hideshima, T., Tai, Y.-T., Laubach, J. P., Raje, N., Magrangeas, F., Minvielle, S., Avet-Loiseau, H., Munshi, N. C., Dorfman, D. M., Richardson, P. G., & Anderson, K. C. (2015). Lenalidomide Enhances Immune Checkpoint Blockade-Induced Immune Response in Multiple Myeloma. *Clinical Cancer Research, 21*(20), 4607.

Gregory R. Warnes, B. B., Lodewijk Bonebakker, Robert Gentleman, Wolfgang Huber Andy Liaw, Thomas Lumley, Martin Maechler, Arni Magnusson, Steffen Moeller, Marc Schwartz, Bill Venables. (2017). gplots, R package.

Grossman, S. R., Zhang, X., Wang, L., Engreitz, J., Melnikov, A., Rogov, P., Tewhey, R., Isakova, A., Deplancke, B., Bernstein, B. E., Mikkelsen,

T. S., & Lander, E. S. (2017). Systematic dissection of genomic features determining transcription factor binding and enhancer function. *Proceedings of the National Academy of Sciences, 114*(7), E1291.

Gunn, M. D., Ngo, V. N., Ansel, K. M., Ekland, E. H., Cyster, J. G., & Williams, L. T. (1998). A B-cell-homing chemokine made in lymphoid follicles activates Burkitts lymphoma receptor-1. *Nature, 391*, 799.

Guo, C., Sonoda, E., Tang, T.-S., Parker, J. L., Bielen, A. B., Takeda, S., Ulrich, H. D., & Friedberg, E. C. (2006). REV1 Protein Interacts with PCNA: Significance of the REV1 BRCT Domain In Vitro and In Vivo. *Molecular Cell, 23*(2), 265-271.

Guo, M., Price, M. J., Patterson, D. G., Barwick, B. G., Haines, R. R., Kania, A. K., Bradley, J. E., Randall, T. D., Boss, J. M., & Scharer, C. D. (2018). EZH2 Represses the B Cell Transcriptional Program and Regulates Antibody-Secreting Cell Metabolism and Antibody Production. *The Journal of Immunology, 200*(3), 1039-1052.

Gupta, D., Treon, S. P., Shima, Y., Hideshima, T., Podar, K., Tai, Y. T., Lin, B., Lentzsch, S., Davies, F. E., Chauhan, D., Schlossman, R. L., Richardson, P., Ralph, P., Wu, L., Payvandi, F., Muller, G., Stirling, D. I., & Anderson, K. C. (2001). Adherence of multiple myeloma cells to bone marrow stromal cells upregulates vascular endothelial growth factor secretion: therapeutic applications. *Leukemia, 15*(12), 1950-1961.

Gupta, S., Jiang, M., Anthony, A., & Pernis, A. B. (1999). Lineage-Specific Modulation of Interleukin 4 Signaling by Interferon Regulatory Factor 4. *The Journal of Experimental Medicine, 190*(12), 1837.

Győry, I., Wu, J., Fejér, G., Seto, E., & Wright, K. L. (2004). PRDI-BF1 recruits the histone H3 methyltransferase G9a in transcriptional silencing. *Nature Immunology, 5*, 299.

Hackett, J. A., Sengupta, R., Zylicz, J. J., Murakami, K., Lee, C., Down, T. A., & Surani, M. A. (2013). Germline DNA demethylation dynamics and imprint erasure through 5-hydroxymethylcytosine. *Science (New York, NY), 339*(6118), 448-452.

Hall, J. M., McDonnell, D. P., & Korach, K. S. (2002). Allosteric regulation of estrogen receptor structure, function, and coactivator recruitment by different estrogen response elements. *Mol Endocrinol, 16*(3), 469-486.

Hanahan, D., & Weinberg, Robert A. (2011). Hallmarks of Cancer: The Next Generation. *Cell, 144*(5), 646-674.

Hanamura, I., Iida, S., Akano, Y., Hayami, Y., Kato, M., Miura, K., Harada, S., Banno, S., Wakita, A., Kiyoi, H., Naoe, T., Shimizu, S., Sonta, S.-i., Nitta, M., Taniwaki, M., & Ueda, R. (2001). Ectopic Expression of MAFB Gene in Human Myeloma Cells Carrying (14;20)(q32;q11) Chromosomal Translocations. *Japanese Journal of Cancer Research, 92*(6), 638-644.

Harada, T., Hideshima, T., & Anderson, K. C. (2016). Histone deacetylase inhibitors in multiple myeloma: from bench to bedside. *International Journal of Hematology, 104*(3), 300-309.

Harbour, J. W., Luo, R. X., Santi, A. D., Postigo, A. A., & Dean, D. C. (1999). Cdk Phosphorylation Triggers Sequential Intramolecular Interactions that Progressively Block Rb Functions as Cells Move through G1. *Cell, 98*(6), 859-869.

Hardiman, G., Rock, F. L., Balasubramanian, S., Kastelein, R. A., & Bazan, J. F. (1996). Molecular characterization and modular analysis of human MyD88. *Oncogene, 13*(11), 2467-2475.

Hashwah, H., Schmid, C. A., Kasser, S., Bertram, K., Stelling, A., Manz, M. G., & Müller, A. (2017). Inactivation of CREBBP expands the germinal center B cell compartment, down-regulates MHCII expression and promotes DLBCL growth. *Proceedings of the National Academy of Sciences, 114*(36), 9701.

Hatjiharissi, E., Ngo, H., Leontovich, A. A., Leleu, X., Timm, M., Melhem, M., George, D., Lu, G., Ghobrial, J., Alsayed, Y., Zeismer, S., Cabanela, M., Nehme, A., Jia, X., Moreau, A. S., Treon, S. P., Fonseca, R., Gertz, M. A., Anderson, K. C., Witzig, T. E., & Ghobrial, I. M. (2007). Proteomic Analysis of Waldenstrom Macroglobulinemia. *Cancer Research, 67*(8), 3777.

He, Y., Fang, J., Taatjes, D. J., & Nogales, E. (2013). Structural visualization of key steps in human transcription initiation. *Nature, 495*, 481.

Heald, R., McLoughlin, M., & McKeon, F. (1993). Human wee1 maintains mitotic timing by protecting the nucleus from cytoplasmically activated cdc2 kinase. *Cell, 74*(3), 463-474.

Heintzman, N. D., Hon, G. C., Hawkins, R. D., Kheradpour, P., Stark, A., Harp, L. F., Ye, Z., Lee, L. K., Stuart, R. K., Ching, C. W., Ching, K. A., Antosiewicz-Bourget, J. E., Liu, H., Zhang, X., Green, R. D., Lobanenkov, V. V., Stewart, R., Thomson, J. A., Crawford, G. E., Kellis, M., & Ren, B. (2009). Histone modifications at human enhancers reflect global cell-type-specific gene expression. *Nature, 459*, 108.

Heintzman, N. D., Stuart, R. K., Hon, G., Fu, Y., Ching, C. W., Hawkins, R. D., Barrera, L. O., Van Calcar, S., Qu, C., Ching, K. A., Wang, W., Weng, Z., Green, R. D., Crawford, G. E., & Ren, B. (2007). Distinct and predictive chromatin signatures of transcriptional promoters and enhancers in the human genome. *Nature Genetics, 39*, 311.

Heise, N., De Silva, N. S., Silva, K., Carette, A., Simonetti, G., Pasparakis, M., & Klein, U. (2014). Germinal center B cell maintenance and differentiation are controlled by distinct NF-κB transcription factor subunits. *The Journal of Experimental Medicine, 211*(10), 2103.

Helin, K., Harlow, E., & Fattaey, A. (1993). Inhibition of E2F-1 transactivation by direct binding of the retinoblastoma protein. *Molecular and Cellular Biology, 13*(10), 6501.

Herbaux, C., Bertrand, E., Marot, G., Roumier, C., Poret, N., Soenen, V., Nibourel, O., Roche-Lestienne, C., Broucqsault, N., Galiègue-Zouitina, S., Boyle, E. M., Fouquet, G., Renneville, A., Tricot, S., Morschhauser, F., Preudhomme, C., Quesnel, B., Poulain, S., & Leleu, X. (2016). BACH2 promotes indolent clinical presentation in Waldenström macroglobulinemia. *Oncotarget, 8*(34), 57451-57459.

Hernando, H., Gelato, K. A., Lesche, R., Beckmann, G., Koehr, S., Otto, S., Steigemann, P., & Stresemann, C. (2016). EZH2 Inhibition Blocks Multiple Myeloma Cell Growth through Upregulation of Epithelial Tumor Suppressor Genes. *Molecular Cancer Therapeutics, 15*(2), 287.

Herviou, L., Jourdan, M., Martinez, A.-M., Cavalli, G., & Moreaux, J. (2019). EZH2 is overexpressed in transitional preplasmablasts and is involved in human plasma cell differentiation. *Leukemia*.

Hewitt, S. L., Yin, B., Ji, Y., Chaumeil, J., Marszalek, K., Tenthorey, J., Salvagiotto, G., Steinel, N., Ramsey, L. B., Ghysdael, J., Farrar, M. A., Sleckman, B. P., Schatz, D. G., Busslinger, M., Bassing, C. H., & Skok, J. A. (2009). RAG-1 and ATM coordinate monoallelic recombination and nuclear positioning of immunoglobulin loci. *Nature Immunology, 10*, 655.

Hideshima, T., Chauhan, D., Shima, Y., Raje, N., Davies, F. E., Tai, Y.-T., Treon, S. P., Lin, B., Schlossman, R. L., Richardson, P., Muller, G., Stirling, D. I., & Anderson, K. C. (2000). Thalidomide and its analogs overcome drug resistance of human multiple myeloma cells to conventional therapy. *Blood, 96*(9), 2943.

Hiebert, S. W., Chellappan, S. P., Horowitz, J. M., & Nevins, J. R. (1992). The interaction of RB with E2F coincides with an inhibition of the transcriptional activity of E2F. *Genes & Development, 6*(2), 177-185.

Hill, Q. A., Rawstron, A. C., de Tute, R. M., & Owen, R. G. (2014). Outcome prediction in plasmacytoma of bone: a risk model utilizing bone marrow flow cytometry and light-chain analysis. *Blood, 124*(8), 1296.

Hirao, A., Kong, Y.-Y., Matsuoka, S., Wakeham, A., Ruland, J., Yoshida, H., Liu, D., Elledge, S. J., & Mak, T. W. (2000). DNA Damage-Induced Activation of p53 by the Checkpoint Kinase Chk2. *Science, 287*(5459), 1824.

Hodge, L. S., Novak, A. J., Grote, D. M., Braggio, E., Ketterling, R. P., Manske, M. K., Price Troska, T. L., Ziesmer, S. C., Fonseca, R., Witzig, T. E., Morice, W. G., Gertz, M. A., & Ansell, S. M. (2011). Establishment and characterization of a novel Waldenström macroglobulinemia cell line, MWCL-1. *Blood, 117*(19), e190.

Hoffmann, I., Draetta, G., & Karsenti, E. (1994). Activation of the phosphatase activity of human cdc25A by a cdk2-cyclin E dependent phosphorylation at the G1/S transition. *Embo j, 13*(18), 4302-4310.

Hong, L., Schroth, G. P., Matthews, H. R., Yau, P., & Bradbury, E. M. (1993). Studies of the DNA binding properties of histone H4 amino terminus. Thermal denaturation studies reveal that acetylation markedly reduces the binding constant of the H4 "tail" to DNA. *J Biol Chem, 268*(1), 305-314.

Horikoshi, M., Hai, T., Lin, Y. S., Green, M. R., & Roeder, R. G. (1988). Transcription factor ATF interacts with the TATA factor to facilitate establishment of a preinitiation complex. *Cell, 54*(7), 1033-1042.

Horn, M., Geisen, C., Cermak, L., Becker, B., Nakamura, S., Klein, C., Pagano, M., & Antebi, A. (2014). DRE-1/FBXO11-Dependent

Degradation of BLMP-1/BLIMP-1 Governs C. elegans Developmental Timing and Maturation. *Developmental Cell, 28*(6), 697-710.
Hoshino, K., Takeda, K., Adachi, O., Takeuchi, O., Akira, S., & Ogawa, T. (2000). Cellular responses to bacterial cell wall components are mediated through MyD88-dependent signaling cascades. *International Immunology, 12*(1), 113-117.
Hsieh, C.-L., Fei, T., Chen, Y., Li, T., Gao, Y., Wang, X., Sun, T., Sweeney, C. J., Lee, G.-S. M., Chen, S., Balk, S. P., Liu, X. S., Brown, M., & Kantoff, P. W. (2014). Enhancer RNAs participate in androgen receptor-driven looping that selectively enhances gene activation. *Proceedings of the National Academy of Sciences, 111*(20), 7319.
Hsieh, P., & Zhang, Y. (2017). The Devil is in the details for DNA mismatch repair. *Proceedings of the National Academy of Sciences, 114*(14), 3552.
Hsin, J.-P., & Manley, J. L. (2012). The RNA polymerase II CTD coordinates transcription and RNA processing. *Genes & Development, 26*(19), 2119-2137.
Huang, P., & Plunkett, W. (1995). Fludarabine-and gemcitabine-induced apoptosis: incorporation of analogs into DNA is a critical event. *Cancer chemotherapy and pharmacology, 36*(3), 181-188.
Huang, S. (1994). Blimp-1 is the murine homolog of the human transcriptional repressor PRDI-BF1. *Cell, 78*(1), 9.
Hugo, W., Zaretsky, J. M., Sun, L., Song, C., Moreno, B. H., Hu-Lieskovan, S., Berent-Maoz, B., Pang, J., Chmielowski, B., Cherry, G., Seja, E., Lomeli, S., Kong, X., Kelley, M. C., Sosman, J. A., Johnson, D. B., Ribas, A., & Lo, R. S. (2016). Genomic and Transcriptomic Features of Response to Anti-PD-1 Therapy in Metastatic Melanoma. *Cell, 165*(1), 35-44.
Hung, K. H., Su, S. T., Chen, C. Y., Hsu, P. H., Huang, S. Y., Wu, W. J., Chen, M. J. M., Chen, H. Y., Wu, P. C., Lin, F. R., Tsai, M. D., & Lin, K. I. (2016). Aiolos collaborates with Blimp-1 to regulate the survival of multiple myeloma cells. *Cell Death And Differentiation, 23*, 1175.
Hunter, Z. R., Xu, L., Yang, G., Tsakmaklis, N., Vos, J. M., Liu, X., Chen, J., Manning, R. J., Chen, J. G., Brodsky, P., Patterson, C. J., Gustine, J., Dubeau, T., Castillo, J. J., Anderson, K. C., Munshi, N. M., & Treon, S. P. (2016). Transcriptome sequencing reveals a profile that corresponds to genomic variants in Waldenström macroglobulinemia. *Blood, 128*(6), 827-838.
Hunter, Z. R., Xu, L., Yang, G., Zhou, Y., Liu, X., Cao, Y., Manning, R. J., Tripsas, C., Patterson, C. J., Sheehy, P., & Treon, S. P. (2014). The genomic landscape of Waldenström macroglobulinemia is characterized by highly recurring MYD88 and WHIM-like CXCR4 mutations, and small somatic deletions associated with B-cell lymphomagenesis. *Blood, 123*(11), 1637-1646.
Hustedt, N., & Durocher, D. (2016). The control of DNA repair by the cell cycle. *Nature Cell Biology, 19*, 1.

Innocente, S. A., Abrahamson, J. L. A., Cogswell, J. P., & Lee, J. M. (1999). p53 regulates a G₂ checkpoint through cyclin B1. *Proceedings of the National Academy of Sciences, 96*(5), 2147.

Ishiguro, K., Kitajima, H., Niinuma, T., Ishida, T., Maruyama, R., Ikeda, H., Hayashi, T., Sasaki, H., Wakasugi, H., Nishiyama, K., Shindo, T., Yamamoto, E., Kai, M., Sasaki, Y., Tokino, T., Nakase, H., & Suzuki, H. (2019). DOT1L inhibition blocks multiple myeloma cell proliferation by suppressing IRF4-MYC signaling. *Haematologica, 104*(1), 155.

Italiano, A., Soria, J.-C., Toulmonde, M., Michot, J.-M., Lucchesi, C., Varga, A., Coindre, J.-M., Blakemore, S. J., Clawson, A., Suttle, B., McDonald, A. A., Woodruff, M., Ribich, S., Hedrick, E., Keilhack, H., Thomson, B., Owa, T., Copeland, R. A., Ho, P. T. C., & Ribrag, V. (2018). Tazemetostat, an EZH2 inhibitor, in relapsed or refractory B-cell non-Hodgkin lymphoma and advanced solid tumours: a first-in-human, open-label, phase 1 study. *The Lancet Oncology, 19*(5), 649-659.

Iwafuchi-Doi, M., & Zaret, K. S. (2014). Pioneer transcription factors in cell reprogramming. *Genes & Development, 28*(24), 2679-2692.

Izumi, T., & Maller, J. L. (1993). Elimination of cdc2 phosphorylation sites in the cdc25 phosphatase blocks initiation of M-phase. *Molecular Biology of the Cell, 4*(12), 1337-1350.

Jacob, J., Kelsoe, G., Rajewsky, K., & Weiss, U. (1991). Intraclonal generation of antibody mutants in germinal centres. *Nature, 354*, 389.

Jacobson, R. H., Ladurner, A. G., King, D. S., & Tjian, R. (2000). Structure and Function of a Human TAFII250 Double Bromodomain Module. *Science, 288*(5470), 1422.

Jaehning, J. A., Stewart, C. C., & Roeder, R. G. (1975). DNA-dependent RNA polymerase levels during the response of human peripheral lymphocytes to phytohemagglutinin. *Cell, 4*(1), 51-57.

Jalali, S., Price-Troska, T., Paludo, J., Villasboas, J., Kim, H.-J., Yang, Z.-Z., Novak, A. J., & Ansell, S. M. (2018). Soluble PD-1 ligands regulate T-cell function in Waldenstrom macroglobulinemia. *Blood Advances, 2*(15), 1985.

Janeway Jr, C. A., Travers, P., Walport, M., & Shlomchik, M. J. (2001). The generation of diversity in immunoglobulins. In *Immunobiology: The Immune System in Health and Disease 5th edition*: Garland Science.

Jansen, J. G., Langerak, P., Tsaalbi-Shtylik, A., van den Berk, P., Jacobs, H., & de Wind, N. (2006). Strand-biased defect in C/G transversions in hypermutating immunoglobulin genes in Rev1-deficient mice. *The Journal of Experimental Medicine, 203*(2), 319.

Jin, Y., Chen, K., De Paepe, A., Hellqvist, E., Krstic, A. D., Metang, L., Gustafsson, C., Davis, R. E., Levy, Y. M., Surapaneni, R., Wallblom, A., Nahi, H., Mansson, R., & Lin, Y. C. (2018). Active enhancer and chromatin accessibility landscapes chart the regulatory network of primary multiple myeloma. *Blood, 131*(19), 2138.

Jinno, S., Suto, K., Nagata, A., Igarashi, M., Kanaoka, Y., Nojima, H., & Okayama, H. (1994). Cdc25A is a novel phosphatase functioning early in the cell cycle. *The EMBO Journal, 13*(7), 1549-1556.
Johanson, T. M., Lun, A. T. L., Coughlan, H. D., Tan, T., Smyth, G. K., Nutt, S. L., & Allan, R. S. (2018). Transcription-factor-mediated supervision of global genome architecture maintains B cell identity. *Nature Immunology, 19*(11), 1257-1264.
Johnson, D. G., Schwarz, J. K., Cress, W. D., & Nevins, J. R. (1993). Expression of transcription factor E2F1 induces quiescent cells to enter S phase. *Nature, 365*(6444), 349-352.
Jourdan, M., Caraux, A., Caron, G., Robert, N., Fiol, G., Rème, T., Bolloré, K., Vendrell, J.-P., Le Gallou, S., Mourcin, F., De Vos, J., Kassambara, A., Duperray, C., Hose, D., Fest, T., Tarte, K., & Klein, B. (2011). Characterization of a Transitional Preplasmablast Population in the Process of Human B Cell to Plasma Cell Differentiation. *The Journal of Immunology, 187*(8), 3931.
Kabashima, K., Haynes, N. M., Xu, Y., Nutt, S. L., Allende, M. L., Proia, R. L., & Cyster, J. G. (2006). Plasma cell S1P₁ expression determines secondary lymphoid organ retention versus bone marrow tropism. *The Journal of Experimental Medicine, 203*(12), 2683.
Kagey, M. H., Newman, J. J., Bilodeau, S., Zhan, Y., Orlando, D. A., van Berkum, N. L., Ebmeier, C. C., Goossens, J., Rahl, P. B., Levine, S. S., Taatjes, D. J., Dekker, J., & Young, R. A. (2010). Mediator and cohesin connect gene expression and chromatin architecture. *Nature, 467*, 430.
Kallies, A., Hasbold, J., Fairfax, K., Pridans, C., Emslie, D., McKenzie, B. S., Lew, A. M., Corcoran, L. M., Hodgkin, P. D., Tarlinton, D. M., & Nutt, S. L. (2007). Initiation of Plasma-Cell Differentiation Is Independent of the Transcription Factor Blimp-1. *Immunity, 26*(5), 555-566.
Kallies, A., Hasbold, J., Tarlinton, D. M., Dietrich, W., Corcoran, L. M., Hodgkin, P. D., & Nutt, S. L. (2004). Plasma Cell Ontogeny Defined by Quantitative Changes in Blimp-1 Expression. *The Journal of Experimental Medicine, 200*(8), 967.
Kallies, A., Hawkins, E. D., Belz, G. T., Metcalf, D., Hommel, M., Corcoran, L. M., Hodgkin, P. D., & Nutt, S. L. (2006). Transcriptional repressor Blimp-1 is essential for T cell homeostasis and self-tolerance. *Nature Immunology, 7*, 466.
Kalushkova, A., Fryknäs, M., Lemaire, M., Fristedt, C., Agarwal, P., Eriksson, M., Deleu, S., Atadja, P., Österborg, A., Nilsson, K., Vanderkerken, K., Öberg, F., & Jernberg-Wiklund, H. (2010). Polycomb Target Genes Are Silenced in Multiple Myeloma. *PLOS ONE, 5*(7), e11483.
Kannouche, P. L., Wing, J., & Lehmann, A. R. (2004). Interaction of Human DNA Polymerase η with Monoubiquitinated PCNA: A Possible Mechanism for the Polymerase Switch in Response to DNA Damage. *Molecular Cell, 14*(4), 491-500.
Kantidakis, T., Saponaro, M., Mitter, R., Horswell, S., Kranz, A., Boeing, S., Aygün, O., Kelly, G. P., Matthews, N., Stewart, A., Stewart, A. F., &

Svejstrup, J. Q. (2016). Mutation of cancer driver MLL2 results in transcription stress and genome instability. *Genes & Development, 30*(4), 408-420.
Kärre, K., Ljunggren, H. G., Piontek, G., & Kiessling, R. (1986). Selective rejection of H–2-deficient lymphoma variants suggests alternative immune defence strategy. *Nature, 319*(6055), 675-678.
Kasinath, V., Faini, M., Poepsel, S., Reif, D., Feng, X. A., Stjepanovic, G., Aebersold, R., & Nogales, E. (2018). Structures of human PRC2 with its cofactors AEBP2 and JARID2. *Science (New York, NY), 359*(6378), 940-944.
Kato, J., Matsushime, H., Hiebert, S. W., Ewen, M. E., & Sherr, C. J. (1993). Direct binding of cyclin D to the retinoblastoma gene product (pRb) and pRb phosphorylation by the cyclin D-dependent kinase CDK4. *Genes Dev, 7*(3), 331-342.
Kawai, T., Adachi, O., Ogawa, T., Takeda, K., & Akira, S. (1999). Unresponsiveness of MyD88-deficient mice to endotoxin. *Immunity, 11*(1), 115-122.
Keller, A. D., & Maniatis, T. (1991). Identification and characterization of a novel repressor of beta-interferon gene expression. *Genes & Development, 5*(5), 868-879.
Keller, A. D., & Maniatis, T. (1991). Selection of sequences recognized by a DNA binding protein using a preparative southwestern blot. *Nucleic acids research, 19*(17), 4675-4680.
Keller, A. D., & Maniatis, T. (1992). Only two of the five zinc fingers of the eukaryotic transcriptional repressor PRDI-BF1 are required for sequence-specific DNA binding. *Molecular and Cellular Biology, 12*(5), 1940.
Kelly, K., Cochran, B. H., Stiles, C. D., & Leder, P. (1983). Cell-specific regulation of the c-myc gene by lymphocyte mitogens and platelet-derived growth factor. *Cell, 35*(3, Part 2), 603-610.
Kent, W. J., Sugnet, C. W., Furey, T. S., Roskin, K. M., Pringle, T. H., Zahler, A. M., Haussler, & David. (2002). The Human Genome Browser at UCSC. *Genome Research, 12*(6), 996-1006.
Kerfoot, Steven M., Yaari, G., Patel, Jaymin R., Johnson, Kody L., Gonzalez, David G., Kleinstein, Steven H., & Haberman, Ann M. (2011). Germinal Center B Cell and T Follicular Helper Cell Development Initiates in the Interfollicular Zone. *Immunity, 34*(6), 947-960.
Kerr, W. G., Cooper, M. D., Feng, L., Burrows, P. D., & Hendershot, L. M. (1989). Mu heavy chains can associate with a pseudo-light chain complex (psi L) in human pre-B cell lines. *Int Immunol, 1*(4), 355-361.
Kieffer-Kwon, K.-R., Nimura, K., Rao, S. S. P., Xu, J., Jung, S., Pekowska, A., Dose, M., Stevens, E., Mathe, E., Dong, P., Huang, S.-C., Ricci, M. A., Baranello, L., Zheng, Y., Tomassoni Ardori, F., Resch, W., Stavreva, D., Nelson, S., McAndrew, M., Casellas, A., Finn, E., Gregory, C., St. Hilaire, B. G., Johnson, S. M., Dubois, W., Cosma, M. P., Batchelor, E., Levens, D., Phair, R. D., Misteli, T., Tessarollo, L., Hager, G., Lakadamyali, M., Liu, Z., Floer, M., Shroff, H., Aiden, E. L., & Casellas, R. (2017). Myc Regulates Chromatin

Decompaction and Nuclear Architecture during B Cell Activation. *Molecular Cell, 67*(4), 566-578.e510.

Kim, J., Sif, S., Jones, B., Jackson, A., Koipally, J., Heller, E., Winandy, S., Viel, A., Sawyer, A., Ikeda, T., Kingston, R., & Georgopoulos, K. (1999). Ikaros DNA-Binding Proteins Direct Formation of Chromatin Remodeling Complexes in Lymphocytes. *Immunity, 10*(3), 345-355.

Kim, J.-A., Im, K., Park, S. N., Kwon, J., Choi, Q., Hwang, S. M., Sekiguchi, N., Yoon, S.-S., Lee, D. S., & Kim, S. Y. (2014). MYD88 L265P mutations are correlated with 6q deletion in Korean patients with Waldenström macroglobulinemia. *BioMed research international, 2014*.

Kim, J. B., & Sharp, P. A. (2001). Positive transcription elongation factor B phosphorylates hSPT5 and RNA polymerase II carboxyl-terminal domain independently of cyclin-dependent kinase-activating kinase. *J Biol Chem, 276*(15), 12317-12323.

Kim, K. H., Kim, W., Howard, T. P., Vazquez, F., Tsherniak, A., Wu, J. N., Wang, W., Haswell, J. R., Walensky, L. D., Hahn, W. C., Orkin, S. H., & Roberts, C. W. M. (2015). SWI/SNF-mutant cancers depend on catalytic and non-catalytic activity of EZH2. *Nature Medicine, 21*, 1491.

Kim, T.-K., Hemberg, M., Gray, J. M., Costa, A. M., Bear, D. M., Wu, J., Harmin, D. A., Laptewicz, M., Barbara-Haley, K., Kuersten, S., Markenscoff-Papadimitriou, E., Kuhl, D., Bito, H., Worley, P. F., Kreiman, G., & Greenberg, M. E. (2010). Widespread transcription at neuronal activity-regulated enhancers. *Nature, 465*, 182.

Kitano, M., Moriyama, S., Ando, Y., Hikida, M., Mori, Y., Kurosaki, T., & Okada, T. (2011). Bcl6 Protein Expression Shapes Pre-Germinal Center B Cell Dynamics and Follicular Helper T Cell Heterogeneity. *Immunity, 34*(6), 961-972.

Kito, K., Yeh, E. T. H., & Kamitani, T. (2001). NUB1, a NEDD8-interacting Protein, Is Induced by Interferon and Down-regulates the NEDD8 Expression. *Journal of Biological Chemistry, 276*(23), 20603-20609.

Kleer, C. G., Cao, Q., Varambally, S., Shen, R., Ota, I., Tomlins, S. A., Ghosh, D., Sewalt, R. G., Otte, A. P., Hayes, D. F., Sabel, M. S., Livant, D., Weiss, S. J., Rubin, M. A., & Chinnaiyan, A. M. (2003). EZH2 is a marker of aggressive breast cancer and promotes neoplastic transformation of breast epithelial cells. *Proc Natl Acad Sci U S A, 100*(20), 11606-11611.

Klein, U., Casola, S., Cattoretti, G., Shen, Q., Lia, M., Mo, T., Ludwig, T., Rajewsky, K., & Dalla-Favera, R. (2006). Transcription factor IRF4 controls plasma cell differentiation and class-switch recombination. *Nature Immunology, 7*, 773.

Knödel, M., Kuss, A. W., Berberich, I., & Schimpl, A. (2001). Blimp-1 over-expression abrogates IL-4- and CD40-mediated suppression of terminal B cell differentiation but arrests isotype switching. *European Journal of Immunology, 31*(7), 1972-1980.

Knutson, S. K., Kawano, S., Minoshima, Y., Warholic, N. M., Huang, K.-C., Xiao, Y., Kadowaki, T., Uesugi, M., Kuznetsov, G., Kumar, N., Wigle,

T. J., Klaus, C. R., Allain, C. J., Raimondi, A., Waters, N. J., Smith, J. J., Porter-Scott, M., Chesworth, R., Moyer, M. P., Copeland, R. A., Richon, V. M., Uenaka, T., Pollock, R. M., Kuntz, K. W., Yokoi, A., & Keilhack, H. (2014). Selective Inhibition of EZH2 by EPZ-6438 Leads to Potent Antitumor Activity in EZH2-Mutant Non-Hodgkin Lymphoma. *Molecular Cancer Therapeutics, 13*(4), 842.

Knutson, S. K., Wigle, T. J., Warholic, N. M., Sneeringer, C. J., Allain, C. J., Klaus, C. R., Sacks, J. D., Raimondi, A., Majer, C. R., Song, J., Scott, M. P., Jin, L., Smith, J. J., Olhava, E. J., Chesworth, R., Moyer, M. P., Richon, V. M., Copeland, R. A., Keilhack, H., Pollock, R. M., & Kuntz, K. W. (2012). A selective inhibitor of EZH2 blocks H3K27 methylation and kills mutant lymphoma cells. *Nature Chemical Biology, 8*, 890.

Kobayashi, M., Aida, M., Nagaoka, H., Begum, N. A., Kitawaki, Y., Nakata, M., Stanlie, A., Doi, T., Kato, L., Okazaki, I.-m., Shinkura, R., Muramatsu, M., Kinoshita, K., & Honjo, T. (2009). AID-induced decrease in topoisomerase 1 induces DNA structural alteration and DNA cleavage for class switch recombination. *Proceedings of the National Academy of Sciences, 106*(52), 22375.

Koch, F., Fenouil, R., Gut, M., Cauchy, P., Albert, T. K., Zacarias-Cabeza, J., Spicuglia, S., de la Chapelle, A. L., Heidemann, M., Hintermair, C., Eick, D., Gut, I., Ferrier, P., & Andrau, J.-C. (2011). Transcription initiation platforms and GTF recruitment at tissue-specific enhancers and promoters. *Nature Structural &Amp; Molecular Biology, 18*, 956.

Kolovos, P., Knoch, T. A., Grosveld, F. G., Cook, P. R., & Papantonis, A. (2012). Enhancers and silencers: an integrated and simple model for their function. *Epigenetics & Chromatin, 5*(1), 1.

Kondo, M., Weissman, I. L., & Akashi, K. (1997). Identification of clonogenic common lymphoid progenitors in mouse bone marrow. *Cell, 91*(5), 661-672.

Konoplev, S., Medeiros, L. J., Bueso-Ramos, C. E., Jorgensen, J. L., & Lin, P. (2005). Immunophenotypic profile of lymphoplasmacytic lymphoma/Waldenstrom macroglobulinemia. *Am J Clin Pathol, 124*(3), 414-420.

Koo, S. J., Fernandez-Montalvan, A. E., Badock, V., Ott, C. J., Holton, S. J., von Ahsen, O., Toedling, J., Vittori, S., Bradner, J. E., & Gorjanacz, M. (2016). ATAD2 is an epigenetic reader of newly synthesized histone marks during DNA replication. *Oncotarget, 7*(43), 70323-70335.

Kornberg, R. D. (1974). Chromatin Structure: A Repeating Unit of Histones and DNA. *Science, 184*(4139), 868-871.

Kouzine, F., Wojtowicz, D., Yamane, A., Resch, W., Kieffer-Kwon, K.-R., Bandle, R., Nelson, S., Nakahashi, H., Awasthi, P., Feigenbaum, L., Menoni, H., Hoeijmakers, J., Vermeulen, W., Ge, H., Przytycka, Teresa M., Levens, D., & Casellas, R. (2013). Global Regulation of Promoter Melting in Naive Lymphocytes. *Cell, 153*(5), 988-999.

Kuerbitz, S. J., Plunkett, B. S., Walsh, W. V., & Kastan, M. B. (1992). Wild-type p53 is a cell cycle checkpoint determinant following irradiation. *Proceedings of the National Academy of Sciences, 89*(16), 7491.

Kulakovskiy, I. V., Vorontsov, I. E., Yevshin, I. S., Sharipov, R. N., Fedorova, A. D., Rumynskiy, E. I., Medvedeva, Y. A., Magana-Mora, A., Bajic, V. B., Papatsenko, D. A., Kolpakov, F. A., & Makeev, V. J. (2018). HOCOMOCO: towards a complete collection of transcription factor binding models for human and mouse via large-scale ChIP-Seq analysis. *Nucleic acids research, 46*(D1), D252-D259.

Kumagai, A., & Dunphy, W. G. (1991). The cdc25 protein controls tyrosine dephosphorylation of the cdc2 protein in a cell-free system. *Cell, 64*(5), 903-914.

Kuo, T.-C. (2005). PhD thesis (Columbia University, NewYork).

Kuo, T. C., & Calame, K. L. (2004). B Lymphocyte-Induced Maturation Protein (Blimp)-1, IFN Regulatory Factor (IRF)-1, and IRF-2 Can Bind to the Same Regulatory Sites. *The Journal of Immunology, 173*(9), 5556.

Kurimoto, K., Yabuta, Y., Hayashi, K., Ohta, H., Kiyonari, H., Mitani, T., Moritoki, Y., Kohri, K., Kimura, H., Yamamoto, T., Katou, Y., Shirahige, K., & Saitou, M. (2015). Quantitative Dynamics of Chromatin Remodeling during Germ Cell Specification from Mouse Embryonic Stem Cells. *Cell Stem Cell, 16*(5), 517-532.

Kurland, J. F., & Tansey, W. P. (2008). Myc-Mediated Transcriptional Repression by Recruitment of Histone Deacetylase. *Cancer Research, 68*(10), 3624.

Kwasnieski, J. C., Fiore, C., Chaudhari, H. G., & Cohen, B. A. (2014). High-throughput functional testing of ENCODE segmentation predictions. *Genome Research, 24*(10), 1595-1602.

Kwon, H., Thierry-Mieg, D., Thierry-Mieg, J., Kim, H.-P., Oh, J., Tunyaplin, C., Carotta, S., Donovan, C. E., Goldman, M. L., Tailor, P., Ozato, K., Levy, D. E., Nutt, S. L., Calame, K., & Leonard, W. J. (2009). Analysis of Interleukin-21-Induced Prdm1 Gene Regulation Reveals Functional Cooperation of STAT3 and IRF4 Transcription Factors. *Immunity, 31*(6), 941-952.

Kwon, K., Hutter, C., Sun, Q., Bilic, I., Cobaleda, C., Malin, S., & Busslinger, M. (2008). Instructive Role of the Transcription Factor E2A in Early B Lymphopoiesis and Germinal Center B Cell Development. *Immunity, 28*(6), 751-762.

Kyle, R. A., Durie, B. G., Rajkumar, S. V., Landgren, O., Blade, J., Merlini, G., Kroger, N., Einsele, H., Vesole, D. H., Dimopoulos, M., San Miguel, J., Avet-Loiseau, H., Hajek, R., Chen, W. M., Anderson, K. C., Ludwig, H., Sonneveld, P., Pavlovsky, S., Palumbo, A., Richardson, P. G., Barlogie, B., Greipp, P., Vescio, R., Turesson, I., Westin, J., & Boccadoro, M. (2010). Monoclonal gammopathy of undetermined significance (MGUS) and smoldering (asymptomatic) multiple myeloma: IMWG consensus perspectives risk factors for progression and guidelines for monitoring and management. *Leukemia, 24*(6), 1121-1127.

Kyle, R. A., Gertz, M. A., Witzig, T. E., Lust, J. A., Lacy, M. Q., Dispenzieri, A., Fonseca, R., Rajkumar, S. V., Offord, J. R., Larson, D. R., Plevak, M. E., Therneau, T. M., & Greipp, P. R. (2003). Review of 1027 patients with newly diagnosed multiple myeloma. *Mayo Clin Proc, 78*(1), 21-33.

Kyle, R. A., Larson, D. R., Therneau, T. M., Dispenzieri, A., Kumar, S., Cerhan, J. R., & Rajkumar, S. V. (2018). Long-Term Follow-up of Monoclonal Gammopathy of Undetermined Significance. *New England Journal of Medicine, 378*(3), 241-249.

Kyle, R. A., Remstein, E. D., Therneau, T. M., Dispenzieri, A., Kurtin, P. J., Hodnefield, J. M., Larson, D. R., Plevak, M. F., Jelinek, D. F., Fonseca, R., Melton, L. J., 3rd, & Rajkumar, S. V. (2007). Clinical course and prognosis of smoldering (asymptomatic) multiple myeloma. *N Engl J Med, 356*(25), 2582-2590.

Kyriakou, C., Advani, R. H., Ansell, S. M., Buske, C., Castillo, J. J., Dreger, P., Gertz, M. A., Giralt, S. A., Leblond, V., Maloney, D. G., Tournilhac, O., & Montoto, S. (2017). Indications for Hematopoietic Stem Cell Transplantation in Patients with Waldenstroms Macroglobulinemia: A Consensus Project of the EBMT Lymphoma Working Party (LWP)/ European Consortium for Waldenstroms Macroglobulinemia (ECWM)/International Waldenstroms Macroglobulinemia Foundation (IWMF). *Blood, 130*(Suppl 1), 2026.

Labib, K., Tercero, J. A., & Diffley, J. F. X. (2000). Uninterrupted MCM2-7 Function Required for DNA Replication Fork Progression. *Science, 288*(5471), 1643.

Lai, F., Orom, U. A., Cesaroni, M., Beringer, M., Taatjes, D. J., Blobel, G. A., & Shiekhattar, R. (2013). Activating RNAs associate with Mediator to enhance chromatin architecture and transcription. *Nature, 494*, 497.

Lambert, S. A., Jolma, A., Campitelli, L. F., Das, P. K., Yin, Y., Albu, M., Chen, X., Taipale, J., Hughes, T. R., & Weirauch, M. T. (2018). The Human Transcription Factors. *Cell, 172*(4), 650-665.

Landgren, O., Kyle, R. A., Pfeiffer, R. M., Katzmann, J. A., Caporaso, N. E., Hayes, R. B., Dispenzieri, A., Kumar, S., Clark, R. J., Baris, D., Hoover, R., & Rajkumar, S. V. (2009). Monoclonal gammopathy of undetermined significance (MGUS) consistently precedes multiple myeloma: a prospective study. *Blood, 113*(22), 5412-5417.

Langmead, B., & Salzberg, S. L. (2012). Fast gapped-read alignment with Bowtie 2. *Nature Methods, 9*, 357.

Lanzavecchia, A. (1985). Antigen-specific interaction between T and B cells. *Nature, 314*(6011), 537.

Lara-Gonzalez, P., Westhorpe, Frederick G., & Taylor, Stephen S. (2012). The Spindle Assembly Checkpoint. *Current Biology, 22*(22), R966-R980.

Lawrence, D. W., & Kornbluth, J. (2016). E3 ubiquitin ligase NKLAM ubiquitinates STAT1 and positively regulates STAT1-mediated transcriptional activity. *Cellular Signalling, 28*(12), 1833-1841.

Le Gallou, S., Caron, G., Delaloy, C., Rossille, D., Tarte, K., & Fest, T. (2012). IL-2 Requirement for Human Plasma Cell Generation:

Coupling Differentiation and Proliferation by Enhancing MAPK–ERK Signaling. *The Journal of Immunology, 189*(1), 161.
LeBien, T. W., & Tedder, T. F. (2008). B lymphocytes: how they develop and function. *Blood, 112*(5), 1570-1580.
Lee, D. Y., Hayes, J. J., Pruss, D., & Wolffe, A. P. (1993). A positive role for histone acetylation in transcription factor access to nucleosomal DNA. *Cell, 72*(1), 73-84.
Leleu, X., Eeckhoute, J., Jia, X., Roccaro, A. M., Moreau, A.-S., Farag, M., Sacco, A., Ngo, H. T., Runnels, J., Melhem, M. R., Burwick, N., Azab, A., Azab, F., Hunter, Z., Hatjiharissi, E., Carrasco, D. R., Treon, S. P., Witzig, T. E., Hideshima, T., Brown, M., Anderson, K. C., & Ghobrial, I. M. (2008). Targeting NF-κB in Waldenstrom macroglobulinemia. *Blood, 111*(10), 5068.
Lemercier, C., Brocard, M.-P., Puvion-Dutilleul, F., Kao, H.-Y., Albagli, O., & Khochbin, S. (2002). Class II Histone Deacetylases Are Directly Recruited by BCL6 Transcriptional Repressor. *277*(24), 22045-22052.
Lenstra, T. L., Benschop, J. J., Kim, T., Schulze, J. M., Brabers, N. A., Margaritis, T., van de Pasch, L. A., van Heesch, S. A., Brok, M. O., Groot Koerkamp, M. J., Ko, C. W., van Leenen, D., Sameith, K., van Hooff, S. R., Lijnzaad, P., Kemmeren, P., Hentrich, T., Kobor, M. S., Buratowski, S., & Holstege, F. C. (2011). The specificity and topology of chromatin interaction pathways in yeast. *Mol Cell, 42*(4), 536-549.
Lenz, G., Davis, R. E., Ngo, V. N., Lam, L., George, T. C., Wright, G. W., Dave, S. S., Zhao, H., Xu, W., Rosenwald, A., Ott, G., Muller-Hermelink, H. K., Gascoyne, R. D., Connors, J. M., Rimsza, L. M., Campo, E., Jaffe, E. S., Delabie, J., Smeland, E. B., Fisher, R. I., Chan, W. C., & Staudt, L. M. (2008). Oncogenic CARD11 Mutations in Human Diffuse Large B Cell Lymphoma. *Science, 319*(5870), 1676.
Leung, T. H., Hoffmann, A., & Baltimore, D. (2004). One nucleotide in a kappaB site can determine cofactor specificity for NF-kappaB dimers. *Cell, 118*(4), 453-464.
Leung-Hagesteijn, C., Erdmann, N., Cheung, G., Keats, Jonathan J., Stewart, A. K., Reece, Donna E., Chung, Kim C., & Tiedemann, Rodger E. (2013). Xbp1s-Negative Tumor B Cells and Pre-Plasmablasts Mediate Therapeutic Proteasome Inhibitor Resistance in Multiple Myeloma. *Cancer Cell, 24*(3), 289-304.
Li, B., Carey, M., & Workman, J. L. (2007). The Role of Chromatin during Transcription. *Cell, 128*(4), 707-719.
Li, H., Handsaker, B., Wysoker, A., Fennell, T., Ruan, J., Homer, N., Marth, G., Abecasis, G., & Durbin, R. (2009). The Sequence Alignment/Map format and SAMtools. *Bioinformatics, 25*(16), 2078-2079.
Li, N., Johnson, D. C., Weinhold, N., Kimber, S., Dobbins, S. E., Mitchell, J. S., Kinnersley, B., Sud, A., Law, P. J., Orlando, G., Scales, M., Wardell, C. P., Försti, A., Hoang, P. H., Went, M., Holroyd, A., Hariri, F., Pastinen, T., Meissner, T., Goldschmidt, H., Hemminki, K., Morgan, G. J., Kaiser, M., & Houlston, R. S. (2017). Genetic

Predisposition to Multiple Myeloma at 5q15 Is Mediated by an ELL2 Enhancer Polymorphism. *Cell Reports, 20*(11), 2556-2564.
Li, P., Spolski, R., Liao, W., Wang, L., Murphy, T. L., Murphy, K. M., & Leonard, W. J. (2012). BATF–JUN is critical for IRF4-mediated transcription in T cells. *Nature, 490*, 543.
Liang, J., Zhang, Y., Jiang, G., Liu, Z., Xiang, W., Chen, X., Chen, Z., & Zhao, J. (2014). MiR-138 Induces Renal Carcinoma Cell Senescence by Targeting EZH2 and Is Downregulated in Human Clear Cell Renal Cell Carcinoma. *Oncology Research Featuring Preclinical and Clinical Cancer Therapeutics, 21*(2), 83-91.
Liberzon, A., Birger, C., Thorvaldsdottir, H., Ghandi, M., Mesirov, J. P., & Tamayo, P. (2015). The Molecular Signatures Database (MSigDB) hallmark gene set collection. *Cell Syst, 1*(6), 417-425.
Lieber, M. R. (2008). The Mechanism of Human Nonhomologous DNA End Joining. *Journal of Biological Chemistry, 283*(1), 1-5.
Lieber, M. R., & Karanjawala, Z. E. (2004). Ageing, repetitive genomes and DNA damage. *Nature Reviews Molecular Cell Biology, 5*, 69.
Lin, F.-R., Kuo, H.-K., Ying, H.-Y., Yang, F.-H., & Lin, K.-I. (2007). Induction of Apoptosis in Plasma Cells by B Lymphocyte–Induced Maturation Protein-1 Knockdown. *Cancer Research, 67*(24), 11914.
Lin, H., & Grosschedl, R. (1995). Failure of B-cell differentiation in mice lacking the transcription factor EBF. *Nature, 376*(6537), 263-267.
Lin, K.-I., Angelin-Duclos, C., Kuo, T. C., & Calame, K. (2002). Blimp-1-dependent repression of Pax-5 is required for differentiation of B cells to immunoglobulin M-secreting plasma cells. *Molecular and cellular biology, 22*(13), 4771-4780.
Lin, K.-I., Kao, Y.-Y., Kuo, H.-K., Yang, W.-B., Chou, A., Lin, H.-H., Yu, A. L., & Wong, C.-H. (2006). Reishi Polysaccharides Induce Immunoglobulin Production through the TLR4/TLR2-mediated Induction of Transcription Factor Blimp-1. *Journal of Biological Chemistry, 281*(34), 24111-24123.
Lin, S.-C., Lo, Y.-C., & Wu, H. (2010). Helical assembly in the MyD88–IRAK4–IRAK2 complex in TLR/IL-1R signalling. *Nature, 465*, 885.
Lin, Y., Wong, K.-k., & Calame, K. (1997). Repression of c-myc transcription by Blimp-1, an inducer of terminal B cell differentiation. *Science, 276*(5312), 596-599.
Lin, Y. C., Jhunjhunwala, S., Benner, C., Heinz, S., Welinder, E., Mansson, R., Sigvardsson, M., Hagman, J., Espinoza, C. A., Dutkowski, J., Ideker, T., Glass, C. K., & Murre, C. (2010). A global network of transcription factors, involving E2A, EBF1 and Foxo1, that orchestrates B cell fate. *Nat Immunol, 11*(7), 635-643.
Litman, R., Peng, M., Jin, Z., Zhang, F., Zhang, J., Powell, S., Andreassen, P. R., & Cantor, S. B. (2005). BACH1 is critical for homologous recombination and appears to be the Fanconi anemia gene product FANCJ. *Cancer Cell, 8*(3), 255-265.
Liu, D., Vader, G., Vromans, M. J. M., Lampson, M. A., & Lens, S. M. A. (2009). Sensing Chromosome Bi-Orientation by Spatial Separation of

Aurora B Kinase from Kinetochore Substrates. *Science, 323*(5919), 1350.
Liu, Q., Guntuku, S., Cui, X.-S., Matsuoka, S., Cortez, D., Tamai, K., Luo, G., Carattini-Rivera, S., DeMayo, F., Bradley, A., Donehower, L. A., & Elledge, S. J. (2000). Chk1 is an essential kinase that is regulated by Atr and required for the G2/M DNA damage checkpoint. *Genes & Development, 14*(12), 1448-1459.
Ljunggren, H.-G., & Kärre, K. (1990). In search of the 'missing self': MHC molecules and NK cell recognition. *Immunology today, 11*, 237-244.
Lohr, J. G., Stojanov, P., Carter, S. L., Cruz-Gordillo, P., Lawrence, M. S., Auclair, D., Sougnez, C., Knoechel, B., Gould, J., Saksena, G., Cibulskis, K., McKenna, A., Chapman, M. A., Straussman, R., Levy, J., Perkins, L. M., Keats, J. J., Schumacher, S. E., Rosenberg, M., Multiple Myeloma Research, C., Getz, G., & Golub, T. R. (2014). Widespread genetic heterogeneity in multiple myeloma: implications for targeted therapy. *Cancer cell, 25*(1), 91-101.
Lois, C., Hong, E. J., Pease, S., Brown, E. J., & Baltimore, D. (2002). Germline transmission and tissue-specific expression of transgenes delivered by lentiviral vectors. *Science, 295*(5556), 868-872.
Long, H. K., Prescott, S. L., & Wysocka, J. (2016). Ever-Changing Landscapes: Transcriptional Enhancers in Development and Evolution. *Cell, 167*(5), 1170-1187.
López-Corral, L., Gutiérrez, N. C., Vidriales, M. B., Mateos, M. V., Rasillo, A., García-Sanz, R., Paiva, B., & San Miguel, J. F. (2011). The Progression from MGUS to Smoldering Myeloma and Eventually to Multiple Myeloma Involves a Clonal Expansion of Genetically Abnormal Plasma Cells. *Clinical Cancer Research, 17*(7), 1692.
Lovén, J., Hoke, Heather A., Lin, Charles Y., Lau, A., Orlando, David A., Vakoc, Christopher R., Bradner, James E., Lee, Tong I., & Young, Richard A. (2013). Selective Inhibition of Tumor Oncogenes by Disruption of Super-Enhancers. *Cell, 153*(2), 320-334.
Lozano, E., Díaz, T., Mena, M.-P., Suñe, G., Calvo, X., Calderón, M., Pérez-Amill, L., Rodríguez, V., Pérez-Galán, P., & Roué, G. (2018). Loss of the Immune Checkpoint CD85j/LILRB1 on Malignant Plasma Cells Contributes to Immune Escape in Multiple Myeloma. *The Journal of Immunology*, ji1701622.
Lu, R., Medina, K. L., Lancki, D. W., & Singh, H. (2003). IRF-4,8 orchestrate the pre-B-to-B transition in lymphocyte development. *17*(14), 1703-1708.
Luger, K., Mäder, A. W., Richmond, R. K., Sargent, D. F., & Richmond, T. J. J. N. (1997). Crystal structure of the nucleosome core particle at 2.8 Å resolution. *389*(6648), 251.
Lukas, J., Parry, D., Aagaard, L., Mann, D. J., Bartkova, J., Strauss, M., Peters, G., & Bartek, J. (1995). Retinoblastoma-protein-dependent cell-cycle inhibition by the tumour suppressor p16. *Nature, 375*(6531), 503-506.

Luse, D. S. (2013). The RNA polymerase II preinitiation complex. Through what pathway is the complex assembled? *Transcription, 5*(1), e27050-e27050.

Ma, J., Gunderson, S. I., & Phillips, C. (2006). Non-snRNP U1A levels decrease during mammalian B-cell differentiation and release the IgM secretory poly(A) site from repression. *Rna, 12*(1), 122-132.

Machanick, P., & Bailey, T. L. (2011). MEME-ChIP: motif analysis of large DNA datasets. *Bioinformatics (Oxford, England), 27*(12), 1696-1697.

Mack, S. C., Pajtler, K. W., Chavez, L., Okonechnikov, K., Bertrand, K. C., Wang, X., Erkek, S., Federation, A., Song, A., Lee, C., Wang, X., McDonald, L., Morrow, J. J., Saiakhova, A., Sin-Chan, P., Wu, Q., Michaelraj, K. A., Miller, T. E., Hubert, C. G., Ryzhova, M., Garzia, L., Donovan, L., Dombrowski, S., Factor, D. C., Luu, B., Valentim, C. L. L., Gimple, R. C., Morton, A., Kim, L., Prager, B. C., Lee, J. J. Y., Wu, X., Zuccaro, J., Thompson, Y., Holgado, B. L., Reimand, J., Ke, S. Q., Tropper, A., Lai, S., Vijayarajah, S., Doan, S., Mahadev, V., Miñan, A. F., Gröbner, S. N., Lienhard, M., Zapatka, M., Huang, Z., Aldape, K. D., Carcaboso, A. M., Houghton, P. J., Keir, S. T., Milde, T., Witt, H., Li, Y., Li, C.-J., Bian, X.-W., Jones, D. T. W., Scott, I., Singh, S. K., Huang, A., Dirks, P. B., Bouffet, E., Bradner, J. E., Ramaswamy, V., Jabado, N., Rutka, J. T., Northcott, P. A., Lupien, M., Lichter, P., Korshunov, A., Scacheri, P. C., Pfister, S. M., Kool, M., Taylor, M. D., & Rich, J. N. (2017). Therapeutic targeting of ependymoma as informed by oncogenic enhancer profiling. *Nature, 553*, 101.

Magnúsdóttir, E., Dietmann, S., Murakami, K., Günesdogan, U., Tang, F., Bao, S., Diamanti, E., Lao, K., Gottgens, B., & Azim Surani, M. (2013). A tripartite transcription factor network regulates primordial germ cell specification in mice. *Nature Cell Biology, 15*, 905.

Magnúsdóttir, E., Kalachikov, S., Mizukoshi, K., Savitsky, D., Ishida-Yamamoto, A., Panteleyev, A. A., & Calame, K. (2007). Epidermal terminal differentiation depends on B lymphocyte-induced maturation protein-1. *Proceedings of the National Academy of Sciences, 104*(38), 14988.

Mandelbaum, J., Bhagat, G., Tang, H., Mo, T., Brahmachary, M., Shen, Q., Chadburn, A., Rajewsky, K., Tarakhovsky, A., Pasqualucci, L., & Dalla-Favera, R. (2010). BLIMP1 is a Tumor Suppressor Gene Frequently Disrupted in Activated B Cell-like Diffuse Large B Cell Lymphoma. *Cancer cell, 18*(6), 568-579.

Margueron, R., Li, G., Sarma, K., Blais, A., Zavadil, J., Woodcock, C. L., Dynlacht, B. D., & Reinberg, D. (2008). Ezh1 and Ezh2 Maintain Repressive Chromatin through Different Mechanisms. *Molecular Cell, 32*(4), 503-518.

Martincic, K., Alkan, S. A., Cheatle, A., Borghesi, L., & Milcarek, C. (2009). Transcription elongation factor ELL2 directs immunoglobulin secretion in plasma cells by stimulating altered RNA processing. *Nature Immunology, 10*, 1102.

Martínez-Calle, N., Pascual, M., Ordoñez, R., San José-Enériz, E., Kulis, M., Miranda, E., Guruceaga, E., Segura, V., Larráyoz, M. J., Bellosillo, B., Calasanz, M. J., Besses, C., Rifón, J., Martín-Subero, J. I., Agirre, X., & Prosper, F. (2019). Epigenomic profiling of myelofibrosis reveals widespread DNA methylation changes in enhancer elements and ZFP36L1 as a potential tumor suppressor gene epigenetically regulated. *Haematologica*, haematol.2018.204917.

Mateos-Gomez, P. A., Gong, F., Nair, N., Miller, K. M., Lazzerini-Denchi, E., & Sfeir, A. (2015). Mammalian polymerase θ promotes alternative NHEJ and suppresses recombination. *Nature, 518*, 254.

Mathieu-Daude, F., Welsh, J., Vogt, T., & McClelland, M. (1996). DNA rehybridization during PCR: the 'Cot effect' and its consequences. *Nucleic Acids Res, 24*(11), 2080-2086.

Matsui, T., Segall, J., Weil, P. A., & Roeder, R. G. (1980). Multiple factors required for accurate initiation of transcription by purified RNA polymerase II. *Journal of Biological Chemistry, 255*(24), 11992-11996.

Matsuoka, S., Huang, M., & Elledge, S. J. (1998). Linkage of ATM to Cell Cycle Regulation by the Chk2 Protein Kinase. *Science, 282*(5395), 1893.

Maul, R. W., Saribasak, H., Martomo, S. A., McClure, R. L., Yang, W., Vaisman, A., Gramlich, H. S., Schatz, D. G., Woodgate, R., Wilson, D. M., 3rd, & Gearhart, P. J. (2011). Uracil residues dependent on the deaminase AID in immunoglobulin gene variable and switch regions. *Nat Immunol, 12*(1), 70-76.

McBlane, J. F., van Gent, D. C., Ramsden, D. A., Romeo, C., Cuomo, C. A., Gellert, M., & Oettinger, M. A. (1995). Cleavage at a V(D)J recombination signal requires only RAG1 and RAG2 proteins and occurs in two steps. *Cell, 83*(3), 387-395.

McCabe, M. T., Graves, A. P., Ganji, G., Diaz, E., Halsey, W. S., Jiang, Y., Smitheman, K. N., Ott, H. M., Pappalardi, M. B., Allen, K. E., Chen, S. B., Della Pietra, A., Dul, E., Hughes, A. M., Gilbert, S. A., Thrall, S. H., Tummino, P. J., Kruger, R. G., Brandt, M., Schwartz, B., & Creasy, C. L. (2012a). Mutation of A677 in histone methyltransferase EZH2 in human B-cell lymphoma promotes hypertrimethylation of histone H3 on lysine 27 (H3K27). *Proceedings of the National Academy of Sciences, 109*(8), 2989.

McCabe, M. T., Ott, H. M., Ganji, G., Korenchuk, S., Thompson, C., Van Aller, G. S., Liu, Y., Graves, A. P., Iii, A. D. P., Diaz, E., LaFrance, L. V., Mellinger, M., Duquenne, C., Tian, X., Kruger, R. G., McHugh, C. F., Brandt, M., Miller, W. H., Dhanak, D., Verma, S. K., Tummino, P. J., & Creasy, C. L. (2012b). EZH2 inhibition as a therapeutic strategy for lymphoma with EZH2-activating mutations. *Nature, 492*, 108.

McMaster, M. L., Berndt, S. I., Zhang, J., Slager, S. L., Li, S. A., Vajdic, C. M., Smedby, K. E., Yan, H., Birmann, B. M., Brown, E. E., Smith, A., Kleinstern, G., Fansler, M. M., Mayr, C., Zhu, B., Chung, C. C., Park, J.-H., Burdette, L., Hicks, B. D., Hutchinson, A., Teras, L. R., Adami, H.-O., Bracci, P. M., McKay, J., Monnereau, A., Link, B. K.,

Vermeulen, R. C. H., Ansell, S. M., Maria, A., Diver, W. R., Melbye, M., Ojesina, A. I., Kraft, P., Boffetta, P., Clavel, J., Giovannucci, E., Besson, C. M., Canzian, F., Travis, R. C., Vineis, P., Weiderpass, E., Montalvan, R., Wang, Z., Yeager, M., Becker, N., Benavente, Y., Brennan, P., Foretova, L., Maynadie, M., Nieters, A., de Sanjose, S., Staines, A., Conde, L., Riby, J., Glimelius, B., Hjalgrim, H., Pradhan, N., Feldman, A. L., Novak, A. J., Lawrence, C., Bassig, B. A., Lan, Q., Zheng, T., North, K. E., Tinker, L. F., Cozen, W., Severson, R. K., Hofmann, J. N., Zhang, Y., Jackson, R. D., Morton, L. M., Purdue, M. P., Chatterjee, N., Offit, K., Cerhan, J. R., Chanock, S. J., Rothman, N., Vijai, J., Goldin, L. R., Skibola, C. F., & Caporaso, N. E. (2018). Two high-risk susceptibility loci at 6p25.3 and 14q32.13 for Waldenström macroglobulinemia. *Nature Communications, 9*(1), 4182.

Medvedovic, J., Ebert, A., Tagoh, H., Tamir, Ido M., Schwickert, T. A., Novatchkova, M., Sun, Q., Huis in 't Veld, Pim J., Guo, C., Yoon, Hye S., Denizot, Y., Holwerda, Sjoerd J. B., de Laat, W., Cogné, M., Shi, Y., Alt, Frederick W., & Busslinger, M. (2013). Flexible Long-Range Loops in the VH Gene Region of the Igh Locus Facilitate the Generation of a Diverse Antibody Repertoire. *Immunity, 39*(2), 229-244.

Medzhitov, R., Preston-Hurlburt, P., Kopp, E., Stadlen, A., Chen, C., Ghosh, S., & Janeway, C. A. (1998). MyD88 Is an Adaptor Protein in the hToll/IL-1 Receptor Family Signaling Pathways. *Molecular Cell, 2*(2), 253-258.

Meijsing, S. H., Pufall, M. A., So, A. Y., Bates, D. L., Chen, L., & Yamamoto, K. R. (2009). DNA binding site sequence directs glucocorticoid receptor structure and activity. *Science (New York, NY), 324*(5925), 407-410.

Meister, S., Schubert, U., Neubert, K., Herrmann, K., Burger, R., Gramatzki, M., Hahn, S., Schreiber, S., Wilhelm, S., Herrmann, M., Jäck, H.-M., & Voll, R. E. (2007). Extensive Immunoglobulin Production Sensitizes Myeloma Cells for Proteasome Inhibition. *Cancer Research, 67*(4), 1783.

Melchers, F., Ten Boekel, E., Seidl, T., Kong, X. C., Yamagami, T., Onishi, K., Shimizu, T., Rolink, A. G., & Andersson, J. (2000). Repertoire selection by pre-B-cell receptors and B-cell receptors, and genetic control of B-cell development from immature to mature B cells. *Immunological Reviews, 175*(1), 33-46.

Mello, J. A., Silljé, H. H. W., Roche, D. M. J., Kirschner, D. B., Nigg, E. A., & Almouzni, G. (2002). Human Asf1 and CAF - 1 interact and synergize in a repair - coupled nucleosome assembly pathway. *EMBO reports, 3*(4), 329.

Méndez, J., & Stillman, B. (2000). Chromatin Association of Human Origin Recognition Complex, Cdc6, and Minichromosome Maintenance Proteins during the Cell Cycle: Assembly of Prereplication Complexes in Late Mitosis. *Molecular and Cellular Biology, 20*(22), 8602.

Mendez, L. M., Polo, J. M., Yu, J. J., Krupski, M., Ding, B. B., Melnick, A., & Ye, B. H. (2008). CtBP is an essential corepressor for BCL6 autoregulation. *Mol Cell Biol, 28*(7), 2175-2186.

Mercer, E. M., Lin, Y. C., Benner, C., Jhunjhunwala, S., Dutkowski, J., Flores, M., Sigvardsson, M., Ideker, T., Glass, C. K., & Murre, C. (2011). Multilineage priming of enhancer repertoires precedes commitment to the B and myeloid cell lineages in hematopoietic progenitors. *Immunity, 35*(3), 413-425.

Messika, E. J., Lu, P. S., Sung, Y.-J., Yao, T., Chi, J.-T., Chien, Y.-h., & Davis, M. M. (1998). Differential Effect of B Lymphocyte–induced Maturation Protein (Blimp-1) Expression on Cell Fate during B Cell Development. *The Journal of Experimental Medicine, 188*(3), 515.

Messika, E. J., Lu, P. S., Sung, Y. J., Yao, T., Chi, J. T., Chien, Y. H., & Davis, M. M. (1998). Differential effect of B lymphocyte-induced maturation protein (Blimp-1) expression on cell fate during B cell development. *J Exp Med, 188*(3), 515-525.

Methot, S. P., & Di Noia, J. M. (2017). Molecular Mechanisms of Somatic Hypermutation and Class Switch Recombination. *Adv Immunol, 133*, 37-87.

Mikhaylichenko, O., Bondarenko, V., Harnett, D., Schor, I. E., Males, M., Viales, R. R., & Furlong, E. E. M. (2018). The degree of enhancer or promoter activity is reflected by the levels and directionality of eRNA transcription. *Genes & development, 32*(1), 42-57.

Mimitou, E. P., & Symington, L. S. (2008). Sae2, Exo1 and Sgs1 collaborate in DNA double-strand break processing. *Nature, 455*, 770.

Minnich, M., Tagoh, H., Bönelt, P., Axelsson, E., Fischer, M., Cebolla, B., Tarakhovsky, A., Nutt, S. L., Jaritz, M., & Busslinger, M. (2016). Multifunctional role of the transcription factor Blimp-1 in coordinating plasma cell differentiation. *Nature Immunology, 17*, 331.

Mirny, L. A. (2010). Nucleosome-mediated cooperativity between transcription factors. *Proceedings of the National Academy of Sciences, 107*(52), 22534.

Mizzen, C. A., Yang, X.-J., Kokubo, T., Brownell, J. E., Bannister, A. J., Owen-Hughes, T., Workman, J., Wang, L., Berger, S. L., Kouzarides, T., Nakatani, Y., & Allis, C. D. (1996). The TAFII250 Subunit of TFIID Has Histone Acetyltransferase Activity. *Cell, 87*(7), 1261-1270.

Montgomery, N. D., Yee, D., Chen, A., Kalantry, S., Chamberlain, S. J., Otte, A. P., & Magnuson, T. (2005). The murine polycomb group protein Eed is required for global histone H3 lysine-27 methylation. *Curr Biol, 15*(10), 942-947.

Monti, S., Chapuy, B., Takeyama, K., Rodig, Scott J., Hao, Y., Yeda, Kelly T., Inguilizian, H., Mermel, C., Currie, T., Dogan, A., Kutok, Jeffery L., Beroukhim, R., Neuberg, D., Habermann, Thomas M., Getz, G., Kung, Andrew L., Golub, Todd R., & Shipp, Margaret A. (2012). Integrative Analysis Reveals an Outcome-Associated and Targetable Pattern of p53 and Cell Cycle Deregulation in Diffuse Large B Cell Lymphoma. *Cancer Cell, 22*(3), 359-372.

Mora-López, F., Reales, E., Brieva, J. A., & Campos-Caro, A. (2007). Human BSAP and BLIMP1 conform an autoregulatory feedback loop. *Blood, 110*(9), 3150.

Morgan, M. A. J., Magnusdottir, E., Kuo, T. C., Tunyaplin, C., Harper, J., Arnold, S. J., Calame, K., Robertson, E. J., & Bikoff, E. K. (2009). Blimp-1/Prdm1 Alternative Promoter Usage during Mouse Development and Plasma Cell Differentiation. *Molecular and Cellular Biology, 29*(21), 5813.

Mori, D., Yano, Y., Toyo-oka, K., Yoshida, N., Yamada, M., Muramatsu, M., Zhang, D., Saya, H., Toyoshima, Y. Y., Kinoshita, K., Wynshaw-Boris, A., & Hirotsune, S. (2007). NDEL1 phosphorylation by Aurora-A kinase is essential for centrosomal maturation, separation, and TACC3 recruitment. *Mol Cell Biol, 27*(1), 352-367.

Morin, R. D., Johnson, N. A., Severson, T. M., Mungall, A. J., An, J., Goya, R., Paul, J. E., Boyle, M., Woolcock, B. W., Kuchenbauer, F., Yap, D., Humphries, R. K., Griffith, O. L., Shah, S., Zhu, H., Kimbara, M., Shashkin, P., Charlot, J. F., Tcherpakov, M., Corbett, R., Tam, A., Varhol, R., Smailus, D., Moksa, M., Zhao, Y., Delaney, A., Qian, H., Birol, I., Schein, J., Moore, R., Holt, R., Horsman, D. E., Connors, J. M., Jones, S., Aparicio, S., Hirst, M., Gascoyne, R. D., & Marra, M. A. (2010). Somatic mutations altering EZH2 (Tyr641) in follicular and diffuse large B-cell lymphomas of germinal-center origin. *Nature genetics, 42*(2), 181-185.

Morin, R. D., Mendez-Lago, M., Mungall, A. J., Goya, R., Mungall, K. L., Corbett, R. D., Johnson, N. A., Severson, T. M., Chiu, R., Field, M., Jackman, S., Krzywinski, M., Scott, D. W., Trinh, D. L., Tamura-Wells, J., Li, S., Firme, M. R., Rogic, S., Griffith, M., Chan, S., Yakovenko, O., Meyer, I. M., Zhao, E. Y., Smailus, D., Moksa, M., Chittaranjan, S., Rimsza, L., Brooks-Wilson, A., Spinelli, J. J., Ben-Neriah, S., Meissner, B., Woolcock, B., Boyle, M., McDonald, H., Tam, A., Zhao, Y., Delaney, A., Zeng, T., Tse, K., Butterfield, Y., Birol, I., Holt, R., Schein, J., Horsman, D. E., Moore, R., Jones, S. J., Connors, J. M., Hirst, M., Gascoyne, R. D., & Marra, M. A. (2011). Frequent mutation of histone-modifying genes in non-Hodgkin lymphoma. *Nature, 476*(7360), 298-303.

Morvan, M. G., & Lanier, L. L. (2015). NK cells and cancer: you can teach innate cells new tricks. *Nature Reviews Cancer, 16*, 7.

Mostoslavsky, R., Singh, N., Tenzen, T., Goldmit, M., Gabay, C., Elizur, S., Qi, P., Reubinoff, B. E., Chess, A., Cedar, H., & Bergman, Y. (2001). Asynchronous replication and allelic exclusion in the immune system. *Nature, 414*(6860), 221-225.

Mould, A. W., Morgan, M. A. J., Nelson, A. C., Bikoff, E. K., & Robertson, E. J. (2015). Blimp1/Prdm1 Functions in Opposition to Irf1 to Maintain Neonatal Tolerance during Postnatal Intestinal Maturation. *PLOS Genetics, 11*(7), e1005375.

Mueller, P. R., Coleman, T. R., Kumagai, A., & Dunphy, W. G. (1995). Myt1: A Membrane-Associated Inhibitory Kinase That Phosphorylates Cdc2 on Both Threonine-14 and Tyrosine-15. *Science, 270*(5233), 86.

Mulero, M. C., Aubareda, A., Schlüter, A., & Pérez-Riba, M. (2007). RCAN3, a novel calcineurin inhibitor that down-regulates NFAT-dependent cytokine gene expression. *Biochimica et Biophysica Acta (BBA) - Molecular Cell Research, 1773*(3), 330-341.

Mundy, G. R., Raisz, L. G., Cooper, R. A., Schechter, G. P., & Salmon, S. E. (1974). Evidence for the Secretion of an Osteoclast Stimulating Factor in Myeloma. *New England Journal of Medicine, 291*(20), 1041-1046.

Muramatsu, M., Kinoshita, K., Fagarasan, S., Yamada, S., Shinkai, Y., & Honjo, T. (2000). Class Switch Recombination and Hypermutation Require Activation-Induced Cytidine Deaminase (AID), a Potential RNA Editing Enzyme. *Cell, 102*(5), 553-563.

Muto, A., Tashiro, S., Nakajima, O., Hoshino, H., Takahashi, S., Sakoda, E., Ikebe, D., Yamamoto, M., & Igarashi, K. (2004). The transcriptional programme of antibody class switching involves the repressor Bach2. *Nature, 429*(6991), 566-571.

Muzio, M., Ni, J., Feng, P., & Dixit, V. M. (1997). IRAK (Pelle) Family Member IRAK-2 and MyD88 as Proximal Mediators of IL-1 Signaling. *Science, 278*(5343), 1612.

Näär, A. M., Boutin, J.-M., Lipkin, S. M., Yu, V. C., Holloway, J. M., Glass, C. K., & Rosenfeld, M. G. (1991). The orientation and spacing of core DNA-binding motifs dictate selective transcriptional responses to three nuclear receptors. *Cell, 65*(7), 1267-1279.

Nagy, M., Chapuis, B., & Matthes, T. (2002). Expression of transcription factors Pu.1, Spi-B, Blimp-1, BSAP and oct-2 in normal human plasma cells and in multiple myeloma cells. *British Journal of Haematology, 116*(2), 429-435.

Nambu, Y., Sugai, M., Gonda, H., Lee, C.-G., Katakai, T., Agata, Y., Yokota, Y., & Shimizu, A. (2003). Transcription-Coupled Events Associating with Immunoglobulin Switch Region Chromatin. *Science, 302*(5653), 2137.

Nasir, A., Norton, J. D., Baou, M., Zekavati, A., Bijlmakers, M.-J., Thompson, S., & Murphy, J. J. (2012). ZFP36L1 Negatively Regulates Plasmacytoid Differentiation of BCL1 Cells by Targeting BLIMP1 mRNA. *PLOS ONE, 7*(12), e52187.

Nera, K.-P., Kohonen, P., Narvi, E., Peippo, A., Mustonen, L., Terho, P., Koskela, K., Buerstedde, J.-M., & Lassila, O. (2006). Loss of Pax5 Promotes Plasma Cell Differentiation. *Immunity, 24*(3), 283-293.

Ng, J.-H., Kumar, V., Muratani, M., Kraus, P., Yeo, J.-C., Yaw, L.-P., Xue, K., Lufkin, T., Prabhakar, S., & Ng, H.-H. (2013). In Vivo Epigenomic Profiling of Germ Cells Reveals Germ Cell Molecular Signatures. *Developmental Cell, 24*(3), 324-333.

Ngo, V. N., Young, R. M., Schmitz, R., Jhavar, S., Xiao, W., Lim, K.-H., Kohlhammer, H., Xu, W., Yang, Y., Zhao, H., Shaffer, A. L., Romesser, P., Wright, G., Powell, J., Rosenwald, A., Muller-Hermelink, H. K., Ott, G., Gascoyne, R. D., Connors, J. M., Rimsza, L. M., Campo, E., Jaffe, E. S., Delabie, J., Smeland, E. B., Fisher, R. I., Braziel, R. M., Tubbs, R. R., Cook, J. R., Weisenburger, D. D.,

Chan, W. C., & Staudt, L. M. (2010). Oncogenically active MYD88 mutations in human lymphoma. *Nature, 470*, 115.
Nie, Z., Hu, G., Wei, G., Cui, K., Yamane, A., Resch, W., Wang, R., Green, Douglas R., Tessarollo, L., Casellas, R., Zhao, K., & Levens, D. (2012). c-Myc Is a Universal Amplifier of Expressed Genes in Lymphocytes and Embryonic Stem Cells. *Cell, 151*(1), 68-79.
Nowak, D. E., Tian, B., Jamaluddin, M., Boldogh, I., Vergara, L. A., Choudhary, S., & Brasier, A. R. (2008). RelA Ser276 Phosphorylation Is Required for Activation of a Subset of NF-κB-Dependent Genes by Recruiting Cyclin-Dependent Kinase 9/Cyclin T1 Complexes. *Molecular and Cellular Biology, 28*(11), 3623.
Nutt, S. L., Fairfax, K. A., & Kallies, A. (2007). BLIMP1 guides the fate of effector B and T cells. *Nature Reviews Immunology, 7*, 923.
Nutt, S. L., Heavey, B., Rolink, A. G., & Busslinger, M. (1999). Commitment to the B-lymphoid lineage depends on the transcription factor Pax5. *Nature, 401*, 556.
Nutt, S. L., Hodgkin, P. D., Tarlinton, D. M., & Corcoran, L. M. (2015). The generation of antibody-secreting plasma cells. *Nature Reviews Immunology, 15*, 160.
O'Neill, L. A. J., & Bowie, A. G. (2007). The family of five: TIR-domain-containing adaptors in Toll-like receptor signalling. *Nature Reviews Immunology, 7*, 353.
Ochiai, K., Katoh, Y., Ikura, T., Hoshikawa, Y., Noda, T., Karasuyama, H., Tashiro, S., Muto, A., & Igarashi, K. (2006). Plasmacytic Transcription Factor Blimp-1 Is Repressed by Bach2 in B Cells. *Journal of Biological Chemistry, 281*(50), 38226-38234.
Ochiai, K., Maienschein-Cline, M., Simonetti, G., Chen, J., Rosenthal, R., Brink, R., Chong, A. S., Klein, U., Dinner, A. R., Singh, H., & Sciammas, R. (2013). Transcriptional regulation of germinal center B and plasma cell fates by dynamical control of IRF4. *Immunity, 38*(5), 918-929.
Oettinger, M. A., Schatz, D. G., Gorka, C., & Baltimore, D. (1990). RAG-1 and RAG-2, adjacent genes that synergistically activate V(D)J recombination. *Science, 248*(4962), 1517.
Ohguchi, H., Hideshima, T., Bhasin, M. K., Gorgun, G. T., Santo, L., Cea, M., Samur, M. K., Mimura, N., Suzuki, R., Tai, Y.-T., Carrasco, R. D., Raje, N., Richardson, P. G., Munshi, N. C., Harigae, H., Sanda, T., Sakai, J., & Anderson, K. C. (2016). The KDM3A–KLF2–IRF4 axis maintains myeloma cell survival. *Nature Communications, 7*, 10258.
Ohinata, Y., Payer, B., O'carroll, D., Ancelin, K., Ono, Y., Sano, M., Barton, S. C., Obukhanych, T., Nussenzweig, M., & Tarakhovsky, A. (2005). Blimp1 is a critical determinant of the germ cell lineage in mice. *Nature, 436*(7048), 207.
Ooi, W. F., Xing, M., Xu, C., Yao, X., Ramlee, M. K., Lim, M. C., Cao, F., Lim, K., Babu, D., Poon, L.-F., Lin Suling, J., Qamra, A., Irwanto, A., Qu Zhengzhong, J., Nandi, T., Lee-Lim, A. P., Chan, Y. S., Tay, S. T., Lee, M. H., Davies, J. O. J., Wong, W. K., Soo, K. C., Chan, W. H., Ong, H. S., Chow, P., Wong, C. Y., Rha, S. Y., Liu, J., Hillmer, A. M.,

Hughes, J. R., Rozen, S., Teh, B. T., Fullwood, M. J., Li, S., & Tan, P. (2016). Epigenomic profiling of primary gastric adenocarcinoma reveals super-enhancer heterogeneity. *Nature Communications, 7*, 12983.

Osterwalder, M., Barozzi, I., Tissières, V., Fukuda-Yuzawa, Y., Mannion, B. J., Afzal, S. Y., Lee, E. A., Zhu, Y., Plajzer-Frick, I., Pickle, C. S., Kato, M., Garvin, T. H., Pham, Q. T., Harrington, A. N., Akiyama, J. A., Afzal, V., Lopez-Rios, J., Dickel, D. E., Visel, A., & Pennacchio, L. A. (2018). Enhancer redundancy provides phenotypic robustness in mammalian development. *Nature, 554*, 239.

Otto, T., & Sicinski, P. (2017). Cell cycle proteins as promising targets in cancer therapy. *Nature Reviews Cancer, 17*, 93.

Ozaki, K., Spolski, R., Ettinger, R., Kim, H.-P., Wang, G., Qi, C.-F., Hwu, P., Shaffer, D. J., Akilesh, S., Roopenian, D. C., Morse, H. C., Lipsky, P. E., & Leonard, W. J. (2004). Regulation of B Cell Differentiation and Plasma Cell Generation by IL-21, a Novel Inducer of Blimp-1 and Bcl-6. *The Journal of Immunology, 173*(9), 5361.

Paiva, B., Corchete, L. A., Vidriales, M.-B., García-Sanz, R., Perez, J. J., Aires-Mejia, I., Sanchez, M.-L., Barcena, P., Alignani, D., Jimenez, C., Sarasquete, M.-E., Mateos, M.-V., Ocio, E. M., Puig, N., Escalante, F., Hernández, J., Cuello, R., García de Coca, A., Sierra, M., Montes, M.-C., González-López, T. J., Galende, J., Bárez, A., Alonso, J., Pardal, E., Orfao, A., Gutierrez, N. C., & San Miguel, J. F. (2015). The cellular origin and malignant transformation of Waldenström macroglobulinemia. *Blood, 125*(15), 2370.

Pan, L., Sato, S., Frederick, J. P., Sun, X.-H., & Zhuang, Y. (1999). Impaired Immune Responses and B-Cell Proliferation in Mice Lacking the Id3 Gene. *Molecular and Cellular Biology, 19*(9), 5969.

Pardoll, D. M. (2012). The blockade of immune checkpoints in cancer immunotherapy. *Nature Reviews Cancer, 12*, 252.

Parker, C. S., & Topol, J. (1984). A Drosophila RNA polymerase II transcription factor contains a promoter-region-specific DNA-binding activity. *Cell, 36*(2), 357-369.

Parker, M. J., Licence, S., Erlandsson, L., Galler, G. R., Chakalova, L., Osborne, C. S., Morgan, G., Fraser, P., Jumaa, H., Winkler, T. H., Skok, J., & Mårtensson, I. L. (2005). The pre - B - cell receptor induces silencing of VpreB and λ5 transcription. *The EMBO Journal, 24*(22), 3895.

Pasare, C., & Medzhitov, R. (2005). Control of B-cell responses by Toll-like receptors. *Nature, 438*, 364.

Pasini, D., Bracken, A. P., Jensen, M. R., Denchi, E. L., & Helin, K. (2004). Suz12 is essential for mouse development and for EZH2 histone methyltransferase activity. *The EMBO Journal, 23*(20), 4061.

Pasqualucci, L., Compagno, M., Houldsworth, J., Monti, S., Grunn, A., Nandula, S. V., Aster, J. C., Murty, V. V., Shipp, M. A., & Dalla-Favera, R. (2006). Inactivation of the PRDM1/BLIMP1 gene in diffuse

large B cell lymphoma. *The Journal of Experimental Medicine, 203*(2), 311.
Pasqualucci, L., Dominguez-Sola, D., Chiarenza, A., Fabbri, G., Grunn, A., Trifonov, V., Kasper, L. H., Lerach, S., Tang, H., Ma, J., Rossi, D., Chadburn, A., Murty, V. V., Mullighan, C. G., Gaidano, G., Rabadan, R., Brindle, P. K., & Dalla-Favera, R. (2011a). Inactivating mutations of acetyltransferase genes in B-cell lymphoma. *Nature, 471*, 189.
Pasqualucci, L., Trifonov, V., Fabbri, G., Ma, J., Rossi, D., Chiarenza, A., Wells, V. A., Grunn, A., Messina, M., Elliot, O., Chan, J., Bhagat, G., Chadburn, A., Gaidano, G., Mullighan, C. G., Rabadan, R., & Dalla-Favera, R. (2011b). Analysis of the coding genome of diffuse large B-cell lymphoma. *Nature Genetics, 43*, 830.
Pavri, R., Gazumyan, A., Jankovic, M., Di Virgilio, M., Klein, I., Ansarah-Sobrinho, C., Resch, W., Yamane, A., San-Martin, B. R., Barreto, V., Nieland, T. J., Root, D. E., Casellas, R., & Nussenzweig, M. C. (2010). Activation-Induced Cytidine Deaminase Targets DNA at Sites of RNA Polymerase II Stalling by Interaction with Spt5. *Cell, 143*(1), 122-133.
Pawlyn, C., Bright, M. D., Buros, A. F., Stein, C. K., Walters, Z., Aronson, L. I., Mirabella, F., Jones, J. R., Kaiser, M. F., Walker, B. A., Jackson, G. H., Clarke, P. A., Bergsagel, P. L., Workman, P., Chesi, M., Morgan, G. J., & Davies, F. E. (2017). Overexpression of EZH2 in multiple myeloma is associated with poor prognosis and dysregulation of cell cycle control. *Blood Cancer Journal, 7*, e549.
Perera, D., Tilston, V., Hopwood, J. A., Barchi, M., Boot-Handford, R. P., & Taylor, Stephen S. (2007). Bub1 Maintains Centromeric Cohesion by Activation of the Spindle Checkpoint. *Developmental Cell, 13*(4), 566-579.
Perkel, J. M., & Atchison, M. L. (1998). A Two-Step Mechanism for Recruitment of Pip by PU.1. *The Journal of Immunology, 160*(1), 241.
Pesenti, M. E., Prumbaum, D., Auckland, P., Smith, C. M., Faesen, A. C., Petrovic, A., Erent, M., Maffini, S., Pentakota, S., Weir, J. R., Lin, Y. C., Raunser, S., McAinsh, A. D., & Musacchio, A. (2018). Reconstitution of a 26-Subunit Human Kinetochore Reveals Cooperative Microtubule Binding by CENP-OPQUR and NDC80. *Mol Cell, 71*(6), 923-939.e910.
Peterson, C. L., & Laniel, M.-A. J. C. B. (2004). Histones and histone modifications. *14*(14), R546-R551.
Peterson, M. L., & Perry, R. P. (1989). The regulated production of mu m and mu s mRNA is dependent on the relative efficiencies of mu s poly(A) site usage and the c mu 4-to-M1 splice. *Molecular and Cellular Biology, 9*(2), 726.
Petrenko, N., Jin, Y., Dong, L., Wong, K. H., & Struhl, K. (2019). Requirements for RNA polymerase II preinitiation complex formation in vivo. *eLife, 8*, e43654.
Pfaffl, M. W. (2001). A new mathematical model for relative quantification in real-time RT–PCR. *Nucleic Acids Research, 29*(9), e45-e45.

Pham, A.-D., & Sauer, F. (2000). Ubiquitin-Activating/Conjugating Activity of TAFII250, a Mediator of Activation of Gene Expression in Drosophila. *Science, 289*(5488), 2357.

Phan, R. T., & Dalla-Favera, R. (2004). The BCL6 proto-oncogene suppresses p53 expression in germinal-centre B cells. *Nature, 432*(7017), 635-639.

Phan, R. T., Saito, M., Basso, K., Niu, H., & Dalla-Favera, R. (2005). BCL6 interacts with the transcription factor Miz-1 to suppress the cyclin-dependent kinase inhibitor p21 and cell cycle arrest in germinal center B cells. *Nature Immunology, 6*, 1054.

Phelan, J. D., Young, R. M., Webster, D. E., Roulland, S., Wright, G. W., Kasbekar, M., Shaffer, A. L., Ceribelli, M., Wang, J. Q., Schmitz, R., Nakagawa, M., Bachy, E., Huang, D. W., Ji, Y., Chen, L., Yang, Y., Zhao, H., Yu, X., Xu, W., Palisoc, M. M., Valadez, R. R., Davies-Hill, T., Wilson, W. H., Chan, W. C., Jaffe, E. S., Gascoyne, R. D., Campo, E., Rosenwald, A., Ott, G., Delabie, J., Rimsza, L. M., Rodriguez, F. J., Estephan, F., Holdhoff, M., Kruhlak, M. J., Hewitt, S. M., Thomas, C. J., Pittaluga, S., Oellerich, T., & Staudt, L. M. (2018). A multiprotein supercomplex controlling oncogenic signalling in lymphoma. *Nature, 560*(7718), 387-391.

Pimentel, H., Bray, N. L., Puente, S., Melsted, P., & Pachter, L. (2017). Differential analysis of RNA-seq incorporating quantification uncertainty. *Nature methods, 14*(7), 687.

Piskurich, J. F., Lin, K.-I., Lin, Y., Wang, Y., Ting, J. P.-Y., & Calame, K. (2000). BLIMP-1 mediates extinction of major histocompatibility class II transactivator expression in plasma cells. *Nature immunology, 1*(6), 526.

Pogo, B. G., Allfrey, V. G., & Mirsky, A. E. (1966). RNA synthesis and histone acetylation during the course of gene activation in lymphocytes. *Proceedings of the National Academy of Sciences of the United States of America, 55*(4), 805-812.

Polach, K. J., & Widom, J. (1996). A Model for the Cooperative Binding of Eukaryotic Regulatory Proteins to Nucleosomal Target Sites. *Journal of Molecular Biology, 258*(5), 800-812.

Popovic, R., Martinez-Garcia, E., Giannopoulou, E. G., Zhang, Q., Zhang, Q., Ezponda, T., Shah, M. Y., Zheng, Y., Will, C. M., Small, E. C., Hua, Y., Bulic, M., Jiang, Y., Carrara, M., Calogero, R. A., Kath, W. L., Kelleher, N. L., Wang, J.-P., Elemento, O., & Licht, J. D. (2014). Histone Methyltransferase MMSET/NSD2 Alters EZH2 Binding and Reprograms the Myeloma Epigenome through Global and Focal Changes in H3K36 and H3K27 Methylation. *PLOS Genetics, 10*(9), e1004566.

Pott, S., & Lieb, J. D. (2014). What are super-enhancers? *Nature Genetics, 47*, 8.

Price, M. J., Patterson, D. G., Scharer, C. D., & Boss, J. M. (2018). Progressive Upregulation of Oxidative Metabolism Facilitates Plasmablast Differentiation to a T-Independent Antigen. *Cell Reports, 23*(11), 3152-3159.

Puga, I., Cols, M., Barra, C. M., He, B., Cassis, L., Gentile, M., Comerma, L., Chorny, A., Shan, M., Xu, W., Magri, G., Knowles, D. M., Tam, W., Chiu, A., Bussel, J. B., Serrano, S., Lorente, J. A., Bellosillo, B., Lloreta, J., Juanpere, N., Alameda, F., Baró, T., de Heredia, C. D., Torán, N., Català, A., Torrebadell, M., Fortuny, C., Cusí, V., Carreras, C., Diaz, G. A., Blander, J. M., Farber, C.-M., Silvestri, G., Cunningham-Rundles, C., Calvillo, M., Dufour, C., Notarangelo, L. D., Lougaris, V., Plebani, A., Casanova, J.-L., Ganal, S. C., Diefenbach, A., Aróstegui, J. I., Juan, M., Yagüe, J., Mahlaoui, N., Donadieu, J., Chen, K., & Cerutti, A. (2011). B cell–helper neutrophils stimulate the diversification and production of immunoglobulin in the marginal zone of the spleen. *Nature Immunology, 13*, 170.

Qi, W., Chan, H., Teng, L., Li, L., Chuai, S., Zhang, R., Zeng, J., Li, M., Fan, H., Lin, Y., Gu, J., Ardayfio, O., Zhang, J.-H., Yan, X., Fang, J., Mi, Y., Zhang, M., Zhou, T., Feng, G., Chen, Z., Li, G., Yang, T., Zhao, K., Liu, X., Yu, Z., Lu, C. X., Atadja, P., & Li, E. (2012). Selective inhibition of Ezh2 by a small molecule inhibitor blocks tumor cells proliferation. *Proceedings of the National Academy of Sciences, 109*(52), 21360.

Rada, C., Di Noia, J. M., & Neuberger, M. S. (2004). Mismatch Recognition and Uracil Excision Provide Complementary Paths to Both Ig Switching and the A/T-Focused Phase of Somatic Mutation. *Molecular Cell, 16*(2), 163-171.

Rada, C., Williams, G. T., Nilsen, H., Barnes, D. E., Lindahl, T., & Neuberger, M. S. (2002). Immunoglobulin Isotype Switching Is Inhibited and Somatic Hypermutation Perturbed in UNG-Deficient Mice. *Current Biology, 12*(20), 1748-1755.

Rada-Iglesias, A., Bajpai, R., Swigut, T., Brugmann, S. A., Flynn, R. A., & Wysocka, J. (2010). A unique chromatin signature uncovers early developmental enhancers in humans. *Nature, 470*, 279.

Radbruch, A., Muehlinghaus, G., Luger, E. O., Inamine, A., Smith, K. G. C., Dörner, T., & Hiepe, F. (2006). Competence and competition: the challenge of becoming a long-lived plasma cell. *Nature Reviews Immunology, 6*, 741.

Raff, M. C., Megson, M., Owen, J. J. T., & Cooper, M. D. (1976). Early production of intracellular IgM by B-lymphocyte precursors in mouse. *Nature, 259*, 224.

Rahl, P. B., Lin, C. Y., Seila, A. C., Flynn, R. A., McCuine, S., Burge, C. B., Sharp, P. A., & Young, R. A. (2010). c-Myc Regulates Transcriptional Pause Release. *Cell, 141*(3), 432-445.

Rajewsky, K. (1996). Clonal selection and learning in the antibody system. *Nature, 381*(6585), 751.

Rajkumar, S. V., Dimopoulos, M. A., Palumbo, A., Blade, J., Merlini, G., Mateos, M.-V., Kumar, S., Hillengass, J., Kastritis, E., Richardson, P., Landgren, O., Paiva, B., Dispenzieri, A., Weiss, B., LeLeu, X., Zweegman, S., Lonial, S., Rosinol, L., Zamagni, E., Jagannath, S., Sezer, O., Kristinsson, S. Y., Caers, J., Usmani, S. Z., Lahuerta, J. J., Johnsen, H. E., Beksac, M., Cavo, M., Goldschmidt, H., Terpos,

E., Kyle, R. A., Anderson, K. C., Durie, B. G. M., & Miguel, J. F. S. (2014). International Myeloma Working Group updated criteria for the diagnosis of multiple myeloma. *The Lancet Oncology, 15*(12), e538-e548.

Ramírez, F., Ryan, D. P., Grüning, B., Bhardwaj, V., Kilpert, F., Richter, A. S., Heyne, S., Dündar, F., & Manke, T. (2016). deepTools2: a next generation web server for deep-sequencing data analysis. *Nucleic Acids Research, 44*(W1), W160-W165.

Ranuncolo, S. M., Polo, J. M., Dierov, J., Singer, M., Kuo, T., Greally, J., Green, R., Carroll, M., & Melnick, A. (2007). Bcl-6 mediates the germinal center B cell phenotype and lymphomagenesis through transcriptional repression of the DNA-damage sensor ATR. *Nature Immunology, 8*, 705.

Ranuncolo, S. M., Polo, J. M., Dierov, J., Singer, M., Kuo, T., Greally, J., Green, R., Carroll, M., & Melnick, A. (2007). Bcl-6 mediates the germinal center B cell phenotype and lymphomagenesis through transcriptional repression of the DNA-damage sensor ATR. *Nat Immunol, 8*(7), 705-714.

Ranuncolo, S. M., Polo, J. M., & Melnick, A. (2008). BCL6 represses CHEK1 and suppresses DNA damage pathways in normal and malignant B-cells. *Blood Cells Mol Dis, 41*(1), 95-99.

Ranuncolo, S. M., Polo, J. M., & Melnick, A. (2008). BCL6 represses CHEK1 and suppresses DNA damage pathways in normal and malignant B-cells. *Blood Cells, Molecules, and Diseases, 41*(1), 95-99.

Rasmussen, E. B., & Lis, J. T. (1993). In vivo transcriptional pausing and cap formation on three Drosophila heat shock genes. *Proc Natl Acad Sci U S A, 90*(17), 7923-7927.

Rastgoo, N., Pourabdollah, M., Abdi, J., Reece, D., & Chang, H. (2018a). Dysregulation of EZH2/miR-138 axis contributes to drug resistance in multiple myeloma by downregulating RBPMS. *Leukemia, 32*(11), 2471-2482.

Rastgoo, N., Pourabdollah, M., Abdi, J., Reece, D., & Chang, H. J. L. (2018b). Dysregulation of EZH2/miR-138 axis contributes to drug resistance in multiple myeloma by downregulating RBPMS. *32*(11), 2471.

Reddy, S. K., Rape, M., Margansky, W. A., & Kirschner, M. W. (2007). Ubiquitination by the anaphase-promoting complex drives spindle checkpoint inactivation. *Nature, 446*, 921.

Reimold, A. M., Ponath, P. D., Li, Y. S., Hardy, R. R., David, C. S., Strominger, J. L., & Glimcher, L. H. (1996). Transcription factor B cell lineage-specific activator protein regulates the gene for human X-box binding protein 1. *The Journal of Experimental Medicine, 183*(2), 393.

Ren, B., Chee, K. J., Kim, T. H., & Maniatis, T. (1999). PRDI-BF1/Blimp-1 repression is mediated by corepressors of the Groucho family of proteins. *Genes & Development, 13*(1), 125-137.

Reth, M., Petrac, E., Wiese, P., Lobel, L., & Alt, F. W. (1987). Activation of V kappa gene rearrangement in pre-B cells follows the expression of

membrane-bound immunoglobulin heavy chains. *Embo j, 6*(11), 3299-3305.
Revilla-I-Domingo, R., Bilic, I., Vilagos, B., Tagoh, H., Ebert, A., Tamir, I. M., Smeenk, L., Trupke, J., Sommer, A., Jaritz, M., & Busslinger, M. (2012). The B-cell identity factor Pax5 regulates distinct transcriptional programmes in early and late B lymphopoiesis. *The EMBO journal, 31*(14), 3130-3146.
Reynolds, A. P., Johnson, A. K., Haugen, E., Rynes, E., Vierstra, J., Stamatoyannopoulos, J. A., Kuehn, M. S., Maurano, M. T., Humbert, R., Sandstrom, R., Thurman, R. E., Thomas, S., & Neph, S. (2012). BEDOPS: high-performance genomic feature operations. *Bioinformatics, 28*(14), 1919-1920.
Rhee, H. S., & Pugh, B. F. (2012). Genome-wide structure and organization of eukaryotic pre-initiation complexes. *Nature, 483*(7389), 295-301.
Rimsza, L. M., Roberts, R. A., Miller, T. P., Unger, J. M., LeBlanc, M., Braziel, R. M., Weisenberger, D. D., Chan, W. C., Muller-Hermelink, H. K., Jaffe, E. S., Gascoyne, R. D., Campo, E., Fuchs, D. A., Spier, C. M., Fisher, R. I., Delabie, J., Rosenwald, A., Staudt, L. M., & Grogan, T. M. (2004). Loss of MHC class II gene and protein expression in diffuse large B-cell lymphoma is related to decreased tumor immunosurveillance and poor patient survival regardless of other prognostic factors: a follow-up study from the Leukemia and Lymphoma Molecular Profiling Project. *Blood, 103*(11), 4251.
Rippe, K., Schrader, A., Riede, P., Strohner, R., Lehmann, E., & Längst, G. (2007). DNA sequence- and conformation-directed positioning of nucleosomes by chromatin-remodeling complexes. *Proceedings of the National Academy of Sciences, 104*(40), 15635.
Roberts, M. J., Chadburn, A., Ma, S., Hyjek, E., & Peterson, L. C. (2013). Nuclear Protein Dysregulation in Lymphoplasmacytic Lymphoma/Waldenström Macroglobulinemia. *American Journal of Clinical Pathology, 139*(2), 210-219.
Robertson, E. J., Charatsi, I., Joyner, C. J., Koonce, C. H., Morgan, M., Islam, A., Paterson, C., Lejsek, E., Arnold, S. J., Kallies, A., Nutt, S. L., & Bikoff, E. K. (2007). Blimp1 regulates development of the posterior forelimb, caudal pharyngeal arches, heart and sensory vibrissae in mice. *Development, 134*(24), 4335.
Roccaro, A. M., Sacco, A., Jia, X., Azab, A. K., Maiso, P., Ngo, H. T., Azab, F., Runnels, J., Quang, P., & Ghobrial, I. M. (2010). microRNA-dependent modulation of histone acetylation in Waldenstrom macroglobulinemia. *Blood*, blood-2010-2001-265686.
Roeder, R. G., & Rutter, W. J. (1969). Multiple Forms of DNA-dependent RNA Polymerase in Eukaryotic Organisms. *Nature, 224*(5216), 234-237.
Roeder, R. G., & Rutter, W. J. (1970). Specific Nucleolar and Nucleoplasmic RNA Polymerases. *Proceedings of the National Academy of Sciences, 65*(3), 675.
Rolink, A. G., Winkler, T., Melchers, F., & Andersson, J. (2000). Precursor B Cell Receptor–Dependent B Cell Proliferation and Differentiation

Does Not Require the Bone Marrow or Fetal Liver Environment. *The Journal of Experimental Medicine, 191*(1), 23.
Ropper, A. H., & Gorson, K. C. (1998). Neuropathies Associated with Paraproteinemia. *New England Journal of Medicine, 338*(22), 1601-1607.
Ross-Innes, C. S., Stark, R., Teschendorff, A. E., Holmes, K. A., Ali, H. R., Dunning, M. J., Brown, G. D., Gojis, O., Ellis, I. O., Green, A. R., Ali, S., Chin, S.-F., Palmieri, C., Caldas, C., & Carroll, J. S. (2012). Differential oestrogen receptor binding is associated with clinical outcome in breast cancer. *Nature, 481*, 389.
Roy, A. L., & Singer, D. S. (2015). Core promoters in transcription: old problem, new insights. *Trends in Biochemical Sciences, 40*(3), 165-171.
Ryan, R. J. H., Nitta, M., Borger, D., Zukerberg, L. R., Ferry, J. A., Harris, N. L., Iafrate, A. J., Bernstein, B. E., Sohani, A. R., & Le, L. P. (2011). EZH2 Codon 641 Mutations are Common in BCL2-Rearranged Germinal Center B Cell Lymphomas. *PLOS ONE, 6*(12), e28585.
Saito, M., Gao, J., Basso, K., Kitagawa, Y., Smith, P. M., Bhagat, G., Pernis, A., Pasqualucci, L., & Dalla-Favera, R. (2007). A Signaling Pathway Mediating Downregulation of BCL6 in Germinal Center B Cells Is Blocked by BCL6 Gene Alterations in B Cell Lymphoma. *Cancer Cell, 12*(3), 280-292.
San Filippo, J., Sung, P., & Klein, H. (2008). Mechanism of Eukaryotic Homologous Recombination. *Annual Review of Biochemistry, 77*(1), 229-257.
Santamaría, D., Barrière, C., Cerqueira, A., Hunt, S., Tardy, C., Newton, K., Cáceres, J. F., Dubus, P., Malumbres, M., & Barbacid, M. (2007). Cdk1 is sufficient to drive the mammalian cell cycle. *Nature, 448*, 811.
Santos-Lozano, A., Morales-Gonzalez, A., Sanchis-Gomar, F., Cristi-Montero, C., Fiuza-Luces, C., Pareja-Galeano, H., Martinez-Lopez, J., Garatachea, N., & Lucia, A. (2016). Response rate to the treatment of Waldenstrom macroglobulinemia: A meta-analysis of the results of clinical trials. *Crit Rev Oncol Hematol, 105*, 118-126.
Savitsky, D., & Calame, K. (2006). B-1 B lymphocytes require Blimp-1 for immunoglobulin secretion. *The Journal of Experimental Medicine, 203*(10), 2305.
Sawadogo, M., & Roeder, R. G. (1985). Interaction of a gene-specific transcription factor with the adenovirus major late promoter upstream of the TATA box region. *Cell, 43*(1), 165-175.
Schaeffer, L., Roy, R., Humbert, S., Moncollin, V., Vermeulen, W., Hoeijmakers, J. H., Chambon, P., & Egly, J. M. (1993). DNA repair helicase: a component of BTF2 (TFIIH) basic transcription factor. *Science, 260*(5104), 58.
Scharer, C. D., Barwick, B. G., Guo, M., Bally, A. P. R., & Boss, J. M. (2018). Plasma cell differentiation is controlled by multiple cell division-coupled epigenetic programs. *Nature Communications, 9*(1), 1698.

Schatz, D. G., & Ji, Y. H. (2011). Recombination centres and the orchestration of V(D)J recombination. *Nature Reviews Immunology, 11*(4), 251-263.
Schaukowitch, K., Joo, J.-Y., Liu, X., Watts, Jonathan K., Martinez, C., & Kim, T.-K. (2014). Enhancer RNA Facilitates NELF Release from Immediate Early Genes. *Molecular Cell, 56*(1), 29-42.
Schebesta, A., McManus, S., Salvagiotto, G., Delogu, A., Busslinger, G. A., & Busslinger, M. (2007). Transcription Factor Pax5 Activates the Chromatin of Key Genes Involved in B Cell Signaling, Adhesion, Migration, and Immune Function. *Immunity, 27*(1), 49-63.
Scheeren, F. A., Nagasawa, M., Weijer, K., Cupedo, T., Kirberg, J., Legrand, N., & Spits, H. (2008). T cell–independent development and induction of somatic hypermutation in human IgM+IgD+CD27+ B cells. *The Journal of Experimental Medicine, 205*(9), 2033.
Schiemann, B., Gommerman, J. L., Vora, K., Cachero, T. G., Shulga-Morskaya, S., Dobles, M., Frew, E., & Scott, M. L. (2001). An essential role for BAFF in the normal development of B cells through a BCMA-independent pathway. *Science, 293*(5537), 2111-2114.
Schmit, F., Cremer, S., & Gaubatz, S. (2009). LIN54 is an essential core subunit of the DREAM/LINC complex that binds to the cdc2 promoter in a sequence-specific manner. *The FEBS Journal, 276*(19), 5703-5716.
Schmitges, F. W., Prusty, A. B., Faty, M., Stutzer, A., Lingaraju, G. M., Aiwazian, J., Sack, R., Hess, D., Li, L., Zhou, S., Bunker, R. D., Wirth, U., Bouwmeester, T., Bauer, A., Ly-Hartig, N., Zhao, K., Chan, H., Gu, J., Gut, H., Fischle, W., Muller, J., & Thoma, N. H. (2011). Histone methylation by PRC2 is inhibited by active chromatin marks. *Mol Cell, 42*(3), 330-341.
Schneider, C. A., Rasband, W. S., & Eliceiri, K. W. (2012). NIH Image to ImageJ: 25 years of image analysis. *Nature Methods, 9*, 671.
Schop, R. F. J., Kuehl, W. M., Van Wier, S. A., Ahmann, G. J., Price-Troska, T., Bailey, R. J., Jalal, S. M., Qi, Y., Kyle, R. A., Greipp, P. R., & Fonseca, R. (2002). Waldenström macroglobulinemia neoplastic cells lack immunoglobulin heavy chain locus translocations but have frequent 6q deletions. *Blood, 100*(8), 2996.
Schop, R. F. J., Van Wier, S. A., Xu, R., Ghobrial, I., Ahmann, G. J., Greipp, P. R., Kyle, R. A., Dispenzieri, A., Lacy, M. Q., Rajkumar, S. V., Gertz, M. A., & Fonseca, R. (2006). 6q deletion discriminates Waldenström macroglobulinemia from IgM monoclonal gammopathy of undetermined significance. *Cancer Genetics and Cytogenetics, 169*(2), 150-153.
Schultz, D. C., Friedman, J. R., & Rauscher, F. J. (2001). Targeting histone deacetylase complexes via KRAB-zinc finger proteins: the PHD and bromodomains of KAP-1 form a cooperative unit that recruits a novel isoform of the Mi-2α subunit of NuRD. *Genes & Development, 15*(4), 428-443.
Sciammas, R., Shaffer, A. L., Schatz, J. H., Zhao, H., Staudt, L. M., & Singh, H. (2006). Graded expression of interferon regulatory factor-4

coordinates isotype switching with plasma cell differentiation. *Immunity, 25*(2), 225-236.
Sciortino, M., Camacho-Leal, M. d. P., Orso, F., Grassi, E., Costamagna, A., Provero, P., Tam, W., Turco, E., Defilippi, P., Taverna, D., & Cabodi, S. (2017). Dysregulation of Blimp1 transcriptional repressor unleashes p130Cas/ErbB2 breast cancer invasion. *Scientific Reports, 7*(1), 1145.
Setz, C. S., Hug, E., Khadour, A., Abdelrasoul, H., Bilal, M., Hobeika, E., & Jumaa, H. (2018). PI3K-Mediated Blimp-1 Activation Controls B Cell Selection and Homeostasis. *Cell Reports, 24*(2), 391-405.
Shaffer, A. L., Emre, N. C. T., Lamy, L., Ngo, V. N., Wright, G., Xiao, W., Powell, J., Dave, S., Yu, X., Zhao, H., Zeng, Y., Chen, B., Epstein, J., & Staudt, L. M. (2008). IRF4 addiction in multiple myeloma. *Nature, 454*, 226.
Shaffer, A. L., Lin, K.-I., Kuo, T. C., Yu, X., Hurt, E. M., Rosenwald, A., Giltnane, J. M., Yang, L., Zhao, H., Calame, K., & Staudt, L. M. (2002). Blimp-1 Orchestrates Plasma Cell Differentiation by Extinguishing the Mature B Cell Gene Expression Program. *Immunity, 17*(1), 51-62.
Shaffer, A. L., Peng, A., & Schlissel, M. S. (1997). In Vivo Occupancy of the κ Light Chain Enhancers in Primary Pro- and Pre-B Cells: A Model for κ Locus Activation. *Immunity, 6*(2), 131-143.
Shaffer, A. L., Shapiro-Shelef, M., Iwakoshi, N. N., Lee, A.-H., Qian, S.-B., Zhao, H., Yu, X., Yang, L., Tan, B. K., Rosenwald, A., Hurt, E. M., Petroulakis, E., Sonenberg, N., Yewdell, J. W., Calame, K., Glimcher, L. H., & Staudt, L. M. (2004). XBP1, Downstream of Blimp-1, Expands the Secretory Apparatus and Other Organelles, and Increases Protein Synthesis in Plasma Cell Differentiation. *Immunity, 21*(1), 81-93.
Shaffer, A. L., Yu, X., He, Y., Boldrick, J., Chan, E. P., & Staudt, L. M. (2000). BCL-6 Represses Genes that Function in Lymphocyte Differentiation, Inflammation, and Cell Cycle Control. *Immunity, 13*(2), 199-212.
Shapiro-Shelef, M., Lin, K.-I., McHeyzer-Williams, L. J., Liao, J., McHeyzer-Williams, M. G., & Calame, K. (2003). Blimp-1 Is Required for the Formation of Immunoglobulin Secreting Plasma Cells and Pre-Plasma Memory B Cells. *Immunity, 19*(4), 607-620.
Shapiro-Shelef, M., Lin, K.-I., Savitsky, D., Liao, J., & Calame, K. (2005). Blimp-1 is required for maintenance of long-lived plasma cells in the bone marrow. *The Journal of Experimental Medicine, 202*(11), 1471.
Sharma, S., & Lichtenstein, A. (2008). Dexamethasone-induced apoptotic mechanisms in myeloma cells investigated by analysis of mutant glucocorticoid receptors. *Blood, 112*(4), 1338.
Shaughnessy, J., Gabrea, A., Qi, Y., Brents, L., Zhan, F., Tian, E., Sawyer, J., Barlogie, B., Bergsagel, P. L., & Kuehl, M. (2001). Cyclin D3 at 6p21 is dysregulated by recurrent chromosomal translocations to immunoglobulin loci in multiple myeloma. *Blood, 98*(1), 217.
Shaulian, E. (2010). AP-1 — The Jun proteins: Oncogenes or tumor suppressors in disguise? *Cellular Signalling, 22*(6), 894-899.

Shen, X., Liu, Y., Hsu, Y.-J., Fujiwara, Y., Kim, J., Mao, X., Yuan, G.-C., & Orkin, S. H. (2008). EZH1 mediates methylation on histone H3 lysine 27 and complements EZH2 in maintaining stem cell identity and executing pluripotency. *Molecular cell, 32*(4), 491-502.

Shi, W., Liao, Y., Willis, S. N., Taubenheim, N., Inouye, M., Tarlinton, D. M., Smyth, G. K., Hodgkin, P. D., Nutt, S. L., & Corcoran, L. M. (2015). Transcriptional profiling of mouse B cell terminal differentiation defines a signature for antibody-secreting plasma cells. *Nature Immunology, 16*, 663.

Shi, Z., Li, Z., Li, Z. J., Cheng, K., Du, Y., Fu, H., & Khuri, F. R. (2014). Cables1 controls p21/Cip1 protein stability by antagonizing proteasome subunit alpha type 3. *Oncogene, 34*, 2538.

Shimshon, L., Michaeli, A., Hadar, R., Nutt, S. L., David, Y., Navon, A., Waisman, A., & Tirosh, B. (2011). SUMOylation of Blimp-1 promotes its proteasomal degradation. *FEBS Letters, 585*(15), 2405-2409.

Shivji, K. K., Kenny, M. K., & Wood, R. D. (1992). Proliferating cell nuclear antigen is required for DNA excision repair. *Cell, 69*(2), 367-374.

Shogren-Knaak, M., Ishii, H., Sun, J.-M., Pazin, M. J., Davie, J. R., & Peterson, C. L. J. S. (2006). Histone H4-K16 acetylation controls chromatin structure and protein interactions. *311*(5762), 844-847.

Shuford, W. W., Klussman, K., Tritchler, D. D., Loo, D. T., Chalupny, J., Siadak, A. W., Brown, T. J., Emswiler, J., Raecho, H., Larsen, C. P., Pearson, T. C., Ledbetter, J. A., Aruffo, A., & Mittler, R. S. (1997). 4-1BB Costimulatory Signals Preferentially Induce CD8⁺ T Cell Proliferation and Lead to the Amplification In Vivo of Cytotoxic T Cell Responses. *The Journal of Experimental Medicine, 186*(1), 47.

Sigurdardottir, E. E., Turesson, I., Lund, S. H., Lindqvist, E. K., Mailankody, S., Korde, N., Bjorkholm, M., Landgren, O., & Kristinsson, S. Y. (2015). The Role of Diagnosis and Clinical Follow-up of Monoclonal Gammopathy of Undetermined Significance on Survival in Multiple Myeloma. *JAMA Oncol, 1*(2), 168-174.

Silljé, H. H. W., & Nigg, E. A. (2001). Identification of human Asf1 chromatin assembly factors as substrates of Tousled-like kinases. *Current Biology, 11*(13), 1068-1073.

Smale, S. T., & Baltimore, D. (1989). The “initiator” as a transcription control element. *Cell, 57*(1), 103-113.

Sneeringer, C. J., Scott, M. P., Kuntz, K. W., Knutson, S. K., Pollock, R. M., Richon, V. M., & Copeland, R. A. (2010). Coordinated activities of wild-type plus mutant EZH2 drive tumor-associated hypertrimethylation of lysine 27 on histone H3 (H3K27) in human B-cell lymphomas. *Proceedings of the National Academy of Sciences, 107*(49), 20980.

Soufi, A., Garcia, Meilin F., Jaroszewicz, A., Osman, N., Pellegrini, M., & Zaret, Kenneth S. (2015). Pioneer Transcription Factors Target Partial DNA Motifs on Nucleosomes to Initiate Reprogramming. *Cell, 161*(3), 555-568.

Spitz, F., & Furlong, E. E. M. (2012). Transcription factors: from enhancer binding to developmental control. *Nature Reviews Genetics, 13*, 613.
Sripathy, S. P., Stevens, J., & Schultz, D. C. (2006). The KAP1 corepressor functions to coordinate the assembly of de novo HP1-demarcated microenvironments of heterochromatin required for KRAB zinc finger protein-mediated transcriptional repression. *Molecular and cellular biology, 26*(22), 8623-8638.
St Clair, S., Giono, L., Varmeh-Ziaie, S., Resnick-Silverman, L., Liu, W. J., Padi, A., Dastidar, J., DaCosta, A., Mattia, M., & Manfredi, J. J. (2004). DNA damage-induced downregulation of Cdc25C is mediated by p53 via two independent mechanisms: one involves direct binding to the cdc25C promoter. *Mol Cell, 16*(5), 725-736.
Stark, R., Brown, G.D. (2011). DiffBind: differential binding analysis of ChIP-Seq peak data. http://bioconductor.org/packages/release/bioc/vignettes/DiffBind/inst/doc/DiffBind.pdf.
Stoll, S., Delon, J., Brotz, T. M., & Germain, R. N. (2002). Dynamic Imaging of T Cell-Dendritic Cell Interactions in Lymph Nodes. *Science, 296*(5574), 1873.
Su, G. H., Chen, H. M., Muthusamy, N., Garrett-Sinha, L. A., Baunoch, D., Tenen, D. G., & Simon, M. C. (1997). Defective B cell receptor-mediated responses in mice lacking the Ets protein, Spi-B. *Embo j, 16*(23), 7118-7129.
Su, I.-h., Basavaraj, A., Krutchinsky, A. N., Hobert, O., Ullrich, A., Chait, B. T., & Tarakhovsky, A. J. N. i. (2003). Ezh2 controls B cell development through histone H3 methylation and Igh rearrangement. *4*(2), 124.
Su, S.-T., Ying, H.-Y., Chiu, Y.-K., Lin, F.-R., Chen, M.-Y., & Lin, K.-I. (2009). Involvement of Histone Demethylase LSD1 in Blimp-1-Mediated Gene Repression during Plasma Cell Differentiation. *Molecular and Cellular Biology, 29*(6), 1421.
Subramanian, A., Tamayo, P., Mootha, V. K., Mukherjee, S., Ebert, B. L., Gillette, M. A., Paulovich, A., Pomeroy, S. L., Golub, T. R., Lander, E. S., & Mesirov, J. P. (2005). Gene set enrichment analysis: A knowledge-based approach for interpreting genome-wide expression profiles. *Proceedings of the National Academy of Sciences, 102*(43), 15545.
Sudakin, V., Chan, G. K. T., & Yen, T. J. (2001). Checkpoint inhibition of the APC/C in HeLa cells is mediated by a complex of BUBR1, BUB3, CDC20, and MAD2. *The Journal of Cell Biology, 154*(5), 925.
Taccioli, G. E., Rathbun, G., Oltz, E., Stamato, T., Jeggo, P. A., & Alt, F. W. (1993). Impairment of V(D)J recombination in double-strand break repair mutants. *Science, 260*(5105), 207.
Takahashi, K., & Yamanaka, S. (2006). Induction of Pluripotent Stem Cells from Mouse Embryonic and Adult Fibroblast Cultures by Defined Factors. *Cell, 126*(4), 663-676.
Takahashi, Y., Rayman, J. B., & Dynlacht, B. D. (2000). Analysis of promoter binding by the E2F and pRB families in vivo: distinct E2F proteins

mediate activation and repression. *Genes & development, 14*(7), 804-816.
Takeda, K., & Akira, S. (2004). TLR signaling pathways. *Seminars in Immunology, 16*(1), 3-9.
Tamura, H., Ishibashi, M., Yamashita, T., Tanosaki, S., Okuyama, N., Kondo, A., Hyodo, H., Shinya, E., Takahashi, H., Dong, H., Tamada, K., Chen, L., Dan, K., & Ogata, K. (2012). Marrow stromal cells induce B7-H1 expression on myeloma cells, generating aggressive characteristics in multiple myeloma. *Leukemia, 27*, 464.
Teif, V. B., Vainshtein, Y., Caudron-Herger, M., Mallm, J.-P., Marth, C., Höfer, T., & Rippe, K. (2012). Genome-wide nucleosome positioning during embryonic stem cell development. *Nature Structural &Amp; Molecular Biology, 19*, 1185.
Tellier, J., Shi, W., Minnich, M., Liao, Y., Crawford, S., Smyth, G. K., Kallies, A., Busslinger, M., & Nutt, S. L. (2016). Blimp-1 controls plasma cell function through the regulation of immunoglobulin secretion and the unfolded protein response. *Nature Immunology, 17*, 323.
Tessarz, P., & Kouzarides, T. (2014). Histone core modifications regulating nucleosome structure and dynamics. *Nature Reviews Molecular Cell Biology, 15*, 703.
The, E. P. C., Dunham, I., Kundaje, A., Aldred, S. F., Collins, P. J., Davis, C. A., Doyle, F., Epstein, C. B., Frietze, S., Harrow, J., Kaul, R., Khatun, J., Lajoie, B. R., Landt, S. G., Lee, B.-K., Pauli, F., Rosenbloom, K. R., Sabo, P., Safi, A., Sanyal, A., Shoresh, N., Simon, J. M., Song, L., Trinklein, N. D., Altshuler, R. C., Birney, E., Brown, J. B., Cheng, C., Djebali, S., Dong, X., Dunham, I., Ernst, J., Furey, T. S., Gerstein, M., Giardine, B., Greven, M., Hardison, R. C., Harris, R. S., Herrero, J., Hoffman, M. M., Iyer, S., Kellis, M., Khatun, J., Kheradpour, P., Kundaje, A., Lassmann, T., Li, Q., Lin, X., Marinov, G. K., Merkel, A., Mortazavi, A., Parker, S. C. J., Reddy, T. E., Rozowsky, J., Schlesinger, F., Thurman, R. E., Wang, J., Ward, L. D., Whitfield, T. W., Wilder, S. P., Wu, W., Xi, H. S., Yip, K. Y., Zhuang, J., Bernstein, B. E., Birney, E., Dunham, I., Green, E. D., Gunter, C., Snyder, M., Pazin, M. J., Lowdon, R. F., Dillon, L. A. L., Adams, L. B., Kelly, C. J., Zhang, J., Wexler, J. R., Green, E. D., Good, P. J., Feingold, E. A., Bernstein, B. E., Birney, E., Crawford, G. E., Dekker, J., Elnitski, L., Farnham, P. J., Gerstein, M., Giddings, M. C., Gingeras, T. R., Green, E. D., Guigó, R., Hardison, R. C., Hubbard, T. J., Kellis, M., Kent, W. J., Lieb, J. D., Margulies, E. H., Myers, R. M., Snyder, M., Stamatoyannopoulos, J. A., Tenenbaum, S. A., Weng, Z., White, K. P., Wold, B., Khatun, J., Yu, Y., Wrobel, J., Risk, B. A., Gunawardena, H. P., Kuiper, H. C., Maier, C. W., Xie, L., Chen, X., Giddings, M. C., Bernstein, B. E., Epstein, C. B., Shoresh, N., Ernst, J., Kheradpour, P., Mikkelsen, T. S., Gillespie, S., Goren, A., Ram, O., Zhang, X., Wang, L., Issner, R., Coyne, M. J., Durham, T., Ku, M., Truong, T., Ward, L. D., Altshuler, R. C., Eaton, M. L., Kellis, M., Djebali, S., Davis, C. A., Merkel, A., Dobin, A., Lassmann, T., Mortazavi, A., Tanzer, A., Lagarde, J., Lin, W., Schlesinger, F., Xue,

C., Marinov, G. K., Khatun, J., Williams, B. A., Zaleski, C., Rozowsky, J., Röder, M., Kokocinski, F., Abdelhamid, R. F., Alioto, T., Antoshechkin, I., Baer, M. T., Batut, P., Bell, I., Bell, K., Chakrabortty, S., Chen, X., Chrast, J., Curado, J., Derrien, T., Drenkow, J., Dumais, E., Dumais, J., Duttagupta, R., Fastuca, M., Fejes-Toth, K., Ferreira, P., Foissac, S., Fullwood, M. J., Gao, H., Gonzalez, D., Gordon, A., Gunawardena, H. P., Howald, C., Jha, S., Johnson, R., Kapranov, P., King, B., Kingswood, C., Li, G., Luo, O. J., Park, E., Preall, J. B., Presaud, K., Ribeca, P., Risk, B. A., Robyr, D., Ruan, X., Sammeth, M., Sandhu, K. S., Schaeffer, L., See, L.-H., Shahab, A., Skancke, J., Suzuki, A. M., Takahashi, H., Tilgner, H., Trout, D., Walters, N., Wang, H., Wrobel, J., Yu, Y., Hayashizaki, Y., Harrow, J., Gerstein, M., Hubbard, T. J., Reymond, A., Antonarakis, S. E., Hannon, G. J., Giddings, M. C., Ruan, Y., Wold, B., Carninci, P., Guigó, R., Gingeras, T. R., Rosenbloom, K. R., Sloan, C. A., Learned, K., Malladi, V. S., Wong, M. C., Barber, G. P., Cline, M. S., Dreszer, T. R., Heitner, S. G., Karolchik, D., Kent, W. J., Kirkup, V. M., Meyer, L. R., Long, J. C., Maddren, M., Raney, B. J., Furey, T. S., Song, L., Grasfeder, L. L., Giresi, P. G., Lee, B.-K., Battenhouse, A., Sheffield, N. C., Simon, J. M., Showers, K. A., Safi, A., London, D., Bhinge, A. A., Shestak, C., Schaner, M. R., Ki Kim, S., Zhang, Z. Z., Mieczkowski, P. A., Mieczkowska, J. O., Liu, Z., McDaniell, R. M., Ni, Y., Rashid, N. U., Kim, M. J., Adar, S., Zhang, Z., Wang, T., Winter, D., Keefe, D., Birney, E., Iyer, V. R., Lieb, J. D., Crawford, G. E., Li, G., Sandhu, K. S., Zheng, M., Wang, P., Luo, O. J., Shahab, A., Fullwood, M. J., Ruan, X., Ruan, Y., Myers, R. M., Pauli, F., Williams, B. A., Gertz, J., Marinov, G. K., Reddy, T. E., Vielmetter, J., Partridge, E., Trout, D., Varley, K. E., Gasper, C., Bansal, A., Pepke, S., Jain, P., Amrhein, H., Bowling, K. M., Anaya, M., Cross, M. K., King, B., Muratet, M. A., Antoshechkin, I., Newberry, K. M., McCue, K., Nesmith, A. S., Fisher-Aylor, K. I., Pusey, B., DeSalvo, G., Parker, S. L., Balasubramanian, S., Davis, N. S., Meadows, S. K., Eggleston, T., Gunter, C., Newberry, J. S., Levy, S. E., Absher, D. M., Mortazavi, A., Wong, W. H., Wold, B., Blow, M. J., Visel, A., Pennachio, L. A., Elnitski, L., Margulies, E. H., Parker, S. C. J., Petrykowska, H. M., Abyzov, A., Aken, B., Barrell, D., Barson, G., Berry, A., Bignell, A., Boychenko, V., Bussotti, G., Chrast, J., Davidson, C., Derrien, T., Despacio-Reyes, G., Diekhans, M., Ezkurdia, I., Frankish, A., Gilbert, J., Gonzalez, J. M., Griffiths, E., Harte, R., Hendrix, D. A., Howald, C., Hunt, T., Jungreis, I., Kay, M., Khurana, E., Kokocinski, F., Leng, J., Lin, M. F., Loveland, J., Lu, Z., Manthravadi, D., Mariotti, M., Mudge, J., Mukherjee, G., Notredame, C., Pei, B., Rodriguez, J. M., Saunders, G., Sboner, A., Searle, S., Sisu, C., Snow, C., Steward, C., Tanzer, A., Tapanari, E., Tress, M. L., van Baren, M. J., Walters, N., Washietl, S., Wilming, L., Zadissa, A., Zhang, Z., Brent, M., Haussler, D., Kellis, M., Valencia, A., Gerstein, M., Reymond, A., Guigó, R., Harrow, J., Hubbard, T. J., Landt, S. G., Frietze, S., Abyzov, A., Addleman, N., Alexander, R. P.,

Auerbach, R. K., Balasubramanian, S., Bettinger, K., Bhardwaj, N., Boyle, A. P., Cao, A. R., Cayting, P., Charos, A., Cheng, Y., Cheng, C., Eastman, C., Euskirchen, G., Fleming, J. D., Grubert, F., Habegger, L., Hariharan, M., Harmanci, A., Iyengar, S., Jin, V. X., Karczewski, K. J., Kasowski, M., Lacroute, P., Lam, H., Lamarre-Vincent, N., Leng, J., Lian, J., Lindahl-Allen, M., Min, R., Miotto, B., Monahan, H., Moqtaderi, Z., Mu, X. J., O'Geen, H., Ouyang, Z., Patacsil, D., Pei, B., Raha, D., Ramirez, L., Reed, B., Rozowsky, J., Sboner, A., Shi, M., Sisu, C., Slifer, T., Witt, H., Wu, L., Xu, X., Yan, K.-K., Yang, X., Yip, K. Y., Zhang, Z., Struhl, K., Weissman, S. M., Gerstein, M., Farnham, P. J., Snyder, M., Tenenbaum, S. A., Penalva, L. O., Doyle, F., Karmakar, S., Landt, S. G., Bhanvadia, R. R., Choudhury, A., Domanus, M., Ma, L., Moran, J., Patacsil, D., Slifer, T., Victorsen, A., Yang, X., Snyder, M., White, K. P., Auer, T., Centanin, L., Eichenlaub, M., Gruhl, F., Heermann, S., Hoeckendorf, B., Inoue, D., Kellner, T., Kirchmaier, S., Mueller, C., Reinhardt, R., Schertel, L., Schneider, S., Sinn, R., Wittbrodt, B., Wittbrodt, J., Weng, Z., Whitfield, T. W., Wang, J., Collins, P. J., Aldred, S. F., Trinklein, N. D., Partridge, E. C., Myers, R. M., Dekker, J., Jain, G., Lajoie, B. R., Sanyal, A., Balasundaram, G., Bates, D. L., Byron, R., Canfield, T. K., Diegel, M. J., Dunn, D., Ebersol, A. K., Frum, T., Garg, K., Gist, E., Hansen, R. S., Boatman, L., Haugen, E., Humbert, R., Jain, G., Johnson, A. K., Johnson, E. M., Kutyavin, T. V., Lajoie, B. R., Lee, K., Lotakis, D., Maurano, M. T., Neph, S. J., Neri, F. V., Nguyen, E. D., Qu, H., Reynolds, A. P., Roach, V., Rynes, E., Sabo, P., Sanchez, M. E., Sandstrom, R. S., Sanyal, A., Shafer, A. O., Stergachis, A. B., Thomas, S., Thurman, R. E., Vernot, B., Vierstra, J., Vong, S., Wang, H., Weaver, M. A., Yan, Y., Zhang, M., Akey, J. M., Bender, M., Dorschner, M. O., Groudine, M., MacCoss, M. J., Navas, P., Stamatoyannopoulos, G., Kaul, R., Dekker, J., Stamatoyannopoulos, J. A., Dunham, I., Beal, K., Brazma, A., Flicek, P., Herrero, J., Johnson, N., Keefe, D., Lukk, M., Luscombe, N. M., Sobral, D., Vaquerizas, J. M., Wilder, S. P., Batzoglou, S., Sidow, A., Hussami, N., Kyriazopoulou-Panagiotopoulou, S., Libbrecht, M. W., Schaub, M. A., Kundaje, A., Hardison, R. C., Miller, W., Giardine, B., Harris, R. S., Wu, W., Bickel, P. J., Banfai, B., Boley, N. P., Brown, J. B., Huang, H., Li, Q., Li, J. J., Noble, W. S., Bilmes, J. A., Buske, O. J., Hoffman, M. M., Sahu, A. D., Kharchenko, P. V., Park, P. J., Baker, D., Taylor, J., Weng, Z., Iyer, S., Dong, X., Greven, M., Lin, X., Wang, J., Xi, H. S., Zhuang, J., Gerstein, M., Alexander, R. P., Balasubramanian, S., Cheng, C., Harmanci, A., Lochovsky, L., Min, R., Mu, X. J., Rozowsky, J., Yan, K.-K., Yip, K. Y., & Birney, E. (2012). An integrated encyclopedia of DNA elements in the human genome. *Nature, 489*, 57.

Thomas, J. O., & Kornberg, R. D. (1975a). Cleavable cross-links in the analysis of histone—histone associations. *FEBS Letters, 58*(1-2), 353-358.

Thomas, J. O., & Kornberg, R. D. (1975b). An octamer of histones in chromatin and free in solution. *Proceedings of the National Academy of Sciences, 72*(7), 2626.

Thompson, E. C., Cobb, B. S., Sabbattini, P., Meixlsperger, S., Parelho, V., Liberg, D., Taylor, B., Dillon, N., Georgopoulos, K., Jumaa, H., Smale, S. T., Fisher, A. G., & Merkenschlager, M. (2007). Ikaros DNA-Binding Proteins as Integral Components of B Cell Developmental-Stage-Specific Regulatory Circuits. *Immunity, 26*(3), 335-344.

Tirode, F., Busso, D., Coin, F., & Egly, J.-M. (1999). Reconstitution of the Transcription Factor TFIIH: Assignment of Functions for the Three Enzymatic Subunits, XPB, XPD, and cdk7. *Molecular Cell, 3*(1), 87-95.

Tonegawa, S. (1983). Somatic generation of antibody diversity. *Nature, 302*(5909), 575-581.

Tooze, R. M., Stephenson, S., & Doody, G. M. (2006). Repression of IFN-γ Induction of Class II Transactivator: A Role for PRDM1/Blimp-1 in Regulation of Cytokine Signaling. *The Journal of Immunology, 177*(7), 4584.

Treon, S. P. (2015). How I treat Waldenström macroglobulinemia. *Blood, 126*(6), 721.

Treon, S. P., Gustine, J., Meid, K., Dubeau, T., Severns, P., Patterson, C., Xu, L., Yang, G., Liu, X., Demos, M., Kofides, A., Chen, J., Munshi, M., Tsakmaklis, N., Chan, G., Yee, A. J., Raje, N., Donnell, E., Hunter, Z., & Castillo, J. J. (2017a). Ibrutinib Is Highly Active As First Line Therapy in Symptomatic Waldenstrom's Macroglobulinemia. *Blood, 130*(Suppl 1), 2767.

Treon, S. P., Gustine, J., Xu, L., Manning, R. J., Tsakmaklis, N., Demos, M., Meid, K., Guerrera, M. L., Munshi, M., Chan, G., Chen, J., Kofides, A., Patterson, C. J., Yang, G., Liu, X., Severns, P., Dubeau, T., Hunter, Z. R., & Castillo, J. J. (2018). MYD88 wild-type Waldenstrom Macroglobulinaemia: differential diagnosis, risk of histological transformation, and overall survival. *British Journal of Haematology, 180*(3), 374-380.

Treon, S. P., Meid, K., Tripsas, C., Heffner, L. T., Eradat, H., Badros, A. Z., Xu, L., Hunter, Z. R., Yang, G., Patterson, C. J., Gustine, J., Castillo, J. J., Matous, J., & Ghobrial, I. M. (2017b). Prospective, Multicenter Clinical Trial of Everolimus as Primary Therapy in Waldenstrom Macroglobulinemia (WMCTG 09-214). *Clinical Cancer Research, 23*(10), 2400-2404.

Treon, S. P., Tripsas, C. K., Meid, K., Warren, D., Varma, G., Green, R., Argyropoulos, K. V., Yang, G., Cao, Y., Xu, L., Patterson, C. J., Rodig, S., Zehnder, J. L., Aster, J. C., Harris, N. L., Kanan, S., Ghobrial, I., Castillo, J. J., Laubach, J. P., Hunter, Z. R., Salman, Z., Li, J., Cheng, M., Clow, F., Graef, T., Palomba, M. L., & Advani, R. H. (2015). Ibrutinib in Previously Treated Waldenström's Macroglobulinemia. *New England Journal of Medicine, 372*(15), 1430-1440.

Treon, S. P., Xu, L., Yang, G., Zhou, Y., Liu, X., Cao, Y., Sheehy, P., Manning, R. J., Patterson, C. J., Tripsas, C., Arcaini, L., Pinkus, G. S., Rodig, S. J., Sohani, A. R., Harris, N. L., Laramie, J. M., Skifter, D. A., Lincoln, S. E., & Hunter, Z. R. (2012). MYD88 L265P Somatic Mutation in Waldenström's Macroglobulinemia. *New England Journal of Medicine, 367*(9), 826-833.

Tsutsui, T., Hesabi, B., Moons, D. S., Pandolfi, P. P., Hansel, K. S., Koff, A., & Kiyokawa, H. (1999). Targeted Disruption of CDK4 Delays Cell Cycle Entry with Enhanced p27(Kip1) Activity. *Molecular and Cellular Biology, 19*(10), 7011.

Tunyaplin, C., Shaffer, A. L., Angelin-Duclos, C. D., Yu, X., Staudt, L. M., & Calame, K. L. (2004). Direct Repression of prdm1 by Bcl-6 Inhibits Plasmacytic Differentiation. *The Journal of Immunology, 173*(2), 1158-1165.

Tunyaplin, C., Shapiro, M. A., & Calame, K. L. (2000). Characterization of the B lymphocyte-induced maturation protein-1 (Blimp-1) gene, mRNA isoforms and basal promoter. *Nucleic Acids Research, 28*(24), 4846-4855.

Turner, C. A., Mack, D. H., & Davis, M. M. (1994). Blimp-1, a novel zinc finger-containing protein that can drive the maturation of B lymphocytes into immunoglobulin-secreting cells. *Cell, 77*(2), 297-306.

Umar, A., Buermeyer, A. B., Simon, J. A., Thomas, D. C., Clark, A. B., Liskay, R. M., & Kunkel, T. A. (1996). Requirement for PCNA in DNA Mismatch Repair at a Step Preceding DNA Resynthesis. *Cell, 87*(1), 65-73.

van Arensbergen, J., van Steensel, B., & Bussemaker, H. J. (2014). In search of the determinants of enhancer–promoter interaction specificity. *Trends in Cell Biology, 24*(11), 695-702.

van den Heuvel, S., & Harlow, E. (1993). Distinct roles for cyclin-dependent kinases in cell cycle control. *Science, 262*(5142), 2050.

van Galen, J. C., Dukers, D. F., Giroth, C., Sewalt, R. G. A. B., Otte, A. P., Meijer, C. J. L. M., & Raaphorst, F. M. (2004). Distinct expression patterns of polycomb oncoproteins and their binding partners during the germinal center reaction. *European Journal of Immunology, 34*(7), 1870-1881.

van Gent, D. C., Fraser McBlane, J., Ramsden, D. A., Sadofsky, M. J., Hesse, J. E., & Gellert, M. (1995). Initiation of V(D)J recombination in a cell-free system. *Cell, 81*(6), 925-934.

van Haaften, G., Dalgliesh, G. L., Davies, H., Chen, L., Bignell, G., Greenman, C., Edkins, S., Hardy, C., O'Meara, S., Teague, J., Butler, A., Hinton, J., Latimer, C., Andrews, J., Barthorpe, S., Beare, D., Buck, G., Campbell, P. J., Cole, J., Forbes, S., Jia, M., Jones, D., Kok, C. Y., Leroy, C., Lin, M.-L., McBride, D. J., Maddison, M., Maquire, S., McLay, K., Menzies, A., Mironenko, T., Mulderrig, L., Mudie, L., Pleasance, E., Shepherd, R., Smith, R., Stebbings, L., Stephens, P., Tang, G., Tarpey, P. S., Turner, R., Turrell, K., Varian, J., West, S., Widaa, S., Wray, P., Collins, V. P., Ichimura, K., Law,

S., Wong, J., Yuen, S. T., Leung, S. Y., Tonon, G., DePinho, R. A., Tai, Y.-T., Anderson, K. C., Kahnoski, R. J., Massie, A., Khoo, S. K., Teh, B. T., Stratton, M. R., & Futreal, P. A. (2009). Somatic mutations of the histone H3K27 demethylase gene UTX in human cancer. *Nature genetics, 41*(5), 521-523.

van Ingen, H., van Schaik, F. M. A., Wienk, H., Ballering, J., Rehmann, H., Dechesne, A. C., Kruijzer, J. A. W., Liskamp, R. M. J., Timmers, H. T. M., & Boelens, R. (2008). Structural Insight into the Recognition of the H3K4me3 Mark by the TFIID Subunit TAF3. *Structure, 16*(8), 1245-1256.

Vannini, A., & Cramer, P. (2012). Conservation between the RNA Polymerase I, II, and III Transcription Initiation Machineries. *Molecular Cell, 45*(4), 439-446.

Vaquerizas, J. M., Kummerfeld, S. K., Teichmann, S. A., & Luscombe, N. M. (2009). A census of human transcription factors: function, expression and evolution. *Nature Reviews Genetics, 10*, 252.

Vasanwala, F. H., Kusam, S., Toney, L. M., & Dent, A. L. (2002). Repression of AP-1 Function: A Mechanism for the Regulation of Blimp-1 Expression and B Lymphocyte Differentiation by the B Cell Lymphoma-6 Protooncogene. *The Journal of Immunology, 169*(4), 1922.

Velichutina, I., Shaknovich, R., Geng, H., Johnson, N. A., Gascoyne, R. D., Melnick, A. M., & Elemento, O. (2010). EZH2-mediated epigenetic silencing in germinal center B cells contributes to proliferation and lymphomagenesis. *Blood, 116*(24), 5247.

Venkatesh, S., Smolle, M., Li, H., Gogol, M. M., Saint, M., Kumar, S., Natarajan, K., & Workman, J. L. (2012). Set2 methylation of histone H3 lysine 36 suppresses histone exchange on transcribed genes. *Nature, 489*, 452.

Veraldi, K. L., Arhin, G. K., Martincic, K., Chung-Ganster, L. H., Wilusz, J., & Milcarek, C. (2001). hnRNP F influences binding of a 64-kilodalton subunit of cleavage stimulation factor to mRNA precursors in mouse B cells. *Mol Cell Biol, 21*(4), 1228-1238.

Vettermann, C., & Schlissel, M. S. (2010). Allelic exclusion of immunoglobulin genes: models and mechanisms. *Immunological reviews, 237*(1), 22-42.

Victora, G. D., Schwickert, T. A., Fooksman, D. R., Kamphorst, A. O., Meyer-Hermann, M., Dustin, M. L., & Nussenzweig, M. C. (2010). Germinal Center Dynamics Revealed by Multiphoton Microscopy with a Photoactivatable Fluorescent Reporter. *Cell, 143*(4), 592-605.

Vincent, S. D., Dunn, N. R., Sciammas, R., Shapiro-Shalef, M., Davis, M. M., Calame, K., Bikoff, E. K., & Robertson, E. J. (2005). The zinc finger transcriptional repressor Blimp1/Prdm1 is dispensable for early axis formation but is required for specification of primordial germ cells in the mouse. *Development, 132*(6), 1315.

Vivier, E., Tomasello, E., Baratin, M., Walzer, T., & Ugolini, S. (2008). Functions of natural killer cells. *Nature Immunology, 9*, 503.

Walker, B. A., Boyle, E. M., Wardell, C. P., Murison, A., Begum, D. B., Dahir, N. M., Proszek, P. Z., Johnson, D. C., Kaiser, M. F., Melchor, L., Aronson, L. I., Scales, M., Pawlyn, C., Mirabella, F., Jones, J. R., Brioli, A., Mikulasova, A., Cairns, D. A., Gregory, W. M., Quartilho, A., Drayson, M. T., Russell, N., Cook, G., Jackson, G. H., Leleu, X., Davies, F. E., & Morgan, G. J. (2015). Mutational Spectrum, Copy Number Changes, and Outcome: Results of a Sequencing Study of Patients With Newly Diagnosed Myeloma. *Journal of Clinical Oncology, 33*(33), 3911-3920.

Wang, H., Hu, X., Ding, X., Dou, Z., Yang, Z., Shaw, A. W., Teng, M., Cleveland, D. W., Goldberg, M. L., Niu, L., & Yao, X. (2004). Human Zwint-1 Specifies Localization of Zeste White 10 to Kinetochores and Is Essential for Mitotic Checkpoint Signaling. *Journal of Biological Chemistry, 279*(52), 54590-54598.

Wang, L., Du, Y., Ward, James M., Shimbo, T., Lackford, B., Zheng, X., Miao, Y.-l., Zhou, B., Han, L., Fargo, David C., Jothi, R., Williams, Carmen J., Wade, Paul A., & Hu, G. (2014). INO80 Facilitates Pluripotency Gene Activation in Embryonic Stem Cell Self-Renewal, Reprogramming, and Blastocyst Development. *Cell Stem Cell, 14*(5), 575-591.

Wang, W.-F., Yan, L., Liu, Z., Liu, L.-X., Lin, J., Liu, Z.-Y., Chen, X.-P., Zhang, W., Xu, Z.-Z., Shi, T., Li, J.-M., Zhao, Y.-L., Meng, G., Xia, Y., Li, J.-Y., & Zhu, J. (2017). HSP70-Hrd1 axis precludes the oncorepressor potential of N-terminal misfolded Blimp-1s in lymphoma cells. *Nature Communications, 8*(1), 363.

Watanabe, K., Tateishi, S., Kawasuji, M., Tsurimoto, T., Inoue, H., & Yamaizumi, M. (2004). Rad18 guides polη to replication stalling sites through physical interaction and PCNA monoubiquitination. *The EMBO journal, 23*(19), 3886-3896.

Welburn, J. P. I., Vleugel, M., Liu, D., Yates, J. R., Lampson, M. A., Fukagawa, T., & Cheeseman, I. M. (2010). Aurora B Phosphorylates Spatially Distinct Targets to Differentially Regulate the Kinetochore-Microtubule Interface. *Molecular Cell, 38*(3), 383-392.

Welinder, E., Mansson, R., Mercer, E. M., Bryder, D., Sigvardsson, M., & Murre, C. (2011). The transcription factors E2A and HEB act in concert to induce the expression of FOXO1 in the common lymphoid progenitor. *Proc Natl Acad Sci U S A, 108*(42), 17402-17407.

Weller, S., Braun, M. C., Tan, B. K., Rosenwald, A., Cordier, C., Conley, M. E., Plebani, A., Kumararatne, D. S., Bonnet, D., Tournilhac, O., Tchernia, G., Steiniger, B., Staudt, L. M., Casanova, J.-L., Reynaud, C.-A., & Weill, J.-C. (2004). Human blood IgM "memory" B cells are circulating splenic marginal zone B cells harboring a prediversified immunoglobulin repertoire. *Blood, 104*(12), 3647.

Weller, S., Faili, A., Garcia, C., Braun, M. C., Le Deist, F., de Saint Basile, G., Hermine, O., Fischer, A., Reynaud, C.-A., & Weill, J.-C. (2001). CD40-CD40L independent Ig gene hypermutation suggests a second B cell diversification pathway in humans. *Proceedings of the National Academy of Sciences, 98*(3), 1166.

Weller, S., Mamani-Matsuda, M., Picard, C., Cordier, C., Lecoeuche, D., Gauthier, F., Weill, J.-C., & Reynaud, C.-A. (2008). Somatic diversification in the absence of antigen-driven responses is the hallmark of the IgM⁺IgD⁺CD27⁺ B cell repertoire in infants. *The Journal of Experimental Medicine, 205*(6), 1331.

Wesche, H., Henzel, W. J., Shillinglaw, W., Li, S., & Cao, Z. (1997). MyD88: An Adapter That Recruits IRAK to the IL-1 Receptor Complex. *Immunity, 7*(6), 837-847.

Whitfield, T. W., Wang, J., Collins, P. J., Partridge, E. C., Aldred, S. F., Trinklein, N. D., Myers, R. M., & Weng, Z. (2012). Functional analysis of transcription factor binding sites in human promoters. *Genome Biol, 13*(9), R50.

Whyte, W. A., Bilodeau, S., Orlando, D. A., Hoke, H. A., Frampton, G. M., Foster, C. T., Cowley, S. M., & Young, R. A. (2012). Enhancer decommissioning by LSD1 during embryonic stem cell differentiation. *Nature, 482*, 221.

Wickham, H. (2016). *ggplot2: Elegant Graphics for Data Analysis*: Springer-Verlag New York.

Wilson, T. M., Vaisman, A., Martomo, S. A., Sullivan, P., Lan, L., Hanaoka, F., Yasui, A., Woodgate, R., & Gearhart, P. J. (2005). MSH2–MSH6 stimulates DNA polymerase η, suggesting a role for A:T mutations in antibody genes. *The Journal of Experimental Medicine, 201*(4), 637-645.

Wohlschlegel, J. A., Dhar, S. K., Prokhorova, T. A., Dutta, A., & Walter, J. C. (2002). Xenopus Mcm10 Binds to Origins of DNA Replication after Mcm2-7 and Stimulates Origin Binding of Cdc45. *Molecular Cell, 9*(2), 233-240.

Wong, C. W., & Privalsky, M. L. (1998). Components of the SMRT corepressor complex exhibit distinctive interactions with the POZ domain oncoproteins PLZF, PLZF-RARalpha, and BCL-6. *J Biol Chem, 273*(42), 27695-27702.

Wong, R. W. J., Ngoc, P. C. T., Leong, W. Z., Yam, A. W. Y., Zhang, T., Asamitsu, K., Iida, S., Okamoto, T., Ueda, R., Gray, N. S., Ishida, T., & Sanda, T. (2017). Enhancer profiling identifies critical cancer genes and characterizes cell identity in adult T-cell leukemia. *Blood, 130*(21), 2326.

Wu, L., Bachrati, C. Z., Ou, J., Xu, C., Yin, J., Chang, M., Wang, W., Li, L., Brown, G. W., & Hickson, I. D. (2006). BLAP75/RMI1 promotes the BLM-dependent dissolution of homologous recombination intermediates. *Proceedings of the National Academy of Sciences of the United States of America, 103*(11), 4068.

Wu, M., Lu, W., Santos, R. E., Frattini, M. G., & Kelly, T. J. (2014). Geminin inhibits a late step in the formation of human pre-replicative complexes. *J Biol Chem, 289*(44), 30810-30821.

Wu, Z. L., Zheng, S. S., Li, Z. M., Qiao, Y. Y., Aau, M. Y., & Yu, Q. (2009). Polycomb protein EZH2 regulates E2F1-dependent apoptosis

through epigenetically modulating Bim expression. *Cell Death And Differentiation, 17*, 801.

Xi, H., Shulha, H. P., Lin, J. M., Vales, T. R., Fu, Y., Bodine, D. M., McKay, R. D. G., Chenoweth, J. G., Tesar, P. J., Furey, T. S., Ren, B., Weng, Z., & Crawford, G. E. (2007). Identification and Characterization of Cell Type–Specific and Ubiquitous Chromatin Regulatory Structures in the Human Genome. *PLOS Genetics, 3*(8), e136.

Xin, B., & Rohs, R. (2018). Relationship between histone modifications and transcription factor binding is protein family specific. *Genome Research, 28*(3), 321-333.

Xiong, Y., Hannon, G. J., Zhang, H., Casso, D., Kobayashi, R., & Beach, D. (1993). p21 is a universal inhibitor of cyclin kinases. *Nature, 366*(6456), 701-704.

Xiong, Y., Liu, L., Xia, Y., Qi, Y., Chen, Y., Chen, L., Zhang, P., Kong, Y., Qu, Y., Wang, Z., Lin, Z., Chen, X., Xiang, Z., Wang, J., Bai, Q., Zhang, W., Yang, Y., Guo, J., & Xu, J. (2019). Tumor infiltrating mast cells determine oncogenic HIF-2α-conferred immune evasion in clear cell renal cell carcinoma. *Cancer Immunology, Immunotherapy*.

Xu, C., Bian, C., Yang, W., Galka, M., Ouyang, H., Chen, C., Qiu, W., Liu, H., Jones, A. E., MacKenzie, F., Pan, P., Li, S. S.-C., Wang, H., & Min, J. (2010). Binding of different histone marks differentially regulates the activity and specificity of polycomb repressive complex 2 (PRC2). *107*(45), 19266-19271.

Xu, H., Xu, K., He, H. H., Zang, C., Chen, C.-H., Chen, Y., Qin, Q., Wang, S., Wang, C., Hu, S., Li, F., Long, H., Brown, M., & Liu, X. S. (2016). Integrative Analysis Reveals the Transcriptional Collaboration between EZH2 and E2F1 in the Regulation of Cancer-Related Gene Expression. *Molecular Cancer Research, 14*(2), 163.

Xu, K., Wu, Z. J., Groner, A. C., He, H. H., Cai, C., Lis, R. T., Wu, X., Stack, E. C., Loda, M., Liu, T., Xu, H., Cato, L., Thornton, J. E., Gregory, R. I., Morrissey, C., Vessella, R. L., Montironi, R., Magi-Galluzzi, C., Kantoff, P. W., Balk, S. P., Liu, X. S., & Brown, M. (2012). EZH2 Oncogenic Activity in Castration-Resistant Prostate Cancer Cells Is Polycomb-Independent. *Science, 338*(6113), 1465-1469.

Xu, Z., Zan, H., Pone, E. J., Mai, T., & Casali, P. (2012). Immunoglobulin class-switch DNA recombination: induction, targeting and beyond. *Nature Reviews Immunology, 12*, 517.

Yaccoby, S., Pearse, R. N., Johnson, C. L., Barlogie, B., Choi, Y., & Epstein, J. (2002). Myeloma interacts with the bone marrow microenvironment to induce osteoclastogenesis and is dependent on osteoclast activity. *British Journal of Haematology, 116*(2), 278-290.

Yamaguchi, Y., Takagi, T., Wada, T., Yano, K., Furuya, A., Sugimoto, S., Hasegawa, J., & Handa, H. (1999). NELF, a multisubunit complex containing RD, cooperates with DSIF to repress RNA polymerase II elongation. *Cell, 97*(1), 41-51.

Yang, G., Buhrlage, S. J., Tan, L., Liu, X., Chen, J., Xu, L., Tsakmaklis, N., Chen, J. G., Patterson, C. J., Brown, J. R., Castillo, J. J., Zhang, W., Zhang, X., Liu, S., Cohen, P., Hunter, Z. R., Gray, N., & Treon, S. P.

(2016). HCK is a survival determinant transactivated by mutated MYD88, and a direct target of ibrutinib. *Blood, 127*(25), 3237.

Yang, G., Zhou, Y., Liu, X., Xu, L., Cao, Y., Manning, R. J., Patterson, C. J., Buhrlage, S. J., Gray, N., Tai, Y.-T., Anderson, K. C., Hunter, Z. R., & Treon, S. P. (2013). A mutation in MYD88 (L265P) supports the survival of lymphoplasmacytic cells by activation of Bruton tyrosine kinase in Waldenström macroglobulinemia. *Blood, 122*(7), 1222.

Yang, H., Qiu, Q., Gao, B., Kong, S., Lin, Z., & Fang, D. (2014). Hrd1-mediated BLIMP-1 ubiquitination promotes dendritic cell MHCII expression for CD4 T cell priming during inflammation. *The Journal of Experimental Medicine, 211*(12), 2467.

Yao, N., Turner, J., Kelman, Z., Stukenberg, P. T., Dean, F., Shechter, D., Pan, Z.-Q., Hurwitz, J., & O'Donnell, M. (1996). Clamp loading, unloading and intrinsic stability of the PCNA, β and gp45 sliding clamps of human, E. coli and T4 replicases. *Genes to Cells, 1*(1), 101-113.

Yap, D. B., Chu, J., Berg, T., Schapira, M., Cheng, S. W. G., Moradian, A., Morin, R. D., Mungall, A. J., Meissner, B., Boyle, M., Marquez, V. E., Marra, M. A., Gascoyne, R. D., Humphries, R. K., Arrowsmith, C. H., Morin, G. B., & Aparicio, S. A. J. R. (2011). Somatic mutations at EZH2 Y641 act dominantly through a mechanism of selectively altered PRC2 catalytic activity, to increase H3K27 trimethylation. *Blood, 117*(8), 2451.

Ye, B. H., Cattoretti, G., Shen, Q., Zhang, J., Hawe, N., de Waard, R., Leung, C., Nouri-Shirazi, M., Orazi, A., Chaganti, R. S., Rothman, P., Stall, A. M., Pandolfi, P. P., & Dalla-Favera, R. (1997). The BCL-6 proto-oncogene controls germinal-centre formation and Th2-type inflammation. *Nat Genet, 16*(2), 161-170.

Ying, H. Y., Su, S. T., Hsu, P. H., Chang, C. C., Lin, I. Y., Tseng, Y. H., Tsai, M. D., Shih, H. M., & Lin, K. I. (2012). SUMOylation of Blimp - 1 is critical for plasma cell differentiation. *EMBO reports, 13*(7), 631.

Yoshida, H., Matsui, T., Yamamoto, A., Okada, T., & Mori, K. (2001). XBP1 mRNA Is Induced by ATF6 and Spliced by IRE1 in Response to ER Stress to Produce a Highly Active Transcription Factor. *Cell, 107*(7), 881-891.

Yoshimura, M., Kohzaki, M., Nakamura, J., Asagoshi, K., Sonoda, E., Hou, E., Prasad, R., Wilson, S. H., Tano, K., Yasui, A., Lan, L., Seki, M., Wood, R. D., Arakawa, H., Buerstedde, J.-M., Hochegger, H., Okada, T., Hiraoka, M., & Takeda, S. (2006). Vertebrate POLQ and POLβ Cooperate in Base Excision Repair of Oxidative DNA Damage. *Molecular Cell, 24*(1), 115-125.

Yu, J., Angelin-Duclos, C., Greenwood, J., Liao, J., & Calame, K. (2000). Transcriptional Repression by Blimp-1 (PRDI-BF1) Involves Recruitment of Histone Deacetylase. *Molecular and Cellular Biology, 20*(7), 2592-2603.

Yuan, D., Gao, N., & Jennings, P. (2010). Interactions Between B Lymphocytes and NK Cells: An Update. In J. Zimmer (Ed.), *Natural*

Killer Cells: At the Forefront of Modern Immunology (pp. 345-368). Berlin, Heidelberg: Springer Berlin Heidelberg.
Yun, M., Wu, J., Workman, J. L., & Li, B. (2011). Readers of histone modifications. *Cell Research, 21*, 564.
Zabidi, M. A., Arnold, C. D., Schernhuber, K., Pagani, M., Rath, M., Frank, O., & Stark, A. (2014). Enhancer–core-promoter specificity separates developmental and housekeeping gene regulation. *Nature, 518*, 556.
Zakharova, I. S., Shevchenko, A. I., & Zakian, S. M. (2009). Monoallelic gene expression in mammals. *Chromosoma, 118*(3), 279-290.
Zan, H., Zhang, J., Al-Qahtani, A., Pone, E. J., White, C. A., Lee, D., Yel, L., Mai, T., & Casali, P. (2011). Endonuclease G plays a role in immunoglobulin class switch DNA recombination by introducing double-strand breaks in switch regions. *Mol Immunol, 48*(4), 610-622.
Zeng, L., Zhang, Q., Li, S., Plotnikov, A. N., Walsh, M. J., & Zhou, M.-M. (2010). Mechanism and regulation of acetylated histone binding by the tandem PHD finger of DPF3b. *Nature, 466*, 258.
Zentner, G. E., & Henikoff, S. (2013). Regulation of nucleosome dynamics by histone modifications. *Nature Structural & Molecular Biology, 20*, 259.
Zhan, F., Hardin, J., Kordsmeier, B., Bumm, K., Zheng, M., Tian, E., Sanderson, R., Yang, Y., Wilson, C., Zangari, M., Anaissie, E., Morris, C., Muwalla, F., van Rhee, F., Fassas, A., Crowley, J., Tricot, G., Barlogie, B., & Shaughnessy, J. (2002). Global gene expression profiling of multiple myeloma, monoclonal gammopathy of undetermined significance, and normal bone marrow plasma cells. *Blood, 99*(5), 1745.
Zhan, F., Tian, E., Bumm, K., Smith, R., Barlogie, B., & Shaughnessy, J. (2003). Gene expression profiling of human plasma cell differentiation and classification of multiple myeloma based on similarities to distinct stages of late-stage B-cell development. *Blood, 101*(3), 1128.
Zhang, H., Okada, S., Hatano, M., Okabe, S., & Tokuhisa, T. (2001). A new functional domain of Bcl6 family that recruits histone deacetylases. *Biochimica et Biophysica Acta (BBA) - Molecular Cell Research, 1540*(3), 188-200.
Zhang, H., Zhang, H., Zhao, M., Lv, Z., Zhang, X., Qin, X., Wang, H., Wang, S., Su, J., Lv, X., Liu, H., Du, W., Zhou, W., Chen, X., & Fei, K. (2013). MiR-138 Inhibits Tumor Growth Through Repression of EZH2 in Non-Small Cell Lung Cancer. *Cellular Physiology and Biochemistry, 31*(1), 56-65.
Zhang, Y., Liu, T., Meyer, C. A., Eeckhoute, J., Johnson, D. S., Bernstein, B. E., Nusbaum, C., Myers, R. M., Brown, M., Li, W., & Liu, X. S. (2008). Model-based analysis of ChIP-Seq (MACS). *Genome Biol, 9*(9), R137.
Zhao, J., Zhai, B., Gygi, S. P., & Goldberg, A. L. (2015). mTOR inhibition activates overall protein degradation by the ubiquitin proteasome

system as well as by autophagy. *Proceedings of the National Academy of Sciences, 112*(52), 15790-15797.
Zhao, W., He, X., Hoadley, K. A., Parker, J. S., Hayes, D. N., & Perou, C. M. (2014). Comparison of RNA-Seq by poly (A) capture, ribosomal RNA depletion, and DNA microarray for expression profiling. *BMC Genomics, 15*(1), 419.
Zhao, Y., Harrison, D. L., Song, Y., Ji, J., Huang, J., & Hui, E. (2018). Antigen-Presenting Cell-Intrinsic PD-1 Neutralizes PD-L1 in cis to Attenuate PD-1 Signaling in T Cells. *Cell Reports, 24*(2), 379-390.e376.
Zhou, Y., Liu, X., Xu, L., Hunter, Z. R., Cao, Y., Yang, G., Carrasco, R., & Treon, S. P. (2014). Transcriptional repression of plasma cell differentiation is orchestrated by aberrant over-expression of the ETS factor SPIB in Waldenström macroglobulinaemia. *British Journal of Haematology, 166*(5), 677-689.
Zhu, H., Zhang, L., Dong, F., Guo, W., Wu, S., Teraishi, F., Davis, J. J., Chiao, P. J., & Fang, B. (2005). Bik/NBK accumulation correlates with apoptosis-induction by bortezomib (PS-341, Velcade) and other proteasome inhibitors. *Oncogene, 24*, 4993.
Zhu, L. J., Gazin, C., Lawson, N. D., Pages, H., Lin, S. M., Lapointe, D. S., & Green, M. R. (2010). ChIPpeakAnno: a Bioconductor package to annotate ChIP-seq and ChIP-chip data. *BMC Bioinformatics, 11*, 237.
Zhu, X., Ling, J., Zhang, L., Pi, W., Wu, M., & Tuan, D. (2007). A facilitated tracking and transcription mechanism of long-range enhancer function. *Nucleic Acids Research, 35*(16), 5532-5544.
Zhu, Z., Chung, W.-H., Shim, E. Y., Lee, S. E., & Ira, G. (2008). Sgs1 Helicase and Two Nucleases Dna2 and Exo1 Resect DNA Double-Strand Break Ends. *Cell, 134*(6), 981-994.
Zhu, Z., Tang, J., Wang, J., Duan, G., Zhou, L., & Zhou, X. (2016). MiR-138 Acts as a Tumor Suppressor by Targeting EZH2 and Enhances Cisplatin-Induced Apoptosis in Osteosarcoma Cells. *PLOS ONE, 11*(3), e0150026.
Zhuang, Y., Soriano, P., & Weintraub, H. (1994). The helix-loop-helix gene E2A is required for B cell formation. *Cell, 79*(5), 875-884.
Zingg, D., Arenas-Ramirez, N., Sahin, D., Rosalia, R. A., Antunes, A. T., Haeusel, J., Sommer, L., & Boyman, O. (2017). The Histone Methyltransferase Ezh2 Controls Mechanisms of Adaptive Resistance to Tumor Immunotherapy. *Cell Reports, 20*(4), 854-867.
Zou, L., Mitchell, J., & Stillman, B. (1997). CDC45, a novel yeast gene that functions with the origin recognition complex and Mcm proteins in initiation of DNA replication. *Molecular and Cellular Biology, 17*(2), 553.

Original publications

Paper I

The BLIMP1 – EZH2 nexus in a non-Hodgkin lymphoma

Kimberley Jade Anderson[1,2,6], Árný Björg Ósvaldsdóttir[1,2,6], Birgit Atzinger[1,2,6], Gunnhildur Ásta Traustadóttir[1,6], Kirstine Nolling Jensen[3,4,6], Aðalheiður Elín Lárusdóttir[1,2,6], Jón Þór Bergþorsson[2,5,6], Ingibjörg Harðardóttir[3,4,6], Erna Magnúsdóttir[1,2,6]

1. Department of Anatomy, Faculty of Medicine, Vatnsmýrarvegur 16, 101 Reykjavik, Iceland
2. Department of Biomedical Science, Faculty of Medicine, 101 Reykjavík, Iceland
3. Department of Biochemistry and Molecular Biology, Faculty of Medicine, 101 Reykjavík, Iceland
4. Department of Immunology, Landspitali-The National University Hospital of Iceland, 101 Reykjavik, Iceland
5. Department of Laboratory Haematology, Landspitali-The National University Hospital of Iceland, 101 Reykjavik, Iceland
6. The University of Iceland Biomedical Center, Vatnsmýrarvegur 16, 101 Reykjavík Iceland

Abstract

Waldenström's macroglobulinemia (WM) is a non-Hodgkin lymphoma, affecting antibody-secreting lymphoplasmacytic cells in the bone marrow. BLIMP1 is a key transcriptional repressor, which drives the transition from B cells to plasma cells and is essential for antibody secretion. Despite this, a potential role for BLIMP1 in WM has not yet been explored. Here we provide evidence of a crucial role for BLIMP1 in the survival of WM cells. We further demonstrate that BLIMP1 is necessary for the expression of the histone methyltransferase EZH2 in both WM and multiple myeloma, most likely through a regulation of proteasomal targeting of EZH2. Chromatin immunoprecipitation analysis and genome wide transcriptome profiling show that the two factors co-operate in regulating genes involved in cancer cell immune evasion. Co-cultures of natural killer cells and WM cells further reveal that both factors participate directly in immune evasion, promoting escape from natural killer cell mediated cytotoxicity. Together, the interplay of BLIMP1 and EZH2 plays a vital role in promoting the survival of WM cells.

Introduction

Waldenström's macroglobulinemia (WM) is a disease characterised by the expansion of monoclonal lymphoplasmacytic cells in the bone marrow, which secrete immunoglobulin M (IgM) (Vijay & Gertz, 2007). Around 3-6 people per million are diagnosed with WM every year, although this varies by geographical region (Brandefors, Melin et al., 2018, Iwanaga, Chiang et al., 2014, Kyle, Larson et al., 2018, Wang, Chen et al., 2012). The activating mutation, $MYD88^{L265P}$, is present in ~96% of untreated patients and serves as a key oncogenic driver of WM, as well as in a subset of activated B cell-like diffuse large B cell lymphoma (ABC-DLBCL) (Treon, Xu et al., 2012, Xu, Hunter et al., 2014, Yu, Li et al., 2018).

The transcription factor B-lymphocyte induced maturation protein-1 (BLIMP1) is a master regulator of terminal B-cell development, and acts via recruitment of co-factors to chromatin (Győry, Wu et al., 2004, Ren, Chee et al., 1999, Yu, Angelin-Duclos et al., 2000). BLIMP1 also has essential functions in the development of many cells and tissues, including primordial germ cells (Ohinata, Payer et al., 2005), the epidermis (Magnúsdóttir, Kalachikov et al., 2007), and the placenta (Vincent, Dunn et al., 2005), to name a few. Interestingly, BLIMP1 is known to be induced downstream of toll like receptor engagement (Morgan, Magnusdottir et al., 2009). Furthermore, LPS-stimulated B cells from MYD88 knock-out mice show decreased expression levels of *Prdm1*, the gene encoding BLIMP1, showing that BLIMP1 is induced downstream of MYD88 (Pasare & Medzhitov, 2005). BLIMP1 was described early on as a repressor of immune signalling mechanisms in B cells, including the Class II transactivator (*CIITA*) (Piskurich, Lin et al., 2000b, Tooze, Stephenson et al., 2006), B cell receptor signalling, and surface antigens and receptors (Shaffer, Lin et al., 2002). It is a key regulator of plasma cell terminal differentiation and antibody secretion (Minnich, Tagoh et al., 2016, Shaffer et al., 2002, Tellier, Shi et al., 2016) and is necessary for the survival of multiple myeloma cells (Lin, Kuo et al., 2007). Conversely, BLIMP1 is frequently inactivated in DLBCL, and is thought to function as a tumour suppressor in that context, consistent with its role in repressing cell cycle genes during the transition from mature B-cells to plasma cells (Calado, Zhang et al., 2010, Mandelbaum, Bhagat et al., 2010, Pasqualucci, Compagno et al., 2006, Shaffer et al., 2002). Furthermore, in WM, there are frequent heterozygous losses of *PRDM1* (Schop, Kuehl et al., 2002), however despite this, BLIMP1 is expressed in a subset of WM lymphoplasmacytic cells (Roberts, Chadburn et al., 2013, Zhou, Liu et al., 2014), consistent with the requirement for BLIMP1 in antibody secretion (Minnich et al., 2016, Savitsky & Calame, 2006, Shapiro-Shelef, Lin et al., 2003). Given the contradictory roles of BLIMP1 in ABC-DLBCL and myeloma, its involvement in WM has been critically under studied.

Another important player in plasma cell differentiation, EZH2 has been described as both a physical and genetic interaction partner of BLIMP1 (Guo, Price et al., 2018, Minnich et al., 2016). The interaction was first suggested in mouse

primordial germ cells (PGCs), where BLIMP1 and EZH2 were found to bind to the same sites on a genome-wide scale (Kurimoto, Yabuta et al., 2015, Magnúsdóttir, Dietmann et al., 2013). EZH2 functions as the catalytic component of the polycomb repressive complex 2, placing methyl groups on lysine 27 of histone 3, typically tri-methylation (H3K27me3), to repress transcription (Czermin, Melfi et al., 2002, Müller, Hart et al., 2002). EZH2 is essential for embryonic development (Carroll, Erhardt et al., 2001). In addition, EZH2 has frequent activating mutations in germinal centre and follicular DLBCL and is a promising therapeutic target (Kim & Roberts, 2016, Morin, Johnson et al., 2010). Surprisingly, while aberrant regulation of histone modifications has been implied in WM pathogenesis (Roccaro, Sacco et al., 2010), the role of EZH2 is yet to be investigated.

In this study, we sought to examine the role of BLIMP1 in WM, and its potential interplay with EZH2 in the disease. We demonstrate for the first time a role for BLIMP1 in regulating WM cell survival and in maintaining EZH2 protein levels. We identify a large overlap in transcriptional targets of the two factors but only a small degree of proximal binding of BLIMP1 with the H3K27me3 mark, implying that the factors repress transcription on an overlapping set of genes in parallel fashion. Finally, we reveal novel roles for BLIMP1 and EZH2 in evasion from natural-killer (NK) cell mediated cytotoxicity.

Results

BLIMP1 is important for cell survival in Waldenström's macroglobulinemia

As BLIMP1 is expressed in $CD19^{+}$ cells in a subset of WM patients (Roberts et al., 2013, Zhou et al., 2014), and given its roles in myeloma and DLBCL, we wanted to determine whether it plays a role in WM. Interestingly, in published transcriptome profiles from WM patients, the mRNA levels of *PRDM1*, the gene encoding BLIMP1, were elevated in WM cells from patients carrying the the $MYD88^{L265P}$ mutation (Hunter, Xu et al., 2016), which is associated with poorer prognosis in WM compared to $MYD88^{WT}$ (Treon, Cao et al., 2014). This suggests that BLIMP1

expression is induced downstream of $MYD88^{L265P}$. As BLIMP1 is known to be expressed in myeloma cell lines, we compared its expression in the myeloma cell line OPM-2 to that of the three WM cell lines RPCI-WM1 (RP), MWCL-1 (MW) and BCWM.1 (BC) by immunofluorescence staining (Fig 1A). All the cell lines expressed BLIMP1, with the RP cells showing relatively uniform expression levels in all cells. However, the MW and BC cells showed more heterogeneous protein levels, with 43% of MW and 18% of BC cells expressing BLIMP1 above background levels. The heterogeneity of BLIMP1 expression in these cell lines does not rule out its importance, as the symptomatic antibody-secreting compartment is likely driven by BLIMP1. To examine the potential role of BLIMP1 in WM, we engineered the RP cell line with two distinct doxycycline (dox)-inducible artificial miRNAs targeting the *PRDM1* mRNA (*PmiR1 and PmiR2)* to knock-down (KD) BLIMP1 or a non-targeting control miRNA (*NTmiR*). The induction of *PmiR1* and *PmiR2* led to a 76% and 60% decrease in BLIMP1 protein respectively (Fig 1B). We also used *PmiR1* to engineer MW cells leading to a 60% reduction in BLIMP1 protein levels (Fig 1C).

BLIMP1 KD in WM cells led to decreased cell survival, with 62% and 71% live cells remaining in RP and MW cell cultures respectively 48h post dox addition, (Fig 1D) and only 3% viable cells remaining in RP cultures at five days after *PmiR1* induction. Despite an initial decrease in viability, by day 5, MW cells recovered their viability, likely due to cells without BLIMP1 KD overtaking the culture as a uniform knock-down in all the cells was not obtained. The proportion of apoptotic cells went up in RP cells by 2.64 and 2.25-fold upon *PmiR1* and *PmiR2* induction respectively, (Fig EV1A). While BLIMP1 KD led to a decrease in viability of MW cells as described above, the increase in apoptosis levels at 48 h did not reach statistical significance (Fig EV1B). The smaller effect of BLIMP1 KD in the MW cell line could be due to having a lower degree of KD in these cells, or because of the high proportion of cells lacking high levels of BLIMP1. Attempts at knocking down BLIMP1 in the BC cell line were inconclusive due to the lack of stable miR transduction and maintenance, presumably because of leakiness of miR expression from the inducible promoter.

We performed a genetic complementation test, where RP *PmiR1* cells were transduced with a lentivirus harbouring either *PmiR1*-resistant BLIMP1-EGFP encoding cDNA or EGFP (Lois, Hong et al., 2002) (Fig 1E). Crucially, this revealed that the decrease in cell viability could be rescued in cells transduced with miR-resistant BLIMP1 (81% viable cells, normalized to BLIMP1-transduced *NTmiR* RP cells) compared to the EGFP control (65% viable cells, normalized to BLIMP1-EGFP-transduced *NTmiR* cells) at 48h post BLIMP1-KD induction (Fig 1F). At five days post BLIMP1-KD induction 57% of the BLIMP1-transduced cells were viable compared to only 3% of the EGFP-transduced cells (Fig 1F). Additionally, 5 days post KD, the miR resistant BLIMP1-transduced cells were still viable (23% resazurin reduction) compared to EGFP-transduced cells (6%) (Fig 1G). Together, these data show that BLIMP1 is a survival factor in WM cells, and that BLIMP1-mediated viability is likely due to the suppression of apoptosis. This is in line with previous findings of BLIMP1 suppressing apoptosis in myeloma through its interaction with Aiolos (Hung, Su et al., 2016).

BLIMP1 expression maintains EZH2 protein levels

The expression of BLIMP1 is induced by MYD88, among other factors. MYD88 is necessary for initiation of the antiviral germinal centre (GC) response (Hou, Saudan et al., 2011). The GC reaction is the mechanism by which B cells undergo somatic hypermutation and class switch recombination in order to increase their affinity to antigens (Basso & Dalla-Favera, 2015). Another essential factor in the GC reaction is the histone methyltransferase EZH2, which drives proliferation of GC B cells (Béguelin, Popovic et al., 2013). Furthermore, EZH2 is necessary for the early T-independent development of plasma cells in response to a viral antigen (Guo et al., 2018). As several lines of evidence from studies of mouse plasmablasts and PGCs show a functional overlap and perhaps a direct interaction between BLIMP1 and EZH2, we sought to investigate the potential interplay between the two factors in WM (Kurimoto et al., 2015, Magnúsdóttir et al., 2013, Minnich et al., 2016). Our first line of inquiry revealed a decrease in EZH2 expression upon BLIMP1 KD in RP cells (Fig 2A). Interestingly, this result was replicated in OPM-2 multiple myeloma

cells harbouring *PmiR1* (Fig 2B). Simultaneous transduction of RP cells with the miR-resistant BLIMP1 construct as above (Fig 1E) restored EZH2 protein levels, confirming the specificity of the KD (Fig 2C, quantified in Fig EV2A). Furthermore, the signal intensities of BLIMP1 and EZH2 within approximately 2×10^4 individual nuclei were positively correlated in two separate experiments ($R^2 = 0.338$, $R^2 = 0.684$). These experiments for the first time, uncover a dependency of EZH2 on BLIMP1 expression.

We then sought to understand the mechanism by which BLIMP1 maintains EZH2 protein levels. To this end, we performed quantitative reverse transcription PCR (RT-qPCR) comparing *PmiR2* to *NTmiR* RP cells upon BLIMP1 KD induction. Consistent with the loss of BLIMP1 protein, we saw a potential increase in steady state *PRDM1* levels due to the loss of BLIMP1 auto-repression (Martins & Calame, 2008) (Fig 2D). However, *EZH2* mRNA levels were not decreased in the RP cell line showing that the loss of EZH2 downstream of BLIMP1 KD is at the post-transcriptional level in this cell line (Fig 2D). The levels of *EZH2* mRNA were slightly decreased in OPM2 myeloma cells (Fig 2E). However, when we treated RP *PmiR1* cells with the proteasome inhibitor MG-132, the EZH2 protein levels were restored to the same levels as that of *NTmiR* cells also treated with proteasome inhibitor (Fig 2F,G). This reveals that the modulation of EZH2 levels by BLIMP1 occurs through the inhibition of proteasome mediated protein degradation.

As EZH2 is known as a key driver of cancer cell transformation (Béguelin et al., 2013, Kleer, Cao et al., 2003) and can play a role in preventing apoptosis (Wu, Zheng et al., 2009), we sought to determine if BLIMP1 mediated WM cell survival is dependent on EZH2. To test this, we genetically complemented the loss of BLIMP1 in the RP *PmiR1* cells by lentiviral transduction of an EZH2 expression construct (Fig 2H). However, the restoration of EZH2 levels did not confer an increase in viability to the BLIMP1 KD cells, with only 2% viable cells remaining 5 days post BLIMP1-KD induction (Fig 2I). Consistent with this, the EZH2-specific catalytic inhibitor tazemetostat did not affect RP cell viability even over a 96 h period (Fig EV2B), despite a dose dependent decrease in H3K27me3 levels (Fig EV2C). Thus, BLIMP1 maintains WM cell survival independently of EZH2.

BLIMP1 KD induces large transcriptional changes

In order to investigate the molecular mechanisms underpinning the above phenotypic observations, we examined the global gene expression changes induced by BLIMP1 KD. We performed transcriptome profiling of the RP *PmiR2* and *NTmiR* cell lines following 48 h of dox treatment. We profiled *PmiR2* rather than the *PmiR1* cells because the lower extent of cell death made them more suitable for RNAseq library construction. Using a q-value cutoff of 0.05, we identified 7814 differentially expressed genes between *PmiR2* and *NTmiR* (Fig 3A and EV Table 1).

As BLIMP1 is the key repressor of the B cell transcriptional program during plasma cell differentiation (Kallies, Hasbold et al., 2004, Minnich et al., 2016, Shaffer et al., 2002, Shapiro-Shelef et al., 2003), we asked whether this mechanism was perturbed in WM where the differentiation process is somewhat halted. Previously characterized B cell lineage targets of BLIMP1, including *CIITA* (Chen, Gilbert et al., 2007, Piskurich, Lin et al., 2000a), *PAX5* (Lin, Angelin-Duclos et al., 2002), *SPIB* and *BCL6* (Shaffer et al., 2002) showed significantly increased expression following BLIMP1 KD (Fig 3B), suggesting that they are repressed by BLIMP1 in WM cells. However, other BLIMP1 targets such as *MYC* (Lin, Wong et al., 1997) and *ID3* (Shaffer et al., 2002) were unaltered. On the other hand, the plasma cell transcription factor *IRF4*, which is important for cell survival in multiple myeloma (Shaffer, Emre et al., 2008), was previously shown to be activated downstream of BLIMP1 in plasma cells (Minnich et al., 2016). Curiously, here we observed it to be induced downstream of BLIMP1 repression and therefore repressed by BLIMP1. Interestingly, and highly relevant to WM pathogenesis and treatment, the BTK inhibitor, *IBTK* was induced upon BLIMP1 KD. The inhibition of BTK via Ibrutinib is now a common treatment modality in WM (Gertz, 2019). Taken together, BLIMP1 does appear to be repressing most but not all of its canonical B cell targets in RP cells. To examine the pro-apoptotic effect of BLIMP1 KD in the RP cell line, we looked at the expression profiles for key apoptosis genes. In line with the phenotype, we observed a large number of apoptosis genes with significantly increased expression following BLIMP1 KD. These included *MAP3K5* (*ASK1*),

XAF1, *CASP4*, *CASP8*, *FAS*, *DFFA*, *JUN* and *BCL2L11* (*BIM*) amongst others (Fig 3C). Finally, we observed a significant de-repression of the *SMURF2* mRNA (EV3A). SMURF2 is an E3 ubiquitin ligase known to target EZH2 for proteasome-mediated degradation and could thus contribute to the decrease in EZH2 protein levels upon the loss of BLIMP1 (Yu, Chou et al., 2013). Taken together, BLIMP1 KD induces extensive gene expression changes in RP including the de-repression of B cell- and apoptosis-related genes, as well as *SMURF2*.

BLIMP1 and EZH2 transcriptionally regulate overlapping pathways

Because of the suggested BLIMP1-EZH2 regulatory relationship (Guo et al., 2018, Magnúsdóttir et al., 2013, Minnich et al., 2016), we wanted to determine to which extent the transcriptional changes brought about by BLIMP1 are dependent on EZH2 catalytic activity. We treated RP cells with the EZH2 catalytic inhibitor, tazemetostat, or DMSO and performed genome wide expression profiling to uncover 450 differentially expressed genes (Fig 3D and EV Table 2). There was an overall smaller amplitude of change for individual genes compared to the changes induced by BLIMP1 KD (Fig EV2C). Nevertheless, there was a highly significant overlap between transcripts increased in *PmiR2* vs. *NTmiR* and in tazemetostat vs. DMSO treated cells (184 genes, p = 1.8e-37) (Fig 3E). Meanwhile, transcripts that showed decreased expression, i.e. genes activated by BLIMP1 or EZH2, overlapped to a much smaller extent, in line with the smaller number of transcripts decreasing in expression with tazemetostat treatment (Fig 3F). Tazemetostat treatment did not induce the same amplitude or extent of transcriptional changes of B cell genes as BLIMP1 KD did, although a number of genes were still significantly de-repressed, including *PIK3CD*, *CCR7* and *ID3* (Fig 3G). Furthermore, consistent with EZH2 inhibition not causing alterations in cell survival, fewer apoptosis genes were differentially expressed compared to the BLIMP1 KD, however a number of apoptosis genes were de-repressed, including *XAF1*, *CASP4*, *FAS* and *JUN* (Fig 3H).

To investigate the pathways jointly regulated by BLIMP1 and EZH2, we performed gene set enrichment analysis using the Hallmarks collection of gene sets (Liberzon, Birger et al., 2015, Subramanian, Tamayo et al., 2005). A number of gene

sets were positively enriched with BLIMP1 KD, including interferon and TNFα responses, apoptosis and the inflammatory response (Fig EV3B). These gene sets are consistent with previous studies demonstrating BLIMP1-mediated repression of interferon responsive genes and apoptosis (Doody, Stephenson et al., 2007, Elias, Robertson et al., 2018a, Hung et al., 2016, Lin et al., 2007, Tooze et al., 2006). Additionally, the unfolded protein response and mTORC1 signalling gene sets were depleted upon BLIMP1 KD (Tellier et al., 2016). Transcriptional changes upon tazemetostat treatment were positively enriched for overlapping sets of genes with BLIMP1 KD, including interferon and TNFα responses (Fig EV3C). While far fewer gene sets were depleted in expression upon tazemetostat treatment, they all overlapped with that of the BLIMP1 KD depleted sets. This suggests that pathways involved in the immune response may be regulated in concert by BLIMP1 and EZH2. Collectively, the transcriptomic analyses demonstrate a large overlap in targets of repression by BLIMP1 and EZH2, highlighting the interplay of the two factors.

BLIMP1 binds to a set of H3K27me3 marked genes at a distance from the mark

Given the large overlap in transcriptional targets and pathways identified above, and the previously published overlaps in genome wide binding of EZH2 and BLIMP1, we next sought to define their direct genomic targets. This should help distinguish gene expression changes resulting from BLIMP1's effect on EZH2 stability, or if BLIMP1 might recruit EZH2 to chromatin.

To this end we performed chromatin immunoprecipitation coupled to deep sequencing (ChIPseq) for H3K27me3, the histone modification catalysed by EZH2, and BLIMP1 in the RP cell line. We identified 14813 peaks for the H3K27me3 mark (EV Table 3), assigned to 4198 genes (EV Table 4), whereas 505 BLIMP1 peaks were identified (EV table 5), assigned to 841 genes (EV Table 6). The previously identified DNA binding motif for BLIMP1 (Kuo & Calame, 2004) was enriched by *de novo* motif analysis in the called BLIMP1 peaks, validating the quality of the experiment (Fig EV4A). Peaks were mapped relative to their assigned transcription start sites (TSS) for BLIMP1 (Fig EV4B) and H3K27me3 (Fig EV4C).

If BLIMP1 recruits EZH2 to chromatin in WM cells, as is suggested in mouse plasmablasts (Minnich et al., 2016), we hypothesised that a large proportion of BLIMP1 peaks would be located in close proximity to H3K27me3 marks. However, only 42 peaks from each factor were present at sites within 10 kb of each other, and this overlap was not statistically significant (Fig 4A). When we plotted signal for H3K27me3 at ± 3 kb flanking BLIMP1 peaks, only a small level of enrichment was observed (Fig 4B). However, when we assigned the peaks from the respective experiments to genes, a significant overlap of 261 genes emerged between BLIMP1 and H3K27me3 in RP cells (Fig 4C), including B-cell genes *PIK3CD* and *POU2F2 (OCT2)*, the STAT1 activator *RNF19B* (*NKLAM*) (Lawrence & Kornbluth, 2016), and the cell-growth inhibitor *NUB1* (Fig 4D).

To test whether these findings can be applied more generally than only to WM cells, we performed ChIPseq for BLIMP1 and H3K27me3 in the OPM-2 (EV Tables 7-10) and NCI-H929 (EV Tables 11-14) myeloma cell lines as well as ChIPseq for EZH2 in NCI-H929 cells (EV Tables 15-16) to reveal the direct binding sites for EZH2, rather than just the polycomb mark. As before, the BLIMP1 consensus binding motif was identified within the called peaks by *de novo* motif analysis (Fig EV4D). When we mapped the peaks relative to their TSS for BLIMP1 (Fig EV4E), H3K27me3 (Fig EV4F) and EZH2 (Fig EV4G), we observed a strong enrichment of signal over TSSs. Interestingly, both the multiple myeloma cell lines displayed a much stronger enrichment of H3K27me3 over TSSs than the RP WM cell line, indicating that H3K27me3 is more often present at distal sites in the RP cell line. There was a strong enrichment for BLIMP1 binding in the OPM-2 and NCI-H929 cell lines over sites bound by BLIMP1 in the RP cell line (Fig EV4H), showing that BLIMP1 binds to mostly the same sites in WM and multiple myeloma. Contrastingly, we observed less enrichment of the H3K27me3 mark in the OPM-2 and NCI-H929 cell lines over sites marked by H3K27me3 in the RP cell line (Fig EV4I). This corresponds to the different enrichments of H3K27me3 over TSSs in th RP cells compared to the myeloma cell lines, suggesting that H3K27me3 has a different distribution in WM compared to myeloma. Interestingly, *SMURF2* was one of the genes bearing both BLIMP1 peaks and the H3K27me3 mark in the RP cell line

(Fig EV4J). As with the RP cells, we rarely observed peaks within a 10kb distance of one another when comparing BLIMP1 and H3K27me3 (Fig EV4K) or BLIMP1 and EZH2 (Fig EV4L) in the OPM-2 and NCI-H929 cell lines. When we plotted the distribution of the H3K27me3 mark and EZH2 over BLIMP1 peaks in NCI-H929 cells there was a small level of enrichment of the H3K27me3 mark flanking the BLIMP1 peaks, which is more likely to reflect general histone distribution than a specific enrichment of the H3K27me3 mark, given the paucity of called H3K27me3 peaks in the proximity of BLIMP1 binding (Fig 4E). Again, we observed a higher degree of overlap between genes assigned to peaks for the respective factors, with a statistically significant overlap between genes bound by BLIMP1 and H3K27me3 in NCI-H929 cells, but not OPM-2 cells (Fig EV4M). Genes bound both by BLIMP1 and EZH2 were not statistically over-represented (Fig EV4N). The above analyses reveal that the majority of BLIMP1 and EZH2 binding to chromatin occur at relatively distal sites between the two factors and their direct regulation on chromatin is therefore unlikely to be due to a direct physical interaction.

In order to determine the direct transcriptional targets of BLIMP1 and EZH2, we compared our ChIPseq and transcription profiling data from the RP cell line. There were 231 and 120 genes associated with BLIMP1 binding that were either induced or repressed upon BLIMP1 KD respectively (Fig 4F-G), in line with previous observations showing that BLIMP1 has a stronger effect in gene repression than activation (Magnúsdóttir et al., 2013, Magnúsdóttir et al., 2007, Minnich et al., 2016, Shaffer et al., 2002). Conversely there were 118 genes associated with the H3K27me3 mark that were induced upon tazemetostat treatment (Fig 4H), but only 7 genes with decreased expression overlapped (Fig 4I). Overall, only approximately 3% of genes marked by H3K27me3 were de-repressed following tazemetostat treatment in these experiments. This indicates that inhibition of EZH2's catalytic activity alone is insufficient to activate most H3K27me3 targets. Meanwhile, approximately one third of BLIMP1-bound genes were direct targets of transcriptional repression, indicating that BLIMP1 binding actively maintains gene repression. Taken together, as BLIMP1 and H3K27me3 are largely present at distinct sites from one another, a great extent of their co-operation is likely through their

binding to different sites on the same genes, as well as through BLIMP1 maintenance of EZH2 protein levels.

BLIMP1 represses transcription of immune surveillance and signalling molecules in concert with EZH2

As gene sets in immune signalling pathways were the most highly enriched upon BLIMP1 KD and EZH2 inhibition, we looked further into the biological significance of these insights. Indeed, immune signalling genes differentially expressed upon BLIMP1 KD can be divided into three mechanistic categories. First, BLIMP1 represses the expression of genes encoding surface ligands that activate T and NK cells, including *ICOSLG*, *TNFSF9*, *CD48*, *MICA*, *CLEC2B*, *ICAM1* and *ITGAM* (Pardoll, 2012, Vivier, Tomasello et al., 2008), MHC class II molecules including *HLA-DMA*, *HLA-DMB* and *CD1D*, along with Class II transactivator (*CIITA)*, and the immune synapse molecule *CAV1* (Fig 5A). Furthermore, MHC class I pathway members, *HLA-A* and *HLA-B* are decreased with BLIMP1 KD, in contrast to previous studies (Doody et al., 2007, Mould, Morgan et al., 2015). Second, BLIMP1 represses both immune-checkpoint inhibitory ligands and their receptors, which are de-repressed in the cells with BLIMP1 KD. These include *TNFRSF14* and *BTLA*, *HAVCR2* and *LGALS9* (Pardoll, 2012, Vivier et al., 2008). Additionally, inhibitory ligands whose receptors are not differentially expressed are also repressed by BLIMP1, including PD-L2, with BLIMP1 binding just downstream of the *PDCDLG2* gene (Fig EV5A). Of note, the PD-1 receptor encoded by *PDCD1* can also have an inhibitory effect on B cell activation (Thibult, Mamessier et al., 2013), and is expressed at a comparable level to its ligand in the RP cell line. The third mechanistic category repressed by BLIMP1 includes genes involved in the repression of downstream signalling from cytokines such as interferons and TNFα. The receptor-encoding genes *IFNGR1*, *IFNAR1*, *IFNLR1*, *TNFRSF1A* and *TNFRSF1B* are all de-repressed upon BLIMP1 KD. So too are downstream players in interferon signalling, *JAK1*, *STAT1*, *STAT2*, *IRF9* and *IFIT1*-3 and *OAS1-3*, as well as TNF pathway members *MAP3K5*, *CASP8* and *CASP9*, which are also apoptosis mediators (Fig 3C).

Around half of the genes discussed above were also significantly changed with tazemetostat treatment (Fig EV5B), including *NCR3LG1*, *CD48*, *LILRB1*, *PDCD1LG2*, *LGALS3* and *STAT1*. Interestingly, while none of the surface molecule genes except for *PDCDLG2* were bound by BLIMP1, some were enriched for H3K27me3 (Fig 5B). Whereas the downstream signalling effectors, *IFIT2* and *STAT1*, were bound by BLIMP1 (Fig 5C), consistent with previous findings in mammary epithelial cells (Elias, Robertson et al., 2018b). In addition, a number of these differentially expressed genes did not bear either H3K27me3 or BLIMP1, and so are likely regulated by secondary effectors or through distal enhancers.

Next, we sought to determine if the genes bearing H3K27me3 marks but not bound by BLIMP1 are repressed by BLIMP1 via the maintenance of EZH2. Using EZH2 overexpression in RP cells with BLIMP1 KD, we performed qPCR and observed that repression of the B cell genes *RCAN3*, *ZFP36L1* and *CIITA* was restored (Fig EV5C). Furthermore, the repression of the immune inhibitory checkpoint ligand *TNFRSF14* and the inhibitory receptor *HAVCR2* was restored upon restoration of EZH2 levels. By comparison, BLIMP1 targets not bearing the H3K27me3 mark such as *STAT1* and *TFEC* were not altered upon EZH2 restoration.

Taken together, BLIMP1 and EZH2 repress the transcription of genes that mediate killing by NK or T cells, inhibitory receptors and their ligands, as well as cytokine receptors and downstream responders. A subset of these targets are regulated by BLIMP1 through EZH2 maintenance, whereas others are regulated independently of EZH2.

BLIMP1 confers evasion from NK cell-mediated cytotoxicity

The transcriptional changes above suggested that BLIMP1 and EZH2 were repressing cytotoxic synapse molecules and receptors, which may lead to escape from immune surveillance. We hypothesised that the KD of BLIMP1 or inhibition of EZH2 could lead to differential activation of NK cell-mediated cytotoxicity. Towards this, we isolated NK cells from human blood and co-cultured them with RP cells treated to induce BLIMP1 KD or with tazemetostat. We assessed NK cell degranulation by staining the NK cells for the expression of CD107a (also called

LAMP-1), which appears on the cell surface upon degranulation. Negative and positive controls are shown in Fig EV5D. The NK cells co-cultured with *PmiR1* RP cells showed a significant increase in the frequency of $CD107a^+$ cells compared to that when co-cultured with *NTmiR* cells, revealing the sensitisation of NK-cells to WM cells upon BLIMP1 KD (Fig 5D-E). Tazemetostat treatment failed to induce changes in NK-cell degranulation, perhaps reflecting its relatively smaller effect on gene expression compared to that of BLIMP1 KD. However, when we measured the effect of BLIMP1 KD or EZH2 inhibition on NK cell-mediated cytotoxicity of RP cells by the level of cytolysis, both BLIMP1 KD and tazemetostat treatment induced statistically significant increases in NK cell-mediated cytotoxicity (Fig 5F). As such, EZH2 inhibition does not appear to affect NK cell activation, with no change in the degranulation of NK cells cultured with DMSO- or tazemetostat-treated RP cells. However, it may sensitise WM cells to cell-mediated cytotoxicity. Collectively, these data indicate that BLIMP1 and EZH2 mediated transcriptional repression drives escape from immune surveillance in WM.

Discussion

BLIMP1, a key driver of plasma cell terminal differentiation has as of yet not been extensively studied in WM, despite its crucial role for antibody secretion (Minnich et al., 2016, Shapiro-Shelef et al., 2003). Antibody secretion is a critical aspect of WM pathology, since a large proportion of WM symptoms are caused by high IgM serum levels (Treon, 2009). In this study we show for the first time direct evidence for the importance of BLIMP1's role in WM cell survival. We further show that BLIMP1 maintains the protein levels of the histone methyltransferase EZH2, demonstrating that the functional interaction between BLIMP1 and EZH2 is more complex than previously thought (Guo et al., 2018, Kurimoto et al., 2015, Magnúsdóttir et al., 2013, Minnich et al., 2016). Furthermore, our scrutiny of the genes regulated by BLIMP1 and EZH2 revealed that the factors collaborate in the evasion of immune surveillance mechanisms. This was evidenced by enhanced degranulation of NK cells co-cultured with BLIMP-1 KD WM cells, as well as enhanced NK cell-mediated WM cellular cytotoxicity upon either BLIMP KD or EZH2 inhibition.

Our finding that BLIMP1 promotes survival in WM cells provides new insight into WM pathology and potentially its aetiology. BLIMP1 is activated downstream of MYD88 signalling in B cells (Pasare & Medzhitov, 2005), and BLIMP1 expression is increased in tumours harbouring the $MYD88^{L265P}$ activating mutation in WM (Hunter et al., 2016). However, $MYD88^{L265P}$ tumours have an increased frequency of heterozygous deletions in the 6q locus containing *PRDM1* (Schop et al., 2002). This is particularly interesting in light of findings showing that high levels of BLIMP1 tend to inhibit proliferation, whereas intermediate levels promote survival and immunoglobulin (Ig) secretion (Kallies et al., 2004, Nutt, Fairfax et al., 2007). Placed in the context of our findings, we can speculate that perhaps the loss of one copy of the *PRDM1* gene upon MYD88 constitutive activation dampens the anti-proliferative effect of BLIMP1 while still maintaining its positive effect on survival and Ig secretion. Indeed, our results demonstrate decreased cell viability with BLIMP1 KD even for the MW cell line that expresses low BLIMP1 levels. It is also interesting to speculate that a complete loss of BLIMP1 during tumorigenesis would more likely result in B cell lymphoma (Pasqualucci et al., 2006), but the loss of Ig secretion ability and plasma cell differentiation would preclude WM tumour formation.

A first line of treatment in WM is rituximab therapy, targeting the B cell specific surface molecule CD20. However, the cells remaining after this treatment present one of the biggest challenges in WM therapy, and rituximab is not recommended for patients exhibiting high serum IgM levels (Gavriatopoulou, Musto et al., 2018). This highlights the importance of the plasma cell compartment in WM, which is likely maintained by BLIMP1. Furthermore, our results demonstrate repression of *IBTK*, an inhibitor of BTK signaling, by BLIMP1, providing a mechanism by which BLIMP1 may potentiate BTK signaling downstream of MYD88 activation. The inhibition of BTK by Ibrutinib is another WM therapy that results in a dramatic reduction in WM symptoms (Treon, Tripsas et al., 2015).

A key question addressed in this study was in elucidating the interplay of BLIMP1 and EZH2 in WM. BLIMP1 shows an overlapping binding pattern with EZH2 in mouse PGCs implicating an interaction between these factors in epigenetic reprogramming during differentiation (Kurimoto et al., 2015, Magnúsdóttir et al.,

2013). This implication was expanded in mouse plasmablasts with the discovery that BLIMP1 physically interacts with EZH2, directing the placement of H3K27me3 to repress B cell genes during the transition to plasma cells (Minnich et al., 2016). In addition, EZH2 aids in the generation of antibody-secreting plasma cells in the mouse and represses BLIMP1 target genes (Guo et al., 2018). Here, we demonstrate that BLIMP1 maintains EZH2 protein levels which could at least in part explain the overlap in transcriptional targets seen by Guo et al. (Guo et al., 2018) in mouse plasmablasts, beyond the mechanism of BLIMP1 potentially recruiting EZH2 to chromatin. However, it is interesting to speculate that the BLIMP1-EZH2 interaction is necessary for normal epigenetic reprogramming during the B cell to plasma cell transition, and the perturbation of this interaction may contribute to the aetiology of B cell malignancies. Interestingly, the restoration of EZH2 levels did not improve cell survival following BLIMP1 KD, indicating that the requirement for BLIMP1 in mediating WM cell survival is through other mechanisms rather than its effect on EZH2.

While both multiple myeloma and normal plasma cells rely on BLIMP1 for their survival (Lin et al., 2007, Shapiro-Shelef et al., 2003, Shapiro-Shelef, Lin et al., 2005) , EZH2 expression is decreased as post-germinal centre B cells transition to plasma cells (Croonquist & Van Ness, 2005, Zhan, Tian et al., 2003), whereas many multiple myeloma cell lines are reliant on EZH2 for cytokine independent growth and thus their more aggressive plasma cell leukemia phenotype (Croonquist & Van Ness, 2005, Hernando, Gelato et al., 2016). Our results indicate that the effects of BLIMP1 on EZH2 levels might extend to myeloma, and perhaps other tumours where the two factors are co-expressed, and warrants further study.

Immune evasion is most extensively studied in relation to solid tumours, but in cancers of immune system cells, the paradigm is somewhat different. Lymphocytes interact with other cells of the immune system not only when they are abnormal, such as in cancer, but also to receive stimulatory and inhibitory signals, regulating their own immune response (de Charette & Houot, 2018). In WM, PD-1 signaling from secreted ligands inhibits T cell responses (Jalali, Price-Troska et al., 2018), but other mechanisms of immune evasion have not been investigated. Our results demonstrate for the first time that BLIMP1 and EZH2 mediate evasion from

NK cell surveillance. This occurs both in terms of NK cell activation and cytotoxicity against WM cells downstream of BLIMP1. Meanwhile, the effect of EZH2 inhibition is restricted to NK-cell mediated cytotoxicity without activation of the NK cells themselves. Based on our transcriptomic profiling, the main mechanism by which BLIMP1 promotes immune evasion in WM is likely to be "hiding" from cytotoxic lymphocytes by transcriptional repression of activating ligands. Whereas, EZH2 is more likely to be de-sensitising WM cells to external cytotoxicity-inducing signals. Interestingly, in melanoma EZH2 promotes evasion from IFNγ-producing cytotoxic T cells (Zingg, Arenas-Ramirez et al., 2017). Investigation into the use of EZH2 inhibition for sensitising WM and other cancer cells to immune-mediated killing should be considered for prospective therapies.

In conclusion, we provide key evidence for a crucial role of BLIMP1 in promoting WM cell survival. In the WM cell context, we discover that BLIMP1 maintains EZH2 protein levels. We show cooperation between BLIMP1 and EZH2 in the repression of immune surveillance genes, among others. Finally, we find that BLIMP1 confers evasion from NK-cell mediated cytotoxicity. In future studies it would be important to investigate the intricate interplay between BLIMP1 and EZH2 in cancers to expand their therapeutic potential.

Materials and Methods

Suspension cell lines

RPCI-WM1 (a gift from Prof. Asher A. Chanan-Khan), BCWM.1 (a gift from Prof. Steven P. Treon) and OPM-2 (#ACC50, Leibniz Institute DSMZ) cell lines were maintained in RPMI media (#SH30255.FS, Hyclone, GE Healthcare Biosciences) supplemented with 10% foetal bovine serum (FBS) (#SV30160.03, Hyclone, GE Healthcare Biosciences, Denmark). The MWCL-1 (a gift from Stephen M. Ansell) and NCI-H929 (#ACC163, Leibniz Institute DSMZ) cell lines were maintained in RPMI media supplemented with 10% FBS 1mM sodium pyruvate (#SH30239.01, Hyclone GE Healthcare Biosciences) and 50μM beta-mercaptoethanol (#0482,

VWR).

Cloning

For knock-down of BLIMP1, artificial miRNA sequences were designed to target the *PRDM1* transcript using the RNAiDesigner tool (Thermo Fisher). These were named *PmiR1* and *PmiR2*. A non-targeting control miRNA (*NTmiR*) was also used as previously described (Hackett, Sengupta et al., 2013). The miRNA sequences were cloned into the tetracycline-inducible pPB-hCMV*1-miR plasmid (Hackett et al., 2013, Murakami, Günesdogan et al., 2016). See Appendix Table 1 for miRNA sequences.

Site directed mutagenesis was used to introduce mutations in coding sequence of the FUW-PRD1-BF1 lentiviral expression construct (Magnúsdóttir et al., 2007) to render it resistant to the targeting miRNAs. The plasmid was amplified using primers listed in Appendix Table 2. FUW-EZH2 was derived first by PCR amplification from the pCMVHA-hEZH2 plasmid (Bracken, Pasini et al., 2003), then incorporated via Gibson assembly (New England Biolabs) into the FUGW backbone (Lois et al., 2002). The pCMVHA hEZH2 plasmid was a gift from Kristian Helin (Addgene plasmid # 24230 ; http://n2t.net/addgene:24230 ; RRID:Addgene_24230).

Construction of knock-down cell lines

Knock-down cell lines were constructed via electroporation 220V, 350µF using Gene Pulser XCell (Bio-Rad) with plasmids containing our miRNA as described above, using the piggyBac transposon system with the piggyBac transposase, the reverse-tetracycline transactivator and a tetracycline-inducible EGFP. Stable cell lines were selected for with 0.5 mg/mL or 1 mg/mL G418 disulfate solution (#A6798, Applichem) for either the RP and MW, or OPM-2 cells respectively for nine days. The RP cells were seeded at a density of 0.5 cells per well in a 96-well plate and clones with the highest KD were used for further analyses. MW and OPM-2 cells were used as a pool of cells directly after antibiotic selection. miRNA expression was induced with 0.2 or 0.5 µg/mL Doxycyline Hyclate (#sc-211380, Santa Cruz Biotechnology) for either the RP and OPM-2, or MW cells respectively.

Lentiviral transduction

Lentivirus was produced by transient transfection of HEK293T cells with the envelope vesicular stomatitis virus G protein (VSVG)-encoding pMD2.G plasmid, the packaging plasmid psPAX2, and either the FUW-PRDI-BF1, FUW-EZH2 or FUGW transfer plasmid. psPAX2 was a gift from Didier Trono (Addgene plasmid #12260; http://n2t.net/addgene:12260; RRID:Addgene_12260). pMD2.G was a gift from Didier Trono (Addgene plasmid #12259; http://n2t.net/addgene:12259; RRID:Addgene_12259).

Viral supernatant was concentrated by ultracentrifugation using 100kDa Amicon centrifugal filters (#UFC910008, Sigma-Aldrich). Suspension cell lines were transduced by spinfection, 800 xg for 30 min with 8 µg/mL polybrene.

Immunofluorescence staining

Cells were cytospun onto glass slides for 3 min at 800 rpm. Samples were fixed and permeabilised 10 min in 4% formaldehyde (#28906, Thermo Fisher Scientific), 0.1% triton-X-100 (#T-9284, Sigma-Aldrich), then blocked for 1 h at room temperature with 0.1% triton-X-100, 1% bovine serum albumin (#A1391, Applichem), and 10% goat serum (#16210064, Gibco). Slides were incubated overnight at 4˚C with primary antibody, anti-BLIMP1 (#9115, Cell Signaling Technologies) at a 1:100 dilution. Nuclei were counterstained with 1µg/mL DAPI (#sc-3598, Santa Cruz Biotechnology). The secondary antibody used was goat anti-rabbit Alexa Fluor 647 (#A21244, Thermo Fisher Scientific) at a 1:1000 dilution. The signal intensity within nuclei was quantified using CellProfiler, with background signal subtracted (Carpenter, Jones et al., 2006).

Protein extraction, SDS-PAGE, and Western Blot

Cells were lysed in protein sample buffer (60mM Tris pH 6.8, 2% SDS, 10% glycerol, 0.01% bromophenol blue, 1.25% β-mercaptoethanol), at 95˚C for 5 min.

Benzonase nuclease (#sc-202391, Santa Cruz Biotechnology) was used to digest chromatin before loading on SDS-PAGE gel. Western blotting was performed as previously described (Burnette, 1981).

RNA Isolation, cDNA synthesis and RT-qPCR

Cells were lysed in TRIsure reagent (#BIO-38032, Bioline), and RNA was extracted according to the manufacturer's instructions. cDNA was synthesised using the GoScript Reverse Transcriptase system (#A5001, Promega), in combination with dNTP mix (#R0191, Thermo Fisher Scientific), random primer 6 (#S1230S, New England Biolabs), murine RNase inhibitor (#M0314S, New England Biolabs) and 1.25mM $MgCl_2$. RT-qPCR was performed using the SensiFAST SYBR Lo-Rox Kit (#BIO-94020, Bioline) on the 7500 Real-Time PCR system (Applied Biosystems). Relative quantitation was calculated according to the Pfaffl method (Pfaffl, 2001), with *ACTB* and *PPIA* used as reference genes. Primer sequences are listed in Appendix Table 3.

Viability, reduction and apoptosis assays

The percentage of live cells was determined by trypan blue exclusion assay (Gibco). The per cent reduction was determined by resazurin assay, with resazurin sodium salt (Santa Cruz Biotechnology) added 5h before the assay end-point, and absorbance measured at 595 and 570nm. Per cent reduction was calculated relative to the fully reduced form of resazurin, resorufin. See Appendix Methods for more details. Apoptosis was assessed using APC-Annexin V (#550474, BD Biosciences) together with Annexin V binding buffer (#556454, BD Biosciences). Staining was carried out according to the manufacturer's instructions and assessed using the MACSQuant analyser (Miltenyi Biotec).

Proteasomal inhibition

To test inhibition of the proteasome, RP *NTmiR* or *PmiR1* cells were treated with 5μM MG-132 (#sc-201270, Santa Cruz Biotechnology) for 4 h, 20 h post dox addition.

RNAseq

The *PmiR2* and *NTmiR* RP cells were treated with 0.2μg/mL dox for 48h. RP cells were treated with 300nM tazemetostat (EPZ-6438, #S7128, Selleckchem) or DMSO for 48h. Total RNA was isolated using TRI-reagent (#AM9738, Thermo Fisher Scientific) according to the manufacturer's instructions, then treated with HL-dsDNase (#70800-201, ArcticZymes), and purified using the RNeasy MinElute Cleanup Kit (#74204, Qiagen). RNAseq libraries were constructed using the NEB NEBNext® Ultra™ Directional RNA Library Prep Kit for Illumina® (#E7420S, New England Biolabs) in combination with the NEBNext® Poly(A) mRNA Magnetic Isolation Module (#E7490S, New England Biolabs). Pooled samples were clustered on paired-end (PE) flowcells using a cBot instrument (Illumina). Sequencing was performed on Illumina HiSeq 2500 using the v4 SBS sequencing kits with a readlength of 2x125 cycles plus a 6 base index read. Primary processing and base calling was done using HCS and RTA. Demultiplexing and generation of FASTQ files was performed using scripts from Illumina (bcl2fastq v.1.8).

RNAseq raw reads were trimmed using Trim Galore (https://www.bioinformatics.babraham.ac.uk/projects/trim_galore/), and pseudoaligned to the hg38 transcriptome and quantified using Kallisto (Bray, Pimentel et al., 2016). Differential expression analysis was performed using the likelihood ratio test in Sleuth (Pimentel, Bray et al., 2017), on a gene level, with a q-value of 0.05, and a $\log_2$ fold-change of ±0.3 as a significance cutoff. Gene set enrichment analysis using the Hallmarks collection of gene sets was run in pre-ranked mode using a list of all detected genes (Liberzon et al., 2015, Subramanian et al., 2005). The rank value was calculated as $-\log_{10}$(q-value) × (sign of fold change).

ChIPseq

Transcription factor ChIP for BLIMP1 and EZH2 was performed as previously described (Boyer, Lee et al., 2005, Magnúsdóttir et al., 2013, Magnúsdóttir et al., 2007). ChIP was carried out for BLIMP1, using 60µL rabbit polyclonal antibody recognising the C-terminal region of BLIMP1 (Kuo & Calame, 2004) with 3×10^7 nuclei, crosslinked with 0.4% formaldehyde. For EZH2, ChIP was performed using 40µL anti-EZH2 (D2C9, #5246, Cell Signaling Technology) with 2×10^7 nuclei, crosslinked with 1% formaldehyde.

Histone ChIP for pan-H3 and the H3K27me3 mark was performed as previously described (Shaffer et al., 2008). ChIP was performed for pan-H3 using 3µL anti-histone H3 (D2B12, #4620S, Cell Signaling Technology). For H3K27me3, ChIP was performed using 5µg anti-H3K27me3 (#ab6002, Abcam). All histone ChIP experiments were performed with 1×10^7 cells per ChIP, crosslinked with 0.4% formaldehyde.

Sequencing was performed as described above. Raw ChIPseq reads were trimmed as above and aligned to the hg38 genome using Bowtie2 (Langmead & Salzberg, 2012). Peaks were called using MACS2 (Zhang, Liu et al., 2008), and tracks were visualised using the UCSC genome browser (Kent, Sugnet et al., 2002). Enrichment over BLIMP1 peaks, H3K27me3 peaks and TSSs was calculated and mapped using Deeptools (Ramírez, Ryan et al., 2016). Overlapping regions were tested for significance using the hypergeometric test in the ChIPPeakAnno package in R (Zhu, Gazin et al., 2010). Overlapping genes were tested for significance using Fisher's exact test in the GeneOverlap package in R (http://shenlab-sinai.github.io/shenlab-sinai/).

NK cell isolation

NK cells were isolated from heparinised buffy coats obtained from healthy human donors, who all provided informed consent, provided by the Icelandic Blood Bank (ethical approval #06-068). PBMCs were first isolated by density gradient centrifugation with Histopaque-1077 (#10771, Sigma-Aldrich), then NK cells were purified by negative enrichment using the NK cell isolation kit (#130-092-657, Miltenyi Biotech) according to the manufacturer's instructions. NK cells were

cultured overnight in RPMI media supplemented with 10% FBS and 10ng/mL IL-2 (R&D Systems).

Degranulation Assay

NK cells were co-cultured with pre-treated RP cells at a 10:1 ratio. Anti-CD107a-PE (clone H4A3, BioLegend) was added to the co-culture media. For the positive control, NK cells in co-culture with RP cells were treated with 2.5µg/mL phorbol 12-myristate 13-acetate and 0.5µg/mL ionomycin. After 1h of co-culture, 2µM monensin was added to every sample and incubated for an additional 4h. Cells were stained with anti-CD56-APC (clone CMSSB, EBioscience), fixed with 1% PFA and analysed on the Sony SH800S flow cytometer. Data were analysed using FlowJo v10.

Cytotoxicity Assay

NK cells were co-cultured with pre-treated RP cells at a 20:1 ratio for 4h. Cytotoxicity was assessed by measurement of the adenylate kinase activity in the culture medium using the ToxiLight assay (#LT07-217, Lonza). Luminescence was measured using a Modulus microplate reader (Promega). Values were normalised to wells containing pre-treated RP cells without NK cells, and are presented as relative luminescence units (RLU).

Data availability

RNAseq and ChIPseq data are available at http://www.ebi.ac.uk/arrayexpress/experiments/E-MTAB-7739 under the accession code: E-MTAB-7739.

Author contributions

EM conceived, designed and supervised the work. KJA, ABO, BA, GAT and AEL performed and designed the experimental work. KNJ performed flow cytometric analyses and contributed to experimental design. KJA performed the bioinformatics analyses. JTB and IH contributed to critical methodologies. KA and EM wrote the paper.

Conflict of interest

The authors declare that they have no conflicts of interest.

Acknowledgements

We thank Arnar Palsson and Dagny A. Runarsdottir for their advice on RNAseq data analysis. We thank Jona Freysdottir and Sunnefa Yeatman Omarsdottir for their advice on the isolation of NK cells. We also thank the group of Eirikur Steingrimsson for many good discussions and advice on the project. We thank Dr. Roopsha Sengupta for providing critical inputs and proof-reading the manuscript.

Funding

This work was supported by project grants from the Icelandic Centre for Research (RANNIS) (grant no. 140950-051) and the Icelandic Cancer Society, a doctoral fellowship from the University of Iceland, and grant from the University of Iceland Eggertssjodur and funds from the COST Project EpiChemBio.

Figure Legends

Figure 1: BLIMP1 promotes survival of WM cells

(A) BLIMP1 expression in myeloma cell line OPM-2 and in WM cell lines RP, MW and BC as detected by immunofluorescence staining, with bar graph representing

percentage of BLIMP1^{bright} cells. Scale bars represent 20µm. **(B)** Immunoblot of BLIMP1 expression following 48h dox induction of RP cells expressing *NTmiR*, *PmiR1* or *PmiR2*, with bar graph representing the quantity of BLIMP1 relative to actin; ****p < 0.0001. **(C)** Immunofluorescence staining of BLIMP1 following 48h dox induction in MW cells expressing *NTmiR*, *PmiR1* or *PmiR2*, with CellProfiler quantification; p = 0.0228. **(D)** Percentage of live cells as determined by Trypan blue exclusion assay in the RP and MW cell lines. RP, p = 0.0019; MW, p = 0.0162. **(E)** Immunoblot depicting lentiviral ectopic expression of EGFP or BLIMP1-EGFP in the RP *PmiR1* cells, next to the RP *NTmiR* cells. **(F)** The percentage of live RP *PmiR1* cells with ectopic EGFP or BLIMP1-EGFP expression determined by the Trypan blue exclusion assay normalised to the percentage of live cells following transduction of RP *NTmiR* cells with EGFP or BLIMP1-EGFP. Day 2, *p = 0.0165; Day 5, ***p = 0.0003. **(G)** Per cent reduction as measured by resazurin assay for RP *PmiR1* cells with EGFP or BLIMP1-EGFP, five days after dox induction. *p = 0.0208. All p-values as determined by student's two-tailed t-test. All graphs plotted as mean of three independent experiments, with error bars representing standard deviation.

Figure 2: BLIMP1 maintains EZH2 protein levels

(A) Immunoblot of BLIMP1 and EZH2 expression following 48h dox-induction of RP cells expressing *NTmiR*, *PmiR1* or *PmiR2*, with quantification of signal relative to actin in bar plot; ***p = 0.0002; ***p = 0.001; **p = 0.0027. **(B)** Immunoblot of BLIMP1 and EZH2 expression following 48h dox-induction of OPM-2 cells expressing *NTmiR* or *PmiR1*, with quantification of signal relative to actin in bar plot; ****p < 0.0001; *p = 0.016. **(C)** Immunofluorescence staining of BLIMP1 and EZH2 expression following 48 h dox-induction of RP cells expressing *NTmiR* or *PmiR1*, transduced with EGFP or BLIMP1-EGFP. Scale bars represent 20 µm. **(D)** RT-qPCR results depicting relative mRNA expression of *PRDM1* and *EZH2* normalised to *PPIA* and *ACTB* in the RP cell line and **(E)** in the OPM-2 cell line. **(F)** Immunoblot of BLIMP1 and EZH2 expression following 24h dox-induction of RP cells expressing *NTmiR* or *PmiR1* treated with DMSO or 5µM MG-132 for 4h. **(G)**

The ratio of EZH2 expression relative to actin for RP *PmiR1* cells divided by RP *NTmiR* cells treated with DMSO or MG132 as in Fig. 2F; p = 0.0134. **(H)** Immunoblot of BLIMP1 and EZH2 expression following 48h dox-induction of RP *NTmiR* cells or *PmiR1* cells transduced with EGFP or EZH2-EGFP. **(I)** Percentage of live cells as determined by Trypan blue exclusion assay in the RP *PmiR1* cells transduced with EGFP or EZH2-EGFP. All p-values as determined by student's two-tailed t-test. All graphs plotted as mean of three independent experiments with error bars representing standard deviation.

Figure 3: BLIMP1 KD induces large transcriptional changes

RNAseq results for **(A)** 48h dox-induced RP cells comparing *PmiR1* to *NTmiR*. Values are plotted as $\log_2$ fold change vs. $-\log_{10}$(qvalue). Red indicates those genes with a q-value ≤ 0.05 and a $\log_2$ fold change ≤ -0.3 or ≥ 0.3. Heat maps depicting the Z-score of the $\log_2$ fold change comparing *PmiR1* to *NTmiR* for three independent replicates looking at **(B)** B cell genes and **(C)** apoptosis genes. **(D)** RNAseq results for RP cells treated for 48h with 300nM tazemetostat compared to vehicle control (DMSO). **(E)** Overlapping genes with increased expression following *PRDM1* KD or tazemetostat treatment. **(F)** Overlapping genes with decreased expression following *PRDM1* KD or tazemetostat treatment. Overlaps tested using Fisher's exact test. Heat maps depicting the Z-score of the $\log_2$ fold change comparing tazemetostat treatment to DMSO for three independent replicates looking at **(G)** B cell genes and **(H)** apoptosis genes.

Figure 4: BLIMP1 and EZH2 are present at a subset of proximal genomic loci

(A) Venn diagram of H3K27me3 and BLIMP1 peaks extended ±10kb, showing overlaps in these regions. (ns) not significant as determined by hypergeometric test. Called peaks determined by overlap from peak calling from two independent experiments. **(B)** Enrichment of signal from ChIPseq tracks ±3kb from the centre of BLIMP1 binding sites. Data depicts representative experiment of two biological replicates. **(C)** Venn diagram of genes assigned to H3K27me3 and BLIMP1 peaks

showing overlapping genes. p= 2.9e-25 as determined by Fisher's exact test. **(D)** ChIPseq tracks for H3K27me3 and BLIMP1 in the RP cell line. Data represents combination of reads from two independent experiments. **(E)** Enrichment of signal from ChIPseq tracks ±10kb from the centre of BLIMP1 binding sites in the NCI-H929 cell line. **(F)** Venn diagram depicting the overlap in genes with significantly increased expression following BLIMP1 KD and genes assigned to BLIMP1 binding sites. p= 7e-15, as determined by Fisher's exact test. **(G)** Venn diagram depicting the overlap in genes with significantly decreased expression following BLIMP1 KD and genes assigned to BLIMP1 binding sites. (ns) not significant as determined by Fisher's exact test. **(H)** Venn diagram depicting genes with significantly increased expression following tazemetostat treatment overlapping with genes assigned to H3K27me3 peaks. p= 7.9e-9, as determined by Fisher's exact test. **(I)** Venn diagram depicting genes with significantly decreased expression following tazemetostat treatment overlapping with genes assigned to H3K27me3 peaks. (ns) not significant, as determined by Fisher's exact test. All ChIPseq experiments were performed as two biological replicates.

Figure 5: BLIMP1 and EZH2 promote immune evasion

(A) Heat maps showing z-score of the log2 fold change for *PmiR2* compared to *NTmiR* and in RP cells with three independent replicates looking at genes involved in stimulation of T and NK cells, MHC molecules, inhibitory ligands and receptors, IFN and TNF receptors and downstream signalling. ChIPseq tracks for H3K27me3 and BLIMP1 in the RP cell line over **(B)** the immune surface molecule genes *HLA-B, MICA, LILRB1, NCR3LG1, TNFRSF1A,* or **(C)** the downstream signalling genes, *IFIT2* and *STAT1*. Data represents combination of reads from two independent experiments. **(D)** Percentage CD56+CD107a+ cells (Q2) representing degranulating NK cells, as determined by flow cytometry following co-culture with RP cells with *NTmiR* or *PmiR1,* or RP cells treated with DMSO or Tazemetostat. One representative experiment is displayed. **(E)** Relative quantification of the degranulation assay **p = 0.0088. **(F)** Cytotoxicity depicted in relative luminescence units (RLU), as measured by adenylate kinase activity in the culture media following

4 h co-culture of NK cells with RP cells expressing *NTmiR* or *PmiR1*, or RP cells treated with DMSO or 1μM Tazemetostat. Cells were co-cultured at the effector:target ratio of 20:1. ****p = 3.1×10^{-5}; *p = 0.02. Results of the degranulation and cytotoxicity assays from four individual donors, performed in two pairs on two separate occasions.

Expanded view

Expanded view figure legends

Expanded view Figure 1

(A) Annexin V staining of dox-induced RP cells with *NTmiR*, *PmiR1* or *PmiR2*; ***p = 0.0004; **p = 0.0071. **(B)** Annexin V staining of dox-induced MW cells with *NTmiR* or *PmiR1*; p = 0.0572.

Expanded view Figure 2

(A) Signal intensity of immunofluorescence staining for BLIMP1 and EZH2 as quantified by CellProfiler from approximately 5000 cells per sample across two independenct replicates. **(B)** Relative growth of RP cells treated with tazemetostat for 96h, shown next to RP cells treated with Ibrutinib for 48h. **(C)** Immunoblot of histone extracts from RP cells stained for H3K27me3 with total H3 as a loading control following 48h tazemetostat treatment at the indicated concentrations. The 0 concentration was treated with vehicle control, DMSO.

Expanded view Figure 3

(A) Graph of RNAseq results depicting normalised transcripts per million (TPM) values for *SMURF2* in RP cells with *NTmiR* and *PmiR1*. Bar plots depicting normalised enrichment score for Hallmarks gene sets identified using GSEA pre-

ranked with FDR-corrected p-value ≤ 0.05 for **(B)** *PmiR1* compared to *NTmiR* and **(C)** tazemetostat treatment compared to DMSO.

Expanded view Figure 4

(A) Motif enrichment analysis showing the top motif for BLIMP1 ChIPseq experiments in the RP cell line. Profiles showing enrichment over ±30 kb regions from TSSs assigned to **(B)** BLIMP1 and **(C)** H3K27me3 peaks in the RP cell line. **(D)** Motif enrichment analysis showing the top motif for BLIMP1 ChIPseq experiments in the OPM-2 and NCI-H929 cell lines. Profiles showing enrichment over ±30 kb regions from TSSs assigned to **(E)** BLIMP1, **(F)** H3K27me3 and **(G)** EZH2 peaks in the OPM-2 and NCI-H929 cell lines. **(H)** Enrichment of BLIMP1 signal in the RP, OPM-2 and NCI-H929 cell lines over BLIMP1 peaks from the RP cell line. **(I)** Enrichment of H3K27me3 signal in the RP, OPM-2 and NCI-H929 cell lines over H3K27me3 peaks from the RP cell line. **(J)** ChIPseq tracks for H3K27me3 and BLIMP1 over the *SMURF2* gene in the RP cell line. **(K)** Venn diagrams of H3K27me3 and BLIMP1 peaks extended ±10kb, showing overlaps in these regions in the OPM-2 and NCI-H929 cell lines. (ns) not significant as determined by hypergeometric test. **(L)** Venn diagram of EZH2 and BLIMP1 peaks extended ±10kb, showing overlaps in these regions in the NCI-H929 cell line. (ns) not significant as determined by hypergeometric test. **(M)** Venn diagrams of overlapping genes assigned to peaks for H3K27me3 or BLIMP1 in the OPM-2 and NCI-H929 cell lines. Significance determined by Fisher's exact test. OPM-2, ns, not significant; NCI-H929, p = 5.9e-20. **(N)** Venn diagram of overlapping genes assigned to peaks for EZH2 or BLIMP1 in the NCI-H929 cell lines. (ns) not significant, as determined by Fisher's exact test.

Expanded view Figure 5

(A) ChIPseq tracks for H3K27me3 and BLIMP1 over the *PDCD1LG2* gene in the RP cell line. **(B)** Heat map showing the z-score of the $_{log2}$ fold change for Tazemetostat compared to DMSO in RP cells with three independent replicates looking at genes involved in stimulation of NK cells, MHC molecules, inhibitory

ligands and receptors, and downstream signalling. **(C)** RT-qPCR from three independent experiments depicting relative mRNA expression comparing RP cells with *NTmiR,* and *PmiR1* transduced with EGFP or EZH2-EGFP. **(D)** Negative control for the degranulation assay, consisting of NK cells cultured alone, and positive control consisting of NK cells in co-culture with RP cells treated with 2.5µg/mL phorbol 12-myristate 13-acetate and 0.5µg/mL ionomycin.

Appendix

Appendix Methods

Resazurin assay

The percentage reduction of resazurin was calculated according to the following formula:

$$\text{Percentage reduction of resazurin} = \frac{(O2 \times A1) - (O1 \times A2)}{(R1 \times N2) - (R2 \times N1)} \times 100$$

Where O1 = molar extinction coefficient (E) of oxidized resazurin at 570 nm (80586); O2= E of oxidized resazurin at 595 nm (117216); R1 = E of reduced resazurin (Red) at 570 nm (155677); R2= E of reduced resazurin at 595 nm (14652); A1 = absorbance of test wells at 570 nm; A2 = absorbance of test wells at 595 nm; N1 = absorbance of negative control well (media plus resazurin but no cells) at 570 nm; N2 = absorbance of negative control well (media plus resazurin but no cells) at 595 nm.

Appendix Table 1: Artificial miRNA sequences

Name	Sequence (5'-3')

PmiR1	G**TACACTTCTCTTCAAACTCAG**GTTTTGGCCACT GACTGACCTGAGTTTAGAGAAGTGTACA
PmiR2	G**TTACTCATCACTCCAATAACC**GTTTTGGCCACT GACTGACGGTTATTGGTGATGAGTAACA
Non-targeting (*NTmiR*)	**AAATGTACTGCGCGTGGAGAC**GTTTTGGCCACT GACTGACGTCTCCACGCAGTACATTT

Appendix Table 2: Primers used for mutagenesis

FUW-P-miR1-mut_Fwd	gaaaaatgcaCATACATTGTGAACGACCAC
FUW-P-miR1-mut_Rev	ctcgaattccgCCTCTGTCCACAGAGTCA

Appendix Table 3: Primers used for qPCR

Primer	**Sequence**
PRDM1_fwd	GGTACACACGGGAGAAAAGC
PRDM1_rev	GAGATTGCTGGTGCTGCTAA
EZH2_fwd	ACATCCTTTTCATGCAACACC
EZH2_rev	GCTCCCTCCAAATGCTGGTA
STAT1_fwd	CTGTGCGTAGCTGCTCCTT
STAT1_rev	GAGTCAAGCTGCTGAAGTTCG
TFEC_fwd	ACATGGGGCTTACAAGTGCT
TFEC_rev	TCAATGAGGTTGTGGTTGTCC
POU2F2_fwd	ACTCATGTTGACGGGCAGC
POU2F2_rev	GGTAGCAGGAACTGAGCAGG

MICA_fwd	ACATTCCATGTTTCTGCTGTTGC
MICA_rev	GACCTGCAGGCTCACGA
LGALS9_fwd	TCAATGGGACCGTTCTCAGC
LGALS9_rev	GAGGGTTGAAGTGGAAGGCA
BCL2L11_fwd	CCTCGGCGCCCTTTCTT
BCL2L11_rev	AGGTTGCTTTGCCATTTGGTC
CASP4_fwd	TGCTGTTTACAAGACCCACG
CASP4_rev	AGAGCCCATTGTGCTGTCTC
OAS2_fwd	CAGGAACCCGAACAGTTCCC
OAS2_rev	AGGACAAGGGTACCATCGGA
PIK3CD_fwd	TGTACGCCGTGATCGAGAAA
PIK3CD_rev	CGGTCTTAAGCTGGTCCTTGT
RCAN3_fwd	GCGCGAATAGAACTCCACGA
RCAN3_rev	GCGGCAGGAGATAGGACTTG
ZFP36L1_fwd	GTCTGCCACCATCTTCGACT
ZFP36L1_rev	TTTCTGTCCAGCAGGCAACC
CIITA_fwd	CATCCTTGGGGAAGCTGAGG
CIITA_rev	CTGTGAGCTGCCTTGGGG
TNFRSF14_fwd	GCAGTGCCAAATGTGTGACC
TNFRSF14_rev	CCTGGACGATGCAGAAGTGG
HAVCR2_fwd	GGCTCTTATCTTCGGCGCT
HAVCR2_rev	GGGAGGTTGGCCAAAGAGAT

PPIA_fwd	CATCTGCACTGCCAAGACTGA
PPIA_rev	TGGCCTCCACAATATTCATGC
ACTIN_fwd	AGGCACCAGGGCGTGAT
ACTIN_rev	GCCCACATAGGAATCCTTCTGAC

References

Basso K, Dalla-Favera R (2015) Germinal centres and B cell lymphomagenesis. Nature Reviews Immunology 15: 172

Béguelin W, Popovic R, Teater M, Jiang Y, Bunting Karen L, Rosen M, Shen H, Yang Shao N, Wang L, Ezponda T, Martinez-Garcia E, Zhang H, Zheng Y, Verma Sharad K, McCabe Michael T, Ott Heidi M, Van Aller Glenn S, Kruger Ryan G, Liu Y, McHugh Charles F et al. (2013) EZH2 Is Required for Germinal Center Formation and Somatic EZH2 Mutations Promote Lymphoid Transformation. Cancer Cell 23: 677-692

Boyer LA, Lee TI, Cole MF, Johnstone SE, Levine SS, Zucker JP, Guenther MG, Kumar RM, Murray HL, Jenner RG, Gifford DK, Melton DA, Jaenisch R, Young RA (2005) Core Transcriptional Regulatory Circuitry in Human Embryonic Stem Cells. Cell 122: 947-956

Bracken AP, Pasini D, Capra M, Prosperini E, Colli E, Helin K (2003) EZH2 is downstream of the pRB-E2F pathway, essential for proliferation and amplified in cancer. Embo j 22: 5323-35

Brandefors L, Melin B, Lindh J, Lundqvist K, Kimby E (2018) Prognostic factors and primary treatment for Waldenström macroglobulinemia – a Swedish Lymphoma Registry study. British Journal of Haematology 183: 564-577

Bray NL, Pimentel H, Melsted P, Pachter L (2016) Near-optimal probabilistic RNA-seq quantification. Nature biotechnology 34: 525

Burnette WN (1981) "Western Blotting": Electrophoretic transfer of proteins from sodium dodecyl sulfate-polyacrylamide gels to unmodified nitrocellulose and radiographic detection with antibody and radioiodinated protein A. Analytical Biochemistry 112: 195-203

Calado DP, Zhang B, Srinivasan L, Sasaki Y, Seagal J, Unitt C, Rodig S, Kutok J, Tarakhovsky A, Schmidt-Supprian M, Rajewsky K (2010) Constitutive Canonical NF-κB Activation Cooperates with Disruption of BLIMP1 in the Pathogenesis of Activated B Cell-like Diffuse Large Cell Lymphoma. Cancer Cell 18: 580-589

Carpenter AE, Jones TR, Lamprecht MR, Clarke C, Kang IH, Friman O, Guertin DA, Chang JH, Lindquist RA, Moffat J, Golland P, Sabatini DM (2006) CellProfiler: image analysis software for identifying and quantifying cell phenotypes. Genome biology 7: R100

Carroll D, Erhardt S, Pagani M, Barton SC, Surani MA, Jenuwein T (2001) The Polycomb-Group Gene Ezh2 Is Required for Early Mouse Development. Molecular and Cellular Biology 21: 4330

Chen H, Gilbert CA, Hudson JA, Bolick SC, Wright KL, Piskurich JF (2007) Positive regulatory domain I-binding factor 1 mediates repression of the MHC class II transactivator (CIITA) type IV promoter. Molecular Immunology 44: 1461-1470

Croonquist PA, Van Ness B (2005) The polycomb group protein enhancer of zeste homolog 2 (EZH2) is an oncogene that influences myeloma cell growth and the mutant ras phenotype. Oncogene 24: 6269

Czermin B, Melfi R, McCabe D, Seitz V, Imhof A, Pirrotta V (2002) Drosophila Enhancer of Zeste/ESC Complexes Have a Histone H3 Methyltransferase Activity that Marks Chromosomal Polycomb Sites. Cell 111: 185-196

de Charette M, Houot R (2018) Hide or defend, the two strategies of lymphoma immune evasion: potential implications for immunotherapy. Haematologica 103: 1256-1268
Doody GM, Stephenson S, McManamy C, Tooze RM (2007) PRDM1/BLIMP-1 Modulates IFN-γ-Dependent Control of the MHC Class I Antigen-Processing and Peptide-Loading Pathway. The Journal of Immunology 179: 7614
Elias S, Robertson EJ, Bikoff EK, Mould AW (2018a) Blimp-1/PRDM1 is a critical regulator of Type III Interferon responses in mammary epithelial cells. Scientific reports 8: 237-237
Elias S, Robertson EJ, Bikoff EK, Mould AW (2018b) Blimp-1/PRDM1 is a critical regulator of Type III Interferon responses in mammary epithelial cells. Scientific Reports 8: 237
Gavriatopoulou M, Musto P, Caers J, Merlini G, Kastritis E, van de Donk N, Gay F, Hegenbart U, Hajek R, Zweegman S, Bruno B, Straka C, Dimopoulos MA, Einsele H, Boccadoro M, Sonneveld P, Engelhardt M, Terpos E (2018) European myeloma network recommendations on diagnosis and management of patients with rare plasma cell dyscrasias. Leukemia 32: 1883-1898
Gertz MA (2019) Waldenström macroglobulinemia: 2019 update on diagnosis, risk stratification, and management. American Journal of Hematology 94: 266-276
Guo M, Price MJ, Patterson DG, Barwick BG, Haines RR, Kania AK, Bradley JE, Randall TD, Boss JM, Scharer CD (2018) EZH2 Represses the B Cell Transcriptional Program and Regulates Antibody-Secreting Cell Metabolism and Antibody Production. The Journal of Immunology 200: 1039-1052
Győry I, Wu J, Fejér G, Seto E, Wright KL (2004) PRDI-BF1 recruits the histone H3 methyltransferase G9a in transcriptional silencing. Nature Immunology 5: 299
Hackett JA, Sengupta R, Zylicz JJ, Murakami K, Lee C, Down TA, Surani MA (2013) Germline DNA demethylation dynamics and imprint erasure through 5-hydroxymethylcytosine. Science (New York, NY) 339: 448-452
Hernando H, Gelato KA, Lesche R, Beckmann G, Koehr S, Otto S, Steigemann P, Stresemann C (2016) EZH2 Inhibition Blocks Multiple Myeloma Cell Growth through Upregulation of Epithelial Tumor Suppressor Genes. Molecular Cancer Therapeutics 15: 287
Hou B, Saudan P, Ott G, Wheeler Matthew L, Ji M, Kuzmich L, Lee Linda M, Coffman Robert L, Bachmann Martin F, DeFranco Anthony L (2011) Selective Utilization of Toll-like Receptor and MyD88 Signaling in B Cells for Enhancement of the Antiviral Germinal Center Response. Immunity 34: 375-384
Hung KH, Su ST, Chen CY, Hsu PH, Huang SY, Wu WJ, Chen MJM, Chen HY, Wu PC, Lin FR, Tsai MD, Lin KI (2016) Aiolos collaborates with Blimp-1 to regulate the survival of multiple myeloma cells. Cell Death And Differentiation 23: 1175
Hunter ZR, Xu L, Yang G, Tsakmaklis N, Vos JM, Liu X, Chen J, Manning RJ, Chen JG, Brodsky P, Patterson CJ, Gustine J, Dubeau T, Castillo JJ, Anderson KC, Munshi NM, Treon SP (2016) Transcriptome sequencing reveals a profile that corresponds to genomic variants in Waldenström macroglobulinemia. Blood 128: 827-838
Iwanaga M, Chiang CJ, Soda M, Lai MS, Yang YW, Miyazaki Y, Matsuo K, Matsuda T, Sobue T (2014) Incidence of lymphoplasmacytic lymphoma/Waldenstrom's macroglobulinaemia in Japan and Taiwan population-based cancer registries, 1996-2003. International journal of cancer 134: 174-80

Jalali S, Price-Troska T, Paludo J, Villasboas J, Kim H-J, Yang Z-Z, Novak AJ, Ansell SM (2018) Soluble PD-1 ligands regulate T-cell function in Waldenstrom macroglobulinemia. Blood Advances 2: 1985
Kallies A, Hasbold J, Tarlinton DM, Dietrich W, Corcoran LM, Hodgkin PD, Nutt SL (2004) Plasma Cell Ontogeny Defined by Quantitative Changes in Blimp-1 Expression. The Journal of Experimental Medicine 200: 967
Kent WJ, Sugnet CW, Furey TS, Roskin KM, Pringle TH, Zahler AM, Haussler, David (2002) The Human Genome Browser at UCSC. Genome Research 12: 996-1006
Kim KH, Roberts CWM (2016) Targeting EZH2 in cancer. Nature Medicine 22: 128
Kleer CG, Cao Q, Varambally S, Shen R, Ota I, Tomlins SA, Ghosh D, Sewalt RGAB, Otte AP, Hayes DF, Sabel MS, Livant D, Weiss SJ, Rubin MA, Chinnaiyan AM (2003) EZH2 is a marker of aggressive breast cancer and promotes neoplastic transformation of breast epithelial cells. Proceedings of the National Academy of Sciences 100: 11606
Kuo TC, Calame KL (2004) B Lymphocyte-Induced Maturation Protein (Blimp)-1, IFN Regulatory Factor (IRF)-1, and IRF-2 Can Bind to the Same Regulatory Sites. The Journal of Immunology 173: 5556
Kurimoto K, Yabuta Y, Hayashi K, Ohta H, Kiyonari H, Mitani T, Moritoki Y, Kohri K, Kimura H, Yamamoto T, Katou Y, Shirahige K, Saitou M (2015) Quantitative Dynamics of Chromatin Remodeling during Germ Cell Specification from Mouse Embryonic Stem Cells. Cell Stem Cell 16: 517-532
Kyle RA, Larson DR, McPhail ED, Therneau TM, Dispenzieri A, Kumar S, Kapoor P, Cerhan JR, Rajkumar SV (2018) Fifty-Year Incidence of Waldenstrom Macroglobulinemia in Olmsted County, Minnesota, From 1961 Through 2010: A Population-Based Study With Complete Case Capture and Hematopathologic Review. Mayo Clinic proceedings 93: 739-746
Langmead B, Salzberg SL (2012) Fast gapped-read alignment with Bowtie 2. Nature Methods 9: 357
Lawrence DW, Kornbluth J (2016) E3 ubiquitin ligase NKLAM ubiquitinates STAT1 and positively regulates STAT1-mediated transcriptional activity. Cellular Signalling 28: 1833-1841
Liberzon A, Birger C, Thorvaldsdottir H, Ghandi M, Mesirov JP, Tamayo P (2015) The Molecular Signatures Database (MSigDB) hallmark gene set collection. Cell systems 1: 417-425
Lin F-R, Kuo H-K, Ying H-Y, Yang F-H, Lin K-I (2007) Induction of Apoptosis in Plasma Cells by B Lymphocyte–Induced Maturation Protein-1 Knockdown. Cancer Research 67: 11914
Lin K-I, Angelin-Duclos C, Kuo TC, Calame K (2002) Blimp-1-dependent repression of Pax-5 is required for differentiation of B cells to immunoglobulin M-secreting plasma cells. Molecular and cellular biology 22: 4771-4780
Lin Y, Wong K-k, Calame K (1997) Repression of c-myc transcription by Blimp-1, an inducer of terminal B cell differentiation. Science 276: 596-599
Lois C, Hong EJ, Pease S, Brown EJ, Baltimore D (2002) Germline transmission and tissue-specific expression of transgenes delivered by lentiviral vectors. Science 295: 868-872
Magnúsdóttir E, Dietmann S, Murakami K, Günesdogan U, Tang F, Bao S, Diamanti E, Lao K, Gottgens B, Azim Surani M (2013) A tripartite transcription factor

network regulates primordial germ cell specification in mice. Nature Cell Biology 15: 905
Magnúsdóttir E, Kalachikov S, Mizukoshi K, Savitsky D, Ishida-Yamamoto A, Panteleyev AA, Calame K (2007) Epidermal terminal differentiation depends on B lymphocyte-induced maturation protein-1. Proceedings of the National Academy of Sciences 104: 14988
Mandelbaum J, Bhagat G, Tang H, Mo T, Brahmachary M, Shen Q, Chadburn A, Rajewsky K, Tarakhovsky A, Pasqualucci L, Dalla-Favera R (2010) BLIMP1 is a Tumor Suppressor Gene Frequently Disrupted in Activated B Cell-like Diffuse Large B Cell Lymphoma. Cancer cell 18: 568-579
Martins G, Calame K (2008) Regulation and Functions of Blimp-1 in T and B Lymphocytes. Annual Review of Immunology 26: 133-169
Minnich M, Tagoh H, Bönelt P, Axelsson E, Fischer M, Cebolla B, Tarakhovsky A, Nutt SL, Jaritz M, Busslinger M (2016) Multifunctional role of the transcription factor Blimp-1 in coordinating plasma cell differentiation. Nature Immunology 17: 331
Morgan MAJ, Magnusdottir E, Kuo TC, Tunyaplin C, Harper J, Arnold SJ, Calame K, Robertson EJ, Bikoff EK (2009) Blimp-1/Prdm1 Alternative Promoter Usage during Mouse Development and Plasma Cell Differentiation. Molecular and Cellular Biology 29: 5813
Morin RD, Johnson NA, Severson TM, Mungall AJ, An J, Goya R, Paul JE, Boyle M, Woolcock BW, Kuchenbauer F, Yap D, Humphries RK, Griffith OL, Shah S, Zhu H, Kimbara M, Shashkin P, Charlot JF, Tcherpakov M, Corbett R et al. (2010) Somatic mutations altering EZH2 (Tyr641) in follicular and diffuse large B-cell lymphomas of germinal-center origin. Nature Genetics 42: 181
Mould AW, Morgan MAJ, Nelson AC, Bikoff EK, Robertson EJ (2015) Blimp1/Prdm1 Functions in Opposition to Irf1 to Maintain Neonatal Tolerance during Postnatal Intestinal Maturation. PLOS Genetics 11: e1005375
Müller J, Hart CM, Francis NJ, Vargas ML, Sengupta A, Wild B, Miller EL, O'Connor MB, Kingston RE, Simon JA (2002) Histone Methyltransferase Activity of a Drosophila Polycomb Group Repressor Complex. Cell 111: 197-208
Murakami K, Günesdogan U, Zylicz JJ, Tang WWC, Sengupta R, Kobayashi T, Kim S, Butler R, Dietmann S, Azim Surani M (2016) NANOG alone induces germ cells in primed epiblast in vitro by activation of enhancers. Nature 529: 403
Nutt SL, Fairfax KA, Kallies A (2007) BLIMP1 guides the fate of effector B and T cells. Nature Reviews Immunology 7: 923
Ohinata Y, Payer B, O'carroll D, Ancelin K, Ono Y, Sano M, Barton SC, Obukhanych T, Nussenzweig M, Tarakhovsky A (2005) Blimp1 is a critical determinant of the germ cell lineage in mice. Nature 436: 207
Pardoll DM (2012) The blockade of immune checkpoints in cancer immunotherapy. Nature Reviews Cancer 12: 252
Pasare C, Medzhitov R (2005) Control of B-cell responses by Toll-like receptors. Nature 438: 364
Pasqualucci L, Compagno M, Houldsworth J, Monti S, Grunn A, Nandula SV, Aster JC, Murty VV, Shipp MA, Dalla-Favera R (2006) Inactivation of the PRDM1/BLIMP1 gene in diffuse large B cell lymphoma. The Journal of Experimental Medicine 203: 311

Pfaffl MW (2001) A new mathematical model for relative quantification in real-time RT–PCR. Nucleic Acids Research 29: e45-e45
Pimentel H, Bray NL, Puente S, Melsted P, Pachter L (2017) Differential analysis of RNA-seq incorporating quantification uncertainty. Nature methods 14: 687
Piskurich JF, Lin K-I, Lin Y, Wang Y, Ting JP-Y, Calame K (2000a) BLIMP-1 mediates extinction of major histocompatibility class II transactivator expression in plasma cells. Nature immunology 1: 526
Piskurich JF, Lin KI, Lin Y, Wang Y, Ting JPY, Calame K (2000b) BLIMP-1 mediates extinction of major histocompatibility class II transactivator expression in plasma cells. Nature Immunology 1: 526
Ramírez F, Ryan DP, Grüning B, Bhardwaj V, Kilpert F, Richter AS, Heyne S, Dündar F, Manke T (2016) deepTools2: a next generation web server for deep-sequencing data analysis. Nucleic Acids Research 44: W160-W165
Ren B, Chee KJ, Kim TH, Maniatis T (1999) PRDI-BF1/Blimp-1 repression is mediated by corepressors of the Groucho family of proteins. Genes & Development 13: 125-137
Roberts MJ, Chadburn A, Ma S, Hyjek E, Peterson LC (2013) Nuclear Protein Dysregulation in Lymphoplasmacytic Lymphoma/Waldenström Macroglobulinemia. American Journal of Clinical Pathology 139: 210-219
Roccaro AM, Sacco A, Jia X, Azab AK, Maiso P, Ngo HT, Azab F, Runnels J, Quang P, Ghobrial IM (2010) microRNA-dependent modulation of histone acetylation in Waldenstrom macroglobulinemia. Blood: blood-2010-01-265686
Savitsky D, Calame K (2006) B-1 B lymphocytes require Blimp-1 for immunoglobulin secretion. The Journal of Experimental Medicine 203: 2305
Schop RFJ, Kuehl WM, Van Wier SA, Ahmann GJ, Price-Troska T, Bailey RJ, Jalal SM, Qi Y, Kyle RA, Greipp PR, Fonseca R (2002) Waldenström macroglobulinemia neoplastic cells lack immunoglobulin heavy chain locus translocations but have frequent 6q deletions. Blood 100: 2996
Shaffer AL, Emre NCT, Lamy L, Ngo VN, Wright G, Xiao W, Powell J, Dave S, Yu X, Zhao H, Zeng Y, Chen B, Epstein J, Staudt LM (2008) IRF4 addiction in multiple myeloma. Nature 454: 226
Shaffer AL, Lin K-I, Kuo TC, Yu X, Hurt EM, Rosenwald A, Giltnane JM, Yang L, Zhao H, Calame K, Staudt LM (2002) Blimp-1 Orchestrates Plasma Cell Differentiation by Extinguishing the Mature B Cell Gene Expression Program. Immunity 17: 51-62
Shapiro-Shelef M, Lin K-I, McHeyzer-Williams LJ, Liao J, McHeyzer-Williams MG, Calame K (2003) Blimp-1 is required for the formation of immunoglobulin secreting plasma cells and pre-plasma memory B cells. Immunity 19: 607-620
Shapiro-Shelef M, Lin K-I, Savitsky D, Liao J, Calame K (2005) Blimp-1 is required for maintenance of long-lived plasma cells in the bone marrow. The Journal of Experimental Medicine 202: 1471
Subramanian A, Tamayo P, Mootha VK, Mukherjee S, Ebert BL, Gillette MA, Paulovich A, Pomeroy SL, Golub TR, Lander ES, Mesirov JP (2005) Gene set enrichment analysis: A knowledge-based approach for interpreting genome-wide expression profiles. Proceedings of the National Academy of Sciences 102: 15545
Tellier J, Shi W, Minnich M, Liao Y, Crawford S, Smyth GK, Kallies A, Busslinger M, Nutt SL (2016) Blimp-1 controls plasma cell function through the regulation of

immunoglobulin secretion and the unfolded protein response. Nature Immunology 17: 323
Thibult M-L, Mamessier E, Gertner-Dardenne J, Pastor S, Just-Landi S, Xerri L, Chetaille B, Olive D (2013) PD-1 is a novel regulator of human B-cell activation. International immunology 25: 129-137
Tooze RM, Stephenson S, Doody GM (2006) Repression of IFN-γ Induction of Class II Transactivator: A Role for PRDM1/Blimp-1 in Regulation of Cytokine Signaling. The Journal of Immunology 177: 4584-4593
Treon SP (2009) How I treat Waldenström macroglobulinemia. Blood 114: 2375
Treon SP, Cao Y, Xu L, Yang G, Liu X, Hunter ZR (2014) Somatic mutations in MYD88 and CXCR4 are determinants of clinical presentation and overall survival in Waldenström macroglobulinemia. Blood 123: 2791
Treon SP, Tripsas CK, Meid K, Warren D, Varma G, Green R, Argyropoulos KV, Yang G, Cao Y, Xu L, Patterson CJ, Rodig S, Zehnder JL, Aster JC, Harris NL, Kanan S, Ghobrial I, Castillo JJ, Laubach JP, Hunter ZR et al. (2015) Ibrutinib in Previously Treated Waldenström's Macroglobulinemia. New England Journal of Medicine 372: 1430-1440
Treon SP, Xu L, Yang G, Zhou Y, Liu X, Cao Y, Sheehy P, Manning RJ, Patterson CJ, Tripsas C, Arcaini L, Pinkus GS, Rodig SJ, Sohani AR, Harris NL, Laramie JM, Skifter DA, Lincoln SE, Hunter ZR (2012) MYD88 L265P Somatic Mutation in Waldenström's Macroglobulinemia. New England Journal of Medicine 367: 826-833
Vijay A, Gertz MA (2007) Waldenström macroglobulinemia. Blood 109: 5096-5103
Vincent SD, Dunn NR, Sciammas R, Shapiro-Shalef M, Davis MM, Calame K, Bikoff EK, Robertson EJ (2005) The zinc finger transcriptional repressor Blimp1/Prdm1 is dispensable for early axis formation but is required for specification of primordial germ cells in the mouse. Development 132: 1315
Vivier E, Tomasello E, Baratin M, Walzer T, Ugolini S (2008) Functions of natural killer cells. Nature Immunology 9: 503
Wang H, Chen Y, Li F, Delasalle K, Wang J, Alexanian R, Kwak L, Rustveld L, Du XL, Wang M (2012) Temporal and geographic variations of Waldenstrom macroglobulinemia incidence: a large population-based study. Cancer 118: 3793-800
Wu ZL, Zheng SS, Li ZM, Qiao YY, Aau MY, Yu Q (2009) Polycomb protein EZH2 regulates E2F1-dependent apoptosis through epigenetically modulating Bim expression. Cell Death And Differentiation 17: 801
Xu L, Hunter ZR, Yang G, Cao Y, Liu X, Manning R, Tripsas C, Chen J, Patterson CJ, Kluk M, Kanan S, Castillo J, Lindeman N, Treon SP (2014) Detection of MYD88 L265P in peripheral blood of patients with Waldenström's Macroglobulinemia and IgM monoclonal gammopathy of undetermined significance. Leukemia 28: 1698
Yu J, Angelin-Duclos C, Greenwood J, Liao J, Calame K (2000) Transcriptional Repression by Blimp-1 (PRDI-BF1) Involves Recruitment of Histone Deacetylase. Molecular and Cellular Biology 20: 2592-2603
Yu X, Li W, Deng Q, Li L, Hsi ED, Young KH, Zhang M, Li Y (2018) MYD88 L265P Mutation in Lymphoid Malignancies. Cancer Research
Yu YL, Chou RH, Shyu WC, Hsieh SC, Wu CS, Chiang SY, Chang WJ, Chen JN, Tseng YJ, Lin YH, Lee W, Yeh SP, Hsu JL, Yang CC, Hung SC, Hung MC (2013) Smurf2-mediated degradation of EZH2 enhances neuron differentiation and improves functional recovery after ischaemic stroke. EMBO Molecular Medicine 5: 531

Zhan F, Tian E, Bumm K, Smith R, Barlogie B, Shaughnessy J (2003) Gene expression profiling of human plasma cell differentiation and classification of multiple myeloma based on similarities to distinct stages of late-stage B-cell development. Blood 101: 1128
Zhang Y, Liu T, Meyer CA, Eeckhoute J, Johnson DS, Bernstein BE, Nusbaum C, Myers RM, Brown M, Li W, Liu XS (2008) Model-based analysis of ChIP-Seq (MACS). Genome biology 9: R137
Zhou Y, Liu X, Xu L, Hunter ZR, Cao Y, Yang G, Carrasco R, Treon SP (2014) Transcriptional repression of plasma cell differentiation is orchestrated by aberrant over-expression of the ETS factor SPIB in Waldenström macroglobulinaemia. British Journal of Haematology 166: 677-689
Zhu LJ, Gazin C, Lawson ND, Pages H, Lin SM, Lapointe DS, Green MR (2010) ChIPpeakAnno: a Bioconductor package to annotate ChIP-seq and ChIP-chip data. BMC bioinformatics 11: 237
Zingg D, Arenas-Ramirez N, Sahin D, Rosalia RA, Antunes AT, Haeusel J, Sommer L, Boyman O (2017) The Histone Methyltransferase Ezh2 Controls Mechanisms of Adaptive Resistance to Tumor Immunotherapy. Cell Reports 20: 854-867

Figure 1

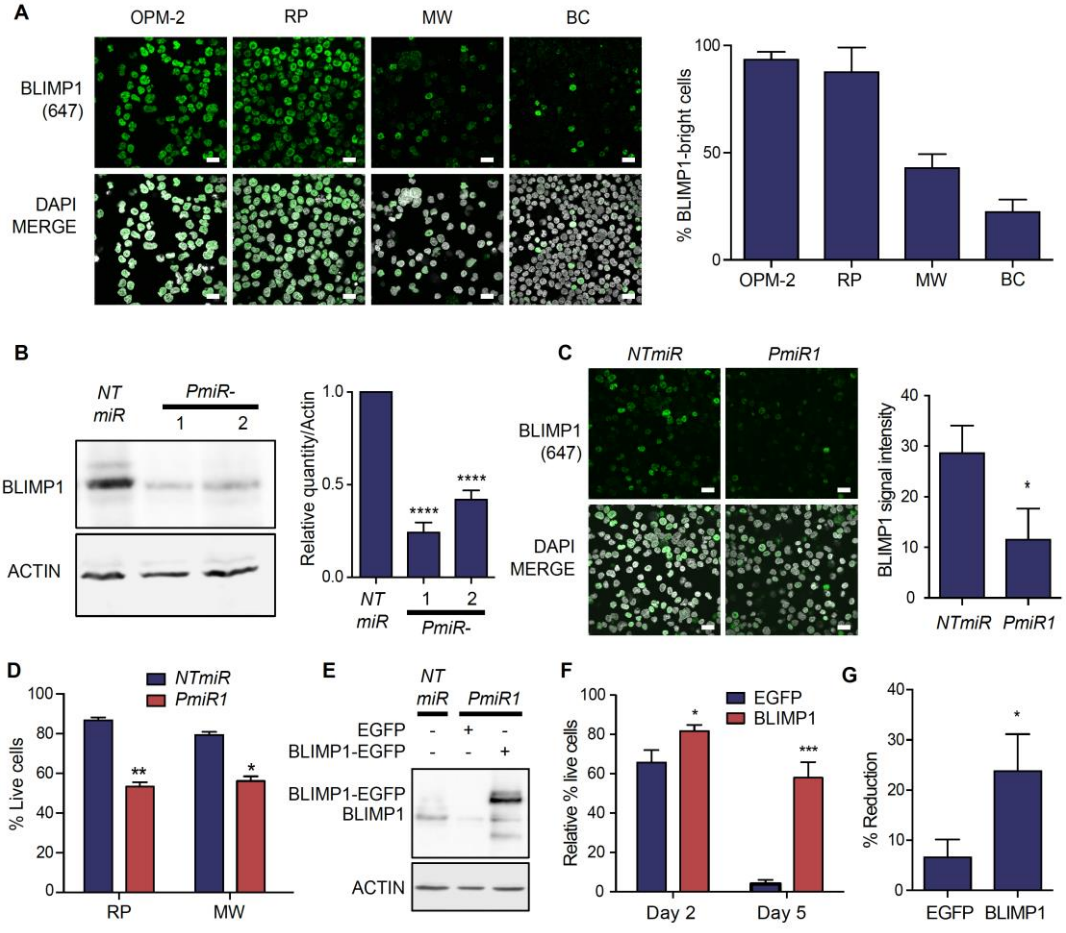

Figure 1: BLIMP1 promotes survival of WM cells

(A) BLIMP1 expression in myeloma cell line OPM-2 and in WM cell lines RP, MW and BC as detected by immunofluorescence staining, with bar graph representing percentage of BLIMP1bright cells. Scale bars represent 20μm. (B) Immunoblot of BLIMP1 expression following 48h dox induction of RP cells expressing NTmiR, PmiR1 or PmiR2, with bar graph representing the quantity of BLIMP1 relative to actin; ****p < 0.0001. (C) Immunofluorescence staining of BLIMP1 following 48h dox induction in MW cells expressing NTmiR, PmiR1 or PmiR2, with cell profiler quantification; p = 0.0228. (D) Percentage of live cells as determined by Trypan blue exclusion assay in the RP and MW cell lines. RP, p = 0.0019; MW, p = 0.0162. (E) Immunoblot depicting lentiviral ectopic expression of EGFP or BLIMP1-EGFP in the RP PmiR1 cells, next to the RP NTmiR cells. (F) The percentage of live RP PmiR1 cells with ectopic EGFP or BLIMP1-EGFP expression determined by the Trypan blue exclusion assay normalised to the percentage of live cells following transduction of RP NTmiR cells with EGFP or BLIMP1-EGFP. Day 2, *p = 0.0165; Day 5, ***p = 0.0003. (G) Per cent reduction as measured by resazurin assay for RP PmiR1 cells with EGFP or BLIMP1-EGFP, five days after dox induction. *p = 0.0208. All p-values as determined by student's two-tailed t-test. All graphs plotted as mean of three independent experiments, with error bars representing standard deviation.

Figure 2

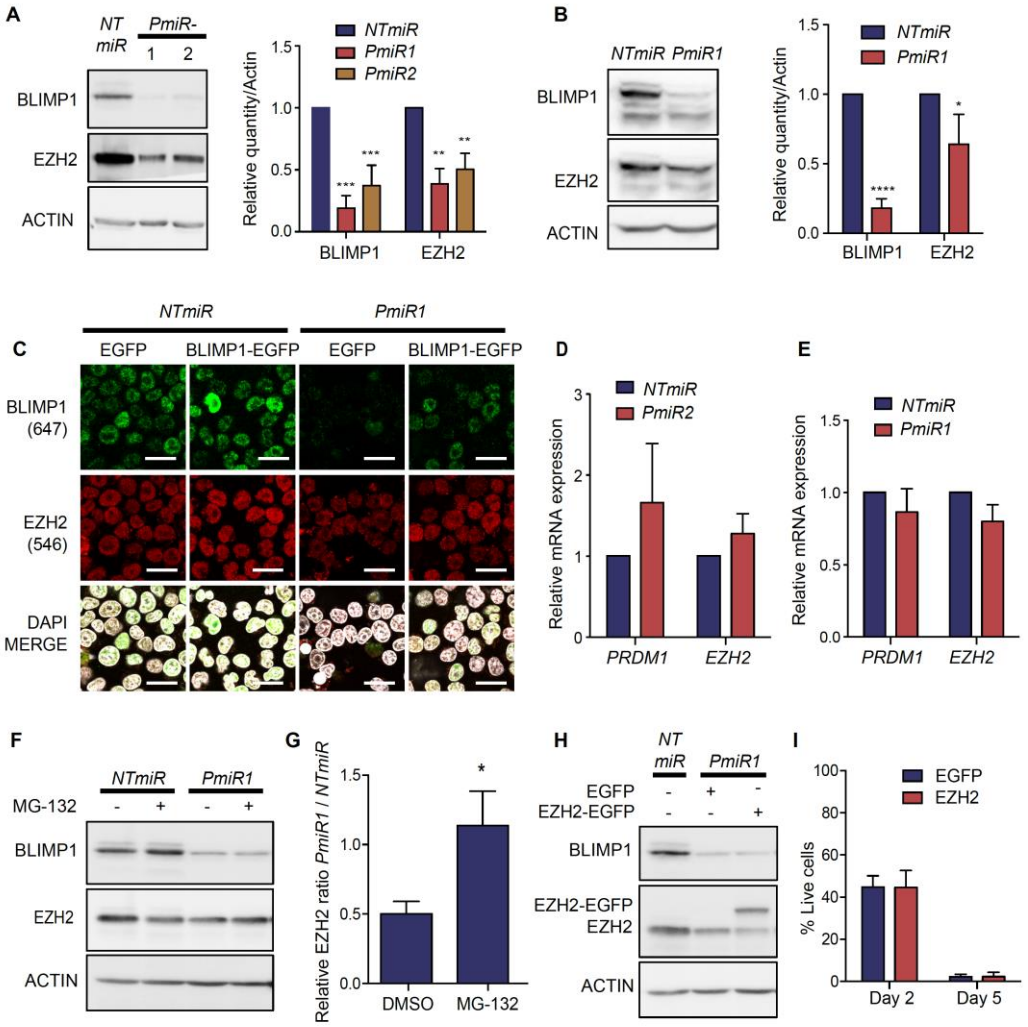

Figure 2: BLIMP1 maintains EZH2 protein levels

(A) Immunoblot of BLIMP1 and EZH2 expression following 48h dox-induction of RP cells expressing NTmiR, PmiR1 or PmiR2, with quantification of signal relative to actin in bar plot; ***p = 0.0002; ***p = 0.001; **p = 0.0027. (B) Immunoblot of BLIMP1 and EZH2 expression following 48h dox-induction of OPM-2 cells expressing NTmiR or PmiR1, with quantification of signal relative to actin in bar plot; ****p < 0.0001; *p = 0.016. (C) Immunofluorescence staining of BLIMP1 and EZH2 expression following 48 h dox-induction of RPCI-WM1 cells expressing NTmiR or PmiR1, transduced with EGFP or BLIMP1-EGFP. Scale bars represent 20 µm. (D) RT-qPCR results depicting relative mRNA expression of PRDM1 and EZH2 normalised to PPIA and ACTB in the RP cell line and (E) in the OPM-2 cell line. (F) Immunoblot of BLIMP1 and EZH2 expression following 24h dox-induction of RP cells expressing NTmiR or PmiR1 treated with DMSO or 5µM MG-132 for 4h. (G) The ratio of EZH2 expression relative to actin for RP PmiR1 cells divided by RP NTmiR cells treated with DMSO or MG132 as in Fig. 2F; p = 0.0134. (H) Immunoblot of BLIMP1 and EZH2 expression following 48h dox-induction of RP NTmiR cells or PmiR1 cells transduced with EGFP or EZH2-EGFP. (I) Percentage of live cells as determined by Trypan blue exclusion assay in the RP PmiR1 cells transduced with EGFP or EZH2-EGFP. All p-values as determined by student's two-tailed t-test. All graphs plotted as mean of three independent experiments with error bars representing standard deviation.

Figure 3

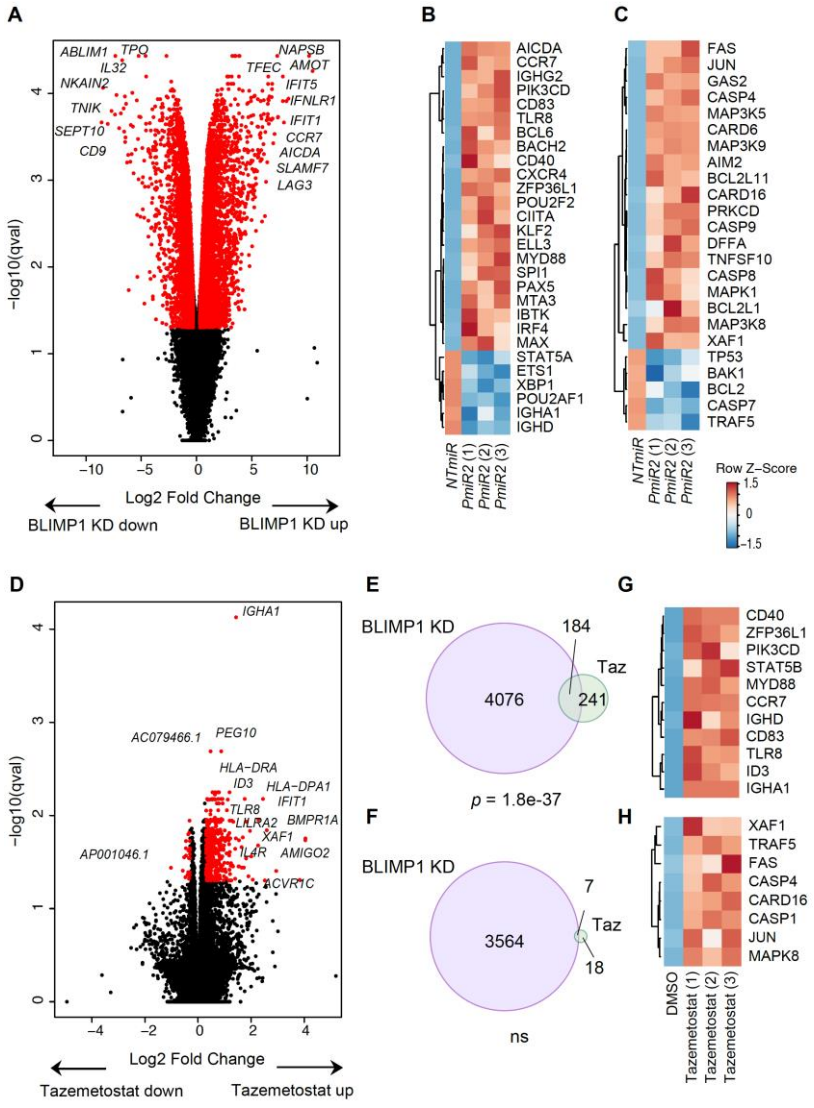

Figure 3: BLIMP1 KD induces large transcriptional changes

RNAseq results for (A) 48h dox-induced RP cells comparing PmiR1 to NTmiR. Values are plotted as log2 fold change vs. –log10(qvalue). Red indicates those genes with a q-value ≤ 0.05 and a log2 fold change ≤ -0.3 or ≥ 0.3. Heat maps depicting the Z-score of the log2 fold change comparing PmiR1 to NTmiR for three independent replicates looking at (B) B cell genes and (C) apoptosis genes. (D) RNAseq results for RP cells treated for 48h with 300nM tazemetostat compared to vehicle control (DMSO). (E) Overlapping genes with increased expression following PRDM1 KD or tazemetostat treatment. (F) Overlapping genes with decreased expression following PRDM1 KD or tazemetostat treatment. Overlaps tested using Fisher's exact test. Heat maps depicting the Z-score of the log2 fold change comparing tazemetostat treatment to DMSO for three independent replicates looking at (G) B cell genes and (H) apoptosis genes.

Figure 4

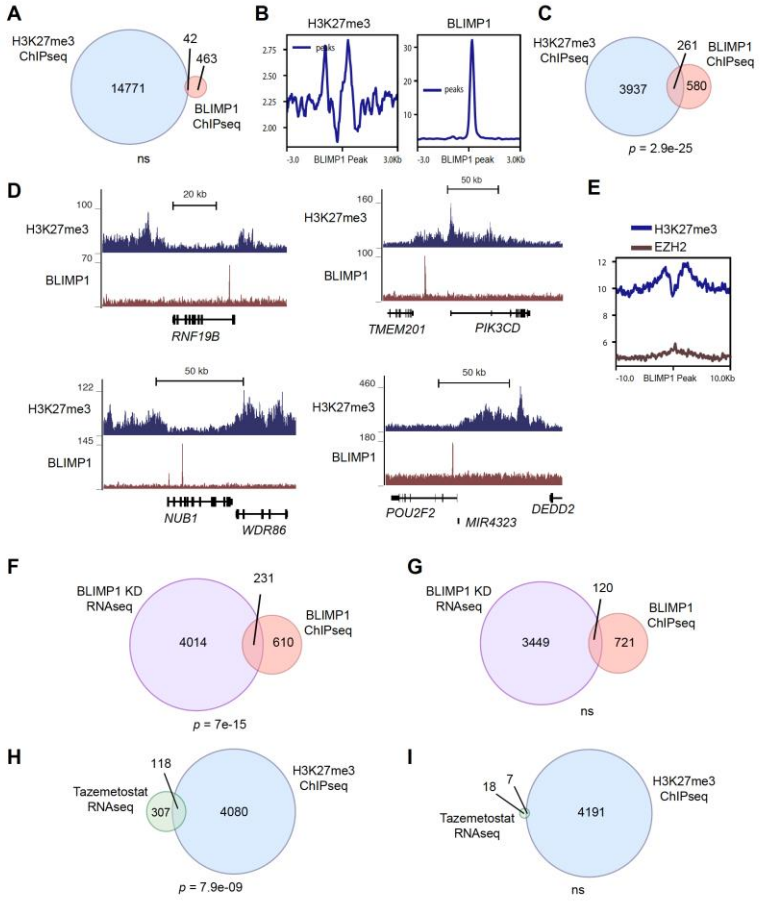

Figure 4: BLIMP1 and EZH2 are present at a subset of proximal genomic loci

(A) Venn diagram of H3K27me3 and BLIMP1 peaks extended ±10kb, showing overlaps in these regions. (ns) not significant as determined by hypergeometric test. Called peaks determined by overlap from peak calling from two independent experiments. (B) Enrichment of signal from ChIPseq tracks ±3kb from the centre of BLIMP1 binding sites. Data depicts representative experiment of two biological replicates. (C) Venn diagram of genes assigned to H3K27me3 and BLIMP1 peaks showing overlapping genes. p= 2.9e-25 as determined by Fisher's exact test. (D) ChIPseq tracks for H3K27me3 and BLIMP1 in the RP cell line. Data represents combination of reads from two independent experiments. (E) Enrichment of signal from ChIPseq tracks ±10kb from the centre of BLIMP1 binding sites in the NCI-H929 cell line. (F) Venn diagram depicting the overlap in genes with significantly increased expression following BLIMP1 KD and genes assigned to BLIMP1 binding sites. p= 7e-15, as determined by Fisher's exact test. (G) Venn diagram depicting the overlap in genes with significantly decreased expression following BLIMP1 KD and genes assigned to BLIMP1 binding sites. (ns) not significant as determined by Fisher's exact test. (H) Venn diagram depicting genes with significantly increased expression following tazemetostat treatment overlapping with genes assigned to H3K27me3 peaks. p= 7.9e-9, as determined by Fisher's exact test. (I) Venn diagram depicting genes with significantly decreased expression following tazemetostat treatment overlapping with genes assigned to H3K27me3 peaks. (ns) not significant, as determined by Fisher's exact test. All ChIPseq experiments were performed as two biological replicates.

Figure 5

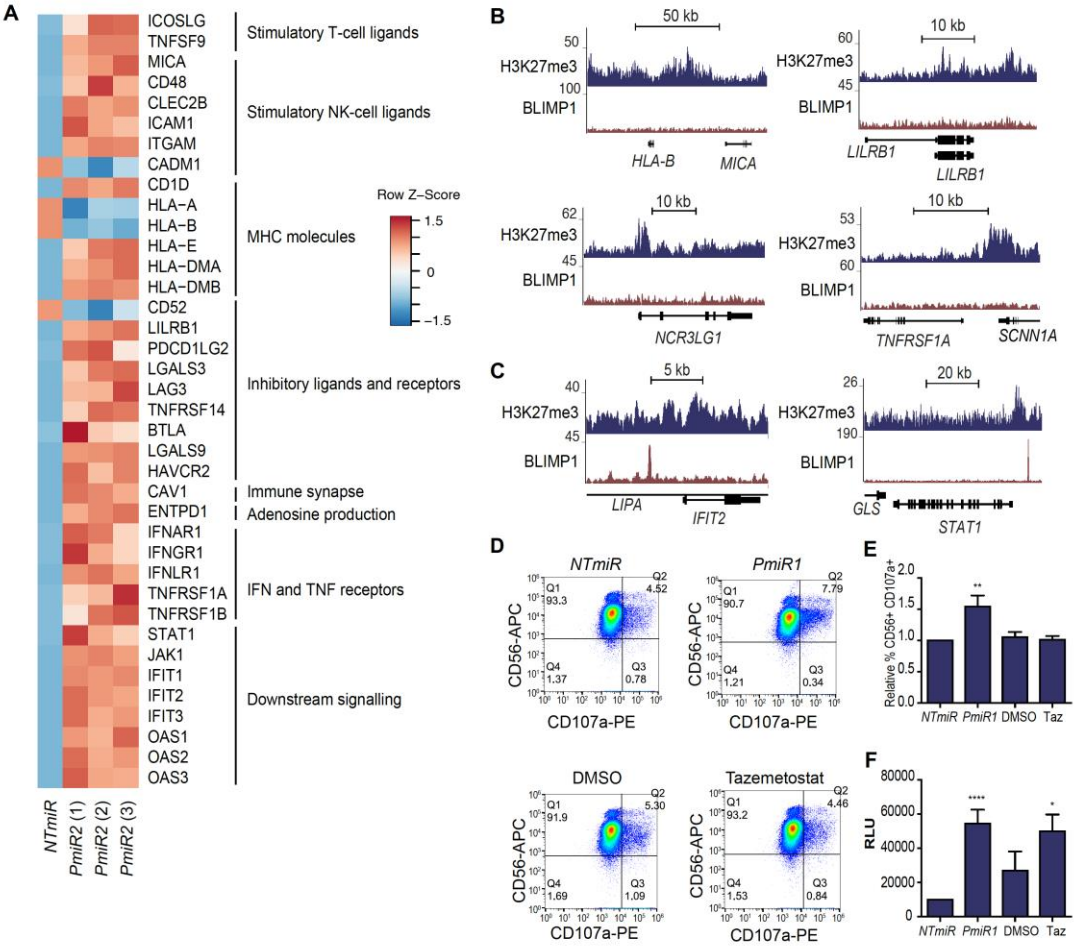

Figure 5: BLIMP1 and EZH2 promote immune evasion

(A) Heat maps showing z-score of the log2 fold change for PmiR2 compared to NTmiR and in RP cells with three independent replicates looking at genes involved in stimulation of T and NK cells, MHC molecules, inhibitory ligands and receptors, IFN and TNF receptors and downstream signalling. ChIPseq tracks for H3K27me3 and BLIMP1 in the RP cell line over (B) the immune surface molecule genes HLA-B, MICA, LILRB1, NCR3LG1, TNFRSF1A, or (C) the downstream signalling genes, IFIT2 and STAT1. Data represents combination of reads from two independent experiments. (D) Percentage CD56+CD107a+ cells (Q2) representing degranulating NK cells, as determined by flow cytometry following co-culture with RP cells with NTmiR or PmiR1, or RP cells treated with DMSO or Tazemetostat. One representative experiment is displayed. (E) Relative quantification of the degranulation assay **p = 0.0088. (F) Cytotoxicity depicted in relative luminescence units (RLU), as measured by adenylate kinase activity in the culture media following 4 h co-culture of NK cells with RP cells expressing NTmiR or PmiR1, or RP cells treated with DMSO or 1μM Tazemetostat. Cells were co-cultured at the effector:target ratio of 20:1. ****p = 3.1×10-5; *p = 0.02. Results of the degranulation and cytotoxicity assays from four individual donors, performed in two pairs on two separate occasions.

Expanded View Figure 1

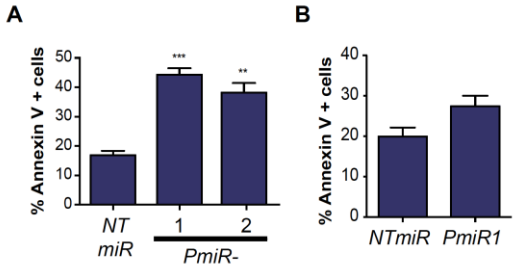

Expanded View Figure 1

(A) Annexin V staining of dox-induced RP cells with NTmiR, PmiR1 or PmiR2; ***p = 0.0004; **p = 0.0071. (B) Annexin V staining of dox-induced MW cells with NTmiR or PmiR1; p = 0.0572.

Expanded View Figure 2

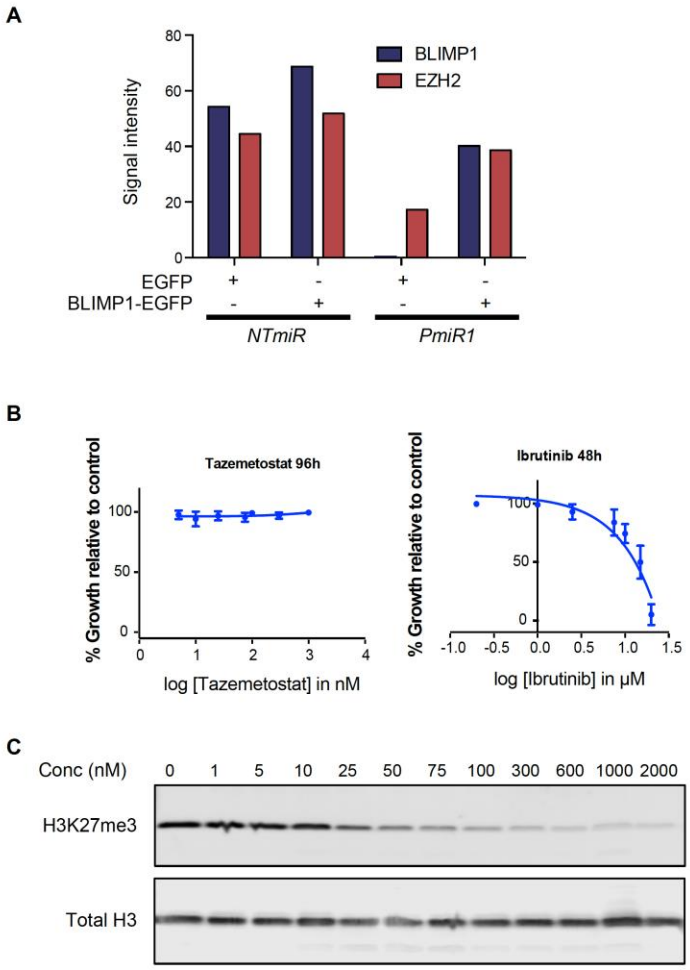

Expanded View Figure 2

(A) Signal intensity of immunofluorescence staining for BLIMP1 and EZH2 as quantified by cell profiler from approximately 5000 cells per sample across two independenct replicates. (B) Relative growth of RP cells treated with tazemetostat for 96h, shown next to RP cells treated with Ibrutinib for 48h. (C) Immunoblot of histone extracts from RP cells stained for H3K27me3 with total H3 as a loading control following 48h tazemetostat treatment at the indicated concentrations. The 0 concentration was treated with vehicle control, DMSO.

Expanded View Figure 3

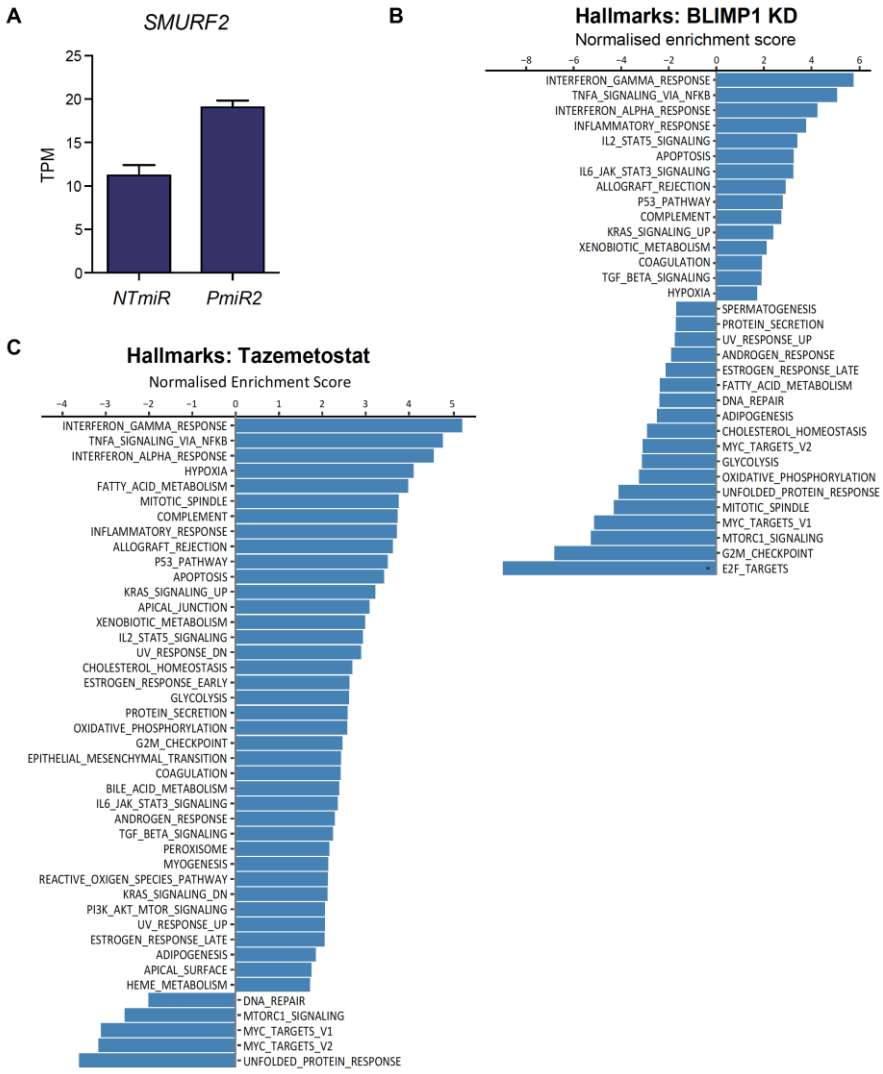

Expanded View Figure 3

(A) Graph of RNAseq results depicting normalised transcripts per million (TPM) values for SMURF2 in RP cells with NTmiR and PmiR1. Bar plots depicting normalised enrichment score for Hallmarks gene sets identified using GSEA pre-ranked with FDR-corrected p-value ≤ 0.05 for (B) PmiR1 compared to NTmiR and (C) tazemetostat treatment compared to DMSO.

Expanded View Figure 4

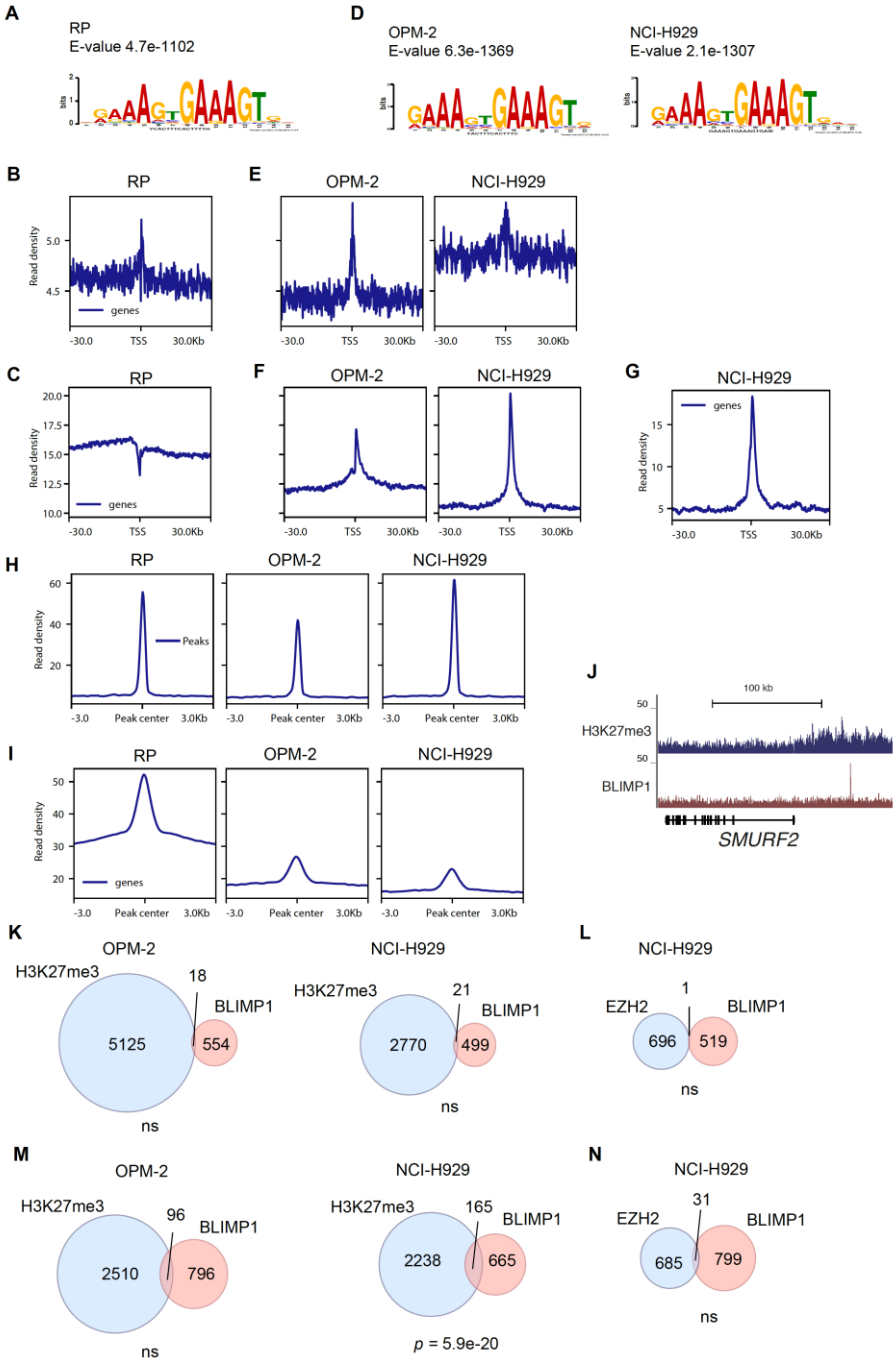

Expanded View Figure 4

(A) Motif enrichment analysis showing the top motif for BLIMP1 ChIPseq experiments in the RP cell line. Profiles showing enrichment over ±30 kb regions from TSSs assigned to (B) BLIMP1 and (C) H3K27me3 peaks in the RP cell line. (D) Motif enrichment analysis showing the top motif for BLIMP1 ChIPseq experiments in the OPM-2 and NCI-H929 cell lines. Profiles showing enrichment over ±30 kb regions from TSSs assigned to (E) BLIMP1, (F) H3K27me3 and (G) EZH2 peaks in the OPM-2 and NCI-H929 cell lines. (H) Enrichment of BLIMP1 signal in the RP, OPM-2 and NCI-H929 cell lines over BLIMP1 peaks from the RP cell line. (I) Enrichment of H3K27me3 signal in the RP, OPM-2 and NCI-H929 cell lines over H3K27me3 peaks from the RP cell line. (J) ChIPseq tracks for H3K27me3 and BLIMP1 over the SMURF2 gene in the RP cell line. (K) Venn diagrams of H3K27me3 and BLIMP1 peaks extended ±10kb, showing overlaps in these regions in the OPM-2 and NCI-H929 cell lines. (ns) not significant as determined by hypergeometric test. (L) Venn diagram of EZH2 and BLIMP1 peaks extended ±10kb, showing overlaps in these regions in the NCI-H929 cell line. (ns) not significant as determined by hypergeometric test. (M) Venn diagrams of overlapping genes assigned to peaks for H3K27me3 or BLIMP1 in the OPM-2 and NCI-H929 cell lines. Significance determined by Fisher's exact test. OPM-2, ns, not significant; NCI-H929, p = 5.9e-20. (N) Venn diagram of overlapping genes assigned to peaks for EZH2 or BLIMP1 in the NCI-H929 cell lines. (ns) not significant, as determined by Fisher's exact test.

Expanded View Figure 5

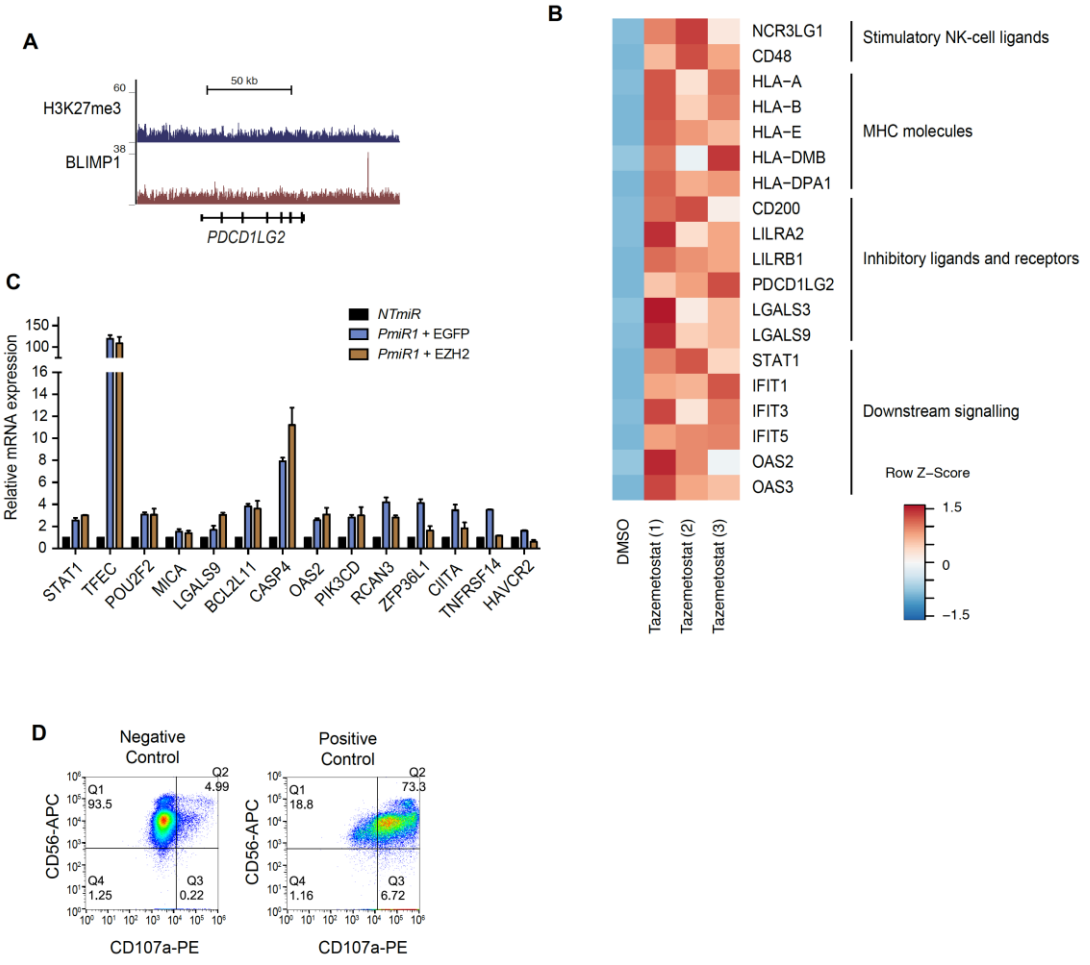

Expanded View Figure 5

(A) ChIPseq tracks for H3K27me3 and BLIMP1 over the PDCD1LG2 gene in the RP cell line. (B) Heat map showing the z-score of the log2 fold change for Tazemetostat compared to DMSO in RP cells with three independent replicates looking at genes involved in stimulation of NK cells, MHC molecules, inhibitory ligands and receptors, and downstream signalling. (C) RT-qPCR from three independent experiments depicting relative mRNA expression comparing RP cells with NTmiR, and PmiR1 transduced with EGFP or EZH2-EGFP. (D) Negative control for the degranulation assay, consisting of NK cells cultured alone, and positive control consisting of NK cells in co-culture with RP cells treated with 2.5µg/mL phorbol 12-myristate 13-acetate and 0.5µg/mL ionomycin.

Appendix

Appendix I: Scripts and codes used for bioinformatics analyses

1 Processing of Raw Data

1.1 FastQC

Analyses were begun using FastQc with the simple command:

```
fastqc <yourfilename>.fastq.gz
```

1.2 Trim Galore

The fastqc html files were examined for quality and adaptor contamination. There was adaptor sequence present for some samples, so all samples were then processed with Trim Galore to remove these. The * represents the file name, and the R1 and R2 are for the paired-end matching reads. The --fastqc command makes the FastQC program run after trimming is complete.

```
trim_galore --fastqc --paired --gzip -t *_R1.fq.gz *_R2.fq.gz" \;
```

- Trimmed files will be output as name_R1_val_1.fq.gz

2 RNAseq

2.1 STAR Aligner

STAR was used to align reads to check for alignment to the human genome. This step was used as an additional quality control of our RNAseq reads.

Making a genome index with STAR (all on one line):

```
STAR --runThreadN 12 --runMode genomeGenerate --genomeDir ./ --genomeFastaFiles /home/kimberl/Ensembl/Homo_sapiens.GRCh38.dna.primary_assembly.fa --sjdbGTFfile /home/kimberl/Ensembl/Homo_sapiens.GRCh38.91.gtf --sjdbOverhang 124
```

Mapping reads and generating sorted .bam files:

```
STAR --runThreadN 12 --genomeDir ~/STAR/genome/ --sjdbGTFfile ~/Homo_sapiens_UCSC_hg38_iGenomes/UCSC/hg38/Annotation/Genes/genes.gtf --readFilesIn file.fastq.gz --readFilesCommand zcat --outSAMtype BAM SortedByCoordinate
```

Generating signal files for visualization on genome browsers for stranded RNA-seq data:

```
STAR --runMode inputAlignmentsFromBAM --inputBAMfile Aligned.sortedByCoord.out.bam --outWigType wiggle --outWigStrand Stranded --runThreadN 12
```

2.2 Kallisto

Kallisto was used for pseudoalignment to the hg38 transcriptome and for quantification of the reads.

2.2.1 First prepare Kallisto index

We used the hg38 transcriptome from ENSEMBL. This was chosen because it has the most annotations. We also included a file containing sequences of rRNAs.

```
kallisto index -i indexfilename.idx Homo_sapiens.GRCh38.cdna.all.fa human_rRNA.fa
```

2.2.2 Running Kallisto

Kallisto was then run on all samples with the --rf-stranded argument because our libraries were strand-specific and this gives us more information.

```
kallisto quant -i indexfilename.idx -o aligned_filename_Kallisto -b 100 --rf-stranded -t 14 trimmed_R1_val_1.fq.gz trimmed_R2_val_2.fq.gz" \;
```

2.3 Sleuth

2.3.1 Prepping for sleuth run

Open R and start a new R script. Set up libraries:

```
library("sleuth")
library("splines")
library("biomaRt")
library("ggthemes")
library("xlsx")
```

Make a .csv file in excel with the metadata of your samples:

Appendix Table I: metadata.csv

sample	miR	treatment	experiment
NTC_PACRCVV_Kallisto	NTC miR	none	KA377
Blimp1_PACRCVW_Kallisto	Blimp1 miR22	none	KA377
EZH2_PACRCVX_Kallisto	EZH2 miR2	none	KA377
EPZ_PACRCVY_Kallisto	WT	Tazemetostat	KA377
DMSO_PACRCVZ_Kallisto	WT	DMSO	KA377
NTC_PACRCWA_Kallisto	NTC miR	none	KA411
Blimp1_PACRCWB_Kallisto	Blimp1 miR22	none	KA411
EZH2_PACRCWC_Kallisto	EZH2 miR2	none	KA411
EPZ_PACRCWD_Kallisto	WT	Tazemetostat	KA411
DMSO_PACRCWE_Kallisto	WT	DMSO	KA411
NTC_PACRCWF_Kallisto	NTC miR	none	KA392
Blimp1_PACRCWG_Kallisto	Blimp1 miR22	none	KA392
EZH2PACRCWH_Kallisto	EZH2 miR2	none	KA392
EPZ_PACRCWI_Kallisto	WT	Tazemetostat	KA392
DMSO_PACRCWJ_Kallisto	WT	DMSO	KA392

Then collect samples and metadata:

```
sample_id <- list.dirs("20180210_Kallisto/.", full.names = TRUE)
kal_dirs <- sample_id[2:16]
all.files = list.files(path ="Kallisto_all/", recursive = TRUE, full.names = TRUE)
s2c <- read.csv("metadata.csv", header=TRUE)
s2c <- dplyr::mutate(s2c, path = kal_dirs)
s2c[] <- lapply(s2c, as.character)
```

Prepare a mart for annotating transcripts. Use it to make a transcript to gene set.

This code is using the Sleuth version 0.29.0, which uses a slightly different method for gene level analysis compared to newer versions of the package.

```
mart <- biomaRt::useEnsembl(biomart="ensembl",
dataset="hsapiens_gene_ensembl")
ttg <- biomaRt::getBM( attributes = c("ensembl_transcript_id",
                                      "ensembl_gene_id", "external_gene_name",
"description"),
                       mart = mart)
ttg <- dplyr::rename(ttg, target_id = ensembl_transcript_id,
                     ens_gene = ensembl_gene_id, ext_gene =
external_gene_name)
head (ttg)
```

2.3.2 Running Sleuth

Here we show an example of how we performed the sleuth run using both treatment and experiment as covariates in the analysis.

```
#Sleuth object with DMSO and Tazemetostat treated cells
s2c_DMSO_Taz <- s2c[c(4,5,9,10,14,15),]
sleuth_ob_DMSO_Taz <- sleuth_prep(s2c_DMSO_Taz, ~treatment +
experiment,
                                  target_mapping = ttg, aggregation_column =
'ens_gene', extra_bootstrap_summary = TRUE)
#Using both covariates in the full model
sleuth_ob_DMSO_Taz <- sleuth_fit(sleuth_ob_DMSO_Taz, ~treatment +
experiment, 'full')
#Reduced model taking only the batch into account
sleuth_ob_DMSO_Taz <- sleuth_fit(sleuth_ob_DMSO_Taz, ~experiment,
'treatment')
design_matrix(sleuth_ob_DMSO_Taz, which_model = "full")
```

Now testing the reduced model against the full, so that we see which genes are different between treatments, given the batch (experiment). We used the likelihood ratio test here.

```
sleuth_ob_DMSO_Taz <- sleuth_lrt(sleuth_ob_DMSO_Taz, 'treatment', 'full')
sleuth_ob_DMSO_Taz_lrt_results <- sleuth_results(sleuth_ob_DMSO_Taz,
'treatment:full', test_type = 'lrt')
#Now selecting only those DEGs with a q-value less than 0.05
sleuth_ob_DMSO_Taz_sig<-
```

```
sleuth_ob_DMSO_Taz_lrt_results[which(sleuth_ob_DMSO_Taz_lrt_results$qval<0.05),]
```

We used principle component analysis and sleuth_live() to look at the data in more detail.

```
sleuth_live(sleuth_ob_DMSO_Taz)
plot_pca(sleuth_ob_DMSO_Taz, pc_x = 1L, pc_y = 2L, use_filtered = TRUE, units = "tpm", color_by = "treatment",text_labels = TRUE)
```

Next, we calculated the log2 fold change from the Kallisto data

```
Taz_table <- kallisto_table(sleuth_ob_DMSO_Taz, use_filtered = TRUE, normalized = TRUE)
Taz_table <- dplyr::select(Taz_table, target_id, tpm, treatment, experiment)
Taz_table <- spread(Taz_table, key = experiment, value = tpm)
Taz_tbl_avtpm <- group_by(Taz_table, target_id)
Taz_tbl_avtpm <- aggregate(Taz_tbl_avtpm[, 3:5], list(Taz_tbl_avtpm$target_id), mean)



DMSO_table <- Taz_table[Taz_table$treatment == c("DMSO"),]
Tazem_table <- Taz_table[Taz_table$treatment == c("Tazemetostat"),]
#Subtracting on a batch-by-batch basis, values for Tazemetostat - DMSO
Taz_diff_table <- within(merge(Tazem_table,DMSO_table,by="target_id"), {
                    KA377 <- KA377.x-KA377.y
                    KA392 <- KA392.x-KA392.y
                    KA411 <- KA411.x-KA411.y
                  })[,c("target_id","KA377","KA392","KA411")]
Taz_diff_table$gene <- ttg$ext_gene[match(Taz_diff_table$target_id, ttg$ens_gene)]

Taz_diff_table <- Taz_diff_table[c(1,5,2:4)]
Taz_diff_table$qval <- sleuth_ob_DMSO_Taz_lrt_results$qval[match(Taz_diff_table$target_id, sleuth_ob_DMSO_Taz_lrt_results$target_id)]
Taz_diff_table$pval <- sleuth_ob_DMSO_Taz_lrt_results$pval[match(Taz_diff_table$target_id, sleuth_ob_DMSO_Taz_lrt_results$target_id)]

#Now calculating log2 fold change batch-by-batch
Taz_fc_table <- within(merge(Tazem_table,DMSO_table,by="target_id"), {
```

```
                    KA377 <- log2(KA377.x/KA377.y)
                    KA392 <- log2(KA392.x/KA392.y)
                    KA411 <- log2(KA411.x/KA411.y)
                  })[,c("target_id","KA377","KA392","KA411")]
Taz_fc_table$gene <- ttg$ext_gene[match(Taz_fc_table$target_id,
ttg$ens_gene)]
Taz_fc_table <- Taz_fc_table[c(1,5,2:4)]
Taz_fc_table$qval <-
sleuth_ob_DMSO_Taz_lrt_results$qval[match(Taz_fc_table$target_id,
sleuth_ob_DMSO_Taz_lrt_results$target_id)]
Taz_fc_table$pval <-
sleuth_ob_DMSO_Taz_lrt_results$pval[match(Taz_fc_table$target_id,
sleuth_ob_DMSO_Taz_lrt_results$target_id)]
Taz_fc_table <- arrange(Taz_fc_table, qval)
Taz_fc_table$mean_log2fc <- rowMeans(subset(Taz_fc_table, select =
c(KA377, KA392, KA411)), na.rm = TRUE)
#Now add a new column containing average tpm
#Set order first
Taz_tbl_avtpm <- Taz_tbl_avtpm[order(match(Taz_tbl_avtpm$Group.1,
Taz_fc_table$target_id)),]
Taz_fc_table$mean_expression_tpm <- rowMeans(subset(Taz_tbl_avtpm,
select = c(KA377, KA392, KA411)), na.rm = TRUE)
Final_taz_fc_tbl <- Taz_fc_table[,c(1,2,6:9)]
write.csv(Final_taz_fc_tbl, "Final_tazemetostat_fc.csv")
Final_taz_fc_sig <- Final_taz_fc_tbl[which(Final_taz_fc_tbl$qval<0.05 &
Final_taz_fc_tbl$mean_log2fc >= 0.3 | Final_taz_fc_tbl$qval<.05 &
Final_taz_fc_tbl$mean_log2fc <= -0.3),]
write.csv(Final_taz_fc_sig, "Final_tazemetostat_DEGs.csv")
```

2.4 Making a volcano plot

We next generated a volcano plot with significant values in red. We set the cutoff as q-value < 0.05 and the mean log2 fold-change < -0.3 and > 0.3.

```
with(Taz_fc_table, plot(mean_log2fc, -log10(qval), pch=20, main="Volcano
plot", xlim=c(-5,5)))
with(subset(Taz_fc_table, qval<.05 & mean_log2fc >= 0.3 | qval<.05 &
mean_log2fc <= -0.3), points(mean_log2fc, -log10(qval), pch=20, col="red"))
with(subset(Taz_fc_table, qval<.05 & abs(mean_log2fc) > 1),
textxy(mean_log2fc, -log10(qval), labs=gene, cex=.8))
```

2.5 Investigating overlapping genes

Here we used the packages VennDiagram and GeneOverlap to create venn diagrams and calculate the statistical significance of the overlaps. We also generated lists of overlapping genes.

```
library("VennDiagram")
dev.off()

BLIMP1_sig_up <- filter(Final_BLIMP1_fc_sig, mean_log2fc > 0)
BLIMP1_sig_down <- filter(Final_BLIMP1_fc_sig, mean_log2fc < 0)
Taz_sig_up <- filter(Final_taz_fc_sig, mean_log2fc > 0)
Taz_sig_down <- filter(Final_taz_fc_sig, mean_log2fc < 0)

#Plotting genes significantly upregulated following KD (no filtering):
venn.plot1 <- venn.diagram(x = list("BLIMP1 KD" =
BLIMP1_sig_up$target_id,
                                    "Tazemetostat" = Taz_sig_up$target_id),
                           filename = NULL,
                           scaled = TRUE, margin = 0.1)
grid.draw(venn.plot1)
dev.off()

Blimp1_taz_olap_up <- BLIMP1_sig_up[BLIMP1_sig_up$target_id %in%
Taz_sig_up$target_id,]
write.csv(Blimp1_taz_olap_up, "BLIMP1_tazemetostat_common_up.csv")

library("GeneOverlap")

Up_olap <- newGeneOverlap(BLIMP1_sig_up$target_id,
Taz_sig_up$target_id, genome.size = NULL,
                          spec = c("hg19.gene"))
Up_olap <- testGeneOverlap(Up_olap)
Up_olap

#Plotting genes significantly downregulated following KD:
dev.off()
venn.plot2 <- venn.diagram(x = list("BLIMP1 KD" =
BLIMP1_sig_down$target_id,
                                    "Tazemetostat" = Taz_sig_down$target_id),
                           filename = NULL,
```

```
                    scaled = TRUE, margin = 0.1)
grid.draw(venn.plot2)
dev.off()

down_olap <- newGeneOverlap(BLIMP1_sig_down$target_id,
Taz_sig_down$target_id, genome.size = NULL,
                     spec = c("hg19.gene"))
down_olap <- testGeneOverlap(down_olap)
down_olap

Blimp1_Taz_olap_down <- BLIMP1_sig_down[BLIMP1_sig_down$target_id
%in% Taz_sig_down$target_id,]
write.csv(Blimp1_Taz_olap_down,
"BLIMP1_tazemetostat_common_down.csv")
```

2.6 GSEA

GSEA was used to identify significantly enriched gene sets within our RNAseq data.For this, we generated ranked gene lists comprising all detected genes assigned to a rank value. The rank value was calculated as -log10(q-value) × (sign of fold change). The genes were then ranked from the highest rank value to the lowest. These lists were generated in R:

```
Taz_all_preranked.score <- Final_taz_fc_tbl[,c(1:3,5)]
Taz_all_preranked.score.up <- filter(Taz_all_preranked.score, mean_log2fc
>0)
Taz_all_preranked_log.score.up <-
log10(1/Taz_all_preranked.score.up$qval)
Taz_all_preranked.score.down <- filter(Taz_all_preranked.score,
mean_log2fc <0)
Taz_all_preranked_log.score.down <- -
log10(1/Taz_all_preranked.score.down$qval)
Taz_all_preranked_log <-
as.data.frame(c(Taz_all_preranked.score.up$gene,
Taz_all_preranked.score.down$gene))
Taz_all_preranked_log$score <- c(Taz_all_preranked_log.score.up,
Taz_all_preranked_log.score.down)
Taz_all_preranked_log <- na.omit(setorder(Taz_all_preranked_log, -score,
na.last = TRUE))
```

```
write.csv(Taz_all_preranked_log,
"20180928_Tazemetostat_all_preranked_log10.csv")
```

This file was then opened in excel, headers of all columns were deleted as well as all columns except for gene names and score. The file was saved as a tab-delimited .txt rile with the .rnk extension. This was then loaded into GSEA preranked program. We used the following settings with the Hallmarks gene set database:

```
Number of Permutations: 1000
Enrichment statistic: classic
Max size: 5000
Min size: 15
Normalisation mode: meandiv
```

2.7 Heatmaps

We plotted heatmaps for our RNAseq samples using lists of significantly differentially expressed genes

```
library(gplots)
library(RColorBrewer)

immune_evasion <- unique(read.csv("Immune_evasion_BLIMP1.csv"))
immune_evasion$Gene <-
immune_evasion$Gene[order(match(immune_evasion$Gene,
ttg$ext_gene))]
BLIMP1_immune_evasion_tbl <- BLIMP1_fc_table[(BLIMP1_fc_table$gene
%in% immune_evasion$Gene),]

BLIMP1_immune_evasion_tbl <- BLIMP1_immune_evasion_tbl[,c(2:5)]
BLIMP1_immune_evasion_tbl <-
data.frame(lapply(BLIMP1_immune_evasion_tbl, function(x) {gsub("Inf", 10,
x)}))

im_order <- read.csv("Immune_evasion_BLIMP1.csv")
BLIMP1_immune_evasion_tbl <-
BLIMP1_immune_evasion_tbl[order(match(BLIMP1_immune_evasion_tbl$ge
ne, im_order$Gene)),]
rownames(BLIMP1_immune_evasion_tbl) <-
BLIMP1_immune_evasion_tbl$gene
BLIMP1_immune_evasion_tbl <- BLIMP1_immune_evasion_tbl[,c(2:4)]
```

```
names <- rownames((BLIMP1_immune_evasion_tbl))

BLIMP1_immune_evasion_tbl <- mutate_all(BLIMP1_immune_evasion_tbl,
function(x) as.numeric(as.character(x)))
rownames(BLIMP1_immune_evasion_tbl) <- c(names)
BLIMP1_immune_evasion_tbl$too <-
rep(0,nrow(BLIMP1_immune_evasion_tbl))
BLIMP1_immune_evasion_tbl$"2" <-
rep(0,nrow(BLIMP1_immune_evasion_tbl))
BLIMP1_immune_evasion_tbl$"3" <-
rep(0,nrow(BLIMP1_immune_evasion_tbl))
BLIMP1_immune_evasion_tbl <- BLIMP1_immune_evasion_tbl[,c(4:6, 1:3)]

colnames(BLIMP1_immune_evasion_tbl) <- c("NTC miR (1)", "NTC miR (2)",
"NTC miR (3)", "PRDM1 miR (1)", "PRDM1 miR (2)", "PRDM1 miR (3)")
BLIMP1_immune_evasion_tbl <- as.matrix(BLIMP1_immune_evasion_tbl)
RBcolors <- colorRampPalette( rev(brewer.pal(9, "RdBu")) )(75)
heatmap.2(BLIMP1_immune_evasion_tbl,
        Rowv = FALSE,
        Colv=FALSE,
        col=RBcolors,
        key=TRUE, keysize=1, symkey=TRUE, density.info='none',
        trace='none',
        ## The following command scales each row so that the gene
expression changes are scaled for each column.
        scale="row",
        margins = c(15,9),
        cexRow=0.7,
        cexCol=1,
        labCol = colnames(BLIMP1_immune_evasion_tbl),
        labRow = rownames(BLIMP1_immune_evasion_tbl),

)
```

3 ChIPseq analyses

We first ran the fastq files through FastQC and Trim Galore as above. Then, we ran Bowtie2 on the trimmed files to align the reads to the hg38 genome.

```
bowtie2 -p14 -x Bowtie2Index/genome -1 name_R1_val_1.fq.gz -2 name_R2_val_2.fq.gz -S name_UCSC.sam
```

Then we converted .sam files to sorted .bam files:

```
samtools view -@ 14 -bS name.sam | samtools sort -o name_aligned.bam
```

We merged the bam files:

```
samtools merge -c -p filename_merge.bam filename1.bam filename2.bam
```

Firstly, we tried to use MACS1.4, but didn't find the peak calling to work so well for the H3K27me3 mark:

```
macs14 -c PACRCXG/*aligned.bam.bam -t PACRCXE/*aligned.bam.bam -g hs -w -S -n 20180206_KA428_NTC_K27me3_UCSC
```

We used the .wig files generated in MACS1.4 to create bigWig files which we then visualised on the UCSC genome browser.

```
wigToBigWig name.wig.gz $HOME/hg38.chrom.sizes UCSC.bw -clip
```

We used MACS2 to call peaks at different q-values. We generally used quite lenient q-values so that we could combine replicates later. We tried the q-values 0.01, 0.001 and 0.0001. For example:

```
MACS2 callpeak -t PACRCUT.bam.bam -c PACRCUS.bam.bam -n 20180322_KA390_RPCI_BLIMP1_macs2_q3 -g hs -q 0.001 -f BAMPE
```

To assess the peak calling, we investigated the peak lists and compared them to tracks for the same experiment visualised on the UCSC genome browser.

We used the bedOps program to remove blacklisted regions with artefacts from the bed files:

```
#!/bin/bash

for i in *.broadPeak

do

echo "BedOps: "$i
```

```
bedops -n $i Centromeric.bed > $i".filtered"

done
```

The blacklisted regions were as follows:

Appendix Table II: Blacklisted regions

Chr	Start	End
1	121301254	143601086
1	148509965	148605901
10	38342249	42345412
11	50639378	54602911
12	34494476	37315449
13	15932666	18445045
14	4116852	18283284
15	16742648	19857282
15	19772028	19788200
16	34561382	34600423
16	38193699	46449179
17	22252871	27419764
18	105511	113219
18	15206107	21026076
18	80262001	80263718
19	24090454	27656388
2	89825185	89842202
2	90322492	94802381
20	26183756	31242950
21	7605039	13270848
22	10213867	15446234
3	90470887	93729259
4	7405	72991
4	49021358	51834385
5	46460491	50216349
6	58351628	60247657
7	56369943	56375294
7	57944754	62051072
8	43618739	46150317
9	43269187	60999358
X	58404711	62941461

Y 1 57227415

- Write column headings into this new file:

```
seqnames start end name score strand fold_enrich X.log10_pval X.log10_qval rel_summit_pos
```

- Now you are ready to load it into R and analyse

3.1 Diffbind

A sample sheet was then prepared in excel combining the selected peak bam files as specified for the diffBind package. For the BLIMP1 ChIPseq in the RPCI-WM1 cell line we used a q-value of 0.001, and for the OPM-2 and NCI-H929 cell lines we used a q-value of 0.0001. For the H3K27me3 ChIPseq we used a q-value of 10e-8 for all cell lines, and for the EZH2 ChIPseq we used a q-value of 0.001. As an example of how we generated consensus peak lists:

```
library(DiffBind)
library(diffloop)
#Creating overlap of RPCI BLIMP1 ChIPSeq replicates called with MACS2
RPCI_BLIMP1_comb <-
dba.peakset(BLIMP1_consensus_cellline,BLIMP1_consensus_cellline$masks$RPCI, bRetrieve = TRUE)
RPCI_BLIMP1_comb <- addchr(RPCI_BLIMP1_comb)
RPCI_BLIMP1_comb <- annotatePeak(RPCI_BLIMP1_comb, TxDb=txdb, annoDb="org.Hs.eg.db")
RPCI_BLIMP1_comb.data <- as.data.frame(RPCI_BLIMP1_comb)
write.csv(RPCI_BLIMP1_comb.data, "RPCI_BLIMP1_comb.csv")
```

Converted peak list to bed file in excel. Saved as tab-delimtited text. Converted to hg19 with UCSC liftover, then ran through the GREAT tool and downloaded gene list from there. This is better than the annotation in R, as you can get multiple gene annotations from one peak if it is in between genes.

3.2 Getting sequences to run in MEME

```
RPCI.Blimp1.seqs <- getSeq(bsG,Complete_RPCI_comb_data )
RPCI.Blimp1.seqs <- as.data.frame(RPCI.Blimp1.seqs)
write.csv(RPCI.Blimp1.seqs, "RPCI_BLIMP1_peaks_sequences.csv")
```

Converted these files to fasta files before running in MEME.

3.3 Deeptools

We used Deeptools to generate plots of raw ChIPseq signals over BLIMP1 binding sites. First, we generated a matrix of ChIPseq signal enrichment using a bigWig file over blimp1 binding sites (designated in a bam file) over + or - 10 kb distances.

```
Deeptools kimberleyanderson$ computeMatrix reference-point -S
H929_K27me3_UCSC_comb_treat.bw  -R H929_BLIMP1_peaks.bed --
missingDataAsZero -b 10000 -a 10000 -bs 25 -p max -o
20180718_H929_K27_over_BLIMP1peaks_10kb
```

We then plotted a heatmap and profile for these

```
plotHeatMap -m 20180718_H929_K27_over_BLIMP1peaks_10kb -o
20180718_H929_K27_overBLIMP1_10kb.pdf --colorMap YlGnBu
```

3.4 Overlapping ChIPseq data

Here we calculated overlaps of ChIPseq data, both directly and by extending the peak regions by 10 kb to either side. This is one example:

```
library("GenomicRanges")
library("ChIPpeakAnno")
#Actual overlap of K27me3 and BLIMP1 for RPCI
RPCI_BLIMP1_combpeaks<- read.table("RPCI_BLIMP1_final.bed.txt")
colnames(RPCI_BLIMP1_combpeaks) <- c("chr", "start", "end")
RPCI_BLIMP1_combpeaks.granges <-
makeGRangesFromDataFrame(RPCI_BLIMP1_combpeaks)
RPCI_K27me3_combpeaks <- read.table("RPCI_K27me3_comb.bed.txt")
colnames(RPCI_K27me3_combpeaks) <- c("chr", "start", "end")
RPCI_K27me3_combpeaks.granges <-
makeGRangesFromDataFrame(RPCI_K27me3_combpeaks)
RPCI_comb_BLIMP1_K27_peakolap <-
findOverlapsOfPeaks(RPCI_BLIMP1_combpeaks.granges,
RPCI_K27me3_combpeaks.granges)
makeVennDiagram(RPCI_comb_BLIMP1_K27_peakolap)

#10kb overlap of BLIMP1 and K27me3 for RPCI
RPCI_comb_BLIMP1_K27_peakolap_10kb <-
```

```
findOverlapsOfPeaks(RPCI_BLIMP1_combpeaks.granges,
                                        RPCI_K27me3_combpeaks.granges,
                                        maxgap = 10000)
makeVennDiagram(RPCI_comb_BLIMP1_K27_peakolap_10kb)
```

3.5 Overlapping ChIPseq and RNAseq data

We performed overlaps using the GeneOverlap package in R and created Venn diagrams using the VennDiagram package. We did the same for genes induced and repressed following BLIMP1 KD or tazemetostat treatment. The same method was used for finding overlapping genes assigned to ChIPseq peaks.

```
library("GeneOverlap")
library("GenomicRanges")
library("dplyr")

BLIMP1_DEGs <- read.csv("20181127_Final_BLIMP1_DEGs.csv",
row.names = 1)
Tazemetostat_DEGs <-
read.csv("20181127_Final_tazemetostat_DEGs.csv", row.names = 1)
BLIMP1_up <- filter(BLIMP1_DEGs, mean_log2fc >0)
BLIMP1_down <- filter(BLIMP1_DEGs, mean_log2fc < 0)
Taz_up <- filter(Tazemetostat_DEGs, mean_log2fc > 0)
Taz_down <- filter(Tazemetostat_DEGs, mean_log2fc < 0)



#BLIMP1 ChIPseq RNAseq overlap up
BLIMP1_olap_up <- newGeneOverlap(BLIMP1_up$gene,
RPCI_BLIMP1_genelist$V1, genome.size = NULL,
                                 spec = c("hg19.gene"))
BLIMP1_olap_up <- testGeneOverlap(BLIMP1_olap_up)
BLIMP1_olap_up
print(BLIMP1_olap_up)

BLIMP1_olap_up_list <- BLIMP1_up[BLIMP1_up$gene %in%
RPCI_BLIMP1_genelist$V1,]
write.csv(BLIMP1_olap_up_list,
"20181127_BLIMP1_ChIPseq_RNAseq_olap_up.csv")
```

```
library("VennDiagram")
#Plotting genes with overlap in ChIPseq and RNAseq:
venn.plot1 <- venn.diagram(x = list("PRDM1 KD RNAseq" =
BLIMP1_up$gene,
                                    "BLIMP1 ChIPseq" = RPCI_BLIMP1_genelist$V1),
                           filename = NULL,
                           scaled = TRUE, margin = 0.1)
grid.draw(venn.plot1)
dev.off()
```